

Alharethi, Abdullah Najih (2025) *Interplay between AMP-activated protein kinase (AMPK) and The Sphingolipid System in Adipose Tissue Regulation.*PhD thesis.

https://theses.gla.ac.uk/85592/

Copyright and moral rights for this work are retained by the author

A copy can be downloaded for personal non-commercial research or study, without prior permission or charge

This work cannot be reproduced or quoted extensively from without first obtaining permission from the author

The content must not be changed in any way or sold commercially in any format or medium without the formal permission of the author

When referring to this work, full bibliographic details including the author, title, awarding institution and date of the thesis must be given

Enlighten: Theses
https://theses.gla.ac.uk/
research-enlighten@glasgow.ac.uk

Interplay between AMP-activated protein kinase (AMPK) and The Sphingolipid System in Adipose Tissue Regulation

Abdullah Naji Alharethi BSc, MSc

Thesis submitted in fulfilment of the requirements for the degree of Doctor of Philosophy

2025

School of Cardiovascular and Metabolic Health, College of Medical, Veterinary and Life Sciences University of Glasgow

Abstract

Introduction: Cardiovascular diseases represent a global health burden, with vascular dysfunction and chronic low-grade inflammation recognised as key pathological drivers. Published evidence highlights the crucial regulatory role of perivascular adipose tissue (PVAT) in maintaining vascular homeostasis. Dysfunctional PVAT with has been implicated in the development of vascular disease. Within this context, sphingosine kinase 1 (SphK1) and its bioactive lipid product, sphingosine-1-phosphate (S1P), is noted as a modulator of vascular tone and inflammation. Furthermore, AMP-activated protein kinase (AMPK) an enzyme which promotes cellular energy homeostasis, serves as a vascular function regulator. The interplay between AMPK signalling and the SphK1/S1P axis within PVAT represents a promising therapeutic target for ameliorating vascular dysfunction. This thesis investigates the functional interactions between AMPK, SphK1/S1P signalling within cultured adipocytes and aortic PVAT, advancing understanding of vascular biology in the hope of identifying novel therapeutic strategies for cardiovascular and metabolic diseases.

Methods and Materials: This chapter outlines the experimental methodologies and analytical techniques used to investigate the interplay between AMPactivated protein kinase (AMPK) and sphingosine-1-phosphate (S1P) in the regulation of adipose tissue, with a particular emphasis on the role of PVAT. Wildtype (WT) and AMPKα1 knockout (KO) mice were employed as experimental models. Vascular function was assessed using wire myography to measure relaxation responses of thoracic aortic rings following exposure to S1P, AMPK activators (AICAR, A-769662, and Compound 991), and their combinations. The contribution of PVAT-derived mediators was investigated by comparing vascular responses in rings with and without intact PVAT. Adipokine secretion was analysed using a proteome-based mouse adipokine array, while nitric oxide (NO) production was quantified using a Sievers 280 NO analyser. Quantitative real-time PCR and western blotting were used to assess gene and protein expression in PVAT, mouse embryonic fibroblasts adipocytes. Additionally, (MEFs), and 3T3-L1 immunofluorescence microscopy was employed to examine the localisation of sphingosine kinase 1 (SphK1). All experiments were conducted under standardised laboratory conditions, and data were analysed using appropriate statistical methods to ensure accuracy, reproducibility, and scientific validity.

Results: Chapter 3 explore the regulatory relationship between AMPK and SphK1 during adipocyte differentiation and in PVAT. Using 3T3-L1 adipocyte cells, mouse embryonic fibroblast (MEF) cells which lack AMPK, and mouse abdominal and thoracic PVAT, SphK1 expression was assessed in adipocytes and in cells lacking AMPK. SphK1 protein levels notably increased during adipocyte differentiation, highlighting a possible role in adipogenesis. In AMPKα1/α2 knockout MEFs, increased SphK1 protein levels were observed without corresponding changes in mRNA expression. Furthermore, tissue-specific differences were noted in PVAT, with distinct regulatory patterns observed between thoracic and abdominal PVAT.

Chpter4 examine the roles of S1P and AMPK activation, using the activator AICAR, in modulating vascular function through PVAT in mouse thoracic aortic rings. S1P alone showed no vasorelaxant effects, while AICAR caused a significant vascular relaxation. S1P and AICAR combined substantially augmented this relaxation, particularly in endothelium-denuded aortic rings containing PVAT. This effect was significantly reduced in AMPKα1 knockout mice, suggesting a critical role for the AMPKα1 subunit. Further experiments suggest that increased secretion of PVAT-derived adiponectin and nitric oxide could be potential mechanisms. S1PR1, a vascular-expressed receptor for S1P was identified as a key mediator of these effects. Findings highlight the complex interplay between S1P signalling, AMPK activation, and PVAT-derived factors in vascular regulation.

Chapter 5 investigate the impact of S1P and different AMPK activators, namely Compound 991 (C991), and A-769662, on vascular relaxation mediated by PVAT in mouse thoracic aortic rings. As in Chapter 4, S1P alone showed no vasorelaxation effects, while each AMPK activator induced significant relaxation, particularly in PVAT-containing vessels. However, combined treatments with S1P and either C991 or A-769662 resulted in non-significant enhanced vascular relaxation, highlighting that the mechanism of AMPK activation may be crucial for this enhancement of relaxation.

Discussion: Chapter 3 demonstrated that AMPK α 1/ α 2 knockout (KO) leads to elevated SphK1 protein expression in MEFs without corresponding changes in mRNA levels, indicating post-transcriptional regulation. This deficiency also enhances

ERK1/2 and JNK signalling, consistent with a shift toward a pro-inflammatory phenotype. Importantly, SphK1 was selectively upregulated in thoracic PVAT of AMPKα1 KO mice, but not in abdominal PVAT, underscoring a depot-specific regulatory role of AMPK.

Chapter 4 demonstrated that while S1P alone exerts limited vasorelaxant effects, its combination with AICAR, an AMPK activator, significantly enhances PVAT-mediated vascular relaxation through nitric oxide and adiponectin pathways. Chapter 5 explored the effects of direct AMPK activators, A-769662 and Compound 991, confirming their ability to induce vascular relaxation, although without the synergistic enhancement observed with AICAR and S1P. The pivotal role of AMPK signalling in integrating metabolic and inflammatory pathways is underscored and its potential as a therapeutic target for vascular dysfunction highlighted.

Conclusion: This thesis provides novel insights into the regulatory interplay between sphingosine-1-phosphate (S1P) signalling, AMPK activation via AICAR, and the functional role of perivascular adipose tissue (PVAT) in modulating vascular relaxation in the mouse thoracic aorta. The combination of AICAR and S1P enhanced vasorelaxation, highlighting the importance of indirect AMPK activation in promoting PVAT-derived adiponectin and nitric oxide. The selective upregulation of SphK1 in AMPK-deficient tissues suggests a shift toward a pro-inflammatory phenotype. These findings identify the SphK1/S1P-AMPK axis as a potential target for improving vascular health.

Table of Contents

Abstra	ct	••••••	ii
Table o	of Co	ntents	v
List of	Tabl	es	ix
List of	Figu	res	x
Acknov	vled	gement	xii
Author	's De	eclaration	. xiii
Abbrev	/iatic	ns	. xiv
Confer	ence	abstracts and publication	. xvi
Chapte	r 1	- Introduction	1
1.1	Ca	rdiovascular disease	2
1.2	Ca	rdiovascular system anatomy	2
1.2	2.1	Endothelium layer	4
1.2	2.2	Vascular smooth muscle layer	4
1.2	2.3	Adventitia and Perivascular adipose tissue	5
1.3	Ad	ipose tissue	5
1.4	Pe	rivascular adipose tissue (PVAT)	7
1.4	4.1	Role of PVAT in vascular tone regulation	9
1.4	4.2	Mechanisms underlying the anti-contractile effect of PVAT	10
1.5	Spł	ningolipid System	12
1.5	5.1	Sphingosine 1 Phosphate overview	12
1.6	Spł	ningosine Kinases	19
1.6	5.1	Regulation of Sphingosine kinase1 (SphK1)	20
1.6	5.2	Regulation of Sphingosine kinase2 (SphK2)	22
1.6	5.3	Sphingosine Kinases inhibitors	23
1.7 regul		e role of Sphingosine Kinase/Sphingosine 1 Phosphate in vascular t	
	7.1 sue f	Role of Sphingosine Kinase/Sphingosine-1-Phosphate in adipose unction	25
-	7.2 ipoge	Role of Sphingosine Kinase/Sphingosine-1-Phosphate in enesis and lipid metabolism	25
-	7.3 sue i	Role of Sphingosine Kinase/Sphingosine-1-Phosphate in adipose nflammation	26
1.8	AM	P-activated protein kinase (AMPK)	27
1.8	3.1	AMPK background	27
1.8	3.2	Pharmacological AMPK activators	29
1.8	3.3	Vascular effect of AMPK	30

1.8.4	Role of AMPK in perivascular adipose tissue	. 32
1.9 F	lypothesis and Aim	. 35
Chapter 2	- Materials and Methods	, 36
2.1 A	Materials	. 37
2.1.1	Animal model	. 37
2.1.2	List of cells and suppliers	. 37
2.1.3	List of materials and suppliers	. 37
2.1.4	List of primary and secondary antibodies for immunoblotting	. 40
2.2 N	Methods	. 41
2.2.1	Genotyping from mouse ear notches	. 41
2.2.2	Wire myography	. 43
2.2.3	Mouse Adipokine Array (Proteome Profile)	. 47
2.2.4	Nitric oxide (NO) assay	. 48
2.2.5	Cell culture procedure	. 49
2.2.6	Analysis of protein expression in PVAT, MEFs and 3T3-L1 cells	. 51
2.2.7	Gene analysis	. 53
2.2.8	Immunofluorescence (IF)	. 56
2.2.9	Statistical analysis	. 57
	-Characterisation of Sphingosine Kinase1 (SphK1) Expression in ipose & Perivascular Adipose Tissues (PVAT)- Effect of AMPKα1 (KO)	
	ntroduction	
	and Objectives	
	Results	
3.3.1	Sphingosine Kinase1 (SphK1) protein level in 3T3-1L adipocytes g differentiation	
3.3.2 expre	Investigation of Sphingosine Kinase 1 (SphK1) gene and protein ession in ΑΜΡΚα1, α2 Knockout Mouse Embryonic Fibroblast (MEF)	
3.3.3 Immu	Visualization of Sphingosine Kinase 1 (SphK1) via nofluorescence in Wild-Type and ΑΜΡΚα1/α2 Knockout Mouse yonic Fibroblasts (MEF) Cells	
	Effect of AMPKα1/α2 Knockout Mouse Embryonic Fibroblasts (MEFon ERK1/2 Protein Levels	
3.3.5 (MEF)	Effect of AMPKα1/α2 Knockout in Mouse Embryonic Fibroblasts cells on JNK protein levels	. 71
3.3.6 abdor	Expression of Sphingosine Kinase 1 (SphK1) Gene and Protein in minal aortic PVAT of Mice.	. 73
3.3.7 Thora	Gene and Protein Expression of Sphingosine Kinase1 (SphK1) in acic Aortic PVAT of AMPKa1 Deficient Mice	. 75

3.	4	Disc	ussion	7
3.	.5	Cond	clusion 8	1
	-		- Investigating the Effect of Sphingosine-1-Phosphate (S1P) and tivator AICAR on Perivascular Adipose Tissue (PVAT) Function .8	
4.	1	Intro	oduction8	4
4.	2	Aim	and Objectives8	7
4.	.3	Resu	ılts8	8
			Vascular relaxation induced by combined S1P and AICAR in WT ngs with intact PVAT8	8
			Relaxation to a combination of S1P and AICAR is not augmented in e (WT) aortic rings with intact endothelium and PVAT	
	4.3. atte		Vascular relaxation to the combination of S1P and AICAR is ed in WT denuded thoracic rings without PVAT9	15
	4.3 com		Effect of AMPKα1 subunit knockout on vascular relaxation to the tion of S1P+AICAR in thoracic PVAT rings9	8
			Effect of S1PR ₁ agonists (SEW2871) and antagonists (W146) and vascular smooth muscle wild-type thoracic PVAT rings10)1
	4.3. com		Effect of S1PR $_2$ agonists (CYM5478) and antagonists (JTE013) d with AICAR on vascular smooth muscle in WT thoracic aorta10)4
			Effect of S1PR $_3$ agonists (CYM5541) and antagonists (CAY10444) in tion with AICAR on vascular smooth muscle in WT thoracic aorta. 10)7
	4.3.	8	Mouse adipokine array (proteome profile)11	0
	4.3.5 proc		Effect of S1P and AICAR in combination on nitric oxide (NO) on in wild-type (WT) thoracic PVAT11	3
			Effect of NO inhibitor (L-NAME) on combination of S1P and AICAR in ded thoracic PVAT11	
4.	4	Disc	ussion11	6
4.	.5	Cond	clusion12	.4
			 How Sphingsine-1-Phosphate (S1P) and AMPK activators- and A769662 affect perivascular adipose tissue functions . 12 	6
5.	.1	Intro	oduction12	.7
5.			and Objectives12	
5.	3	Resu	ılts13	0
		ular	Effect of the combination of S1P and Compound 991 (C991) on smooth muscle relaxation in wild-type (WT) thoracic rings with 'AT13	0
		ular	Effect of the combination of S1P plus Compound 991 (C991) on smooth muscle relaxation in AMPKα1 KO thoracic rings with intact13	3
			Effect of the combination of S1P plus A769662 on vascular smooth elaxation in wild-type thoracic aortic rings with intact PVAT13	6

	4 Effect of a combination of S1P plus A-769662 on relaxation in acs from AMPKα1 KO mice with intact PVAT	
5.4	Discussion	. 142
5.5	Conclusion	. 148
Chapter	6 - General discussion	149
6.1	Summary and General discussion	.150
6.2	Limitations	.155
6.3	Conclusion	.157
Chapter	7 References	158
Appendi	ces	184

List of Tables

Table 1-1 Agonists and antagonists of the sphingosine-1-phosphate receptors and their activity across S1PR1-S1PR5	
	10
Table 2-1 The primary antibodies used for immunoblotting	40
Table 2-2 The secondary antibodies used for immunoblotting	41
Table 2-3 List of DNA primers in genotyping process.	42
Table 2-4 List of drugs and stock concentrations used	45
Table 2-5 TaqMan probes	56
Table 4-1 Semi-quantitative assessment of vasorelaxation in mouse thoracic aorta in response to S1P receptor agonists, AICAR, and their co-application; plus signs indicate degree of qualitative	
relaxation	. 117
Table 7-1 Contractile responses (mean ± SEM) to KPSS and phenylephrine under varying ET (±) and PV	ΑT
(±) conditions.	. 184

List of Figures

Figure 1-1: The structure of the vascular wall	3
Figure 1-2: Overview of Sphingosine-1-Phosphate (S1P) synthesis and metabolism.	14
Figure 1-3 The S1P-S1PRs signalling pathways	17
Figure 1-4 Schematic overview of the transcriptional, post-transcriptional, and post-translational regulation of SphK1	22
Figure 1-5: AMPK α, β, and γ subunits	28
Figure 2-1: The genotyping of Wild-Type (WT) and AMPKα1 Knockout (KO) mice	43
Figure 2-2: Representative images of mouse thoracic aorta mounted in a small-vessel wire myograph	44
Figure 2-3: The components of the wire myograph.	47
Figure 3-1: Expression of Sphingosine Kinase 1 (SphK1) during 3T3-L1 adipogenesis	63
Figure 3-2: Gene and protein expression of SphK1 in MEF cells	65
Figure 3-3: Immunofluorescence confocal microscopy of SphK1 in MEF cells	68
Figure 3-4: Protein levels of ERK1/2 in MEF cells.	70
Figure 3-5: Protein levels of JNK in MEF cells	72
Figure 3-6: Gene and protein expression of SphK1 in abdominal aortic PVAT of mice	74
Figure 3-7: Gene and protein expression of SphK1 and pAMPK in thoracic aortic PVAT of mice	76
Figure 4-1: Functional assessment of endothelium-denuded thoracic aortic rings with PVAT in Wild-Type (WT) mice.	
Figure 4-2: Functional assessment of endothelium-intact thoracic aortic rings with PVAT in Wild-Type mice.	94
Figure 4-3: Functional assessment of endothelium-denuded thoracic aortic rings without PVAT in Wild- Type mice	97
Figure 4-4: Functional evaluation of endothelium-denuded thoracic aortic rings with perivascular adipos tissue in AMPKα1 KO mice1	
Figure 4-5: Functional assessment of SEW2871, a selective S1PR1 agonist, in endothelium-denuded thoracic aortic rings with PVAT in Wild-Type (WT) mice1	.03
Figure 4-6: Functional evaluation of CYM5478, a selective S1PR2 agonist, in endothelium-denuded thoracic aortic rings with PVAT in Wild-Type (WT) mice1	06
Figure 4-7: Functional assessment of CYM5541, a selective S1PR3 agonist, in endothelium-denuded thoracic aortic rings with PVAT in Wild-Type (WT) mice1	.09
Figure 4-8: Adipokine profiling of thoracic PVAT-conditioned media following S1P and AICAR treatments in Wild-Type mice	
Figure 4-9: Combined effects of S1P and AICAR on nitric oxide production in thoracic aortic PVAT of Wild Type mice	
Figure 4-10: Relaxation to S1P and AICAR and the role of Nitric Oxide (NO) in endothelium-denuded mouse thoracic aortic rings with PVAT1	15
Figure 5-1: Functional assessment of relaxation in endothelium-denuded thoracic aortic rings with PVAT from wild-type (WT) mice	
Figure 5-2: Functional evaluation of endothelium-denuded thoracic aortic rings with PVAT in AMPKα1 knockout (KO) mice	35
Figure 5-3: Functional evaluation of endothelium-denuded thoracic aortic rings with PVAT in wild-type (WT) mice	38

Figure 5-4: Functional evaluation of endothelium-denuded thoracic aortic rings with PVAT in AMPKα1	L
knockout (KO) mice	. 141
Figure 5-5: Mechanisms of AMPK regulation by pharmacological activators	1/1/
rigure 3-3. Mechanisms of Alvirk regulation by pharmacological activators	. 144

Acknowledgement

This PhD journey has been both a deeply enriching and transformative experience, and I am profoundly grateful to all those who have supported, guided, and encouraged me throughout.

I would like to express my sincere appreciation to my supervisors, Professor Simon Kennedy and Professor Craig Daly, for their exceptional guidance, constructive feedback, and unwavering support. Their mentorship has played a pivotal role in shaping my scientific thinking and enabling the successful completion of this research.

I am also thankful to the research teams of Professor Kennedy, Dr. Ian Salt, and Professor Will Fuller for their collaborative support and technical contributions, which added great value to my work. My special thanks go to Mr. John McAbney for his expert training in wire myography and for his continued assistance and encouragement throughout my experimental studies.

This research would not have been possible without the generous funding and support provided by Najran University, the Saudi Cultural Bureau in London, and the Government of the Kingdom of Saudi Arabia. I am sincerely grateful for the opportunity and resources that made this academic journey possible.

On a personal note, I dedicate this work to my father, Naji who passed away in 2019. His steadfast support and deep belief in the value of education continue to guide and inspire me every step of the way. I pray that Allah grants him the highest place in paradise. I also extend my heartfelt thanks to my mother, Karemah who's love, prayers, and encouragement have been a constant source of strength. I am deeply grateful to my wife, Nawal Alharthi for her patience, understanding, and sacrifices during this journey, and to my sons, Bandar and Badr who have brought joy and motivation to my life.

Author's Declaration

I hereby declare that this thesis is entirely my own work except where otherwise stated. It has not been submitted either in whole or in part for any other degree or qualification. The research presented herein was conducted in the laboratory of Professor Simon Kennedy & Professor Craig Daly, within the School of Cardiovascular and Metabolic Health, College of Medical, Veterinary and Life Sciences, University of Glasgow, Glasgow, United Kingdom.

Abdullah Naji N Alharethi

October 2025

Abbreviations

3T3-L1 Fibroblast cell line isolated from 3T3 mouse embryo

A769662 6,7-Dihydro-4-hydroxy-3-(2'-hydroxy[1,1'-biphenyl]-4-yl)-6-oxo-

thieno[2,3-b]pyridine-5-carbonitrile

ACC Acetyl-CoA Carboxylase

ACh Acetylcholine

ADRF Adipocyte-Derived Relaxing Factor

AICAR 5-Aminoimidazole-4-Carboxamide 1-8-D-Ribonucleoside

BAT Brown adipose tissue
BCA Bicinchoninic acid
C.M Conditioned medium

Ca²⁺ Calcium ions

CaMKKB Calcium/Calmodulin-dependent Protein Kinase Kinase B

cAMP Cyclic adenosine 3',5' -monophosphate

CAY10444 (4R)-2-undecyl-4-thiazolidinecarboxylic acid

CerS Ceramide synthases

cGMP Cyclic guanosine monophosphate

CVD Cardiovascular Diseases

CYM5478 1-[2-[2,5-dimethyl-1-(phenylmethyl)-1H-pyrrol-3-yl]-2-oxoethyl]-5-

(trifluoromethyl)-2(1H)-pyridinone

CYM5541 N,N-dicyclohexyl-5-cyclopropyl-1,2-oxazole-3-carboxamide

DMEM Dulbecco's modified eagles' medium

DMSO Dimethyl sulfoxide

DTT Dithiothreitol

EAT Epididymal adipose tissue

ECs Endothelial cells

EGF Epidermal growth factor eNOS Endothelial NO Synthase

ERK 1/2 Extracellular signal-regulated kinase 1/2

EWAT Epidydimal white adipose tissue

FCS Foetal calf serum H_2S Hydrogen sulfide HFD High fat diet

IBMX 3-isobutyl-1-methylxanthine

JNK Jun N-terminal kinase

JTE013 3-(2,6-dichloropyridin-4-yl)-1-[(1,3-dimethyl-4-propan-2-

ylpyrazolo[4,5-e]pyridin-6-yl)amino]urea

KPSS High potassium physiological salt solution

LPS Lipopolysaccharide

MAPK Mitogen-activated protein kinases

NO Nitric oxide

NOA 280i Sievers Nitric Oxide Analyzer 280i

NOS Nitric oxide synthase

PBS Phosphate buffered saline
PCR Polymerase Chain Reaction

PE Phenylephrine

PI3Ks Phosphatidylinositol 3-kinases

PKA Protein kinase A
PKB Protein kinase B
PKC Protein kinase C

PPARγ Peroxisome Proliferator-Activated Receptor γ

PSS Physiological salt solution
PVAT Perivascular adipose tissue

RISC RNA interference silencing complex

ROS Reactive Oxygen Species S1P Sphingosine 1 Phosphate

S1PP S1P phosphatases

S1PR Sphingosine 1 Phosphate receptor

SAT Subcutaneous Adipose Tissue

SDS-PAGE SDS-polyacrylamide gel electrophoresis

SEW2871 5-[4-phenyl-5-(trifluoromethyl)-2-thienyl]-3-[3-

(trifluoromethyl)phenyl]-1,2,4-oxadiazole

siRNA Small interfering RNA
SphK Sphingosine kinase
Spms2 Spinster homolog 2

T2DM Type 2 Diabetes Mellitus

TBS Tris-buffered saline

TBST Tris-buffered saline - Tween 20

TEMED N, N, N', N'-tetramethylenediamine

TNF-α Tumour Necrosis Factor α

TZDs Thiazolidinediones

UCP-1 Uncoupling protein 1

VAT Visceral adipose tissue

VSMC Vascular smooth muscle cell

W146 [(3R)-3-amino-4-[(3-hexylphenyl)amino]-4-oxobutyl]-phosphonic acid
ZMP 5-aminoimidazole-4-carboxamide-1-B-D-furanosyl 5'-monophosphate

Conference abstracts and publication

Abdullah Naji; Craig Daly; Simon Kennedy; (2022) The Effect of AMPKα1 Deletion on Sphingosine Kinase 1 Protein Expression in Adipose Tissue. British Pharmacology Society Meeting, September (2022), Liverpool. *Br. J. Pharmacol.* 180(4): 526.

Abdullah Naji; Craig Daly; Simon Kennedy; (2022) The Effect of AMPKα1 Deletion on Sphingosine Kinase 1 Protein Expression in Adipose Tissue. 5th European Workshop on AMPK and AMPK-related kinases, September (2022), Glasgow.

Abdullah Naji; Craig Daly; Simon Kennedy; (2023). Perivascular adipose tissue (PVAT) augments relaxation of denuded mouse aortic to a combination of Sphingosine-1-Phosphate (S1P) plus the AMPK activator AICAR. Scottish Cardiovascular Forum, February (2023), Aberdeen.

Abdullah Naji; Craig Daly; Simon Kennedy; (2023) Perivascular adipose tissue (PVAT) augments relaxation of denuded mouse aortic to a combination of Sphingosine-1-Phosphate (S1P) plus the AMPK activator AICAR. 19th World Congress of Basic & Clinical Pharmacology, July (2023), Glasgow. *Br. J. Pharmacol.* 180 (S1), 189. P0886.

Hwej, A., Al-Ferjani, A., Alshuweishi, Y., **Naji, A.**, Kennedy, S. and Salt, I.P., 2024. Lack of AMP-activated protein kinase-α1 reduces nitric oxide synthesis in thoracic aorta perivascular adipose tissue. *Vascular Pharmacology*, *157*, *p.107437*.

Chapter 1 - Introduction

1.1 Cardiovascular disease

Cardiovascular disease refers collectively to disorders that impact the heart and blood vessels, including conditions such as coronary heart disease, cerebrovascular disease, and peripheral arterial disease. The World Health Organization (WHO) reported in 2021 that cardiovascular disease was responsible for approximately 32% of global deaths in 2019, with heart attacks and strokes accounting for 85% of these fatalities. In the United States alone, heart disease led to the deaths of around 695,000 individuals in 2021, representing roughly one in every five deaths (Tsao et al., 2023). Furthermore, an estimated seven million individuals in the United Kingdom are currently living with cardiovascular diseases, which are recognized as the leading cause of mortality in the country. Key contributing factors to the development of cardiovascular disease include: hypertension, smoking, elevated cholesterol levels, diabetes, and obesity (Robinson, 2021).

WHO Organization (2000), defines obesity as an abnormal or excessive accumulation of adipose tissue to an extent that may negatively impact health. Since the 1980s, the prevalence of obesity has risen significantly across most countries and is now regarded as a global pandemic, responsible for over 2.8 million deaths annually (Boutari and Mantzoros, 2022). Obesity is a critical risk factor for cardiovascular disease and is closely associated with other risk factors, such as hypertension, hyperlipidaemia, insulin resistance and its closely-associated condition type 2 diabetes (T2D) (Powell-Wiley, Poirier et al. 2021).

1.2 Cardiovascular system anatomy

The cardiovascular system, also known as the circulatory system, is responsible for transporting oxygenated blood from the lungs, hormones from endocrine glands, nutrients from the digestive system, and metabolic waste products from cells to various body systems. Additionally, it plays a crucial role in regulating body temperature. The circulatory system comprises three main components: the heart, blood, and blood vessels, the latter of which includes arteries, veins, arterioles, and capillaries. The heart, a muscular organ located in the chest cavity, is essential for ensuring an adequate supply of oxygenated blood to end organs

and tissues through the vascular network. Blood vessels facilitate the transport of oxygen-rich blood and essential nutrients from the heart to the rest of the body via the systemic circulation, before returning deoxygenated blood back to the heart, where it is then directed to the lungs through the pulmonary circulation for reoxygenation (Matienzo and Bordoni 2020).

The walls of blood vessels are composed of three distinct layers: the tunica intima, tunica media, and tunica adventitia. The tunica intima, the innermost layer, is comprised of a single layer of endothelial cells (ECs), which provide a smooth surface, enhancing blood flow, supported by an elastic lamina. Surrounding this layer, the tunica media, or middle layer, consists primarily of vascular smooth muscle cells (VSMCs) and elastic fibres, which play a vital part in the regulation of vascular tone and blood pressure. The outermost layer, the tunica adventitia (or tunica externa), is composed of two sub-layers: the adventitia compacta, a layer containing collagen fibres and fibroblast cells, and the perivascular adipose tissue (PVAT), which is found surrounding most blood vessels. All of these support the structural integrity and functionality of the blood vessels (Daly, 2019) (Figure 1-1).

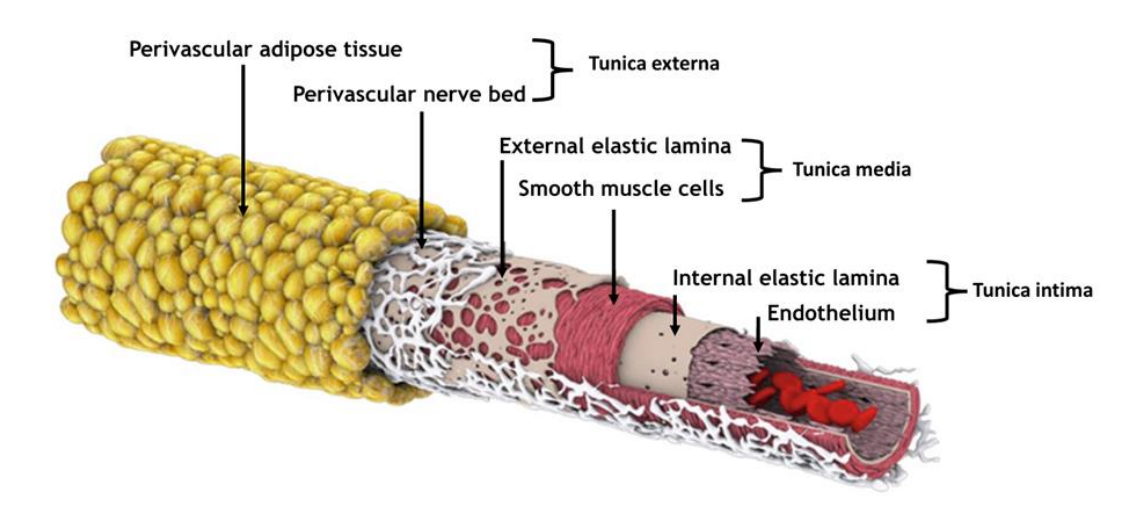


Figure 1-1: The structure of the vascular wall

This figure shows the three distinct layers: the tunica intima, tunica media, and tunica adventitia (tunica externa) (Daly, 2019).

1.2.1 Endothelium layer

The endothelium is a single layer of cells that lines the interior surface of blood vessels, serving as a critical interface between the vascular wall and circulating blood. This endothelial layer performs numerous essential functions that contribute to overall cardiovascular health and the maintenance of vascular homeostasis. Endothelial cells play a fundamental role in several physiological processes, including: acting as a structural barrier between blood vessels and surrounding tissues; mediating inflammatory and immune responses; regulating blood clotting and anticoagulation; facilitating metabolic activities; promoting angiogenesis; and controlling vascular tone (Krüger-Genge, Blocki et al. 2019). Additionally, the endothelium synthesizes and releases various bioactive molecules, such as nitric oxide (NO), which exerts vasodilatory effects that are crucial for regulating blood flow and blood pressure, thereby ensuring proper perfusion of organs and tissues (Deanfield, Halcox and Rabelink 2007). Endothelial cells also produce endothelin, a peptide which assists in the regulation of blood pressure and flow by causing blood vessels to constrict.

1.2.2 Vascular smooth muscle layer

Vascular smooth muscle cells (VSMCs) are essential components of the blood vessel wall and play a crucial role in regulating vascular tone, vessel diameter, and overall haemodynamic stability. By mediating contraction and relaxation, VSMCs directly influence blood flow and blood pressure. These cells respond to various physiological stimuli, including hormones such as angiotensin II, and neurotransmitters like noradrenaline, by actively contracting. This vasoconstriction leads to a reduction in vessel diameter, thereby increasing blood pressure and vascular resistance. Conversely, VSMCs relax in response to vasodilatory signals, such as NO released by endothelial cells, which diffuses into VSMCs and stimulates the production of cyclic guanosine monophosphate (cGMP), ultimately promoting muscle relaxation (Wilson, 2011, Walford and Loscalzo, 2003).

In addition to their role in vascular tone regulation, VSMCs contribute to vascular homeostasis by prompting the vascular wall to contract, thereby regulating the size of the blood vessels. Intracellular calcium levels, which are crucial for smooth

muscle contraction, are regulated through voltage-gated calcium channels. The opening of these channels facilitates calcium ion (Ca²⁺) influx, triggering contraction, whereas the activation of potassium (K⁺) channels leads to K⁺ efflux, hyperpolarizing the cell membrane and subsequently closing calcium channels. This reduction in intracellular calcium concentration results in smooth muscle relaxation.

VSMCs also have a significant part to play in vascular repair and adaptation under pathological conditions such as chronically raised blood pressure. In response to vascular injury, they exhibit phenotypic plasticity, transitioning from a contractile phenotype to a proliferative and migratory state, as well as adopting a myofibroblast-like phenotype to aid in tissue remodelling and repair (Chen et al., 2023b).

1.2.3 Adventitia and Perivascular adipose tissue

Perivascular adipose tissue forms the outer connective tissue layer that envelops most blood vessels. Its function is analogous to that of the serosa, which serves as a protective tissue layer surrounding many body organs. A detailed examination of the structure and function of PVAT will be provided in Section 1.4.

1.3 Adipose tissue

Adipose tissue (AT) primarily consists of adipocytes, alongside various other cell types such as endothelial cells, fibroblasts, pericytes, preadipocytes, and multiple immune cell types, such as macrophages, T cells, B cells, mast cells, and others. These non-adipocyte cellular components collectively form the stromal vascular fraction (SVF) of AT (Richard et al., 2020). AT plays a crucial role in endocrine signalling by secreting a diverse range of bioactive molecules, known as adipocytokines. These adipocytokines act as circulating hormones that facilitate inter-organ communication and contribute to the regulation of key physiological processes, including energy homeostasis, lipid and glucose metabolism, reproductive function, and immune response (CoelhoOliveira and Fernandes, 2013, Koenen et al., 2021). Adipose tissue has three main types: white adipose tissue (WAT), brown adipose tissue (BAT), and beige (brite) adipose tissue, each with distinct functions, phenotypes, and anatomical distributions (Li *et al.*, 2022;

Stanek *et al.*, 2021). BAT is primarily involved in non-shivering thermogenesis, generating heat through mitochondrial uncoupling protein 1 (UCP-1), which is essential for maintaining body temperature (Koenen et al., 2021). WAT, on the other hand, serves as the main site for energy storage, endocrine signalling, and insulin sensitivity, making up the largest proportion of AT in mammals, including humans (Koenen et al., 2021). Beige AT, interspersed within WAT, exhibits thermogenic properties similar to BAT but at a lower capacity (Richard et al., 2020; Li et al., 2022).

AT is further categorized into visceral and subcutaneous depots. Visceral AT, which surrounds internal organs, is highly metabolically active and linked to metabolic diseases, whereas subcutaneous AT acts as a buffering system for excess nutrient storage (LeeDesprés and Koh, 2013). Historically, AT was considered a passive energy reservoir; however, recent studies have established its role as a major endocrine organ, secreting adipokines, cytokines, and chemokines that influence systemic metabolism and organ functions (Qi et al., 2018).

In obesity, WAT undergoes pathological expansion, predominantly through adipocyte hypertrophy, which can lead to local hypoxia and increased infiltration of immune cells. This dysfunctional state promotes the secretion of proinflammatory cytokines including IL-6, TNF- α , and MCP-1. For example, TNF- α has been shown to decrease eNOS expression/activity by approximately ~50%, thereby impairing endothelial function (Kwaifa et al., 2020; Dschietzig et al., 2012). These inflammatory mediators contribute to insulin resistance, cardiovascular diseases (CVDs), and metabolic syndrome (Koenen et al., 2021). Dysfunctional WAT also promotes endothelial dysfunction and atherosclerosis by impairing vascular homeostasis (Kwaifa et al., 2020). Visceral WAT, which may account for up to 10% of total body fat mass, contributes disproportionately to circulating free fatty acids, further driving metabolic and vascular dysfunction (van Dam et al., 2017). For instance, in obesity, WAT can become inflamed and release excessive proinflammatory cytokines like TNF- α , which inhibits eNOS, the enzyme responsible for NO production in blood vessels. Consequently, NO levels are reduced, leading to endothelial dysfunction and impaired vasodilation. In contrast, BAT helps regulate lipid metabolism by taking up and oxidizing lipids for heat production. Cold exposure for 24 h reduces plasma triglyceride (TG) concentrations by 43%,

while BAT uptake of TG-derived activity increases by 139-150% and retention rises by 168-464% compared with controls (Khedoe et al., 2015). Similarly, BAT activation lowers plasma triglycerides by about 54% and total cholesterol by 25%, resulting in a 43% reduction in atherosclerotic lesion area in APOE*3-Leiden.CETP mice (Berbée et al., 2015).

The distribution of WAT and BAT varies, based on genetics, age, sex, and environmental factors such as diet, exercise, and temperature. In humans, subcutaneous WAT accounts for up to 80% of body fat, while intra-abdominal WAT represents 10-20% in men and 5-8% in women (Ibrahim, 2010, Berryman and List, 2017). In mice, BAT is most prominent in the interscapular region and is commonly used as a model for BAT studies (Lidell et al., 2013).

1.4 Perivascular adipose tissue (PVAT)

Perivascular adipose tissue is a specialized form of adipose tissue that encases the majority of systemic blood vessels, including the aorta and major arteries such as the carotid, coronary, and mesenteric vessels (Kim et al., 2020). PVAT is increasingly recognized as an integral component of the vascular wall, actively contributing to vascular homeostasis through the secretion of adipokines and other bioactive molecules (Szasz and Webb, 2012). These include adiponectin, leptin, cytokines, reactive oxygen species (such as superoxide and hydrogen peroxide (H₂O₂), as well as hydrogen sulphide (H₂S) and nitric oxide, which are key signalling molecules involved in various physiological and metabolic processes (Almabrouk *et al.*, 2017). Nitric oxide is among several vasoactive substances secreted by PVAT to regulate vascular function through both endothelium-dependent and endothelium-independent mechanisms.

The released NO can diffuse into the endothelium and influence vascular tone, an important interaction in the maintenance of vascular homeostasis. NO from PVAT is able to improve endothelial function as it promotes vasodilation and reduces oxidative stress. However, in pathological conditions such as obesity or inflammation, PVAT's ability to produce NO may be impaired, contributing to endothelial dysfunction (Lynch et al., 2013, Greenstein et al., 2009, Xia et al., 2016, Hwej et al., 2024). This highlights the critical role of NO in promoting the

vasorelaxant effects associated with PVAT. The synthesis of NO is facilitated by three distinct isoforms of nitric oxide synthase (NOS): endothelial NOS (eNOS) and neuronal NOS (nNOS), both of which are calcium-dependent, as well as inducible NOS (iNOS), which typically operates independently of calcium signalling (Förstermann and Sessa, 2012).

Previous research has highlighted the role of PVAT in modulating vascular function, particularly in attenuating vascular contraction across various vascular beds, including coronary vessels (Aghamohammadzadeh et al., 2013) and rat mesenteric arteries (Verlohren *et al.*, 2004). The composition of PVAT varies depending on the anatomical location, consisting of white adipocytes, brown adipocytes, or a combination of both (Gao *et al.*, 2007; Cinti, 2011; Fitzgibbons *et al.*, 2011).

The regulatory function of PVAT in vascular tone is significantly compromised under pathological conditions such as obesity and atherosclerosis, leading to vascular dysfunction (Szasz and Webb 2012; Chang *et al.*, 2020). Alterations in the secretory profile of PVAT have been observed in hypertension, obesity, and other cardiovascular diseases, disrupting the balance between its anti-contractile and pro-contractile effects, which further contributes to vascular impairment (RamirezO'Malley and Ho, 2017).

Additionally, PVAT exhibits considerable heterogeneity, even within the same blood vessel. In rats, PVAT surrounding the abdominal aorta primarily resembles white adipose tissue, with larger adipocytes and markedly lower expression of thermogenic genes, whereas PVAT around the thoracic aorta displays a brown adipose-like phenotype characterized by ~3-fold higher UCP-1 expression and increased mitochondrial content (Padilla et al., 2013). Similar regional differences have been noted in rodents more broadly, with thoracic PVAT exhibiting BAT-like features and abdominal PVAT more WAT-like, suggesting region-specific functional roles in vascular homeostasis (Brown et al., 2014).

1.4.1 Role of PVAT in vascular tone regulation

Historically, PVAT was primarily regarded as a structural component that provided mechanical support to blood vessels and protected them from adjacent tissues. Consequently, it was frequently removed in vascular research due to concerns that it might impede the diffusion of exogenous substances. As a result, its functional significance remained largely overlooked for many years. However, emerging clinical and experimental evidence has established that PVAT plays a crucial role in maintaining vascular homeostasis through paracrine interactions with blood vessels (Lian and Gollasch, 2016; Chang *et al.*, 2020). Through engagement with vascular smooth muscle cells and endothelial cells, PVAT secretes a diverse array of vasoactive molecules that regulate vascular tone by modulating vasodilation and vasoconstriction (Kim et al., 2020).

The paracrine influence of PVAT was first documented in 1991, when Soltis and Cassis reported that PVAT-intact rat aortic rings exhibited a diminished contractile response to norepinephrine. This effect was attributed to norepinephrine uptake by PVAT, which is characterized by a dense sympathetic innervation (Soltis and Cassis, 1991). Subsequent research by Löhn et al. (2002) further demonstrated that PVAT attenuates vasoconstriction induced by angiotensin II, serotonin, and phenylephrine. Their findings indicated that this anticontractile effect is mediated through the activation of potassium channels and tyrosine kinase in VSMCs, rather than through nitric oxide-dependent pathways. This led to the identification of PVAT-derived relaxing factors (PVRFs), which include adiponectin, leptin, omentin, NO, angiotensin 1-7, hydrogen sulphide, hydrogen peroxide, prostacyclin, and methyl palmitate (Fésüs *et al.*, 2007; Lee *et al.*, 2009; Victorio *et al.*, 2016).

Conversely, PVAT also secretes perivascular adipose tissue-derived contracting factors (PVCFs), such as superoxide anion, tumour necrosis factor- α , prostaglandins, catecholamines, chemerin, and thromboxane A2 (Gao *et al.*, 2006; Mendizábal *et al.*, 2013; Meyer *et al.*, 2013). Certain mediators, including hydrogen peroxide, leptin, hydrogen sulphide, and prostanoids, exhibit dual vasorelaxant and vasoconstrictive properties, with their effects being influenced by variables such as concentration, vascular region, contractile state, pathological

conditions, and species-specific factors (Hayabuchi *et al.*, 1998; Gao and Lee, 2001; Cacanyiova *et al.*, 2019).

Overall, the current body of literature suggests that healthy PVAT predominantly exerts an anticontractile influence on vascular function. However, the ultimate regulatory outcome is determined by the balance between its vasodilatory and vasoconstrictive factors, highlighting its complex and dynamic role in vascular physiology (Meyer *et al.*, 2013).

1.4.2 Mechanisms underlying the anti-contractile effect of PVAT

The paracrine vasorelaxant effects of perivascular adipose tissue (PVAT)-derived relaxing factors have been extensively studied. However, understanding of the precise mechanisms underlying their influence on vascular function remains incomplete (Agabiti-Rosei *et al.*, 2018) although it is widely accepted that PVAT regulates vascular tone through two primary pathways: endothelium-dependent and endothelium-independent.

1.4.2.1 Endothelium dependent mechanisms

The vascular endothelium plays a fundamental role in modulating vascular tone by releasing vasoactive factors, including vasodilators such as NO, prostacyclin (PGI₂), and endothelium-derived hyperpolarizing factor (EDHF), as well as vasoconstrictors such as thromboxane A₂ (TXA₂) and endothelin-1 (ET-1) (Khaddaj Mallat *et al.*, 2017; Shimokawa and Godo, 2020). NO, one of the most potent endothelium-derived vasodilators, activates soluble guanylate cyclase (sGC) in vascular smooth muscle cells, leading to increased cyclic GMP levels and activation of intracellular signalling pathways that induce vascular relaxation (Kim et al., 2020). The production of NO is mediated by endothelial nitric oxide synthase.

PVAT's anticontractile effects may be attributed to its ability to release NO or other PVRFs, such as adiponectin, leptin, and angiotensin-(1-7). These mediators contribute to both endothelium-dependent and endothelium-independent vasorelaxation, thereby playing a critical role in the regulation of vascular tone (Gao *et al.*, 2007; Lee *et al.*, 2009; Gálvez-Prieto *et al.*, 2012; Lynch *et al.*, 2013; Victorio *et al.*, 2016; Sena *et al.*, 2017). The PVRFs could potentially diffuse through the adventitia, media and internal elastic lamina through various

mechanisms, such as paracrine signalling, matrix remodelling, cell migration, or possibly vasa vasorum pathways.

Additionally, PVRFs may indirectly induce VSMC relaxation by stimulating endothelial NO production, leading to the activation of ATP-sensitive and voltage-gated potassium (K⁺) channels in a calcium-dependent manner (Dubrovska *et al.*, 2004; Lee *et al.*, 2009). This interplay between PVAT-derived factors and endothelial signalling pathways highlights the complexity of PVAT-mediated vascular regulation.

1.4.2.2 Endothelium-Independent Mechanisms

PVAT also exerts direct effects on VSMCs, as evidenced by its ability to induce vasorelaxation in endothelium-denuded blood vessels. Studies indicate that PVAT from different vascular regions, such as the thoracic aorta, abdominal aorta, and mesenteric artery, modulates vascular tone through activation of specific potassium channels in VSMCs. However, the precise K⁺ channel subtypes involved differ, according to vessel type and species.

Löhn et al. (2002) demonstrated that in the thoracic aorta of Sprague-Dawley rats, PVAT-induced vasorelaxation in response to serotonin is mediated by ATP-sensitive K^+ (K_{ATP}) channels and tyrosine kinase activation in a calcium-dependent, endothelium-independent manner. In contrast, subsequent research by Gao et al. (2007) in the thoracic aorta of Wistar rats found that PVAT-mediated relaxation is primarily facilitated by calcium-activated K^+ (K_{Ca}) channels rather than K_{ATP} or delayed rectifier K^+ (K_V) channels. Their findings further suggest that PVAT-derived relaxation involves H_2O_2 -induced activation of sGC, leading to smooth muscle relaxation.

Further studies have identified variations in the types of K⁺ channels responsible for PVAT-mediated vasorelaxation across different vascular beds and species. For instance, delayed rectifier K⁺ (K_V) channels contribute to PVAT-induced relaxation in the mesenteric arteries of Sprague-Dawley rats (Verlohren *et al.*, 2004; Fésüs *et al.*, 2007), whereas voltage-dependent K⁺ channels mediate this effect in the thoracic aorta of Wistar Kyoto rats (Lee et al., 2011). Additionally, K_{Ca} channels have been implicated in PVAT-induced relaxation in human internal thoracic

arteries (Gao et al., 2005). In mouse mesenteric arteries, adiponectin-induced vasorelaxation has been linked to the activation of delayed rectifier K^+ (K_r) and large-conductance calcium-activated K^+ (BK_{Ca}) channels (Fésüs et al., 2007; Lynch et al., 2013). The variability in K^+ channel activation suggests that the regulatory mechanisms of PVAT-derived relaxation are highly context-dependent, influenced by vascular bed-specific characteristics and interspecies differences.

1.5 Sphingolipid System

Sphingolipids represent a very important group of cellular lipids that are increasingly recognized for their role in metabolic disorders, including obesity and type 2 diabetes (T2D). These lipids influence various physiological processes through their bioactive metabolites, such as ceramide, sphingosine, sphingomyelin, and sphingosine-1-phosphate (S1P). Among these, ceramide and S1P have been identified as key regulators of inflammatory pathways within adipose tissue. Their involvement in adipose inflammation is mediated through the stimulation of adipocytes and immune cells, leading to the secretion of proinflammatory cytokines and chemokines. This inflammatory response has been associated with the progression of metabolic syndromes, further underscoring the significance of sphingolipids in metabolic dysfunction (FangPyne and Pyne, 2019, Kang et al., 2013).

1.5.1 Sphingosine 1 Phosphate overview

Sphingosine-1-phosphate is a biologically active metabolite derived from sphingosine, first identified in 1990 as a key regulator of cell growth (Olivera and Spiegel, 1993). This lipid signalling molecule is synthesized by a variety of cell types, including erythrocytes, platelets, endothelial cells, and adipocytes (Ito et al., 2013, Thuy et al., 2014, MendelsonEvans and Hla, 2014). Functioning as a crucial mediator in multiple cellular processes, S1P is integral to both normal physiological functions and pathological conditions. Its involvement in cardiovascular health is considerable, as it influences vascular integrity, immune cell trafficking, and inflammatory responses (Thuy et al., 2014).

1.5.1.1 Sphingosine-1-phosphate synthesis and degradation

The formation of S1P is a complex multi-step process that begins with the production of ceramide, a key intermediate in sphingolipid metabolism. Ceramide synthesis occurs through three distinct pathways (Figure 1-2): de novo biosynthesis, sphingomyelin metabolism, and direct conversion from sphingosine via ceramide synthase (CerS). The de novo pathway begins in the endoplasmic reticulum, where serine and palmitoyl-CoA undergo condensation through the enzyme serine palmitoyltransferase (SPT), leading to the formation of 3ketodihydrosphingosine. This intermediate is then reduced by 3ketodihydrosphingosine reductase (3KDHR) to produce dihydrosphingosine, which is subsequently acetylated by ceramide synthases (CerS) to generate dihydroceramide. The final step in ceramide synthesis involves dihydroceramide desaturase (DES), which introduces a double bond to form ceramide (Pulkoski-GrossDonaldson and Obeid, 2015, Pyne and Pyne, 2000). Once formed, ceramide can be further metabolized into sphingosine through the catalytic activity of ceramidase. Sphingosine is then phosphorylated, or subjected to enzymatic conversion, by sphingosine kinase, resulting in the formation of S1P (MendelsonEvans and Hla, 2014, Gandy and Obeid, 2013). The degradation of S1P is mediated by two distinct pathways: it can either be metabolised and irreversibly split by S1P lyase (S1PL) into phosphoethanolamine and hexadecanal, ensuring sphingolipid balance and cellular signalling regulation, or it can be recycled back into sphingosine through dephosphorylation by S1P phosphatases (S1PP) (Pulkoski-GrossDonaldson and Obeid, 2015, Pyne and Pyne, 2000). Beyond its metabolic transformations, S1P plays a crucial role as a bioactive lipid mediator. It functions both extracellularly, through interactions with S1P receptors, and intracellularly, where it acts as a second messenger regulating various signalling pathways within cellular compartments (Spiegel and Milstien, 2003).

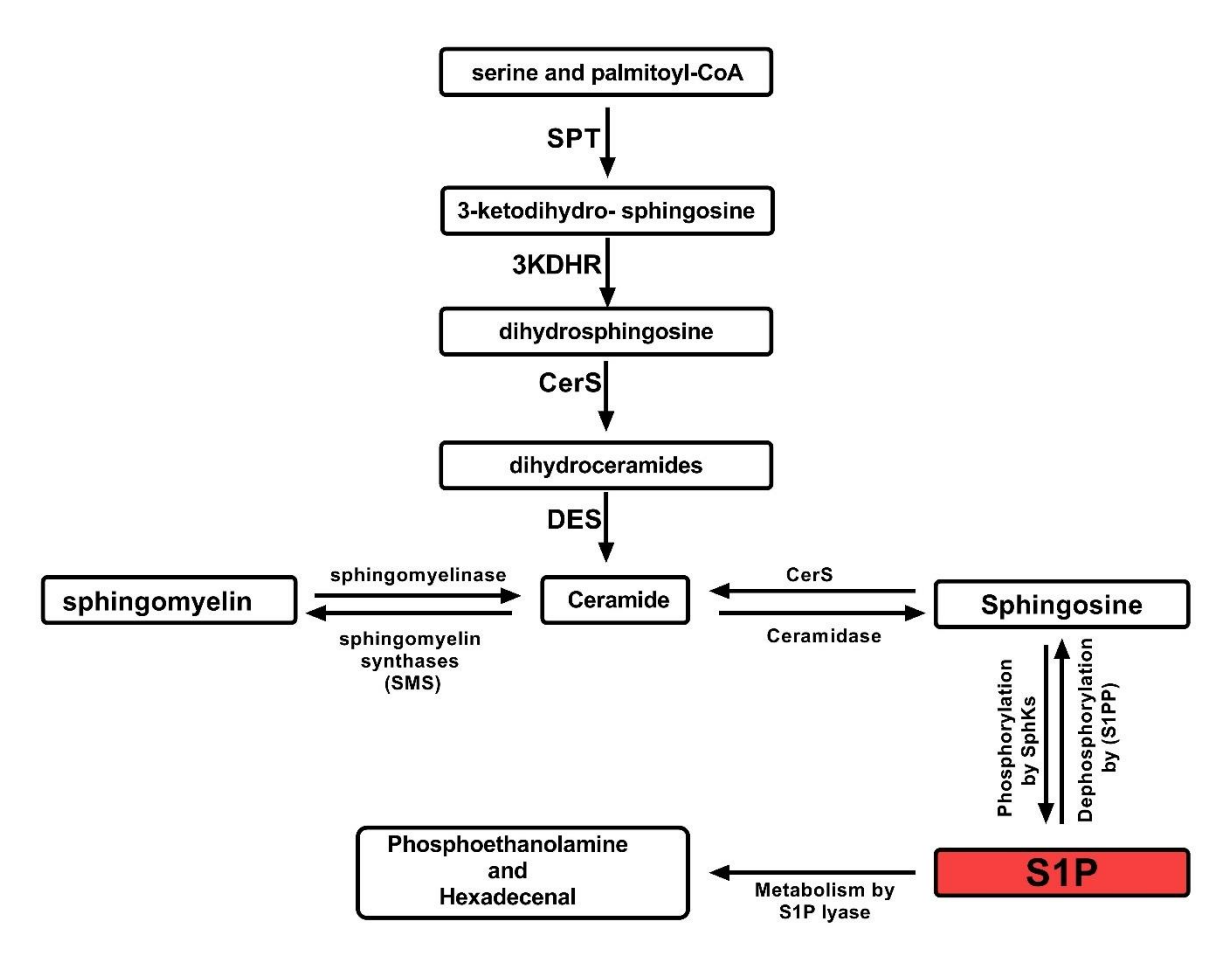


Figure 1-2: Overview of Sphingosine-1-Phosphate (S1P) synthesis and metabolism.

Ceramide can be generated through three primary pathways: (1) hydrolysis of sphingomyelin by the enzyme sphingomyelinase; (2) the de novo biosynthetic pathway, which begins with palmitoyl-CoA and serine and proceeds through a series of enzymatic reactions involving serine palmitoyltransferase (SPT), 3-ketodihydrosphingosine reductase (3-KDHR), ceramide synthases (CerS), and dihydroceramide desaturase (DES); and (3) the salvage pathway, in which sphingosine is reconverted to ceramide by ceramide synthases (CerS). Sphingosine can also be phosphorylated by sphingosine kinase to form sphingosine-1-phosphate (S1P), a bioactive lipid mediator. S1P is further degraded by sphingosine-1-phosphate lyase (S1PL) into phosphoethanolamine and hexadecanal, completing its catabolic pathway.

1.5.1.2 Sphingosine-1 phosphate transporter

S1P is actively transported across cell membranes by specific transporter proteins that play essential roles in its physiological and pathological functions. Two major classes of S1P transporters have been identified: spinster homolog 2 (Spns2) and the ATP-binding cassette (ABC) transporters. Spns2, a member of the major facilitator superfamily (MFS), is a non-ATP-dependent transporter and the first identified S1P transporter in mammals (Chen et al., 2023a). It is primarily located in the plasma membrane and is responsible for the cellular export of S1P. Overexpression of Spns2 in various models, including zebrafish and mammalian cells, has been shown to enhance S1P secretion (Kawahara et al., 2009), while its deletion or downregulation markedly reduces extracellular S1P release and lowers

circulating S1P concentrations. For example, endothelial Spns2 deletion reduced plasma S1P to ~54% of control (0.39 \pm 0.03 μ M in controls vs 0.21 \pm 0.01 μ M in Spns2-/- mice; Fukuhara et al., 2012). Consistent with reduced extracellular S1P, plasma from Spns2-deficient mice induces less S1PR1 internalization in a GFPtagged S1PR1 reporter assay, indicating diminished receptor engagement (Nijnik et al., 2012). In parallel, ABC transporters, such as ABCA1 and ABCC1, have also been implicated in S1P export in various cell types including astrocytes (Sato et al., 2007), mast cells (Mitra et al., 2006), and adipocytes (Theodoulou and Kerr, 2015). Inhibition or silencing of these transporters results in a reduction of extracellular S1P, although some studies have shown inconsistent effects following their overexpression or knockout, indicating possible cell-type-specific roles or compensatory mechanisms (Hisano et al., 2011). Once secreted, S1P circulates in the bloodstream predominantly bound to carrier proteins, including high-density lipoprotein (HDL), low-density lipoprotein (LDL), very-low-density lipoprotein (VLDL), and albumin. Approximately 50% of plasma S1P is associated with HDL, particularly via binding to apolipoprotein M (ApoM), which serves as a chaperone, stabilising S1P and regulating its bioavailability (JozefczukGuzik and Siedlinski, 2020). This transport system ensures tight control over extracellular S1P levels, which is crucial for maintaining vascular homeostasis and immune cell trafficking.

1.5.1.3 Sphingosine-1 phosphate receptors

Sphingosine-1-phosphate receptors belong to the G-protein-coupled receptor (GPCR) family and include five subtypes: S1PR1, S1PR2, S1PR3, S1PR4, and S1PR5, each composed of approximately 400 amino acids (O'Sullivan and Dev, 2013). These receptors share a conserved structural framework characterized by seven transmembrane α-helices spanning the lipid bilayer, creating a polar internal tunnel. The N-terminal region and three extracellular loops extend outward, while the C-terminal region and three intracellular loops are oriented towards the cytoplasm (Pulkoski-GrossDonaldson and Obeid, 2015, Spiegel and Milstien, 2003). The expression of S1P receptors varies across different tissues. S1PR1, S1PR2, and S1PR3 are predominantly found in the cardiovascular system, exhibiting distinct distribution patterns among major cardiovascular cell types and adipose cells (Cannavo et al, 2017). In contrast, S1PR4 is primarily expressed in lymphoid tissues, while S1PR5 is predominantly expressed in the central nervous system,

particularly in oligodendrocytes, but has also been detected in peripheral tissues. Upon S1P binding, these receptors initiate intracellular signalling by activating specific G-protein subunits, including Gi, Gq, and G12/13, which regulate diverse downstream signalling pathways (O'Sullivan and Dev, 2013, LiXu and Testai, 2016, Spiegel and Milstien, 2003, Jun et al., 2006, Mastrandrea, 2013). Each receptor subtype is linked to distinct G-protein interactions, leading to unique functional outcomes in different physiological contexts (Figure 1-3).

S1PR₁

Identified in 1990 in human umbilical vein endothelial cells (HUVECs (O'Sullivan and Dev, 2013)), S1PR1 was the first member of the EDG family of GPCRs to be characterized (Hla and Maciag, 1990, YohNoriko and Naotoshi, 2002). It is broadly expressed across various cell types, including endothelial cells, vascular smooth muscle cells, fibroblasts, epithelial cells, and adipocytes (Goetzl et al., 2004, Karuppuchamy et al., 2017, Mastrandrea, 2013). S1PR1 receptor signalling is primarily mediated through its interaction with Gi proteins (Gonda et al., 1999, Okamoto et al., 1998, YohNoriko and Naotoshi, 2002). Upon activation, S1PR1 triggers a range of intracellular responses, including the inhibition of adenylyl cyclase, activation of phospholipase C (PLC), and mobilization of intracellular Ca²⁺ (Okamoto et al., 1998, Kluk and Hla, 2002). Additionally, S1PR1 signalling engages key pathways such as Ras-ERK and phosphatidylinositol 3-kinase (PI3K), which are critical for regulating various cellular processes (O'Sullivan and Dev, 2013).

S1PR₂

Initially identified in a rat aortic cDNA library, S1PR2 was discovered during research on vascular signalling pathways (Okazaki et al., 1993, YohNoriko and Naotoshi, 2002). S1P has been reported to have a high affinity for S1PR₂ (Gonda et al., 1999). This receptor is widely distributed across various tissues, including the lung, heart, brain, kidney, spleen, adrenal glands, and adipose tissue (Ishii et al., 2001, Mastrandrea, 2013).

S1PR₃

Originally discovered in a human genomic library during studies on cannabinoid receptors, S1PR3 shares approximately 50% sequence similarity with S1PR1 and S1PR2. It is widely distributed across various tissues and organs, including the lung, heart, stomach, brain, thymus, kidney, adrenal glands, spleen, and adipose tissue (Kluk and Hla, 2002). Additionally, S1PR3 signalling is associated with the activation of Ras and extracellular signal-regulated kinases (ERK), highlighting its role in regulating various cellular functions such as cell proliferation, migration, inflammation, and vascular tone (Sanchez and Hla, 2004).

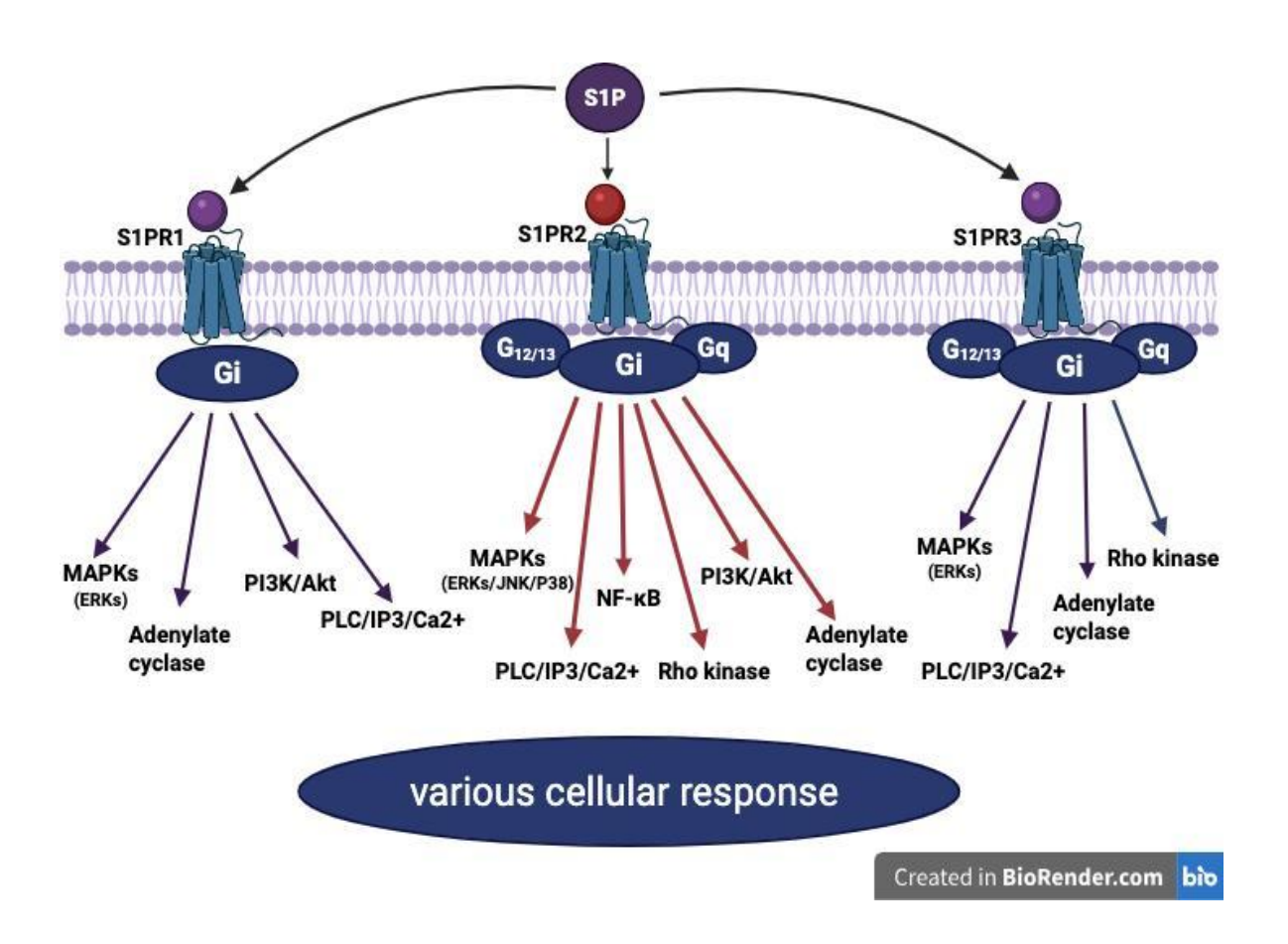


Figure 1-3 The S1P-S1PRs signalling pathways.

This figure depicts the signalling cascades initiated by sphingosine-1-phosphate receptors (S1PRs), specifically S1PR1, S1PR2, and S1PR3. Each receptor engages distinct intracellular pathways, modulating a wide range of cellular responses and physiological processes. Abbreviations: Sphingosine 1 Phosphate (S1P), Sphingosine 1 Phosphate receptor (S1PR), Mitogen-Activated Protein Kinases (MAPKs), Nuclear factor-KB (NF-KB), Phosphoinositide 3-kinase/ protein kinase B (PI3K)/Akt, Phospholipase C (PLC), inositol trisphosphate (IP3).

1.5.1.4 Sphingosine 1 Phosphate agonists and antagonists

S1P receptors exhibit specificity for their natural ligands, S1P and dihydro-S1P (ContosIshii and Chun, 2000). In addition to these endogenous ligands, several synthetic small-molecule agonists have been developed for experimental research. Among these, SEW2871 selectively targets S1PR1 (Sanna et al., 2004), CYM5478 acts as a potent and selective S1PR2 agonist (Herr et al., 2016), and CYM5541 is designed specifically for S1PR3 activation (Jo et al., 2012).

Selective antagonists have also been identified for blocking S1P receptor activity. S1PR1 is inhibited by W146 (Sanna et al., 2006), while JTE-013 serves as a highly selective antagonist for S1PR2 (Salomone and Waeber, 2011, Pitman et al., 2022). The activity of S1PR3 can be suppressed using BML-241 (CAY10444) (Salomone and Waeber, 2011) (Table 1-1).

Table 1-1 Agonists and antagonists of the sphingosine-1-phosphate receptors and their activity across S1PR1–S1PR5

Role	S1PR1	S1PR2	S1PR3	S1PR4	S1PR5
S1PR1-	EC ₅₀ ≈ 20.7 nM	No activation	No activation	No activation	No activation
selective		≤ 10 µM	≤ 10 µM	≤ 10 µM	≤ 10 µM
agonist					
S1PR2-	≤25% efficacy;	EC ₅₀ ≈ 119 nM		≤25% efficacy;	≤25% efficacy;
selective	≥10× weaker vs		≥10× weaker	≥10× weaker	≥10× weaker
agonist	S1PR2				
S1PR3-	No activation	No activation	EC ₅₀ ≈ 72-132	No activation	No activation
selective	up to >10 μM	up to >50 μM	nM	up to >50 μM	up to >25 μM
agonist					
S1PR1-	K _i ≈ 77 nM	No effect ≤ 10	No effect ≤ 10	Not reported	No effect ≤ 10
selective		μΜ	μΜ		μΜ
antagonist					
S1PR2-	No antagonism	IC ₅₀ = 17 ± 6	No antagonism	IC50 ≈ 237 nM	Not reported
selective	≤10 µM	nM	≤10 µM		
antagonist					
S1PR3-	No antagonism	No antagonism	IC50 ≈ 4.6 µM	No antagonism	No antagonism
selective	≤10 µM	≤10 µM		≤10 µM	≤10 µM
antagonist					
	S1PR1- selective agonist S1PR2- selective agonist S1PR3- selective agonist S1PR1- selective antagonist S1PR2- selective antagonist S1PR2- selective antagonist	S1PR1- selective agonist S1PR2- selective agonist S1PR2- selective agonist S1PR3- selective agonist S1PR1- selective antagonist S1PR2- S1PR2- S1PR2- No activation up to >10 μM S1PR1- selective antagonist S1PR2- selective antagonist S1PR3- selective antagonist S1PR3- selective antagonist S1PR3- selective antagonist S1PR3- selective antagonism ≤10 μM	S1PR1- selective agonist S1PR2- selective agonist S1PR2- selective ≥10× weaker vs agonist S1PR3- selective agonist S1PR1- selective antagonist S1PR1- selective antagonist S1PR2- S1PR2- S1PR3- No activation up to >10 μM up to >50 μM No effect ≤ 10 μM S1PR2- selective antagonist S1PR2- selective antagonist S1PR3- selective ≤10 μM S1PR3- selective ≤10 μM No antagonism ≤10 μM ≤10 μM	S1PR1- selective agonist $S1PR2$ - $S1PR2$ - $S1PR3$ - No activation $S1PR2$ - $S1PR3$ - No activation $S1PR3$ - No activation $S1PR3$ - Selective antagonist $S1PR3$ - No antagonism $S1PR3$ - $S1PR3$ - $S1PR3$ - No antagonism $S1PR3$ - $S1PR3$ - $S1PR3$ - $S1PR3$ - No antagonism $S1PR3$ - $S1PR3$ - No antagonism $S1PR3$ - $S1PR3$ - $S1PR3$ - No antagonism $S1PR3$ -	S1PR1- selective agonist S1PR2- selective agonist S1PR3- selective agonist S1PR1- selective agonist S1PR3- S1PR1- selective agonist S1PR3- S1PR1- selective antagonist S1PR2- S1PR1- selective antagonist S1PR2- S1PR3- S1PR1- selective antagonist S1PR2- S1PR3- S1PR3- No antagonism S1PR3- selective antagonist S1PR3- No antagonism S1PR3- S1PR3- No antagonism S1PR3- S1PR3- No antagonism S1PR3- S1PR3- No antagonism S1PR3- S1PR3- S1PR3- S1PR3- No antagonism S1PR3-

Fingolimod (FTY720) was the first S1P receptor modulator approved for clinical use in the treatment of multiple sclerosis (MS). As a prodrug, FTY720 undergoes phosphorylation, primarily by sphingosine kinase 2 (SphK2), to form phospho-

FTY720, which activates all S1P receptors except S1PR2. This activation leads to receptor internalization and degradation, thereby modulating immune responses (Brinkmann et al., 2010). Siponimod is a second-generation S1P receptor modulator with high selectivity for S1PR1 and S1PR5. Although it initially acts as an agonist at S1PR1, sustained receptor engagement leads to receptor internalisation and degradation, resulting in functional antagonism. This mechanism underlies its immunomodulatory effect and forms the basis for its FDA approval in 2019 for the treatment of multiple sclerosis (Coyle et al., 2024).

1.6 Sphingosine Kinases

Sphingosine kinase is a key enzyme responsible for the synthesis of sphingosine-1phosphate. Two isoforms, SphK1 and SphK2, have been identified, each encoded by distinct genes located on different chromosomes—SphK1 on chromosome 17 and SphK2 on chromosome 19 (Cannavo et al., 2017). Despite their structural similarities, an important distinction lies in the additional regions present in SphK2 at both the N-terminal and central regions, extending its amino acid sequence by approximately 250 residues (JozefczukGuzik and Siedlinski, 2020). Both isoforms contain a C-terminal region (CTR), an N-terminal region (NTR), an ATP-binding site, and a sphingosine recognition domain. Both SphK1 and SphK2 are expressed across the range of human tissues, but their expression levels vary. SphK1 is predominantly found in the heart, spleen, lungs, and leukocytes, whereas SphK2 is primarily expressed in the liver (Venkataraman et al., 2006). Three variants of SphK1 have been identified in humans: SphK1a and SphK1b (both 51 kDa) and SphK1c, which has a molecular weight between 42.5 kDa and 51 kDa. In contrast, SphK2 has two known isoforms, SphK2a and SphK2b. Additionally, several alternative splice variants of both SphK isoforms have been identified in rodents, differing mainly at the N-terminal region (Alemany et al., 2007). The subcellular localization of SphK isoforms also differs significantly. SphK1 is primarily found in the cytoplasm but can translocate to the plasma membrane upon activation. In contrast, SphK2 is mainly localized to the endoplasmic reticulum and has also been associated with mitochondrial compartments (Cannavo et al., 2017).

1.6.1 Regulation of Sphingosine kinase1 (SphK1)

The regulation of Sphingosine Kinase 1 occurs at multiple levels, including transcriptional, post-transcriptional, and post-translational modifications, influencing its expression, localization, and activity within cells (Figure 1-4).

1.6.1.1 Transcriptional Regulation

Several transcription factors control SphK1 gene expression. Specificity Protein 1 (Sp1) plays a critical role in the regulation of certain processes in cells, including growth, differentiation, apoptosis, immune response and others. It is crucial in upregulating SphK1 in response to nerve growth factor (NGF) in PC12 cells (Sobue et al., 2005). Activator Protein 1 (AP-1) regulates gene expression in response to various stimuli, such as cytokines, growth factors, stress, and infections, and plays a crucial role in cellular processes like differentiation, proliferation, and apoptosis. AP-1 mediates transcriptional activation in glioblastoma cells following IL-1B stimulation (Paugh et al., 2009). Additionally, Sp1 and AP-2 binding sites in the SphK1 promoter facilitate its upregulation in neuroblastoma cells upon exposure to glial-derived neurotrophic factor (Murakami et al., 2007). Transcription factors of the AP-2 family (AP- 2α to AP- 2ϵ) regulate gene expression in both developmental-stage and adult tissues and are implicated in metabolic disorders. In the context of obesity, where expanding adipose tissue often becomes hypoxic, transcriptional responses involving hypoxia-inducible factors (HIFs) and AP-2 may alter lipid signalling pathways. Specifically, HIF-2α has been shown to regulate SphK1 expression, with its knockdown reducing SphK1 levels in hypoxic glioma cells (Anelli et al., 2008). Other transcriptional regulators include LIM-domain-only protein 2 (LMO2) (Matrone et al., 2017) and E2F family members E2F1 and E2F7 (Hazar-Rethinam et al., 2015).

1.6.1.2 Post-Transcriptional Regulation

MicroRNAs (miRNAs) contribute to the negative regulation of SphK1 by either degrading its mRNA or inhibiting its translation (KimHan and Siomi, 2009). For instance, miR-124 enhances SphK1 mRNA degradation in ovarian cancer cells (Zhang et al., 2013), while miR-506 inhibits its translation in hepatocellular carcinoma (Lu et al., 2015). Recent studies have identified additional miRNAs,

such as miR-3677 in osteosarcoma (Yao et al., 2020) and miRNA-6862 in neural cells that downregulate SphK1 expression (Xue et al., 2021).

1.6.1.3 Post-Translational Regulation

and intracellular localisation are tightly regulated SphK1 activity phosphorylation and protein-protein interactions. Phosphorylation at Ser225 is a critical modification that promotes the translocation of SphK1 to the plasma membrane, positioning the enzyme near S1P transporters. This spatial arrangement facilitates the efficient synthesis and export of S1P, thereby enabling autocrine and paracrine activation of S1P receptors. Pro-inflammatory stimuli, including TNF-α, IL-1B, and LPS, have been shown to enhance SphK1 activity by promoting Ser225 phosphorylation and subsequent membrane translocation (Pitson et al., 2003, Billich et al., 2005, Lee et al., 2019). However, alternative pathways, independent of Ser225 phosphorylation, can also regulate SphK1, such as Gq-mediated translocation in response to muscarinic receptor activation and bradykinin signalling (ter Braak et al., 2009, Bruno et al., 2018). Additionally, CIB1, a calcium-binding protein, facilitates SphK1 membrane translocation to the plasma membrane in HeLa cells (Jarman et al., 2010).

1.6.1.4 Protein-Protein Interactions

SphK1 activity is further regulated by interactions with various proteins, which can either enhance or inhibit its functioning. Activation is promoted by binding to Src family protein tyrosine kinases (PTKs), δ -Catenin in hippocampal cells (Fujita et al., 2004). Moreover, Filamin A in melanoma cells (Maceyka et al., 2008), and TRAF2 in HEK293T cells (Xia et al., 2002). Conversely, inhibitory interactions have been reported with proteins such as SKIP (SphK1 Interacting Protein 1) in HEK cells (Lacaná et al., 2002), PECAM-1 in HEK293 cells (Fukuda et al., 2004), and FHL2 in cardiomyocytes (Sun et al., 2006).

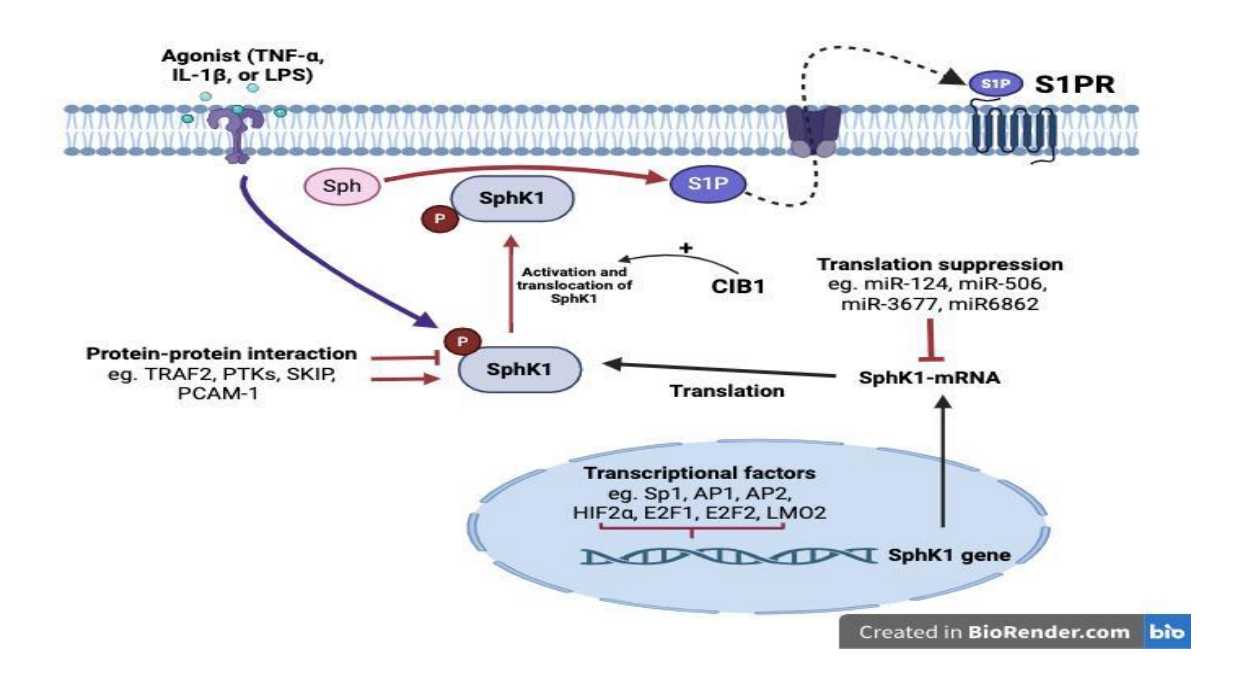


Figure 1-4 Schematic overview of the transcriptional, post-transcriptional, and post-translational regulation of SphK1.

SphK1 expression is regulated at multiple levels. Transcriptionally, factors such as Sp1, AP-1, AP-2, HIF-1 α , E2F1, E2F2, and LMO2 modulate its promoter activity. Post-transcriptionally, non-coding RNAs including miR-124, miR-506, miR-3677, and miR-6862 suppress its translation. Post-translationally, SphK1 is activated by phosphorylation in response to inflammatory stimuli like IL-1 β and TNF- α , and its membrane translocation is promoted by CIB1. At the plasma membrane, SphK1 converts sphingosine to S1P, which is exported to act on S1P receptors. Protein–protein interactions further fine-tune its enzymatic activity.

1.6.2 Regulation of Sphingosine kinase2 (SphK2)

Compared to SphK1, the regulation of SphK2 remains less extensively studied. However, similarly to SphK1, its enzymatic activity can be rapidly enhanced in response to various external stimuli. Pro-inflammatory cytokines such as TNF- α and IL-1B, as well as growth factors like EGF, have been shown to activate SphK2 (MastrandreaSessanna and Laychock, 2005). Given the structural similarities between SphK1 and SphK2, it is not surprising that both isoforms share common activation mechanisms. SphK2 activation is mediated through phosphorylation by ERK1/2, a mechanism also observed in SphK1. However, while SphK1 phosphorylation occurs at Ser225, SphK2 is phosphorylated at distinct sites, specifically Ser351 and Thr578, further highlighting differences in their regulatory control (Hait et al., 2007).

1.6.3 Sphingosine Kinases inhibitors

The search for effective inhibitors targeting SphK1 and SphK2 has been an area of significant research interest. Initial inhibitors, such as L-threodihydrosphingosine (DHS), N,N-dimethylsphingosine (DMS), and N,N,N-trimethylsphingosine (TMS), were among the first compounds identified. However, their broad activity profile led to off-target effects, as they also inhibited other kinases, including protein kinase C (PKC) and ceramide synthase (Pitman and Pitson, 2010). To enhance selectivity, a series of non-lipidic small molecules, including SKI-I, SKI-II, SKI-III, and SKI-IV, were synthesized. These compounds effectively lower S1P levels and are widely used as non-selective inhibitors of SphKs (French et al., 2003). Further progress in this field resulted in the development of selective SphK1 inhibitors such as PF543, VPC96091, SK1-I (BML258), and compound 82 (Bu et al., 2021). Among these, PF543 has emerged as the most extensively used SphK1 inhibitor, as it promotes SphK1 proteasomal degradation, leading to a reduction in S1P levels (Byun et al., 2013). Its role in modulating S1P concentrations has been validated in various cellular and animal models (Yi et al., 2023, Schnute et al., 2012). For SphK2 inhibition, several selective inhibitors have been identified, including (R)-FTY720-Ome (ROME), ABC294640, SG-12, K145, SKI-II, and trans-12a (Neubauer and Pitson, 2013). Among these, ROME functions as a competitive inhibitor with high specificity for SphK2, showing no inhibitory effect on SphK1, even at elevated concentrations (Lim et al., 2011). Studies have demonstrated that ROME effectively decreases both SphK2 expression and S1P levels in prostate cancer cells (Watson et al., 2013).

1.7 The role of Sphingosine Kinase/Sphingosine 1 Phosphate in vascular tone regulation

Vascular tone is dynamically regulated by various circulating mediators that induce either vasoconstriction or vasodilation. Among these, S1P has emerged as a critical endogenous modulator of vascular function. The effects of S1P on vascular tone are mediated through both endothelium-dependent and endothelium-independent mechanisms, involving distinct receptor subtypes and signalling pathways.

Endothelium-Dependent Regulation

S1P plays a vital role in maintaining vascular homeostasis by enhancing endothelial barrier integrity and promoting vasodilation, primarily via S1PR1 activation; it binds to S1PR1, which is primarily responsible for barrier enhancement, and the interaction stabilizes endothelial junctions and reduces vascular leakage. Experimental studies have demonstrated that S1P stimulates endothelial nitric oxide synthase activation through signalling cascades involving calcium-sensitive and PI3K/Akt pathways. The engagement of S1PR1 and S1PR3 on endothelial cells leads to eNOS phosphorylation and subsequent nitric oxide production, a key mediator of vasorelaxation. This effect has been observed in various models, including rat aortic rings and coronary arteries, where S1P-induced vasodilation was mediated by eNOS-dependent NO release (Alganga et al., 2019, Mair et al., 2010). Furthermore, S1PR3 activation has been implicated in vasodilation within the mouse aorta in response to FTY720, an S1P analogue, through an Aktdependent eNOS phosphorylation mechanism (Tölle et al., 2005). Additionally, intracellular S1P has been found to regulate eNOS expression by interacting with heat shock protein 90 (hsp90) (Roviezzo et al., 2006), a chaperone protein essential for eNOS enzymatic activity and NO production (Brouet et al., 2001).

Endothelium-Independent Regulation

In vascular smooth muscle cells, S1P primarily induces vasoconstriction through activation of S1PR2, with lower contributions from S1PR1 and S1PR3 (AlewijnsePeters and Michel, 2004). S1P-mediated vasoconstriction occurs via two primary mechanisms: (1) increased intracellular calcium (Ca²⁺) levels resulting from K⁺ channel depolarization, through the following mechanisms: inhibiting voltage - gated K⁺ channels, which leads to a lower potassium efflux; stimulating an influx of calcium into vascular smooth muscle cells; activation of Rho Kinase. This leads to the activation of myosin light chain kinase (MLCK) and smooth muscle contraction, and (2) Ca²⁺ sensitization via the G12/13-RhoA-Rho kinase pathway, which enhances contractility independent of direct Ca²⁺ influx (Hemmings, 2006, Hemmings et al., 2006).

Rho Kinase Activation: S1P activates Rho kinase, which sensitizes the contractile machinery to calcium, enhancing vasoconstriction. The effects of S1P on vascular

constriction also vary depending on receptor distribution in different vascular beds. In rat cerebral arteries, vasoconstriction is mediated through S1PR2 and S1PR3, which induce Rho-kinase-dependent Ca²⁺ release from the sarcoplasmic reticulum. However, the aortic response to S1P is significantly lower, likely due to the reduced expression of S1PR2 and S1PR3 in this vessel type (Coussin et al., 2002). Additionally, S1P can promote vasoconstriction by stimulating L-type Ca²⁺ channels, leading to extracellular Ca²⁺ influx and contraction (Bischoff et al., 2000). Other pathways, including the phosphorylation of p38 MAPK and ERK1/2, also contribute to S1P-induced VSMC contraction (Hemmings, 2006). Notably, intracellular S1P can independently modulate vascular tone by activating store-operated calcium entry (SOCE) channels, which facilitate calcium influx into VSMCs and contribute to vasoconstriction (El-Shewy et al., 2018).

1.7.1 Role of Sphingosine Kinase/Sphingosine-1-Phosphate in adipose tissue function

Sphingosine kinases and their bioactive product, sphingosine-1-phosphate, play a crucial role in adipose tissue function and metabolism. These signalling molecules are involved in various cellular processes, including adipogenesis, lipid metabolism, and inflammatory responses within adipose depots. SphK1 and SphK2 are widely expressed in different adipose tissue types, including subcutaneous adipose tissue (SAT), epididymal white adipose tissue (EWAT) (Zhang et al., 2014, Kitada et al., 2016), and brown adipose tissue (BAT) (Morishige et al., 2023), as well as in cultured 3T3-L1 adipocytes (Hashimotolgarashi and Kosaka, 2009, Kitada et al., 2016), Similarly, S1P receptors (S1PR1, S1PR2, and S1PR3) are detected in 3T3-L1 adipocytes (Mastrandrea, 2013, Lee et al., 2017), differentiated rat white adipocytes (Jun et al., 2006), epididymal adipose tissue (EAT), and inguinal SAT (Chakrabarty et al., 2022). Additionally, studies indicate that S1P concentrations are elevated in obesity, with increased levels detected in the adipose tissue of both obese humans and animal models (Samad et al., 2006, Guitton et al., 2020).

1.7.2 Role of Sphingosine Kinase/Sphingosine-1-Phosphate in adipogenesis and lipid metabolism

Extensive research has explored the involvement of sphingolipid signalling components, including SphK1, SphK2, and S1P receptors, in adipogenesis and lipid

metabolism. Studies have shown that SphK1 and SphK2 activity increases during adipocyte differentiation, leading to enhanced S1P production. For instance, in 3T3-L1 adipocytes, the activation of SphKs during adipogenesis correlates with increased lipid droplet accumulation and the upregulation of adipogenic markers (Hashimotolgarashi and Kosaka, 2009). Pharmacological or genetic inhibition of SphK1 significantly reduces lipid accumulation, suggesting its essential role in adipocyte maturation. Similarly, another study reported that inhibiting SphK1 with SPHK-I2 suppressed lipid droplet formation in mature adipocytes (Mastrandrea, 2013). While SphK1 activation appears to promote adipogenesis, the role of S1PR activation in adipocyte differentiation is more complex. Studies indicate that S1P can inhibit adipogenesis, as treatment of 3T3-L1 preadipocytes with S1P suppresses differentiation and lipid accumulation. This inhibition is associated with the downregulation of key transcriptional regulators, including PPARy, C/EBPα, and adiponectin (Moon et al., 2014). Consistently, pharmacological or genetic inhibition of S1PR2 enhances adipogenesis and lipid accumulation, alongside increased expression of adipogenic transcription factors (MoonJeong and Park, 2015, JeongMoon and Park, 2015). Furthermore, mice deficient in S1P lyase, an enzyme responsible for S1P degradation, exhibited reduced adiposity compared to wild-type controls, suggesting that S1P metabolism plays a regulatory role in fat storage (Bektas et al., 2010).

1.7.3 Role of Sphingosine Kinase/Sphingosine-1-Phosphate in adipose tissue inflammation

SphK1 and SphK2 and their bioactive lipid product, S1P, play a pivotal role in the regulation of adipose tissue inflammation, particularly in the context of obesity. Evidence from both human (Ito et al., 2013, Nojiri et al., 2014) and animal studies (Wang et al., 2014) indicates that SphK1 expression is significantly upregulated in obese models, correlating with elevated S1P levels in both adipose tissue and systemic circulation (Hashimotolgarashi and Kosaka, 2009).

The pro-inflammatory role of SphK1 in adipose tissue has been demonstrated through its ability to induce the production of inflammatory cytokines, including TNF- α , IL-6, and IL-1B. In contrast, genetic deletion of SphK1 results in an increase in anti-inflammatory adipocytokines such as IL-10 and adiponectin, indicating a

potential protective effect against inflammation (Wang et al., 2014). Furthermore, SphK1 inhibition has been shown to mitigate LPS-induced inflammation, reinforcing its role as a key modulator of inflammatory responses in adipose tissue (TousFerrer-Lorente and Badimon, 2014). S1P, synthesized by both SphK1 and SphK2, further contributes to adipose tissue inflammation by promoting cytokine secretion in adipocytes. Among S1P receptors, S1PR2 has been identified as a major driver of inflammation, as its genetic deletion or pharmacological inhibition attenuates inflammatory responses in adipose tissue (Kitada et al., 2016, Asano et al., 2023). Conversely, S1PR1 activation appears to exert anti-inflammatory effects, reducing TNF- α expression and macrophage infiltration (Asano et al., 2023), highlighting the differential roles of S1P receptor subtypes in adipose tissue homeostasis.

Chronic inflammation within adipose tissue is closely linked to insulin resistance and metabolic dysfunction. SphK1/S1P signalling has been shown to worsen insulin resistance and impair glucose metabolism, as evidenced by studies demonstrating that SphK1-deficient mice exhibit improved insulin sensitivity and glucose tolerance following a high-fat diet (Olefsky and Glass, 2010, Wang et al., 2014, Osborn and Olefsky, 2012). Moreover, the inhibition or genetic deletion of S1PR2 enhances metabolic function by reducing inflammation and improving insulin sensitivity (Kitada et al., 2016).

1.8 AMP-activated protein kinase (AMPK)

1.8.1 AMPK background

AMP-activated protein kinase (AMPK) is a central regulator of cellular energy homeostasis, functioning as a downstream component of a protein kinase cascade that senses intracellular energy levels and governs both cellular and systemic metabolism (Salt and Hardie, 2017). Its activation is triggered by an increase in AMP or ADP relative to ATP, which occurs in response to metabolic stressors such as hypoxia, nutrient deprivation, or ischaemia (Hardie, 2011, Carling, 2017). Upon activation, AMPK stimulates ATP-generating pathways, including fatty acid oxidation, while concurrently inhibiting ATP-consuming processes such as

lipogenesis, cholesterol synthesis, protein synthesis, and gluconeogenesis, ensuring cellular energy balance (Carling, 2017; Palmer and Salt, 2021).

Structurally, AMPK is a heterotrimeric complex comprising a catalytic α -subunit and two regulatory β - and γ -subunits, with multiple isoforms (α 1, α 2, β 1, β 2, γ 1, γ 2, and γ 3) that enable tissue-specific functional diversity (Hardie, 2011). In the endothelium and adipose tissue, AMPK predominantly exists in its α 1 isoform, whereas skeletal and cardiac muscles primarily express α 2 (Salt and Hardie, 2017).

The α -subunit features an N-terminal catalytic serine/threonine kinase domain, containing a highly conserved Thr172 residue, which is critical for AMPK activation, while its C-terminal region interacts with the β -subunit (Salt and Hardie, 2017). The β -subunit functions as a scaffold, linking the γ -subunit and the C-terminal domain of the α -subunit, while also containing a carbohydrate-binding module (CBM)/glycogen-binding domain (GBD), which allows AMPK to interact with glycogen (Carling, 2017; Juszczak *et al.*, 2020). Meanwhile, the γ -subunit contains four cystathionine- β -synthase (CBS) motifs, which facilitate the binding of adenine nucleotides (AMP, ADP, and ATP), playing a crucial role in AMPK's allosteric regulation (RossJensen and Hardie, 2016) (Figure 1-5).

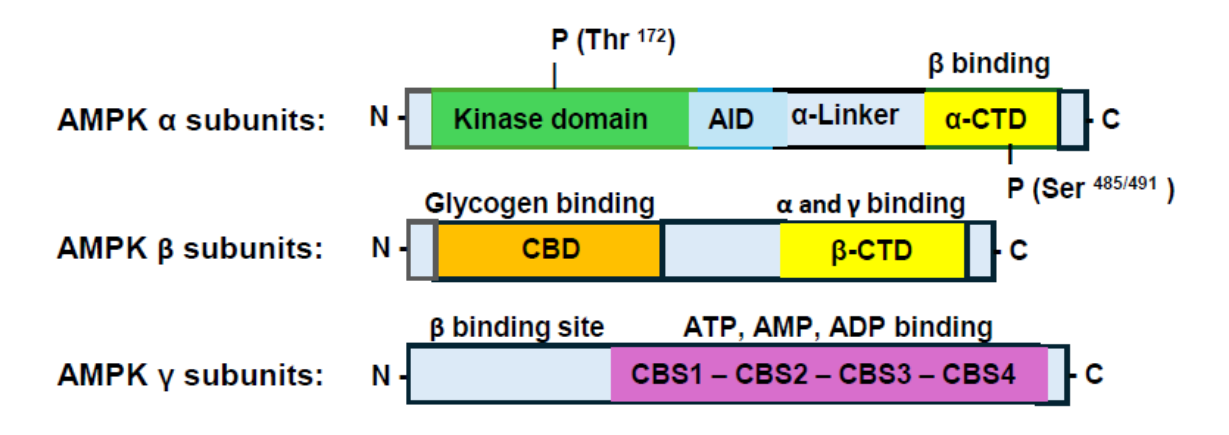


Figure 1-5: AMPK α , β , and γ subunits.

The AMPK α subunit contains an N-terminal serine/threonine kinase domain, which is phosphorylated at Thr172 for activation, regulated by an autoinhibitory domain (AID) and negatively modulated via Ser 485/491 phosphorylation. The β subunit functions as a scaffold, interacting with the α and γ subunits through its β -CTD and binding glycogen via its CBD. The γ subunit contains four CBS domains, which bind ATP, AMP, and ADP, with AMP binding inducing allosteric activation, stabilizing the AMPK complex, and enhancing phosphorylation by upstream kinases, ensuring energy balance and metabolic regulation (Juszczak *et al.*, 2020).

The activation of AMPK is primarily driven by AMP and ADP binding to CBS domains of the γ-subunit, which induces a conformational change that enhances Thr172 phosphorylation by upstream kinases, leading to a 100-fold increase in AMPK activity (Towler and Hardie, 2007; Carling, 2017). Simultaneously, AMP binding inhibits the dephosphorylation of Thr172 by protein phosphatases, further sustaining AMPK activation (Davies et al., 1995; Salt & Hardie, 2017). Beyond allosteric activation by AMP, AMPK can also be activated through direct phosphorylation at Thr172 by upstream kinases, primarily liver kinase B1 (LKB1) and Ca²⁺/calmodulin-dependent protein kinase kinase 2 (CaMKK2) (Shaw et al., 2004; Hawley et al., 2005; Woods et al., 2005). LKB1-mediated activation occurs in response to low-energy conditions, such as exercise and starvation (Herzig and Shaw, 2018), whereas CaMKK2-dependent activation is triggered by intracellular Ca²⁺ flux, which can be induced by endothelial-acting hormones such as thrombin and vascular endothelial growth factor (VEGF) (Stahmann et al., 2010; Hardie, 2018). Given its fundamental role in metabolic regulation, AMPK is targeted by numerous pharmacological agents, natural compounds, and hormones. Some of these agents, including metformin and thiazolidinediones, are already clinically utilized in the treatment of type 2 diabetes (T2D), highlighting AMPK's therapeutic potential in metabolic diseases.

1.8.2 Pharmacological AMPK activators

A diverse range of compounds with distinct structures have been developed to experimentally activate AMPK, with a variety of different mechanisms of action. One class of AMPK activators consists of prodrugs that undergo intracellular conversion into AMP analogues through cellular enzymatic processes. A well-established compound in this category is AICAR (5-aminoimidazole-4-carboxamide ribonucleoside), an adenosine analogue that enters cells via adenosine transporters and is subsequently phosphorylated by adenosine kinase to produce ZMP, an AMP mimetic (Hardie, 2016). By binding to the same regulatory sites as AMP, ZMP mimics AMP's effects on AMPK activation without altering adenine nucleotide ratios, although it is less potent than AMP itself (Hardie, 2016; Salt & Hardie, 2017). AICAR has been extensively utilized for AMPK activation in intact cells, tissues, and animal models, yet its limited specificity and off-target effects have been reported (Kopietz et al., 2021; Ahwazi et al., 2021). Another prodrug-

based AMPK activator, Compound 13 (C13), follows a mechanism similar to AICAR. Once inside the cell, C13 is processed by cellular esterases into Compound 2 (C2), an AMP analogue that has been shown to activate AMPK more effectively than AMP or ZMP (Gómez-Galeno et al., 2010; Salt & Hardie, 2017).

Beyond AMP analogue-based regulation, recent advances have led to the development of allosteric AMPK activators that directly bind to AMPK at specific regulatory sites. Among these are A769662, a thienopyridone compound, and 991, a benzimidazole derivative (Cool et al., 2006; Calabrese et al., 2014). Both compounds activate AMPK by binding to the allosteric drug and metabolite (ADaM) site, a regulatory pocket situated between the β-CBM and the N-lobe on the α subunit (Xiao et al., 2013). Notably, these allosteric activators display selectivity for AMPK complexes containing the β1 isoform rather than β2, influencing their potential application in tissue-specific AMPK modulation (Xiao et al., 2013). The preferential activation of β1-containing AMPK complexes by A769662 was further validated by studies showing that its effects are abolished by an S108A mutation in β1, which prevents phosphorylation at this residue (Willows et al., 2017). Similarly, 991 also exhibits a degree of selectivity for β1-containing AMPK complexes, though its activity is reduced rather than abolished when β1 carries the S108A mutation compared to wild-type β1 AMPK (Willows et al., 2017).

1.8.3 Vascular effect of AMPK

Extensive research has identified AMPK as a key regulatory enzyme in the vascular system, playing a crucial role in modulating endothelial function and governing vascular smooth muscle cell activity to maintain vascular homeostasis and haemodynamic stability.

1.8.3.1 Role of AMPK in the vascular endothelium

AMPK is a key regulator of endothelial function, particularly in vascular tone modulation, NO production, and endothelial protection. Both AMPKα1 and AMPKα2 isoforms are expressed in endothelial cells, with AMPKα1 being the dominant form (Morrow et al., 2003; Goirand et al., 2007). However, AMPKα2 also plays an essential role in maintaining endothelial integrity, as its deletion has been

associated with increased oxidative stress and endothelial dysfunction (Wang et al., 2010).

The activation of endothelial AMPK is triggered by various physiological stressors, including hypoxia, low glucose levels, shear stress, and hormonal stimulation from factors such as adiponectin and angiotensin II (Nagata et al., 2003; Ouchi et al., 2004; Zhang et al., 2006; Chen et al., 2009; Wang et al., 2012; Salt & Hardie, 2017). Additionally, AMPK activation can be induced by several pharmacological agents, such as metformin (Hattori et al., 2006), thiazolidinediones (Boyle et al., 2008), SGLT2 inhibitors (Mancini et al., 2018), statins (Sun et al., 2006), and fenofibrate (Murakami et al., 2006).

One of AMPK's key roles in the vascular endothelium is its regulation of eNOS phosphorylation and nitric oxide production, a function it shares with the PI3K/Akt pathway. While these are distinct signalling routes, some evidence suggests potential crosstalk between AMPK and PI3K/Akt in modulating endothelial function (Rodríguez et al., 2021). AMPK facilitates the phosphorylation of eNOS at Ser1177, thereby enhancing NO synthesis and promoting vasodilation (Morrow et al., 2003; Cheng et al., 2007; Reihill et al., 2007; Rossoni et al., 2011). Pharmacological AMPK activators, such as AICAR, metformin, and adiponectin, have been shown to increase eNOS activity and NO bioavailability, contributing to endothelium-dependent relaxation in both human and animal models (Ford and Rush, 2011; Dolinsky *et al.*, 2013; Chen *et al.*, 2019).

Beyond its role in vasodilation, AMPK has anti-inflammatory, anti-atherogenic, and cytoprotective effects. It mitigates oxidative stress, inflammation, endothelial apoptosis, and ER stress, while simultaneously enhancing angiogenesis and endothelial cell survival (Colombo and Moncada, 2009; Jansen et al., 2020; Kim et al., 2010; Dong et al., 2010; Nagata et al., 2003). Through NF- κ B signalling inhibition, AMPK suppresses the expression of pro-inflammatory cytokines (TNF- α) and adhesion molecules (ICAM-1, VCAM-1, and E-selectin), all of which play a crucial role in endothelial dysfunction and the progression of atherosclerosis (Hattori et al., 2006; Ewart et al., 2008; Katerelos et al., 2010). Moreover, AMPK activation by canagliflozin has been observed to inhibit IL-1B-stimulated pro-inflammatory chemokine secretion in human endothelial cells, further highlighting

its anti-inflammatory properties and contribution to vascular homeostasis (Mancini et al., 2018).

1.8.3.2 Role of AMPK in the vascular smooth muscle cells

AMPK is a key regulator of VSMC function, influencing vasoconstriction and vasodilation in response to various physiological and pathological stimuli. Dysfunction of AMPK in VSMCs has been linked to vascular diseases such as hypertension and atherosclerosis. Both AMPK α 1 and α 2 isoforms are expressed in VSMCs, with α 1 being predominant, while α 1 is the main regulatory subunit contributing to AMPK activity (Goirand et al., 2007; Rodríguez et al., 2021).

AMPK plays a crucial role in endothelium-independent vasodilation. Studies have demonstrated that AMPK activation using AICAR induces potent relaxation in the mouse aorta, independent of endothelium and eNOS (Goirand et al., 2007; Almabrouk et al., 2017). Similarly, A769662-induced AMPK activation in mouse mesenteric arteries promotes vasodilation by reducing intracellular calcium levels through SERCA activation and BK_{Ca} channel stimulation (Schneider et al., 2015). In human and rat renal resistance arteries, AMPK-induced relaxation occurs via both endothelium-dependent (NO and IK_{Ca} channel activation) and endothelium-independent (SERCA activation) mechanisms (Rodríguez et al., 2020).

In addition to promoting vasodilation, AMPK inhibits VSMC contraction by phosphorylating and rendering myosin light chain kinase (MLCK) inactive, thereby reducing myosin light chain phosphorylation and attenuating vasoconstriction (Horman et al., 2008). Furthermore, acetylcholine (Lee & Choi, 2013) and ROS (e.g., H₂O₂) (Zhang et al., 2008a) have been shown to induce endothelium-independent vascular relaxation via an AMPK-LKB1-dependent pathway, which inhibits MLCK and reduces contractility.

1.8.4 Role of AMPK in perivascular adipose tissue

Perivascular adipose tissue has emerged as an active regulator of vascular function, exerting paracrine effects on both vascular smooth muscle cells and endothelial cells. AMPK is expressed not only in VSMCs and ECs but also in PVAT, where its activation plays a crucial role in the ability of PVAT to regulate vascular contractility and homeostasis. While AMPK's functions in ECs and VSMCs have been

extensively studied (Ewart et al., 2008; Bijland et al., 2013; Mancini et al., 2017), its role in PVAT regulation remains less explored.

A previous study from our laboratory demonstrated that global deletion of AMPKα1 significantly impaired the anticontractile function of PVAT in endothelium-denuded mouse aortic vessels, suggesting that AMPK is essential for PVAT-mediated vasoregulation (Almabrouk et al., 2014). AMPK has also been implicated in regulating adiponectin production and secretion, a key vasoprotective adipokine released by PVAT (Lihn et al., 2004; Giri et al., 2006). This was further supported by findings that AMPKα1 knockout mice exhibited reduced adiponectin secretion from PVAT, leading to impaired vascular relaxation. Moreover, exogenous addition of adiponectin restored vasorelaxation in both knockout and wild-type aortic rings without PVAT (Almabrouk et al., 2017).

Dysregulation of AMPK activity in PVAT has been linked to inflammation and adipokine imbalance, particularly under conditions of metabolic stress. For instance, palmitic acid (PA) treatment of rat PVAT led to reduced AMPK activity, an increase in NF-κB phosphorylation, and dysregulated adipokine expression (Sun et al., 2014; Chen et al., 2016; Ma et al., 2017). However, pre-treatment with AMPK activators, including metformin, AICAR, salicylate, resveratrol, diosgenin, and methotrexate, reversed these effects by suppressing NF-κB activation, reducing pro-inflammatory cytokine expression, and enhancing adiponectin and PPARγ levels (Sun et al., 2014; Chen et al., 2016; Ma et al., 2017). Additionally, conditioned medium (CM) from PA-stimulated PVAT impaired endothelium-dependent vasodilation, but this effect was reversed following AMPK activation, further emphasizing its protective role in PVAT function (Sun et al., 2014; Chen et al., 2016; Ma et al., 2017).

Obesity, a major risk factor for cardiovascular diseases such as hypertension, atherosclerosis, and coronary artery disease, is associated with increased PVAT mass, structural alterations, and functional impairment (Stanek et al., 2021). AMPK has been identified as a protective mechanism against obesity-induced PVAT dysfunction. Studies from our laboratory revealed that high-fat diet (HFD) induces inflammatory infiltration in PVAT, reduces AMPK phosphorylation, decreases adiponectin secretion, and attenuates PVAT's anticontractile function (Almabrouk et al., 2018). Furthermore, studies in HFD-fed rats demonstrated that PVAT

dysfunction was associated with increased IKKB activation, reduced AMPK phosphorylation, and elevated serum TNF- α levels, while adiponectin levels were significantly decreased (Chen et al., 2016). However, AMPK activation using diosgenin effectively reversed these effects, highlighting AMPK's potential as a therapeutic target for counteracting obesity-induced PVAT dysfunction (Chen et al., 2016).

1.9 Hypothesis and Aim

Perivascular adipose tissue (PVAT) plays a vital role in supporting vascular function by releasing vasorelaxant mediators, notably adiponectin and nitric oxide (NO), which are essential for regulating vascular tone and mitigating vascular dysfunction. The synthesis and availability of these mediators are tightly controlled by intracellular metabolic regulators, particularly AMP-activated protein kinase (AMPK), which facilitates adiponectin secretion and stimulates NO production, thereby contributing to the anti-contractile properties of PVAT. Sphingosine-1-phosphate (S1P), a bioactive lipid mediator, also influences vascular tone by modulating the production of adiponectin and NO; however, the specific mechanisms underlying its action within PVAT remain incompletely understood. This study hypothesises that the combined presence of S1P and AMPK activation within PVAT enhances vasorelaxation through the increased release of adiponectin and NO. It is further proposed that this vasodilatory effect is diminished in the absence of AMPKα1, underscoring its essential role in mediating the actions of S1P within PVAT.

The specific aims of this study are:

- 1. To investigate the expression and role of sphingosine kinase1 (SphK1)/S1P signalling pathways in wild-type (WT) and AMPKα1 knockout (KO) mice.
- 2. To evaluate whether AMPK activation (using AICAR) and S1P receptor stimulation (S1PR1-3), as well as the combination of S1P with AICAR, promote vasorelaxation in aortic rings from WT and AMPKα1 KO mice, and to assess the contribution of PVAT-derived adipokines including NO and adiponectin using conditioned media and targeted pharmacological approaches.
- 3. To examine the vascular effects of direct AMPK activators (C991 and A-769662), both independently and in combination with S1P in WT and AMPKα1 KO mice, to further define the role of AMPK and S1P in PVAT-mediated vascular regulation.

Chapter 2 - Materials and Methods

2.1 Materials

2.1.1 Animal model

Wild-type (Sv129-WT) male and female mice aged between 12-20 weeks were initially purchased from Harlan Laboratories (Oxon, UK) and global AMPKα1 knock-out (KO) mice were generously provided by Benoit Viollet (Institut Cochin, Paris, France). Three genotypes were used: Wild-type, heterozygous and AMPKα1 knock-out (KO). All mice were bred in-house and maintained together under identical conditions, being housed and fed a standard chow diet in the Central Research Facility (CRF) at the University of Glasgow. All experimental procedures were carried out in accordance with the United Kingdom Home Office Legislation under the Animals (Scientific Procedure) Act 1986 (project license PP1756142 which was approved by the Glasgow University Animal Welfare and Ethical Review Board) and guidelines from Directive 2010/63/EU of the European Parliament on the protection of animals used for scientific purposes.

2.1.2 List of cells and suppliers

3T3-L1 preadipocytes were originally purchased from American Type Culture Collection, (Manassas, VI, USA) and kindly supplied by Prof. G. W. Gould (University of Strathclyde, Glasgow, UK).

Wild type and AMPK $\alpha 1/\alpha 2$ (AMPK-/-) double knockout mouse embryonic fibroblasts (MEFs) were a kind gift from Dr. Benoit Viollet, Institute Cochin, Paris, France (Laderoute *et al.*, 2006).

2.1.3 List of materials and suppliers

Tocris Bioscience, Bristol, UK

Sphingosine 1 Phosphate (#1370)

SEW2871 (#2284)

CYM5541 (#4897)

JTE 013 (#2392)

W146 (#3602)

Troglitazone (#3114)

Cayman Chemical, USA

CYM 5478 (#29024)

CAY10444 (#CAY10005033)

Sigma-Aldrich Ltd, Gillingham, Dorset, UK

Phenylephrine (#P6126)

Acetylcholine (#A6625)

Dexamethasone

3-Isobutyl-1-methylxanthine (IBMX) (#I5879)

Porcine Insulin (#I5523)

L-NAME (#N5751)

Abcam, Cambridge, UK

A769662 (#ab120335)

AOBIOUS Inc., Gloucester, MA, USA

Compound 991 (#AOB8150).

Toronto Research Chemicals Inc, Ontario, Canada

AICAR (5-aminoimidazole-4-carboxamide-1-beta-4-ribofuranoside) (#A611700)

Fisher Scientific UK Ltd, Loughborough, Leicestershire, UK

Bovine serum albumin (BSA)(#PB1600-100)

NuPAGE™ LDS Sample Buffer (4X) (#NP0007)

Pierce[™] BCA Protein Assay Kits (#23277)

Invitrogen (GIBCO Life Technologies Ltd), Paisley, UK

Dulbecco's modified Eagles media (DMEM), high glucose

Dulbecco's modified Eagles media (DMEM)+GlutaMAX

Foetal calf serum (FCS) (USA origin)

Foetal calf serum (FCS) (EU origin)

Newborn calf serum (NCS)

Phosphate buffered saline (PBS)

Penicillin/streptomycin

DNA Gel Stain (#S33102)

Trypsin

Corning tissue culture T75/T150 flasks

New England Biolabs Inc, UK

Blue Prestained Protein Standard, Broad Range (11-250 kDa) (#P7719S)

VWR International Ltd, Lutterworth, Leicestershire, UK

Falcon tissue culture 10 cm diameter dishes

Falcon tissue culture 6 well plates

Anachem, Luton, UK

DNAreleasy

Invitrogen (Life Technologies Ltd), Paisley, UK

SYBR™ Safe DNA Gel Stain (#S33102)

Premier International Foods, Cheshire, UK

Dried skimmed milk.

VECTOR Laboratory (2BScientific)

VECTASHIELD® Antifade Mounting Medium with DAPI (#H-1200)

Severn Biotech Ltd, Kidderminster, Hereford, UK

Acrylamide:Bisacrylamide (37.5:1; 30% (w/v) Acrylamide) (#20-2100-10)

R&D SYSTEMS a Biotechne brand, Abingdon, UK

Mouse Adipokine Array Kit (#ARY013)

2.1.4 List of primary and secondary antibodies for immunoblotting

2.1.4.1 Primary antibodies for Western blotting

The primary antibodies used for immunoblotting are listed in table 2-1. All antibodies were prepared in TBST with 5% (w/v) BSA. These antibodies were applied to nitrocellulose membranes that had been blocked with TBS containing 5% (w/v) milk powder.

Table 2-1 The primary antibodies used for immunoblotting

Antibody	Source(Catalouge.N)	Species	Dilution
phospho-ACC	Cell Signalling Technology,	Rabbit	1:1000
(S79)	Hertfordshire, UK, (#3661)		
ACC	Cell Signalling Technology,	Rabbit	1:1000
	Hertfordshire, UK, (#3662)		
Phospho-AMPK	Cell Signalling Technology,	Rabbit	1:1000
(T172)	Hertfordshire, UK, (#2531)		
ΑΜΡΚα	Cell Signalling Technology,	Rabbit	1:1000
	Hertfordshire, UK, (#2532)		
SphK1	Santa Cruz (sc-365401)	Mouse	1:500
ERK 1/2	Cell Signalling Technology(#9102)	Rabbit	1:1000
JNK	Cell Signalling Technology(#9252)	Rabbit	1:1000
B-actin	Cell Signalling Technology, UK, (#4970)	Rabbit	1:1000

2.1.4.2 Secondary antibodies for Western blotting

The secondary antibody as described in table 2-2 was applied to all blots and incubated for 1 hour at room temperature.

Table 2-2 The secondary antibodies used for immunoblotting

Conjugate	Epitope	species	Dilution	Source(Catalouge.N)
IRDye®	Rabbit	Donkey	1:10000	LI-COR Biosciences, USA (# 926-
800CW				32213)
IRDye®	Rabbit	Donkey	1:10000	LI-COR Biosciences, USA (# 926-
680CW				68073)
IRDye®	Mouse	Donkey	1:10000	LI-COR Biosciences, USA (# 926-
800CW				32212)
IRDye®	Mouse	Donkey	1:10000	LI-COR Biosciences, USA (# 925-
680CW				68072)

2.2 Methods

2.2.1 Genotyping from mouse ear notches

2.2.1.1 DNA extraction and polymerase chain reaction (PCR)

Ear notches were numbered and collected from the CRF building at the University of Glasgow when the mice were 6 weeks old. These notches were then stored in ear notch tubes at -20°C. DNA extraction was then performed from the ear notches of both male and female WT and AMPKα1 knock-out (KO) mice.

Ear notches were then transferred to PCR tubes and 10µl of DNAreleasy (Anachem LS02, UK) was added to lyse the ear notch tissues. All samples were then incubated for 7 minutes on a thermocycler under the following conditions: initial denaturation 75°C for 5 minutes, followed by denaturation at 96°C for 2 minutes and then held at 20°C. The DNA concentration was subsequently diluted by adding 90µl of Nuclease-free water into each sample. This stock DNA was stored at 4°C until used for polymerase chain reaction (PCR).

The PCR technique was employed to amplify both wild-type (Sv129-WT) and global AMPKa1 knock-out (KO) genes. The experiment involved two main steps: PCR amplification and gel electrophoresis. Each PCR tube was filled with a total volume of 25.3 µl of the following: 13.75µl of GoTaq (Promega M5122, UK), 8.45µl

of distilled water, and 0.55μl of each of the forward and reverse primers of WT and AMPKα1 KO. Subsequently, 2μl of prepared DNA from each mouse was added to PCR tubes. The sequences of the primers are shown in table 2-3.

The PCR tubes were then placed in a PCR machine which was programmed as follows: 95°C for 5 minutes to allow initial DNA denaturation. This was followed by further denaturation at 95°C for 30 seconds, annealing at 58°C for 40 seconds and extension at 72°C for 10 minutes. This cycle of denaturing, annealing and extension was repeated 40 times.

Table 2-3 List of DNA primers in genotyping process.

All forward and reverse primers were purchased from ThermoFisher.

Primer	Туре	Sequence (5'-3')	Annealing temp.	Product size (bp)
Wild	Forward primer	AGCCGACTTTGGTAAAGGATG	64.0	
Type	Reverse primer	CCCACTTTCCATTTTCTCCA	63.7	Approx 500
Knaskaut	Forward primer	GGGCTGCAGGAATTCGATATCAA	69.8	
Knockout	Reverse primer	CCTTCCTGAAATGACTTCTA	58.9	Approx 500

2.2.1.2 Agarose gel electrophoresis

A 2% (w/v) agarose gel was then prepared by dissolving 1g of agarose (ThermoFisher, UK) in 50ml Tris-Acetate-EDTA (TAE) buffer. The mixture was heated in a microwave on high power for two minutes until the agarose was completely dissolved. To this solution, 5µl of SYBR Safe DNA stain (Invitrogen, UK) was then added and subsequently the solution was poured into a casting tray with combs in place and allowed to set for 30 minutes at room temperature.

Subsequently, the gel was then transferred into the electrophoresis tank and covered with TAE buffer. A volume of $6\,\mu\text{L}$ of DNA ladder (Promega G2101, UK) was loaded into the first well, followed by loading $10\,\mu\text{L}$ of each sample into individual, separate wells for electrophoretic analysis. The gel was then subjected to electrophoresis at 100V for 30 minutes using a Flowgen powerpack (Bio-Rad, UK) at room temperature.

Finally, the DNA bands were visualised and photographed using UV light (Bio-Rad, UK) and images were analysed using QuantityOne software (Figure 2-1).

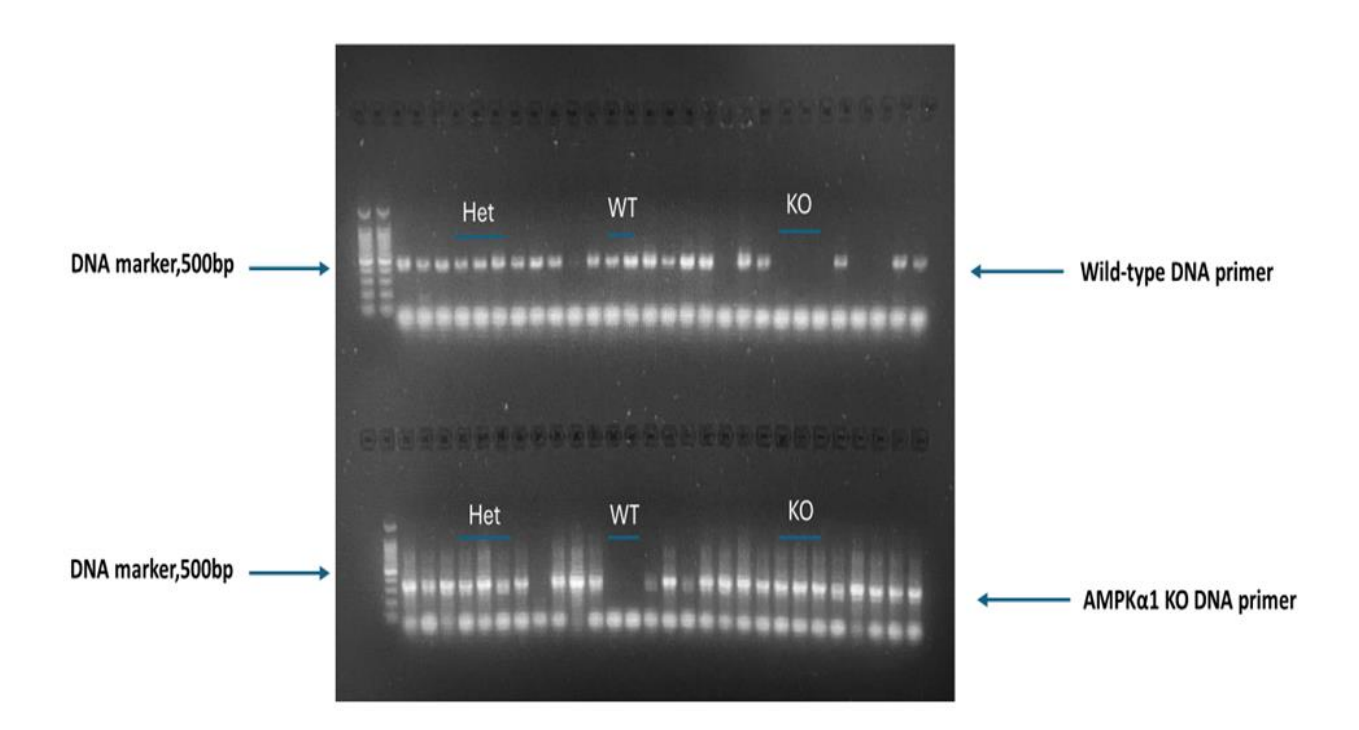


Figure 2-1: The genotyping of Wild-Type (WT) and AMPKα1 Knockout (KO) mice.

Mice genotyping was conducted by analyzing PCR-amplified products derived from ear notch samples. The DNA fragments were separated using gel electrophoresis, with a DNA ladder placed on the left side of the agarose gel for reference. The upper portion of the gel displayed the PCR products generated using primers that target wild-type (WT) alleles, while the lower portion exhibited the products from primers specific to AMPK α 1 KO alleles. The gel indicated examples of heterozygous (Het), wild-type (WT), and knockout (KO) genotypes.

2.2.2 Wire myography

2.2.2.1 Isolation and dissection of thoracic aorta mice

Wild-type (Sv129-WT) and global AMPK α 1 knockout (KO) mice were euthanized by gradually increasing the concentration of CO $_2$ within a closed chamber, in accordance with ethical guidelines. Immediately following euthanasia, the heart

and thoracic aorta were carefully excised and transferred into cold physiological salt solution (PSS) composed of 119 mM NaCl, 25 mM NaHCO₃, 4.7 mM KCl, 1.2 mM KH₂PO₄, 1 mM MgSO₄, 11 mM glucose, and 2.5 mM CaCl₂, to preserve tissue integrity for further experimentation. The entire heart and thoracic aorta were then carefully isolated and placed in a Petri dish containing cold PSS to maintain tissue viability for subsequent procedures. Thoracic aortae were then dissected, and, in some experiments, they were cleaned of the surrounding perivascular adipose tissues (PVAT), while other segments were left with intact PVAT (Figure 2-2). The vessels were then cut into 1-2 mm rings using fine dissecting scissors under a binocular microscope for subsequent aortic functional studies. Endothelium removal was carried out by gently rubbing the intimal surface of the rings with forceps, while in some segments, the endothelium was left intact.

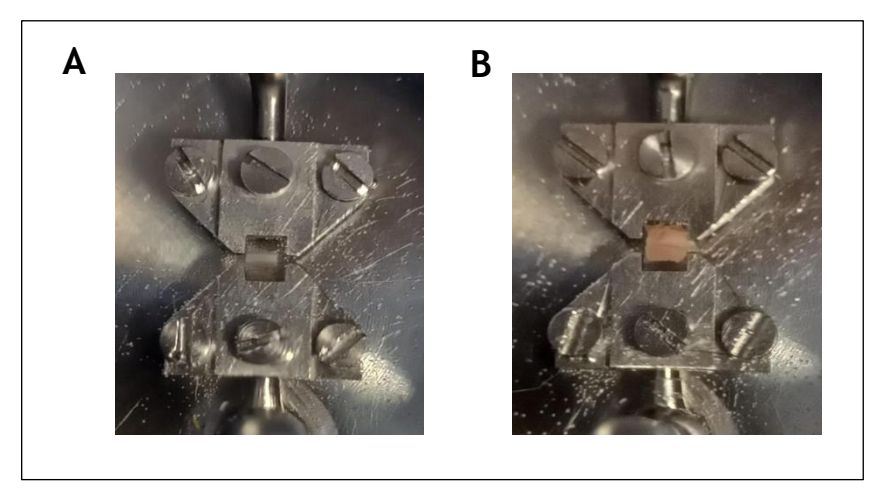


Figure 2-2: Representative images of mouse thoracic aorta mounted in a small-vessel wire myograph.

Two-millimetre aortic rings were threaded onto two stainless-steel wires and mounted between a force transducer (for isometric tension recording) and an adjustable micrometer jaw (for setting passive tension). Changes in vessel tone were recorded continuously via the LabChart software. (A) Thoracic aorta with PVAT removed. (B) Thoracic aorta with intact PVAT.

2.2.2.2 Mounting the tissue

The aortic rings were mounted in a four-channel wire myograph (Danish Myo Technology, Denmark) (Figure 2-3). Vessels were gassed with a mixture of 95% O₂, 5% CO₂ at 37 °C in 5 ml of PSS, allowing for equilibration for 30 mins. The rings were then stretched stepwise, in approximately 2mN steps with 5-minute intervals between each stretch until reaching the optimal tension of 9.81 mN. Viability of vessels was confirmed by two successive additions of 5 ml high-potassium

physiological salt solution (KPSS; composition in mM: NaCl 62.5, KCl 62.5, NaHCO₃ 25, KH₂PO₄ 1.2, MgSO₄ 1.2, CaCl₂ 2.5, glucose 11.1). In KPSS, the elevated K⁺ concentration is achieved by isotonic replacement of NaCl with KCl to maintain overall ionic balance and osmolarity. All rings were then constricted using phenylephrine (PE) at a concentration of 1 μM until the vessel reached a consistent level of contraction. The vessels were then tested with 3 μM of the endothelium-dependent vasodilator acetylcholine (ACh) in order to check the function of the endothelium. A relaxation to acetylcholine (ACh) < 20% was indicative of successful endothelial removal and relaxation to acetylcholine (ACh) > 50% was indicative of an intact endothelial layer (Furchgott and Zawadzki, 1980; Förstermann *et al.*, 1986; Wu and Bohr, 1990; Buchwalow *et al.*, 2008; Ewart *et al.*, 2017; Alganga *et al.*, 2019; Hwej *et al.*, 2024).

The effects of Sphingosine-1-Phosphate (S1P) and selective S1P receptor agonists including SEW2871 (S1PR1 agonist, Tocris Bioscience, UK), CYM5541 (S1PR3 agonist, Tocris Bioscience, UK), and CYM5478 (S1PR3 agonist, Cayman Chemical, USA) as well as AMPK activators such as AICAR (Toronto Research Chemicals, Canada), A769662 (Abcam, Cambridge, UK), and Compound 991 (AOBIOUS Inc., Gloucester, MA, USA), were assessed on vascular reactivity. Experiments were conducted using aortic rings pre-contracted with phenylephrine (1 μ M), followed by the construction of cumulative concentration-response curves (Table 2-4).

Table 2-4 List of drugs and stock concentrations used

Drugs	Stock concentration	Diluent
S1P	1 mM	PBS
SEW2871	10 mM	Ethanol
CYM5478	1 mM	DMSO
CYM5541	10 mM	Ethanol
W146	10 mM	NaOH

JTE013	10 mM	Ethanol
CAY10444	10 mM	DMSO
AICAR	100 mM	PBS
C991	10 mM	DMSO
A769662	100 mM	DMSO
L-NAME	100 mM	d.H ₂ O

For S1P and its receptor agonists, concentrations ranging from 3×10^{-9} to 3×10^{-6} M were applied at 15-minute intervals consistent with protocols routinely used in our laboratory and overlapping with previously published wire-myograph studies, which typically apply S1P in the low nanomolar to micromolar range (Salomone *et al.*, 2008; Alganga et al.,2017). For the indirect AMPK activator AICAR, cumulative concentrations ranging from 5×10^{-4} to 2×10^{-3} M were administered at similar intervals. This range was adapted from protocols previously established in our laboratory (1×10^{-4} to 2×10^{-3} M) and modified here to enhance vascular responsiveness and enable direct comparison with S1P co-application experiments. The direct AMPK activators A-769662 and C991 were applied cumulatively over 1×10^{-6} to 5×10^{-4} M consistent with dose-response protocols previously employed in our laboratory (Ewart et al., 2017).

In addition, the combined effects of S1P or S1P receptor agonists with AMPK activators were evaluated to determine potential synergistic or additive interactions on vascular tone. Concentration-response curves were generated in aortic rings both with and without PVAT, to assess the specific contribution of PVAT-derived factors to these responses.

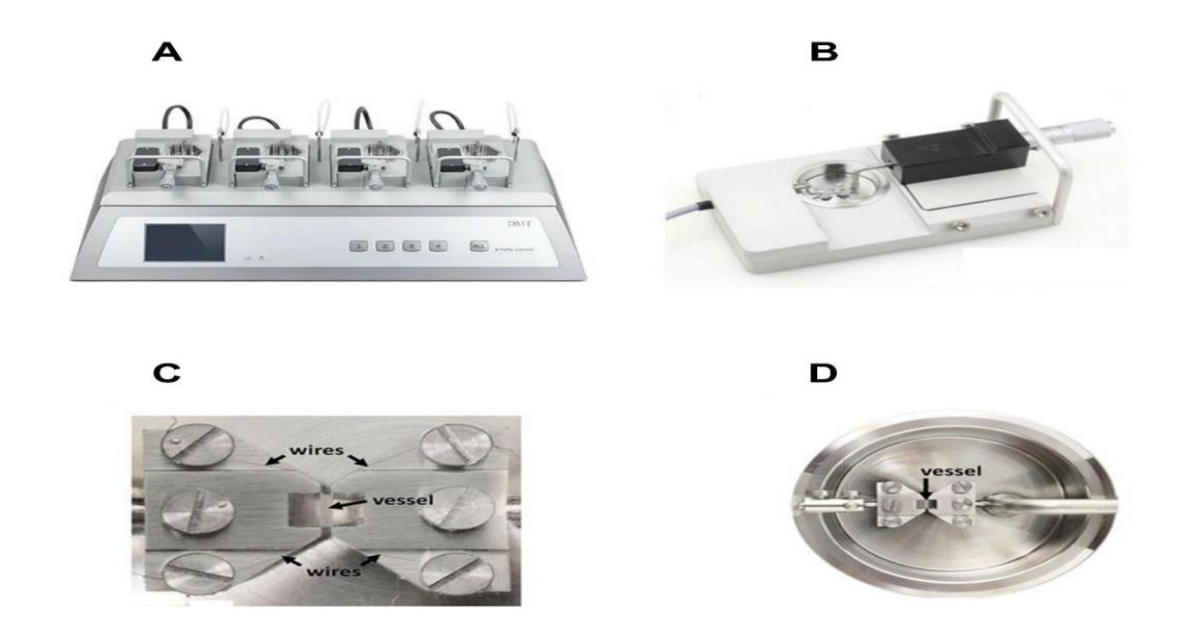


Figure 2-3: The components of the wire myograph.

(a) the DMT multi-chamber 620M Wire Myograph, (b) a myograph unit equipped with a force transducer on the left and a micrometre on the right, (c) a detailed view of the jaws, screws, wires, and a mounted vessel segment, (d) an organ bath unit featuring jaws and a mounted vessel segment adapted from Danish Myo Technology, (Denmark Aarhus Denmark).

2.2.3 Mouse Adipokine Array (Proteome Profile)

Adipokine expression profiling was conducted using the Mouse Adipokine Array (Proteome Profiler, ARY013, R&D Systems, a Bio-Techne brand, UK), capable of detecting 38 adipokines in duplicate on a nitrocellulose membrane, following the manufacturer's instructions.

PVAT samples were freshly isolated and incubated in cold PSS under different treatment conditions: control (PSS only), S1P (10 μ M), AICAR (2 mM), or a combination of S1P (10 μ M) and AICAR (2 mM). Incubations were carried out for 4 hours prior to further analysis. After treatment, the conditioned PSS media were collected, centrifuged to remove debris, and stored at -80 °C until analysis.

Prior to loading, membranes were incubated with blocking buffer for 60 minutes on a rocking platform shaker at room temperature. Each 1 mL sample of conditioned PSS was mixed with 0.5 mL array buffer and 15 μ L mouse adipokine detection antibody cocktail, and the mixture was incubated at room temperature for 60 minutes. After aspirating the blocking buffer from the membranes, the sample-antibody mixture was added and incubated overnight at 2-8 °C with gentle rocking.

Following incubation, membranes were washed twice with washing buffer to eliminate unbound materials. Membranes were then incubated with 2 mL of IRDye 800CW Streptavidin (diluted 1:2000) for 30 minutes at room temperature. Membrane images were captured using an Odyssey Imaging System (LI-COR, USA), and the signal intensity for each adipokine was quantified using Image Studio software (LI-COR, USA).

The resulting data were imported into Microsoft Excel, normalized to internal positive controls provided on the membrane, and further analyzed statistically using GraphPad Prism 8.0 software (GraphPad, California, USA).

2.2.4 Nitric oxide (NO) assay

The thoracic aortic PVAT of WT mice was gathered and weighed. These tissues were then subsequently immersed in 1 ml of oxygenated physiological buffer solution (NaCl 119 mM, NaHCO₃ 25 mM, KCl 4.7 mM, KH₂PO₄ 1.2 mM, MgSO₄ 1 mM, glucose 11 mM, and CaCl₂ 2.5 mM) and incubated under various treatment conditions: untreated control, S1P (S1P, 10 µM), AICAR (2 mM), and a combination of S1P and AICAR at 37°C for a duration of 4 hours in the myograph chamber. 100 µL of the conditioned media, which contained substances released from the PVAT was collected. Subsequently, 400 μL of methanol (v/v) was added to the collected media, and the mixture was centrifuged at 13.000xg at 4°C for 20 minutes. The resulting supernatant was then collected and stored at -80°C for subsequent analysis of nitric oxide (NO) content utilising a Sievers 280 NO analyser. The NO analyzer determines the amount of NO produced by the tissues by measuring the concentration of nitrite (NO₂⁻), which forms from the reaction between NO released from the tissues and the dissolved oxygen in the conditioned medium. To prepare the equipment, a reducing agent solution was prepared by mixing 5 mL of glacial acetic acid with 50 mg of sodium iodide (NaI) dissolved in 1.5 mL of deionized water. This solution was added to the purge vessel and flushed with nitrogen (N₂) gas for 30 minutes to remove any trace of NO₂⁻. After purging, the purge vessel was sealed, and the reducing agent was refluxed under a nitrogen atmosphere. Before each experiment, a standard curve for NO2 was constructed using a 100 mM sodium nitrite (NaNO2) standard solution. Serial dilutions of 50 µM, 10 µM, 1 µM, and 100 nM were prepared and injected into the purge vessel using an Exmire microsyringe (ITO Corporation, Japan). This standard curve served as a reference for quantifying the nitrite levels in the samples. Following the calculation of the standard curve, supernatant samples from WT thoracic PVAT mice were injected into the purge vessel. To ensure accurate measurements, injections were made at one-minute intervals, allowing the output curve to return to baseline between each sample. The output, measured in millivolts (mV), was then correlated with the NO_2^- concentration in the sample by referencing the previously constructed NO_2^- standard curve.

2.2.5 Cell culture procedure

2.2.5.1 Cell culture plastic ware

Mouse embryonic fibroblasts (MEFs) and 3T3-L1 preadipocytes were obtained from the American Type Culture Collection (ATCC, USA). MEFs were cultured in Corning T75 flasks and 6-well plates, while 3T3-L1 cells were maintained in Corning T75 flasks, Falcon 10 cm dishes, and 6-well plates, under standard cell culture conditions.

2.2.5.2 Recovery of cryopreserved cell stock from liquid nitrogen

Cryogenic vials containing frozen cell stocks were retrieved from liquid nitrogen storage and rapidly thawed in a 37 $^{\circ}$ C water bath. Once thawed, the cell suspension was transferred under sterile conditions into a T75 flask containing pre-warmed Dulbecco's Modified Eagle Medium (DMEM), supplemented with 10% fetal bovine serum (FBS) and 1% penicillin-streptomycin, previously equilibrated to 37 $^{\circ}$ C in an atmosphere of 10% (v/v) CO₂. The cells were incubated overnight at 37 $^{\circ}$ C in a humidified incubator with 10% (v/v) CO₂.

The following day, the culture medium was aspirated to remove any residual cryoprotective agents and non-viable cells, and replaced with fresh, pre-warmed complete medium to support optimal cell recovery and growth.

2.2.5.3 MEFs and 3T3-1L cells culture growth media

Mouse embryonic fibroblasts (MEFs) were grown in Dulbecco's Modified Eagle Medium (DMEM) that was enriched with 10% (v/v) fetal calf serum (FCS) and 100 U/mL (w/v) of penicillin and streptomycin. The cells were cultured at 37° C in a humidified environment containing 10% (v/v) CO_2 , with the culture medium being refreshed every 48 hours.

3T3-L1 cells were cultured as fibroblasts (passage 3-7) in T75 flasks using DMEM supplemented with 10% (v/v) newborn calf serum (NCS) and 100 U/mL (w/v) of penicillin and streptomycin. The cells were maintained at $37^{\circ}C$ in a humidified atmosphere containing 10% (v/v) CO_2 , with the medium being replaced every 48 hours.

2.2.5.4 3T3-L1 preadipocytes differentiation protocol

To induce the differentiation of 3T3-L1 preadipocytes into mature adipocytes, a specialized DMEM medium containing 10% (v/v) fetal calf serum (FCS) and an adipogenic cocktail was utilized. The cocktail comprised 0.5 mM IBMX, 0.25 μ M dexamethasone, 1 μ g/mL insulin, and 5 μ M troglitazone. Before use, the medium was filter-sterilized using a 0.2 μ m filter. After three days, the medium was switched to DMEM containing 10% (v/v) fetal calf serum (FCS), 5 μ M troglitazone, and 1 μ g/mL insulin. The cells were then incubated in this new medium for an additional three days. Following this period, the medium was aspirated and replaced with DMEM supplemented with 10% (v/v) FCS. Adipocytes were utilized for experimentation between 8-12-days post-differentiation. Throughout all procedures, the cells were maintained in a humidified environment at 37°C with 10% (v/v) CO₂.

2.2.5.5 Passaging of MEFs and 3T3-L1 cells

When cells cultured in T75 flasks reached approximately 80% confluence, the growth medium was discarded, and the cells were briefly rinsed with 10 mL of pre-warmed sterile phosphate-buffered saline (PBS) to remove residual serum and debris. Following rinsing, 3 mL of sterile 0.05% (w/v) trypsin-EDTA solution was added to each flask, and the cells were incubated at 37 °C in an atmosphere of 10% (v/v) CO2 until complete detachment was observed under the microscope. To neutralize the trypsin, an appropriate volume of pre-warmed DMEM growth medium supplemented with 10% fetal bovine serum (FBS) was added. The resulting cell suspension was collected and aliquoted for downstream applications.

For reseeding, cells were typically plated at a density of 5×10^4 to 1×10^5 cells per well (for 6-well plates) or adjusted appropriately depending on the experimental requirements.

2.2.6 Analysis of protein expression in PVAT, MEFs and 3T3-L1 cells

2.2.6.1 Preparation of lysates from mouse PVAT

Wild type (Sv129) and AMPK α 1 knockout mice were euthanized using CO₂. The thoracic and abdominal PVAT from these mice was quickly excised and snap-frozen in liquid nitrogen. The tissues were then homogenized in four volumes of lysis buffer using hand-held disposable pestles and tubes (Sigma) at 4°C. Following homogenization, the samples were kept on ice for 30 minutes. The lysates were subsequently centrifuged at 21,910 x g for 15 minutes at 4°C. The resulting supernatants were collected and stored at -20°C.

2.2.6.2 Preparation of lysates from MEFs and 3T3-L1 cells

Cells being cultured in 6-well plates were initially washed and then incubated in serum-free DMEM for 2 hours at 37° C. This was followed by a 1-hour incubation at 37° C in 1 ml of Krebs-Ringer Phosphate (KRP) buffer, which consisted of 119 mM NaCl, 5 mM NaHCO₃, 4.7 mM KCl, 1.3 mM CaCl₂, 1.2 mM MgSO₄, 1.2 mM NaH₂PO₄, 5 mM glucose, and 0.1% (w/v) bovine serum albumin. Test substances were subsequently introduced to the wells for varying durations at 37° C. After the incubation, the medium was discarded, and 0.1-0.2 ml of ice-cold lysis buffer was added. The cells were then scraped into microcentrifuge tubes. The cell extracts were then centrifuged at 21,910 x g for 15 minutes at 4°C. The resulting supernatants were stored at -20°C until further use.

2.2.6.3 Bicinchoninic acid (BCA) method

The protein concentration of cell and tissue lysates was measured using the bicinchoninic acid (BCA) assay. To begin, a working reagent (WR) was prepared by combining BCA Reagent A and BCA Reagent B in a 50:1 ratio. In a 96-well plate, duplicate samples of bovine serum albumin (BSA) standards were prepared in the following concentrations: 0 μ g, 0.025 μ g, 0.125 μ g, 0.25 μ g, 0.5 μ g, 0.75 μ g, 1.0 μ g, 1.5 μ g, and 2 μ g, each adjusted to a final volume of 10 μ L with distilled water. Similarly, 2 μ L of each lysate sample, in duplicate, was added to the wells and brought up to 10 μ L with distilled water. Subsequently, 200 μ L of the working reagent was added to all wells containing either the samples or the BSA standards. The plate was

then covered and incubated at 37°C for 15 minutes. Absorbance was read at 570 nm using a plate reader.

2.2.6.4 Separation of protein by SDS-PAGE and western blotting

Equal amounts of protein lysate, as determined by the BCA assay, were resolved using SDS-PAGE. The SDS-PAGE was conducted with 1.5 mm thick vertical slab gels containing 10% acrylamide. These slab gels were prepared using Bio-Rad Mini-Protean III gel units, featuring a stacking gel approximately 2 cm deep. The lysates were mixed with 4X complete sample buffer in a 3:1 ratio and then heated to 95°C for 5 minutes in a heating block prior to SDS-PAGE separation. Pre-stained broadrange protein markers (10-250 kDa) were used as standards. Electrophoresis was carried out using the Bio-Rad Protean III system at a constant voltage of 80 V for the stacking gel and up to 150 V for the separating gel until the tracking dye reached the bottom and good resolution of the molecular mass markers was achieved.

The gel was subsequently transferred onto a nitrocellulose membrane using an iBlot 2 gel transfer device set at 20 V for 7 minutes (ThermoFisher, UK). The membrane was then incubated with shaking at room temperature for one hour in a blocking buffer, prepared by dissolving 5% (w/v) dried skimmed milk powder (Marvel, UK) in Tris-buffered saline (TBS). The purpose of the blocking buffer was to prevent non-specific background bands. The blot was washed three times for 15 minutes each with TBS (50 mM Tris-Cl, pH 7.6, and 150 mM NaCl).

Following the washes, the membranes were incubated overnight at 4°C with a primary antibody diluted in TBST (Table 2-1). The next day, the membrane was washed again three times for 15 minutes each with TBS. Subsequently, the secondary antibody (Table 2-2) was added, and the membrane was shaken for one hour at room temperature, followed by additional washes with TBS.

2.2.6.5 Protein expression quantification

Densitometric quantification of band intensity was performed using Image Studio Lite software (LI-COR).

2.2.7 Gene analysis

2.2.7.1 RNA Extraction from MEF Cells

Wild-type (WT) and AMPK α 1/ α 2 knockout (KO) mouse embryonic fibroblast (MEF) cells were cultured in 6-well plates using Dulbecco's Modified Eagle Medium (DMEM) supplemented with 10% (v/v) fetal bovine serum (FBS) and incubated at 37 °C in a humidified atmosphere containing 10% CO₂. Upon reaching the desired confluence, the medium was aspirated, and the cells were gently washed twice with cold phosphate-buffered saline (PBS) to remove any residual serum or media components.

Total RNA was extracted using the Qiagen RNeasy Mini Kit (Qiagen, Germany), following the manufacturer's protocol. All steps were performed at room temperature unless otherwise specified. A volume of 350 μ L of RLT lysis buffer was added directly to each well, and the lysate was collected using a cell scraper. The lysate was transferred to a RNeasy spin column, then centrifuged at 17,000 × g for 2 minutes to homogenize.

Next, an equal volume of 70% (v/v) ethanol was added to each lysate and mixed gently by pipetting. The resulting mixture was applied to a new RNeasy spin column and centrifuged at full speed for 1 minute. After discarding the flow-through, 700 μ L of RW1 wash buffer was added to the column and centrifuged for 30 seconds at full speed. Following another flow-through removal, 500 μ L of RPE buffer was added and centrifuged for 30 seconds, then repeated with another 500 μ L RPE wash for 2 minutes. To remove residual buffer, the columns were transferred to fresh 2 mL collection tubes and centrifuged for 3 minutes at full speed.

Finally, the columns were transferred to new 1.5 mL RNase-free microcentrifuge tubes, and RNA was eluted in 30 μ L of RNase-free water by centrifugation at full speed for 1 minute. RNA purity and concentration were assessed using a NanoDrop spectrophotometer, measuring absorbance at 260 nm and 280 nm. The A260/A280 ratio was used as an indicator of RNA quality, and only samples within acceptable purity thresholds were retained. All RNA samples were stored at -80 $^{\circ}$ C until further use.

2.2.7.2 RNA Extraction from PVAT

Thoracic aortic perivascular adipose tissue (PVAT) was isolated from wild-type (WT) and AMPKα1 knockout (KO) mice and immersed in physiological salt solution (PSS) for 30 minutes at 37 °C. Total RNA was extracted using the RNeasy Lipid Tissue Mini Kit (Qiagen, Germany), following the centrifugation-based protocol recommended by the manufacturer.

Briefly, PVAT samples were transferred into 2 mL RNase-free collection tubes containing two stainless steel beads (5 mm diameter), and 1 mL of QIAzol lysis reagent was added. Tissues were then homogenized using a TissueLyser LT system (Qiagen) for 5 minutes. The homogenates were incubated at room temperature (15-25 °C) for 5 minutes to allow complete dissociation.

Following homogenization, $200 \, \mu L$ of chloroform was added to each sample, and the tubes were shaken vigorously for 15 seconds. After standing for 2-3 minutes at room temperature, samples were centrifuged at $12,000 \times g$ for 15 minutes at 4 °C, resulting in phase separation. The upper aqueous phase, containing the RNA, was carefully transferred to a new tube and mixed with an equal volume of 70% ethanol, followed by thorough vortexing.

The mixture was then applied to an RNeasy Mini spin column placed in a 2 mL collection tube and centrifuged at $8,000 \times g$ for 15 seconds at room temperature. The column was subsequently washed with $350 \, \mu L$ of Buffer RW1, followed by centrifugation at $8,000 \times g$ for 15 seconds. To eliminate genomic DNA contamination, $80 \, \mu L$ of DNase I solution was added directly onto the spin column membrane, and the column was incubated at room temperature for 15 minutes.

Next, the column was washed again with 350 μ L of Buffer RW1 and centrifuged. After discarding the flow-through, 500 μ L of Buffer RPE was added and centrifuged for 15 seconds at $8,000 \times g$, followed by a second wash with another 500 μ L of Buffer RPE, centrifuged for 2 minutes. To remove residual buffer, the column was placed in a fresh 2 mL collection tube and centrifuged to ensure complete drying.

Finally, the spin column was transferred to a 1.5 mL RNase-free microcentrifuge tube, and 30 μ L of RNase-free water was applied directly to the membrane to elute the RNA. The column was centrifuged at 8,000 × g for 1 minute to collect the eluate. RNA

concentration and purity were assessed using a NanoDrop™ 1000 spectrophotometer, and the samples were stored at -80 °C until further analysis.

2.2.7.3 cDNA Synthesis via Reverse Transcription

Total RNA extracted from MEF cells and PVAT was reverse transcribed into complementary DNA (cDNA) using the High-Capacity cDNA Reverse Transcription Kit (Applied Biosystems, Thermo Fisher Scientific, USA), following the manufacturer's protocol. For each 20 μ L reaction, 1 μ g of DNase I-treated RNA was diluted to 10 μ L with RNase-free water, placed in 0.5 mL PCR tubes, and kept on ice. The reverse transcription mix—comprising 2 μ L of 10× RT buffer, 0.8 μ L of 25× dNTP mix (100 mM), 2 μ L of 10× RT random primers, 1 μ L of Multiscribe Reverse Transcriptase, and 4.2 μ L of RNase-free water—was added to each tube, vortexed, and centrifuged at 17,000×g for 15 seconds. The tubes were placed in a thermal cycler and subjected to the following cycling conditions: 25 °C for 10 min, 37 °C for 120 min, 85 °C for 5 min, and then held at 4 °C. Synthesised cDNA was stored at -80 °C for later use.

2.2.7.4 Quantitative Real-Time PCR (qPCR)

Quantitative real-time PCR (qPCR) was performed to assess the expression of target genes using TaqMan probes and TaqMan Universal PCR Master Mix (Thermo Fisher Scientific). Each 10 μL reaction in a 384-well plate contained 2 μL of cDNA, 1 μL of the specific TaqMan gene expression assay (Table 2-5), 2 μL of nuclease-free water, and 5 μL of master mix. All reactions were prepared in triplicate, sealed with optical adhesive film, centrifuged at 2,000 × g for 5 minutes, and analysed using the QuantStudio[™] 7 Flex Real-Time PCR System. The thermal profile included an initial denaturation at 95 °C for 10 minutes, followed by 40 cycles of 95 °C for 15 seconds and 60 °C for 1 minute, and a final extension at 55 °C for 80 cycles. Expression data were analysed using the QuantStudio [™] software and normalised to TATA box binding protein (TBP) mRNA, with relative expression levels calculated using the ΔΔCt method (Rao et al., 2013).

Table 2-5 TaqMan probes

TaqMan probe name	Species	Assay ID
Sphingosine kinase 1(SphK1)	Mouse	Mm00448841_g1
TATA box binding protein (Tbp)	Mouse	Mm01277042_m1

2.2.8 Immunofluorescence (IF)

Immunofluorescence was performed to visualize the presence of the enzyme sphingosine kinase in cultured cells under the microscope. MEF cells were grown on 6 well plates containing sterilised 13 mm diameter glass coverslips. Coverslips of MEF cells were washed with cold PBS and fixed in 4% (w/v) paraformaldehyde (Santa Cruz, USA) for 20 minutes at room temperature. The coverslips were then washed three times in PBS and incubated in quenching buffer (50 mM NH₄Cl in PBS) for 10 minutes, washed again three times in PBS before incubating them in permeabilization buffer (0.1% (w/v) Triton X-100 in PBS) for 20 min. After washing three times in PBS, they were blocked in immunofluorescence (IF) buffer (PBS containing 0.1% (v/v) donkey serum) for 30 minutes. MEFs were then incubated at room temperature overnight in permeabilization media (PBS containing 2% (w/v) BSA, 0.1% (w/v) saponin, 20 mmol/L glycine). SphK1 primary antibody (Santa Cruz, sc-365401, dilution 1:100) was prepared in IF buffer, then added to the coverslips and these were then incubated overnight at room temperature. Next day, the coverslips were then washed in IF buffer three times and further incubated in Alexa Fluor® 594-conjugated anti-mouse IgG secondary antibody (diluted in IF buffer (1:100), Invitrogen) for 1 hour at room temperature. Cells were then triple washed three times with PBS. The coverslips were then incubated overnight in VECTASHILD Antifade mounting Medium with DAPI (Vector Laboratories) to stain the nuclei. The slides were then visualised by utilising a Ziess LSM 880 confocal microscope equipped with a 63x oil immersion objective lens.

2.2.9 Statistical analysis

All data are presented as a relative change (mean ± SEM) from the control baseline or normalized to the reference group for each experiment, as specified. Statistical analyses were conducted using Prism software (GraphPad Software). Depending on the requirements of the experiment, Student's t-tests, and one or two-way ANOVA (with Tukey's multiple comparison tests, respectively) were performed. A p-value <0.05 was considered statistically significant. In this study, N refers to the number of independent experiments from which tissues or cells were obtained.

Chapter 3 -Characterisation of Sphingosine Kinase1 (SphK1) Expression in Mouse Adipose & Perivascular Adipose Tissues (PVAT)- Effect of AMPKα1 Knockout (KO)

3.1 Introduction

Sphingosine kinases (SphKs) are lipid kinases responsible for catalysing the phosphorylation of sphingosine to produce sphingosine-1-phosphate (S1P), representing one of the primary enzymatic pathways for S1P biosynthesis (Wattenberg et al, 2006). SphKs exist in two isoforms, SphK1 and SphK2, both of which catalyse the conversion of sphingosine into S1P. This phosphorylated lipid acts as a multifunctional signalling molecule implicated in key cellular processes, including cell proliferation, migration, and survival (Cannavo et al, 2017). SphK1 is closely associated with assisting cell survival, proliferation, and inflammation, whereas SphK2 associates more with apoptosis, mitochondrial function, and epigenetic regulation (Alkafaas, 2024).

Recent studies have highlighted the complex role of SphK1 in adipogenesis, inflammation, and insulin sensitivity, positioning it as a potential therapeutic target for metabolic disorders (Anderson et al, 2020). In particular, SphK1 expression is significantly upregulated during adipocyte differentiation. A study using 3T3-L1 cells revealed a 37.6-fold increase in SphK1 expression, along with a 6.6-fold increase in SphK2 expression, as the cells differentiated into adipocytes (Hashimoto et al, 2009). Additionally, inhibition of SphK1 attenuates adipocyte differentiation, suggesting its importance in adipogenesis (Mastrandrea, 2013). S1P produced by SphK1 mediates its effects through G protein-coupled receptors (GPCR), which regulate key cellular functions. GPCRs are widespread on eukaryotic cells, including adipocytes. During adipocyte differentiation, the expression levels of GPCRs can undergo significant change; to illustrate, some are upregulated or downregulated depending on what stage of differentiation has been reached and also on the type of adipocyte, i.e., whether white, brown or beige (Im et al., 2021). However, the role of SphK1 in adipose tissue appears to be context-dependent (Chun et al, 2002). For instance, Under physiological conditions, SphK1 contributes to adipocyte homeostasis, as evidenced by findings that adipocyte-specific deletion of SphK1 leads to marked adipocyte hypertrophy and dysregulation of genes involved in lipid metabolism and mature adipocyte function (Lambert, 2021). However, in the context of obesity, SphK1 expression is significantly upregulated in adipose tissue from both diet-induced obese mice and obese individuals with type 2 diabetes (Wang et al, 2014). This paradoxical increase suggests that while SphK1 is necessary for normal adipocyte development, its overactivation during metabolic stress may contribute to adipose tissue dysfunction and inflammation (Chun et al., 2002), highlighting a potentially dual role depending on metabolic context.

SphK1 has also been implicated in adipose tissue inflammation and insulin resistance. Studies have shown that the genetic deletion or pharmacological inhibition of SphK1 in obese mouse models reduces adipose tissue macrophage infiltration, lowers the expression of pro-inflammatory cytokines, and improves insulin sensitivity (Ross et al, 2013; Wang et al, 2014). These findings suggest that SphK1 may be a critical mediator of obesity-related inflammation and metabolic dysfunction.

AMPK is a heterotrimeric serine/threonine kinase that acts as a cellular energy sensor, regulating various metabolic pathways to maintain energy balance (Hardie, 2011). Structurally, AMPK consists of three subunits: a catalytic alpha subunit, and regulatory beta and gamma subunits. These subunits form different isoforms that are expressed across a variety of tissues (Hawley et al, 1996). All cell types express AMPK in one form or another, but the AMPKα1 isoform has a vital function in the regulation of cellular energy metabolism and is notably active in cells where energy demand is not constant, such as adipocytes, muscle cells, liver cells and others. AMPKα1, predominantly expressed in mouse tissues (Yang et al, 2010) and human endothelial cells (Schulz et al, 2005), plays a key anti-inflammatory role by protecting endothelial cells from inflammatory stimuli (Salt & Palmer, 2012). This is done through several mechanisms, such as inhibiting NF-κB signalling, thereby reducing the expression of pro-inflammatory genes (Zhang et al., 2011), and modulating cytokine production, thus lowering inflammatory responses (Mancini and Salt, 2018).

In a previous study, our laboratory conducted research on the impact of a high-fat diet (HFD) on wild-type (WT) and AMPKα1 knockout (KO) mice, focusing on perivascular adipose tissue (PVAT). The findings indicate that in mice lacking AMPKα1, there was an increased infiltration of macrophages into PVAT, present even in the absence of HFD. Feeding wild-type mice HFD led to increased inflammatory cell infiltration of the PVAT and the conclusion was that deletion of the AMPK isoform phenocopies some of the effects of HFD in the PVAT (Almabrouk

et al, 2018). This underscores the critical role of AMPKα1 in modulating inflammation and maintaining PVAT homeostasis, particularly under metabolic stress caused by HFD. In obesity, adipose tissue inflammation is often associated with elevated levels of pro-inflammatory cytokines such as tumour necrosis factoralpha (TNF-α), interleukin-1 beta (IL-1β), and interleukin-6 (IL-6) (Lee et al, 2009). These cytokines drive chronic inflammation by activating key signalling pathways, including nuclear factor kappa B (NF-κB) and mitogen-activated protein kinases (MAPKs) (Salt & Palmer, 2012). Notably, SphK1 and its product S1P, are central to the activation of several signalling pathways, including the MAPK pathways (ERK, p38, JNK), and the AKT pathway (Kluk & Hla, 2002). The interplay between these signalling cascades and both AMPK and SphK1 signalling suggests a complex regulatory network in adipose tissue homeostasis. Elucidating the interplay between these signalling cascades could provide a more comprehensive understanding of adipose tissue biology and perhaps ultimately identify therapeutic targets in cardiometabolic disease.

3.2 Aim and Objectives

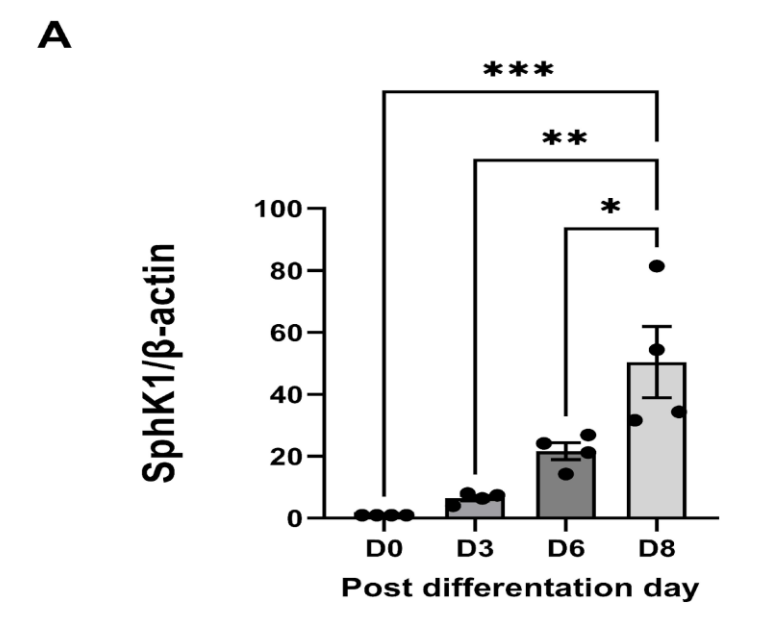
Although AMPK is a central regulator of adipose tissue metabolism, its influence on SphK1 expression and associated signalling pathways is not well defined. This chapter seeks to characterise the regulatory role of AMPK in modulating SphK1 expression and downstream signalling in both adipose tissue and cultured adipocyte cells. The specific objectives are as follows:

- 1. To characterize the expression profile of SphK1 throughout the process of 3T3-IL adipocyte differentiation.
- 2. To investigate the effects of deficiency of both AMPK α 1 and α 2 on SphK1 expression at both the mRNA and protein levels in Mouse Embryonic Fibroblast (MEF) cells.
- 3. To evaluate the consequences of AMPK α 1 and α 2 knockout on the activation of ERK1/2 and JNK signalling pathways in MEF cells, with an emphasis on their potential interaction with SphK1 expression.
- 4. To explore the effects of global AMPKα1 deficiency on SphK1 expression in PVAT from mouse abdominal and thoracic aorta.

3.3 Results

3.3.1 Sphingosine Kinase1 (SphK1) protein level in 3T3-1L adipocytes during differentiation

This experiment was designed to confirm the expression of SphK1 in an adipose tissue-derived cell line and to investigate how its expression changes during the differentiation of preadipocytes into mature adipocytes. The differentiation process, which is induced using a standard chemical induction cocktail, is described in detail in the Methods chapter. Cells were harvested and lysed to produce protein samples at distinct time points: day 0, day 3, day 6, and day 8. The samples were analysed for protein content and subjected to immunoblotting analysis to assess SphK1 expression throughout the adipogenic process. The results demonstrated a pronounced, time-dependent increase in SphK1 protein levels, with peak expression observed on day 8, where it was significantly elevated (***P<0.001) compared to day 0 and also to day 3 (**P<0.01). A significant increase (*P<0.05) in SphK1 levels was also observed between days 6 and 8 (Figure 3-1).



В

D0 D3 D6 D8

34 KDa SphK1

42 KDa β-actin

Figure 3-1: Expression of Sphingosine Kinase 1 (SphK1) during 3T3-L1 adipogenesis.

Preadipocytes from the 3T3-L1 cell line were induced to differentiate into mature adipocytes using the protocol described in the Methods section (Section 2.2.5.4). Cell lysates were collected at specific time points during the differentiation process (day 0, 3, 6 and 8) and resolved by SDS-PAGE, followed by immunoblotting, using specific antibodies against SphK1. Panels (A) and (B) represent a quantitative graph and a representative immunoblotting image respectively, illustrating the temporal changes in SphK1 protein expression throughout the adipogenic process. SphK1 protein levels were normalized to the level of B-actin for an accurate comparison. The data shown represent the mean \pm SEM of 4 independent experiments. Statistical significance was assessed using one-way ANOVA followed by a Tukey test, with significance levels indicated by asterisks (*P < 0.05, **P < 0.01, ***P < 0.001).

3.3.2 Investigation of Sphingosine Kinase 1 (SphK1) gene and protein expression in AMPKα1, α2 Knockout Mouse Embryonic Fibroblast (MEF) Cells

Based on the observed increase in SphK1 expression during adipogenesis, between day 3 and day 8 (Figure 3-1), it was essential to further investigate the regulatory mechanisms that influence SphK1 expression in cells. To gain a deeper understanding of this regulation, the role of AMPK in modulating SphK1 expression was examined. In order to do this, a comparison was made between SphK1 gene and protein expression in WT MEF cells and AMPKa1 & a2 KO MEF cells.

mRNA was extracted from WT and KO MEF cells and subsequently analyzed by quantitative PCR (qPCR), as detailed in the methodology section. The analysis of SphK1 gene expression revealed no statistically significant difference between AMPKα1 & α2 KO MEFs and WT controls.

The protein levels of SphK1 in WT and KO MEF cells were analyzed through Western blotting, as described in the methodology section. The presence of AMPK activity was confirmed by examining the phosphorylation status of its substrate, ACC at Ser79, which was also used to validate the genotype of the cells. Consistent with expectations, the phosphorylation of ACC (pACC) was significantly higher in WT cells and almost absent in AMPK α 1 & α 2 KO cells (**P<0.01), indicating virtually no AMPK activity in KO cells. Notably, SphK1 protein expression was significantly elevated in KO cells compared to WT cells (**P<0.01) (Figure 3-2).

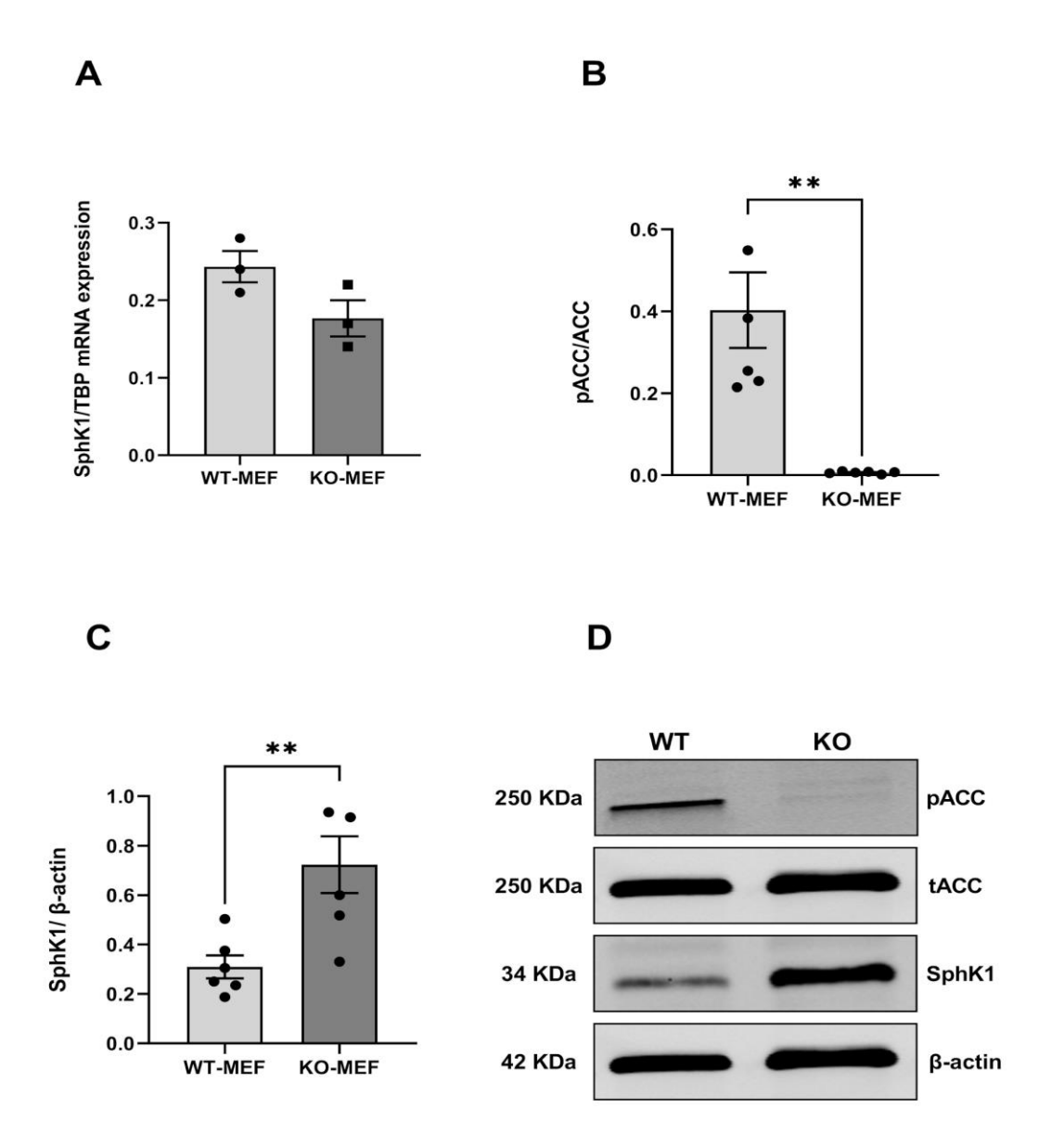


Figure 3-2: Gene and protein expression of SphK1 in MEF cells.

Wild-type (WT) and AMPK α 1 & α 2 knockout (KO) MEF cells were cultured, and cell lysates were extracted for analysis. Panel (A) displays SphK1 mRNA expression, quantified by qPCR and normalized to TATA-box binding protein (TBP) expression, with no significant differences observed (N=3). Panel (B) presents analysis of ACC phosphorylation at Ser79 (pACC S79), assessed by Western blotting of cell lysates and normalized to total ACC levels, revealing a significant reduction in pACC levels in KO cells compared to WT cells (**P < 0.01, N=6). Panel (C) illustrates SphK1 protein expression, analyzed by immunoblotting and normalized to β -actin levels, showing a significant increase in SphK1 protein in KO cells compared to WT control (**P < 0.01, N=6). Panel (D) representative immunoblotting images. All data are expressed as the mean \pm SEM, with statistical significance determined via an unpaired t-test.

3.3.3 Visualization of Sphingosine Kinase 1 (SphK1) via Immunofluorescence in Wild-Type and AMPKα1/α2 Knockout Mouse Embryonic Fibroblasts (MEF) Cells

The elevation of SphK1 protein expression in AMPK α 1 & α 2 KO MEFs compared to WT MEFs (Figure 3-2) was further investigated using immunofluorescence analysis followed by confocal microscopy. In this experimental setup, WT and AMPK α 1/ α 2 KO MEF cells were cultured on coverslips and subsequently incubated with a primary antibody specific to SphK1, followed by incubation with an Alexa Fluor® 594-conjugated anti-mouse IgG secondary antibody. They were then processed according to the detailed immunofluorescence protocol described in the Methods section.

In line with the findings from SphK1 protein expression, confocal microscopy revealed a markedly higher expression of SphK1 in AMPK α 1 & α 2 KO cells compared to WT cells. The fluorescence intensity corresponding to SphK1 was significantly elevated in the KO MEFs, providing a clear visualization of this upregulation. Statistical validation of these results demonstrated a highly statistically significant difference in SphK1 expression between the KO and WT MEF cells (****P<0.001) (Figure 3-3).

Α SphK1 Merged Control WT-MEF Control **KO-MEF**

В

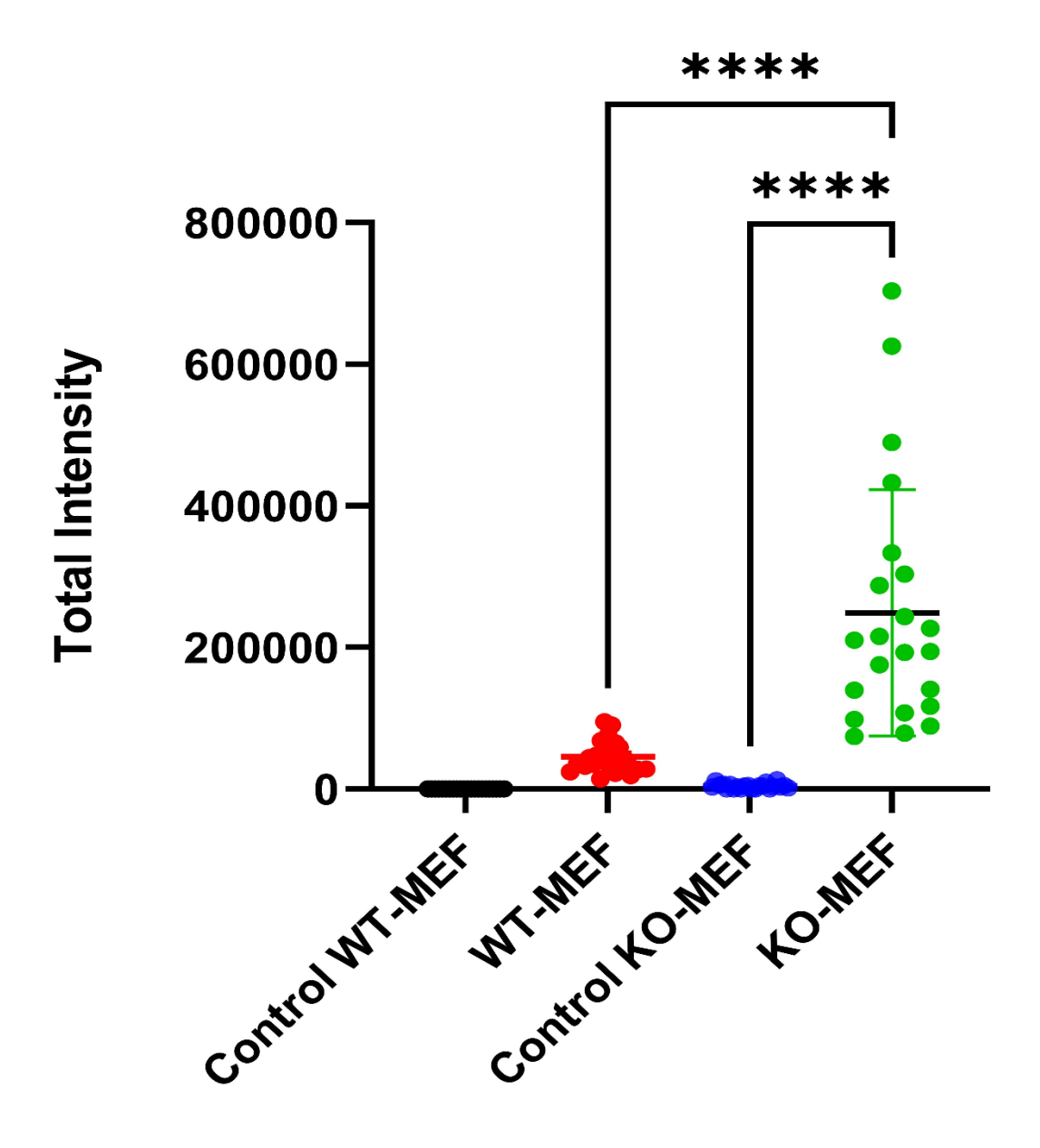


Figure 3-3: Immunofluorescence confocal microscopy of SphK1 in MEF cells.

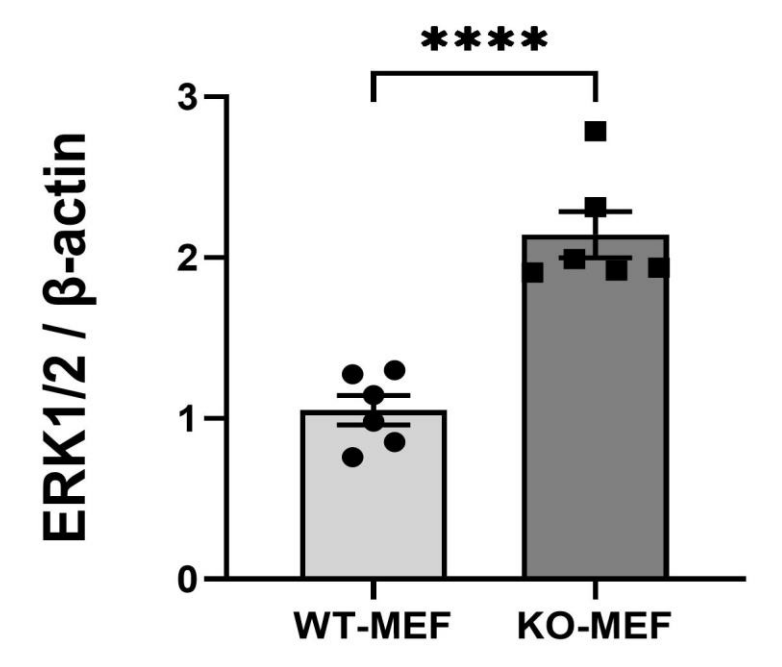
Wild-type (WT) and AMPK α 1 & α 2 MEF cells were cultured to investigate the expression levels of SphK1. To visualize the localization and expression of SphK1, coverslips containing MEF cells were incubated with specific SphK1 antibodies and analyzed using immunofluorescence confocal microscopy. Panel (A) gives representative confocal micrographs showing SphK1 immunofluorescence in WT and AMPK α 1/ α 2 KO MEF cells. DAPI was used to stain cell nuclei. The images reveal increased fluorescence intensity observed in AMPK α 1/ α 2 KO cells, consistent with elevated SphK1 protein levels. Images were acquired using a Zeiss LSM confocal microscope at 63× magnification. Scale bar = 20 μ m. Panel (B) graphically summarises data from five independent experiments, with 22 cells analyzed in each group (****P < 0.001). The results are expressed as the mean ± SEM, and statistical significance was determined using a one-way ANOVA (Tukey test).

3.3.4 Effect of AMPKα1/α2 Knockout Mouse Embryonic Fibroblasts (MEF) Cells on ERK1/2 Protein Levels

Given that SphK1 protein levels were significantly elevated in AMPK α 1 & α 2 KO cells compared to WT cells (Figure 3-2), it would be important to explore how the absence of AMPK α 1 & α 2 further affects SphK1 function. Since ERK activation is necessary for SphK1 activation, which in turn increases S1P levels (Pitson et al, 2003), we next investigated the role of AMPK in modulating ERK1/2 protein levels. Specifically, we compared ERK1/2 protein levels between WT and AMPK α 1/ α 2 KO MEF cells.

Western blot analysis on both WT and AMPK α 1/ α 2 KO MEF cells was used to assess ERK1/2 protein levels, as detailed in the methodology section. The results showed that ERK1/2 activation was significantly higher in AMPK α 1/ α 2 KO cells compared to WT cells (****P<0.001). These findings are consistent with the observed increase in SphK1 expression in KO cells, and support the interconnected roles of AMPK, ERK1/2, and SphK1 in cellular signalling pathways in adipocytes (Figure 3-4).

Α



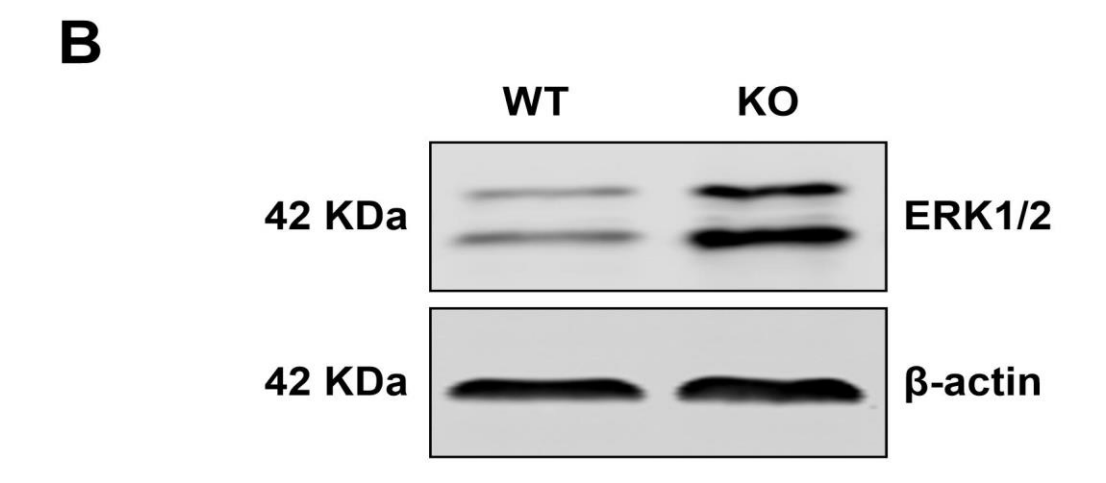


Figure 3-4: Protein levels of ERK1/2 in MEF cells.

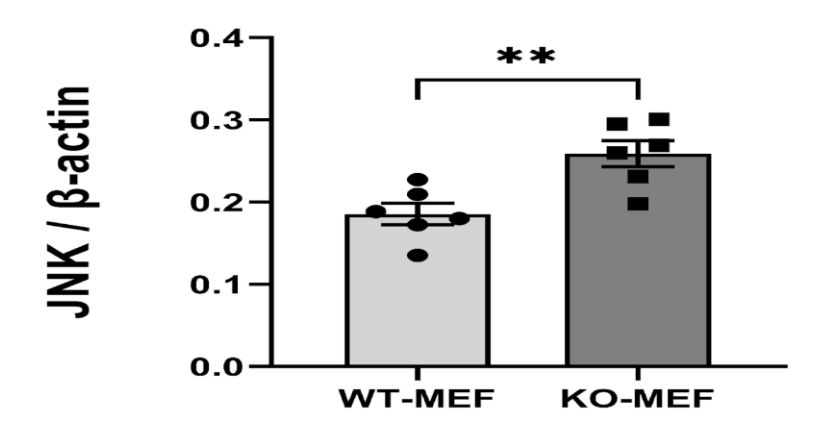
Wild-type (WT) and AMPK α 1/ α 2 knockout (KO) MEF cells were cultured, and cell lysates were collected for subsequent analysis. Panel (A) presents the levels of ERK1/2 protein, which were assessed by immunoblotting and normalized to β -actin levels. The results indicate a significant increase in ERK1/2 protein in KO cells compared to WT controls (****P < 0.001, N=6). Panel (B) displays representative immunoblotting images. Data are presented as the mean \pm SEM, with statistical significance determined using Prism Software via an unpaired t-test.

3.3.5 Effect of AMPKα1/α2 Knockout in Mouse Embryonic Fibroblasts (MEF) cells on JNK protein levels

Given the significant elevation of SphK1 and ERK1/2 protein levels in AMPK α 1/ α 2 KO cells compared to WT cells (Figure 3-2 and Figure 3-4), a further exploration of the impact of AMPK α 1/ α 2 deficiency on other inflammatory pathways was merited. AMPK is known to exhibit protective, anti-inflammatory effects in endothelial cells when exposed to inflammatory factors (He et al, 2015). Reduced AMPK activity has been associated with increased inflammation in adipose tissues (Almabrouk et al, 2018). To understand the role of AMPK in modulating other inflammatory pathways such as MAPK, we investigated the expression of JNK protein levels in WT and KO MEF cells.

Western blot analysis was performed on lysates from both WT and AMPK α 1/ α 2 KO MEF cells, as described in the methodology section. The results revealed that JNK activation was significantly higher in AMPK α 1/ α 2 KO cells compared to WT cells (**P<0.01). These findings align with the observed increases in SphK1 and ERK1/2 expression in KO cells and suggest a broader impact of AMPK deficiency on MAPK signalling pathways (Figure 3-5).

A



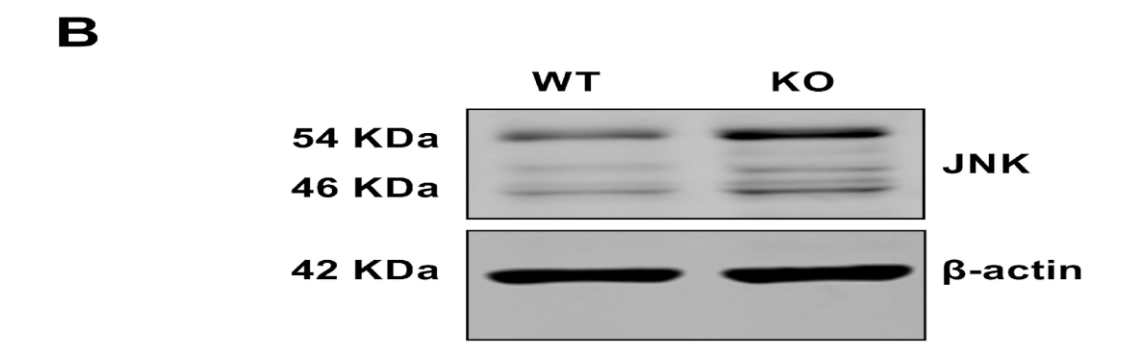


Figure 3-5: Protein levels of JNK in MEF cells.

Wild-type (WT) and AMPK α 1/ α 2 knockout (KO) MEF cells were cultured, and cell lysates were prepared for analysis. Panel (A) shows the JNK protein levels, which were measured by immunoblotting and normalized to β -actin levels. The results demonstrate a significant increase in JNK protein levels in KO cells compared to WT controls (**P < 0.01, N=6). Panel (B) provides representative images of the immunoblots. Data are expressed as the mean \pm SEM, with statistical significance assessed using an unpaired t-test.

3.3.6 Expression of Sphingosine Kinase 1 (SphK1) Gene and Protein in abdominal aortic PVAT of Mice.

To assess if the changes observed in SphK1 protein levels in KO MEF cells were also present in a more physiologically representative tissue and the role that AMPK plays in nay effects seen, we then studied SphK1 expression in mouse perivascular adipose tissue (PVAT). Specifically, we compared the expression of the SphK1 gene and protein in the abdominal aortic PVAT of WT and AMPKα1 KO mice.

mRNA was extracted from the abdominal PVAT of WT and AMPKα1 KO mice, and quantitative PCR (qPCR) was performed as described in the methodology section. The analysis revealed no statistically significant difference in SphK1 gene expression between AMPKα1 KO mice and WT controls.

Additionally, the protein expression of SphK1 in the abdominal PVAT of WT and AMPKα1 KO mice was assessed via Western blotting, following the procedures detailed in the methodology section. The activity of AMPK in abdominal PVAT was verified by examining the phosphorylation of AMPK at Thr172, which confirmed the genotype of the PVAT samples. As expected, the phosphorylation of AMPK (pAMPK) was significantly higher in WT PVAT than in AMPKα1 KO PVAT (*P<0.05). However, similar to the qPCR results, there was no statistically significant difference in SphK1 protein expression levels between AMPKα1 KO and WT abdominal PVAT (Figure 3-6).

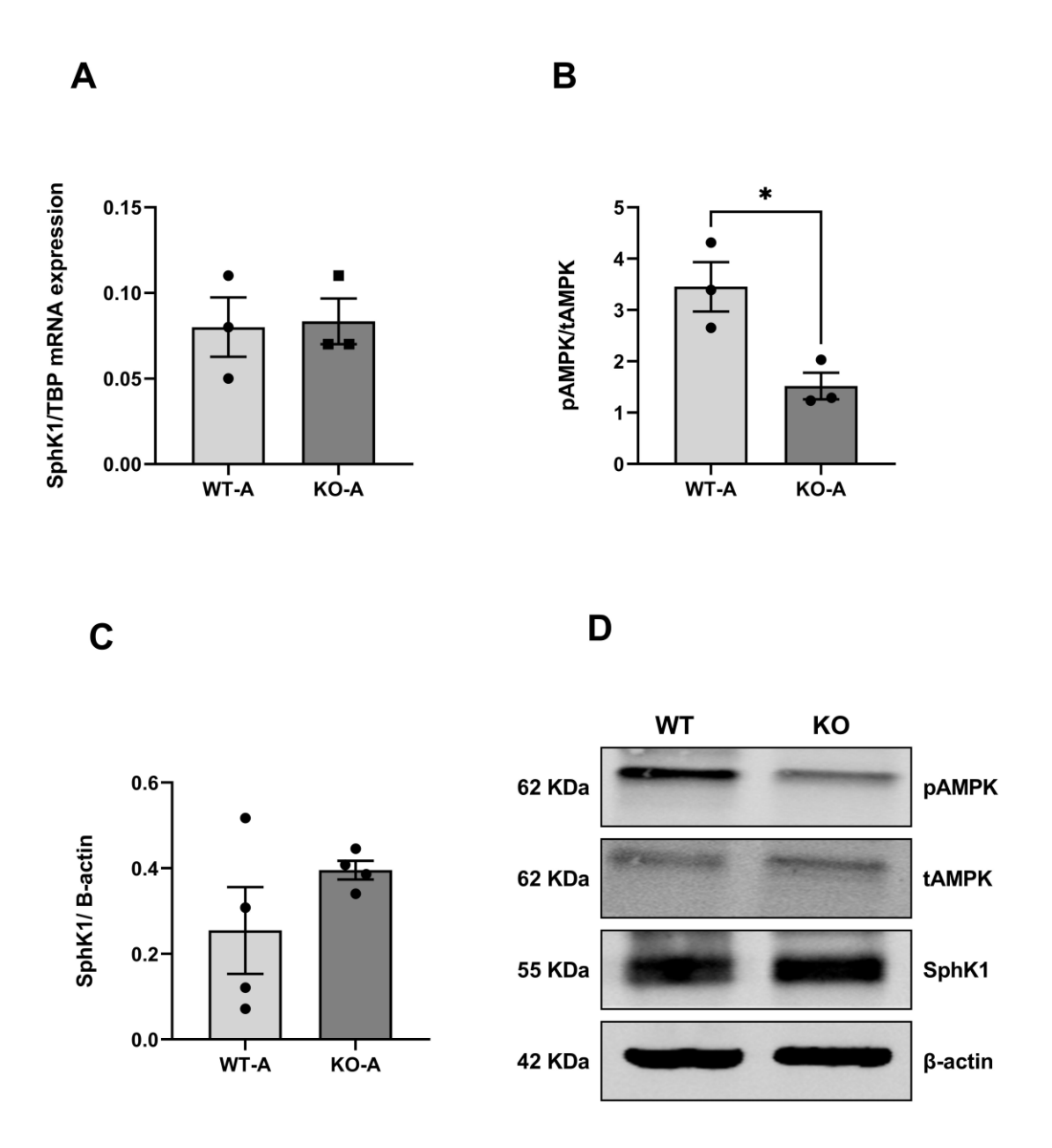


Figure 3-6: Gene and protein expression of SphK1 in abdominal aortic PVAT of mice.

Wild-type (WT) and AMPK α 1 knockout (KO) perivascular adipose tissue (PVAT) was isolated from the abdominal aortic region of mice, and lysates were prepared for further analysis. Panel (A) depicts the expression of SphK1 mRNA, as quantified by qPCR, with normalization to TATA-box binding protein (TBP) expression. The results indicate no significant differences between the WT and KO groups (N=3). Panel (B) shows the analysis of AMPK phosphorylation at Thr172 (pAMPK Thr172), which was evaluated via Western blotting of cell lysates and normalized to total AMPK levels. The findings demonstrate a significant reduction in pAMPK levels in KO PVAT compared to WT (*P < 0.05, N=3). Panel (C) presents the analysis of SphK1 protein expression, which was assessed by immunoblotting and normalized to β -actin levels. As with the mRNA results, no significant differences were observed between the genotypes (N=4). Panel (D) provides representative images from the immunoblotting experiments. All data are expressed as the mean \pm SEM, with statistical significance determined using an unpaired t-test.

3.3.7 Gene and Protein Expression of Sphingosine Kinase1 (SphK1) in Thoracic Aortic PVAT of AMPKα1 Deficient Mice

Since there is a difference in the brown to white adipose ratio between abdominal and thoracic aortic PVAT, we decided to repeat the gene and protein experiments using samples of PVAT from WT and KO mouse thoracic aorta.

RNA was extracted from the thoracic PVAT of WT and AMPKa1 KO mice, and quantitative PCR (qPCR) was conducted as outlined in the methodology section. The analysis revealed no statistically significant difference in SphK1 gene expression between the AMPKa1 KO mice and WT controls.

Protein levels of SphK1 in the thoracic PVAT of WT and AMPK α 1 KO mice were evaluated through Western blotting, following the procedures described in the methodology section. The activation of AMPK by phosphorylation at Thr172, was used to confirm the genotype of the PVAT samples. As anticipated, the phosphorylation of AMPK (pAMPK) was significantly higher in WT PVAT compared to AMPK α 1 KO PVAT (*P<0.05).

In contrast to the abdominal aortic PVAT where there was no difference in SphK1 protein expression, KO thoracic aortic PVAT showed a significantly higher SphK1 protein expression (**P<0.01) (Figure 3-7). This is in agreement with what was found in the MEF cells when AMPK α 1/ α 2 was deleted (Figure 3-2).

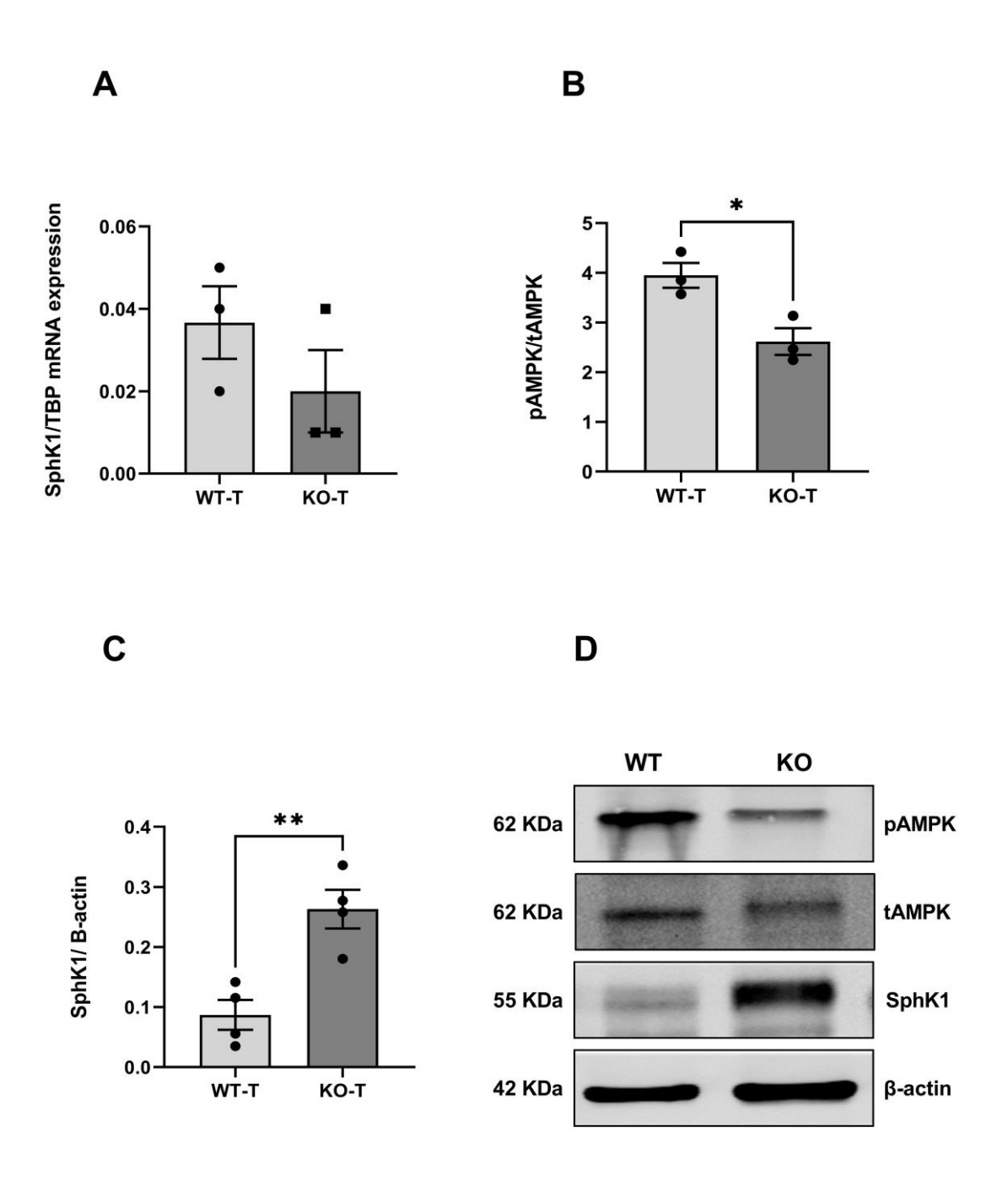


Figure 3-7: Gene and protein expression of SphK1 and pAMPK in thoracic aortic PVAT of mice.

Wild-type (WT) and AMPK α 1 knockout (KO) perivascular adipose tissue (PVAT) was isolated from the thoracic aorta of mice, and lysates were prepared for analysis. Panel (A) shows SphK1 mRNA expression, quantified by qPCR and normalized to TATA-box binding protein (TBP) levels. The results indicate no significant differences between WT and KO PVAT mice (N=3). Panel (B) presents the analysis of AMPK phosphorylation at Thr172 (pAMPK Thr172), assessed by Western blotting of cell lysates and normalized to total AMPK levels. A significant reduction in pAMPK levels was observed in KO PVAT compared to WT PVAT (*P < 0.05, N=3). Panel (C) illustrates SphK1 protein expression, analyzed by immunoblotting and normalized to β -actin levels. The results demonstrate a significant increase in SphK1 protein levels in KO PVAT compared to WT PVAT samples (**P < 0.01, N=4). Panel (D) provides representative immunoblotting images. All data are expressed as the mean \pm SEM, with statistical significance determined using Prism Software via an unpaired t-test.

3.4 Discussion

The results presented in this chapter indicate that SphK1 protein levels increased significantly during differentiation of 3T3 adipocytes, peaking at day 8 (Figure 3-1). In terms of the involvement of AMPK, the data showed that in AMPK α 1/ α 2 knockout (KO) MEF cells, SphK1 protein expression was significantly higher compared to wild-type (WT) cells, despite no difference in gene expression (Figure 3-2). Furthermore, in KO MEF cells the fluorescence intensity associated with SphK1 was significantly increased and appeared to show a cytoplasmic distribution. This finding further confirms the upregulation of SphK1 in the absence of AMPK α 1/ α 2 (Figure 3-3). Similarly, ERK1/2 and JNK activation were significantly elevated in AMPK α 1/ α 2 KO MEF cells (Figure 3-4 and 3-5). Using mouse perivascular adipose tissue (PVAT), the relationship between SphK1 and AMPK was found to be tissue specific. Abdominal PVAT showed no significant differences in SphK1 gene or protein expression between AMPKa1 KO and WT mice (Figure 3-6) while in thoracic PVAT, SphK1 protein levels were significantly higher in AMPKα1 KO mice compared to WT, despite no difference in gene expression (Figure 3-7). These findings provide important insights into the complex relationship between AMPK and sphingosine kinase 1 across various cellular and tissue contexts, with potential implications for the regulation of adipose tissue function and inflammation. This would include processes such as adipocyte differentiation and inflammatory signalling pathway modulation within adipose tissue. These findings contribute to a deeper understanding of the crosstalk between these key metabolic regulators and raises key questions about the role that these pathways play in PVAT and adipose function, which will be further investigated in subsequent chapters.

During adipogenesis, a time-dependent increase in SphK1 protein levels was observed, aligning with the findings of Hashimoto et al,.(2009) who reported a progressive induction of SphK1 protein expression in 3T3-L1 cells during differentiation. In their study, SphK1 protein levels began to rise noticeably from day 3 and reached a peak around day 8. This pattern aligns with the present findings, in which SphK1 protein expression reached its highest level by day 8, which was the final time point assessed. This selection was based on the well-established completion of 3T3-L1 adipocyte differentiation at this stage, as

reported by Hashimoto et al. (2009). Further supporting the role of SphK1 as a key mediator of adipocyte maturation and metabolic function. This suggests that SphK1 plays a fundamental role in regulating the developmental processes necessary for fully functional adipocytes, contributing to lipid storage and metabolic activity (Mastrandrea, 2013). To further explore the role of SphK1 in adipogenesis, future studies could employ pharmacological inhibitors or siRNAmediated knockdown of SphK1 during the differentiation of preadipocytes. The effects on adipocyte development could be assessed by examining the expression of key adipogenic markers, such as PPARy, C/EBPα, and aP2, in addition to evaluating lipid droplet formation. These strategies would help determine whether SphK1 is required at the initiation of differentiation, during its progression, or throughout the entire process. Moreover, these data could provide valuable insights into the signalling pathways through which SphK1 regulates adipocyte differentiation. These findings reinforce the significance of SphK1 in adipogenesis, pointing to its potential as a target for modulating adipocyte differentiation and metabolic health in the context of obesity and related diseases.

Regarding AMPK regulation of SphK1 in MEF cells, one of the study's key observations is the substantial increase in SphK1 protein levels in AMPKα1/α2 KO MEFs, despite unchanged SphK1 gene expression. This finding suggests a posttranscriptional regulatory mechanism by which AMPK modulates SphK1, possibly influencing its protein stability or translation efficiency (Wang et al, 2014). The discrepancy between protein and mRNA levels highlights the importance of posttranscriptional modifications in SphK1 regulation, a crucial aspect that necessitates further investigation. To further investigate the post-transcriptional regulation of SphK1 by AMPK, future studies could employ cycloheximide, a wellestablished protein synthesis inhibitor, to measure the degradation rate of SphK1 protein in WT and AMPK-deficient MEF cells. If SphK1 degrades more slowly in the knockout cells, this would suggest that AMPK plays a role in promoting its turnover. In addition, to explore whether AMPK affects SphK1 at the level of translation. methods such as polysome profiling or ribosome footprinting could be used to assess the efficiency of SphK1 mRNA translation. Together, these approaches would help clarify whether AMPK regulates SphK1 expression by influencing protein degradation, translation, or both, thereby providing deeper insight into

the mechanisms involved. Understanding this regulatory layer is essential for fully elucidating AMPK's influence on SphK1 and its broader role in adipocyte function and metabolism.

The simultaneous upregulation of SphK1, ERK1/2, and JNK observed in AMPK α 1/ α 2 KO MEF cells provides strong evidence of a regulatory crosstalk between AMPK and MAPK signalling pathways. The activation of ERK1/2, which is required for SphK1 activation (Pitson et al, 2003), highlights the interconnected nature of these pathways, suggesting that AMPK may exert control over SphK1 through MAPK signalling. Furthermore, the increased activation of JNK in AMPK-deficient cells points to a pro-inflammatory state, consistent with AMPK's well-documented anti-inflammatory effects (Salt & Palmer, 2012). This result supports the hypothesis that SphK1 may contribute to inflammatory signalling in the absence of AMPK, potentially through enhanced MAPK pathway activation.

A key finding of this study is the tissue-specific regulation of SphK1 by AMPK in PVAT. In AMPKα1 KO mice, SphK1 protein expression was significantly elevated in thoracic PVAT, while it remained unchanged in abdominal PVAT. This difference likely reflects the distinct metabolic and inflammatory characteristics of these depots. Thoracic PVAT shares several features with brown adipose tissue (BAT), including high mitochondrial density and thermogenic capacity (Fitzgibbons et al., 2011). BAT-like adipose depots are highly metabolically active and rely on AMPK signalling to maintain mitochondrial function, regulate adipogenic transcription factors, and suppress inflammatory responses (Wang et al., 2021). Supporting this, Yang et al. (2016) demonstrated that AMPK α 1 ablation in neonatal mice led to reduced BAT mass, decreased UCP1 expression, and lower mitochondrial content, highlighting the importance of AMPKα1 in BAT development and functionality. In contrast, abdominal PVAT more closely resembles white adipose tissue (WAT), which is primarily involved in lipid storage and exhibits a different metabolic profile (Szasz and Webb, 2012). The absence of AMPKα1 in thoracic PVAT appears to compromise its anti-inflammatory regulatory function, resulting in the upregulation of sphingosine kinase 1 (SphK1), a kinase known to promote proinflammatory signalling. This aligns with the findings of Gabriel et al. (2017), who reported that SphK1 expression is elevated in adipose tissue macrophages and contributes to inflammation, particularly under lipotoxic conditions. Supporting this notion, Almabrouk et al. (2018) demonstrated increased infiltration of inflammatory cells in the thoracic PVAT of AMPKα1 knockout mice, further indicating a shift toward a pro-inflammatory phenotype in the absence of AMPKα1. Collectively, these findings suggest that AMPKα1 deficiency disrupts PVAT homeostasis, potentially through enhanced SphK1 expression and activation of downstream mitogen-activated protein kinase (MAPK) pathways, including ERK1/2 and JNK, both of which were upregulated in the present study. The observed post-transcriptional regulation of SphK1 in thoracic PVAT, similar to that seen in MEF cells, further emphasizes the complexity of this regulatory mechanism, underscoring the need to consider depot-specific factors when studying adipose tissue biology.

Implications and Future Directions

This study highlights the depot-specific role of AMPK in regulating SphK1 expression and inflammatory pathways within perivascular adipose tissue. The selective increase of SphK1 in thoracic PVAT following AMPKα1 deletion suggests that AMPK is essential for maintaining an anti-inflammatory state in metabolically active fat depots. These findings point to AMPK-SphK1 signalling as a potential target for preventing PVAT dysfunction and its contribution to vascular inflammation in metabolic disease. The pro-inflammatory state is associated with elevated levels of SphK1, ERK1/2, and JNK in AMPK-deficient conditions. In this study, AMPKα1 deficiency was associated with elevated levels of SphK1, ERK1/2, and JNK, indicating a pro-inflammatory state in perivascular adipose tissue (PVAT). These findings are consistent with those of Almabrouk et al. (2014), who reported that AMPKα1 knockout mice exhibited increased macrophage infiltration, reduced adiponectin secretion, and loss of the anticontractile function of PVAT. These alterations suggest a protective role of AMPK in maintaining PVAT function and suppressing vascular inflammation. Similarly, in human studies, reduced AMPK activity in the visceral adipose tissue of morbidly obese individuals has been linked with increased inflammatory signalling and insulin resistance, emphasising AMPK's relevance in metabolic disease (Gauthier et al., 2011). Furthermore, Mancini and colleagues highlighted the anti-inflammatory role of AMPK, showing that its activation suppresses pro-inflammatory signalling pathways such as NF-kB and JNK in adipose tissue, ultimately reducing cytokine-mediated inflammation (Bijland,

Mancini, and Salt, 2013). Collectively, these findings reinforce the idea that AMPK plays a central role in controlling inflammation in adipose tissues and suggest that therapeutic strategies targeting AMPK-SphK1-MAPK signalling may help counteract inflammation and dysfunction in obesity-related vascular and metabolic disorders.

Future experiments should aim to clarify the link between AMPK, SphK1, and inflammation at both the gene and protein levels. One approach would be to treat adipose-derived cells or cultured PVAT explants with pharmacological AMPK activators (such as AICAR or A-769662) or inhibitors (such as Compound C) and measure changes in SphK1 mRNA and protein expression using quantitative PCR and Western blotting. Similarly, using SphK1-specific inhibitors (e.g., SKI-II) could help assess whether blocking SphK1 reverses inflammation-related changes downstream of AMPK deficiency. Levels of key inflammatory markers such as TNF-α, IL-6, and IL-1β could be assessed in parallel by qPCR and ELISA to establish functional links between AMPK activity, SphK1 regulation, and inflammation. Together, these experiments would provide a clearer understanding of how AMPK modulates SphK1 expression and its contribution to inflammatory responses in adipose tissue.

3.5 Conclusion

This study has revealed complex regulatory interactions between AMPK and SphK1 that are dependent on adipose tissue depot location. These findings suggest that AMPK plays a critical role in maintaining the functional and inflammatory balance of perivascular adipose tissue (PVAT), particularly in thoracic regions. The data highlight the importance of considering depot-specific differences in adipose tissue biology and underscore the involvement of AMPK, SphK1, and MAPK pathways in regulating adipose tissue homeostasis. These regulatory mechanisms are likely to have significant implications for metabolic health and the development of obesity-related disorders. Notably, differences observed between wild-type and AMPKα1 knockout mice were more prominent in thoracic PVAT compared to abdominal PVAT, guiding the direction of subsequent investigations. Building on these findings, the next chapter will focus specifically on thoracic aorta to assess PVAT and its regulation of vascular function using wire myography. These experiments will examine the effect of AMPK activation via AICAR on

endothelial and vascular smooth muscle cell function in thoracic aortic rings. Additionally, the study will investigate whether SphK1 and its product, S1P, affect AMPK activation under these experimental conditions.

Chapter 4 - Investigating the Effect of Sphingosine-1-Phosphate (S1P) and the AMPK Activator AICAR on Perivascular Adipose Tissue (PVAT) Function

4.1 Introduction

The cardiovascular system transports oxygen and nutrients via the heart and an extensive network of blood vessels composed of the endothelium, vascular smooth muscle, and adventitia (Aaronson et al., 2020; Chaudhry et al., 2022). Surrounding these layers, perivascular adipose tissue (PVAT) is increasingly recognised as an active endocrine organ, not just structural support, playing a key role in vascular tone and inflammation (Touyz et al., 2018; Chang et al., 2020). PVAT influences the underlying vasculature through paracrine signalling, releasing bioactive molecules including adipokines, reactive oxygen species (ROS), nitric oxide (NO), and hydrogen sulfide (H₂S) (Szasz & Webb, 2012). In healthy states, PVAT-derived adiponectin and NO help maintain vascular homeostasis by promoting vasodilation and reducing oxidative stress (Xia & Li, 2017; Chen et al., 2003). However, in pathological conditions such as obesity, diabetes, and hypertension, PVAT becomes inflamed and secretes vasoconstrictors and pro-inflammatory cytokines, contributing to vascular dysfunction (Ketonen et al., 2010; Zou et al., 2016; Qi et al., 2018).

Sphingosine-1-phosphate (S1P) is a bioactive lipid that modulates vascular function via binding to five G protein-coupled receptors (S1PR1-S1PR5), which are differentially expressed on endothelial cells, vascular smooth muscle cells (VSMCs), and immune cells (Chun et al., 2002; Peters & Alewijnse, 2007). In the cardiovascular system, S1PR1, S1PR2, and S1PR3 are the predominant subtypes with distinct cellular distributions and roles (Constantinescu et al., 2022; Wang et al., 2023). For instance, S1PR1 is largely found in cardiomyocytes, S1PR3 in cardiac fibroblasts, and S1PR2 in both cell types (Cannavo et al., 2017). S1P signalling modulates endothelial barrier integrity (Wilkerson and Argraves, 2014), angiogenesis (ArgravesWilkerson and Argraves, 2010), immune cell trafficking (Cartier and Hla, 2019), and vascular tone (Igarashi and Michel, 2009). S1P signalling can mediate both vasoconstriction and vasodilation, depending on the receptor subtype, vascular bed, and other signalling mediators (WaeberBlondeau and Salomone, 2004). Additionally, S1P influences the secretion of PVAT-derived factors, such as adipokines and NO, which are crucial for maintaining vascular homeostasis (DantasIgarashi and Michel, 2003).

Numerous selective small-molecule agonists have been developed to study S1P receptor subtype-specific functions in vascular biology. SEW2871 selectively targets S1PR1, while CYM54 and CYM55 are used to activate S1PR2 and S1PR3, respectively. These pharmacological tools facilitate the dissection of receptor-specific signalling pathways involved in S1P-mediated vascular responses. Further details on their specificity and mechanisms are discussed in Section 1.5.1.3 of the general introduction.

AMPK contributes to aortic relaxation by phosphorylating AMPKα1 in vascular smooth muscle, a process regulated by upstream kinases such as liver kinase B1 (LKB1) and Ca²⁺/calmodulin-dependent protein kinase kinase 2 (CaMKK2), which respond to shifts in cellular energy status. Importantly, smooth muscle contraction and relaxation are closely linked to the phosphorylation state of the myosin regulatory light chain (MLC) (Goirand et al., 2007). Studies with AMPKα1 knockout (KO) mice have demonstrated that vascular relaxation responses are significantly reduced, underscoring the pivotal role of this isoform in AMPK-mediated vascular effects (Almabrouk et al., 2017). The absence of AMPKα1 disrupts eNOS phosphorylation and NO production, thereby impairing vasodilation (Hwej et al., 2024). Additionally, In AMPKα1 knockout mice, PVAT generates significantly lower levels of adiponectin compared to WT mice, highlighting the essential role of AMPKα1 in regulating adiponectin production within adipose tissue (Almabrouk et al., 2017).

A variety of structurally diverse compounds have been utilized in experiments to activate AMPK. One class of AMPK activators comprises prodrugs that are metabolized within cells to produce an AMP analogue through enzymatic conversion. A prominent compound in this class is AICAR, an adenosine analogue. In human aortic smooth muscle cells and isolated rabbit aortae, treatment with AICAR has been shown to induce phosphorylation of AMPK and acetyl-CoA carboxylase, a key downstream target of AMPK, thus inhibiting growth factor-induced cell proliferation (Igata et al., 2005). Complementing these findings, Abdulqader and Kennedy (2020) demonstrated that AICAR enhances nitric oxide (NO) production in PVAT in a rabbit model. Their study revealed that PVAT incubated with AICAR generated significantly higher levels of NO compared to

untreated controls, suggesting that AICAR-induced AMPK activation in PVAT contributes to NO-mediated modulation of vascular function.

Despite the growing recognition of PVAT, S1P, and AMPK as critical modulators of vascular tone, their interactions together remain poorly understood. This study aims to elucidate the mechanisms by which S1P and AICAR, individually and in combination, influence vascular relaxation in thoracic aortic rings, with a focus on the roles of PVAT, AMPKα1, NO, and adiponectin. By examining these interactions, the study will provide functional insights into PVAT-mediated vascular regulation and help identify potential therapeutic targets for cardiovascular diseases. More specifically, the regulatory roles of AMPKa1 and AMPKα2 can be more clearly defined. This would have a number of benefits. First, regarding tissue-specific functions, the two isoforms are mainly expressed in different tissues, and a clearer knowledge of their roles may help in the design of strategies for specific tissues. Also, dysregulation of AMPK isoforms has been associated with various diseases, which include diabetes, cancer, and cardiovascular disorders. A deeper understanding of the distinct roles they play might give insight into disease mechanisms and potential treatments. Finally, in terms of therapeutic targeting, it may be possible to improve the development of better targeted therapies by selectively inhibiting AMPKα1 or AMPKα2.

4.2 Aim and Objectives

The main aim is to investigate the underlying mechanisms of the effects of S1P and AICAR on vascular relaxation, with a specific focus on the roles of PVAT, $AMPK\alpha1$, NO, and adiponectin. Objectives are:

- To evaluate the individual effects of S1P and AICAR on vascular relaxation in thoracic aortic rings from both wild-type (WT) and AMPKα1 knockout (KO) mice, under endothelium-intact and denuded conditions, and in the presence or absence of PVAT.
- 2. To determine the combined effects of S1P and AICAR on vascular relaxation in WT and AMPK α 1 KO thoracic aortic rings, with an emphasis on the contribution of PVAT to the observed responses.
- 3. To assess the role of S1P receptor subtypes (S1PR1, S1PR2, and S1PR3) in mediating vascular relaxation using receptor-specific agonists and antagonists.
- 4. To analyse the role of NO in the effects observed and measure NO production by PVAT.
- 5. To examine the effects of S1P and AICAR on the secretion of PVAT-derived adipokines, including adiponectin, and to determine their contribution to vascular relaxation.
- 6. To compare vascular responses between WT and AMPK α 1 KO mice and elucidate the role of AMPK α 1 in modulating the effects of S1P, AICAR, and PVAT.

4.3 Results

4.3.1 Vascular relaxation induced by combined S1P and AICAR in WT aortic rings with intact PVAT.

To investigate the effects of sphingolipids and AMPK on vascular function in the mouse aorta, thoracic aortic rings with intact PVAT were isolated from WT mice and subsequently denuded of endothelium. The rings were then mounted on a wire myograph, and all rings exhibited a stable baseline tone, contraction in response to both additions of 5 ml KPSS, a robust contraction to phenylephrine (1 μ M), and showed no acetylcholine-evoked relaxation (3 μ M), confirming effective endothelial removal. Pre-contraction with 1 μ M phenylephrine was established as outlined in the methods section, cumulative concentration-response curves were constructed to S1P and to the AMPK activator AICAR, followed by a protocol in which S1P and AICAR were applied together to evaluate any augmentation of relaxation (Figure 4-1A).

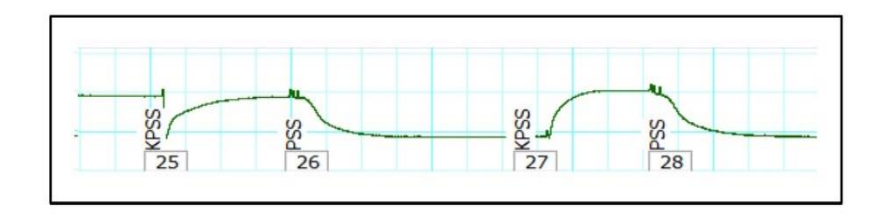
Cumulative addition of S1P alone (3×10^{-9} to 3×10^{-6} M) did not produce a significant relaxation in rings-containing PVAT. The maximum relaxation observed was 6.5 \pm 4.2% (n=6) in S1P-treated rings compared to 1.5 \pm 1.5% (n=6) in untreated, time-control rings (Figure 4-1B).

In a separate set of rings, AICAR $(5\times10^{-4} \text{ to } 2\times10^{-3} \text{ M})$ was added to the endothelium-denuded aortic rings-containing PVAT. AICAR caused a significant relaxation, with a maximum of 40.3 \pm 6.4% (n=6) observed in treated rings compared to 1.5 \pm 1.5% (n=6) in untreated, time-control rings (Figure 4-1C).

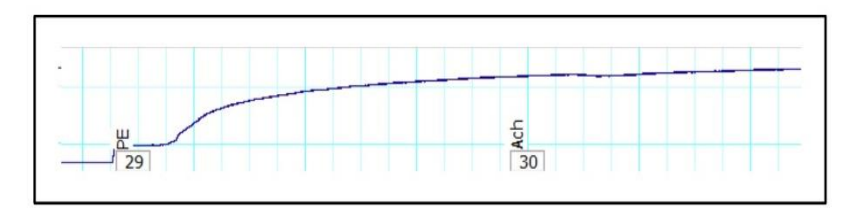
In a further set of experiments, rings were treated with a combination of S1P $(3\times10^{-9} \text{ to } 3\times10^{-6} \text{ M})$ and AICAR $(5\times10^{-4} \text{ to } 2\times10^{-3} \text{ M})$ added simultaneously. The combination caused an augmented relaxation compared to that seen to AICAR alone. The maximum relaxation observed with the combination treatment was 72.6 \pm 6.4% (n=6), which was significantly greater than the relaxation induced by AICAR alone $(40.3 \pm 6.5\%, n=6)$ (Figure 4-1D).

Α

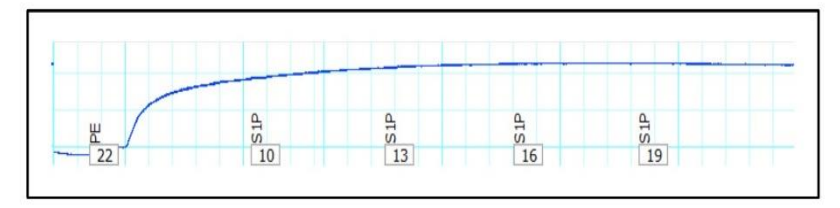




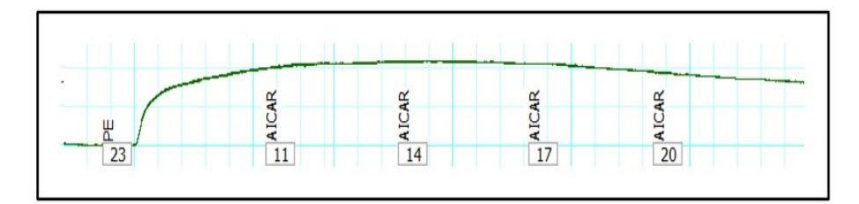
PE & Ach



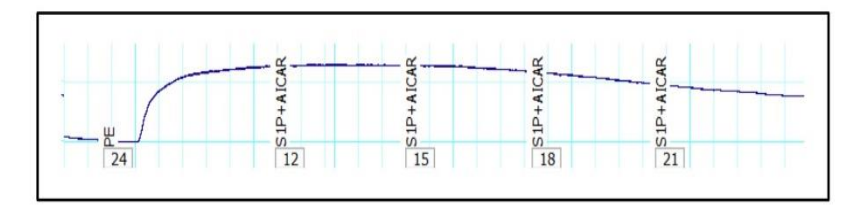
PE - S1P CRC

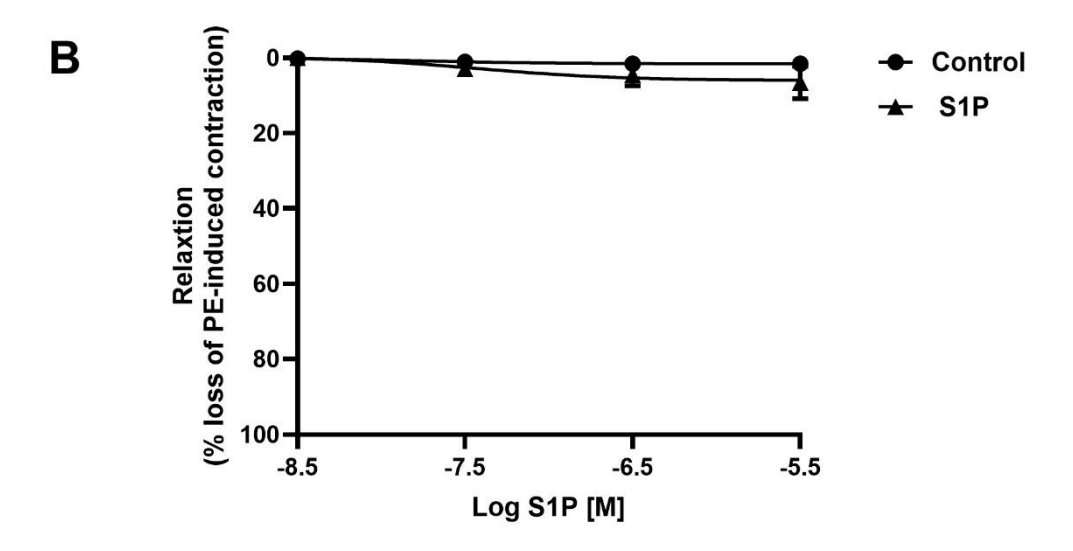


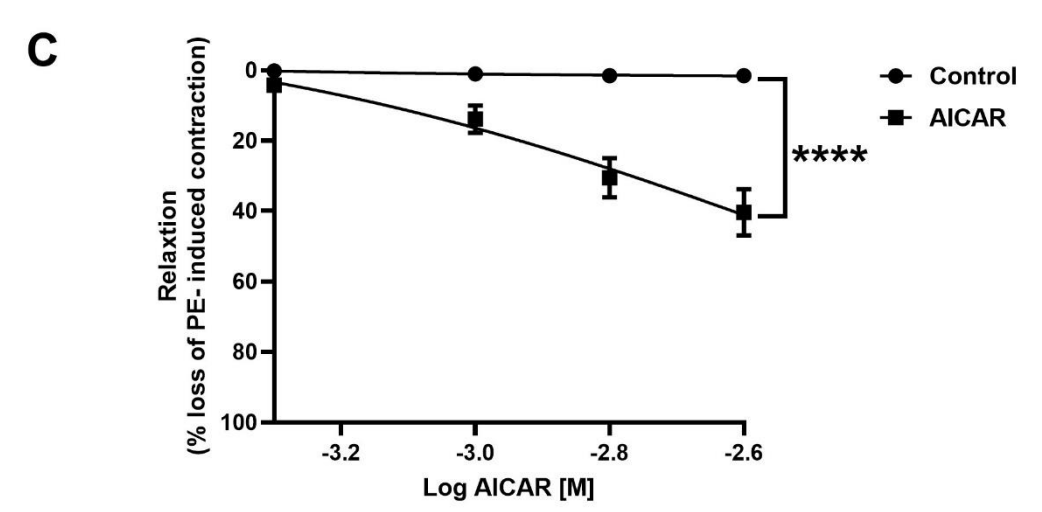
PE - AICAR CRC



PE - S1P+AICAR CRC







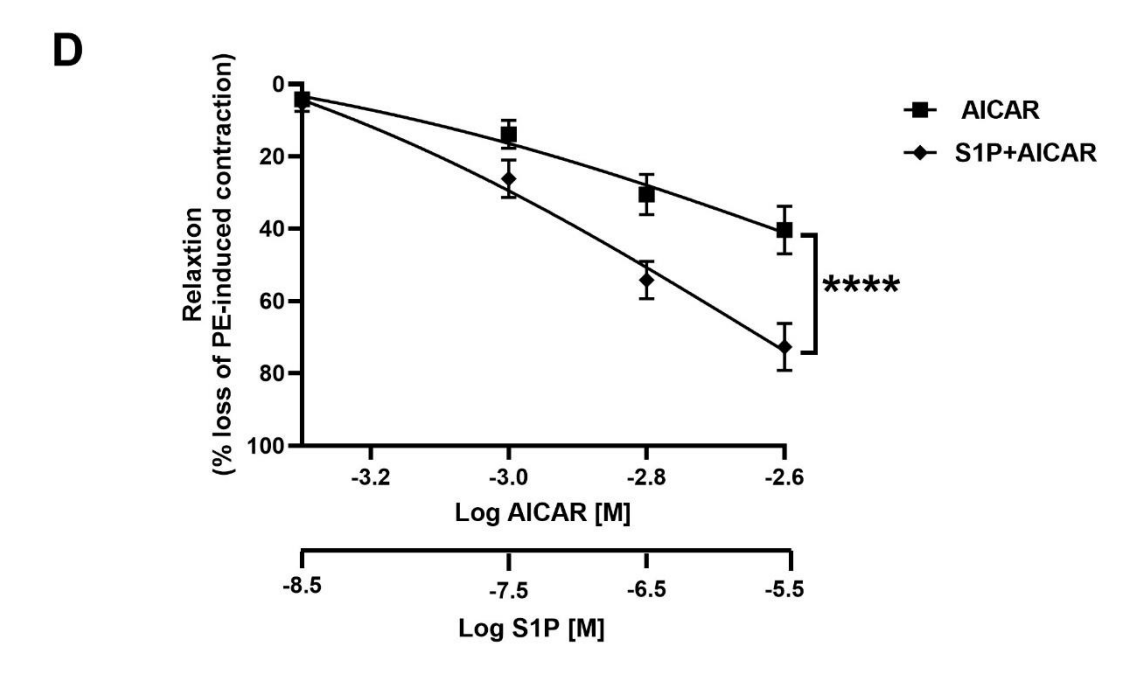


Figure 4-1: Functional assessment of endothelium-denuded thoracic aortic rings with PVAT in Wild-Type (WT) mice.

(A) Representative experimental trace from WT endothelium-denuded aortic mice rings with intact PVAT. After KPSS verification of contractile integrity, rings were pre-contracted with phenylephrine (1 μ M); absence of acetylcholine-induced relaxation (3 μ M) confirmed successful denudation. Cumulative additions of S1P (3×10⁻⁹ to 3×10⁻⁶ M), AICAR (5×10⁻⁴ to 2×10⁻³ M), and S1P + AICAR were then applied on a stable PE tone. (B) Relaxation responses to sphingosine-1-phosphate (S1P) were examined at concentrations ranging from 3×10⁻⁹ to 3×10⁻⁶ M and compared to those of untreated (control) PVAT-containing aortic rings (n=6). (C) Relaxation responses to the AMP-activated protein kinase (AMPK) activator AICAR were assessed at concentrations ranging from 5×10⁻⁴ to 2×10⁻³ M and compared with the responses of untreated PVAT-containing aortic rings (n=6). (D) The impact of combined treatment with S1P and AICAR on the concentration–response curves were evaluated in PVAT-containing aortic rings, and results compared to those obtained with AICAR treatment alone (n=6). Statistical analysis was performed using two-way ANOVA, followed by Tukey's post hoc test with ****P < 0.001.

4.3.2 Relaxation to a combination of S1P and AICAR is not augmented in Wild-type (WT) aortic rings with intact endothelium and PVAT.

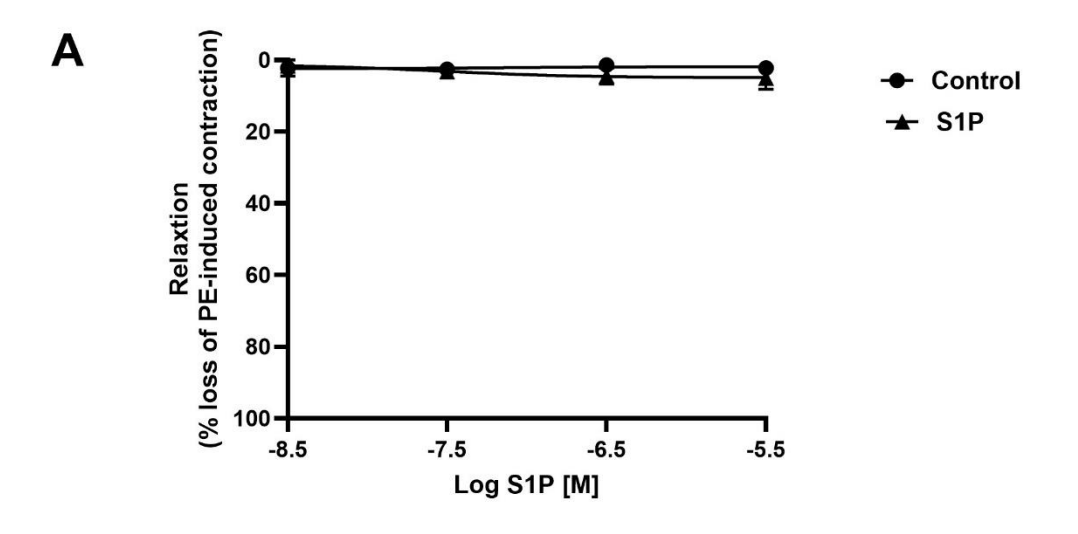
Based on the augmented relaxation in denuded thoracic aortic rings containing PVAT to a combination of S1P and AlCAR (Figure 4-1D), the experiments were repeated in endothelium-intact thoracic aortic rings. As with the experiments in 4.3.1 (above), rings were mounted on a wire myograph and pre-contracted with 1 μ M phenylephrine.

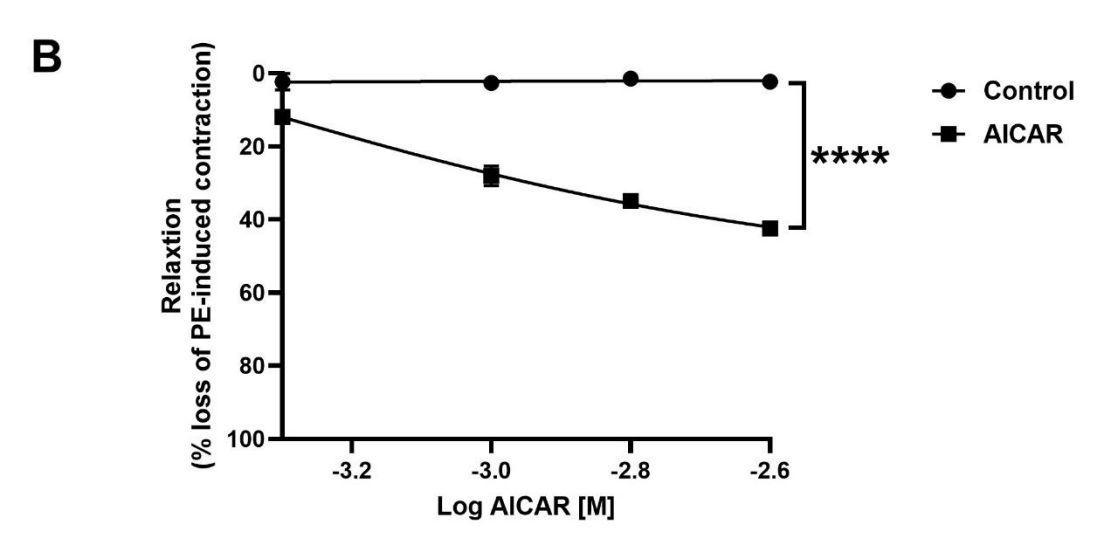
Cumulative concentration-response curves to S1P (3×10^{-9} to 3×10^{-6} M) were constructed in endothelium-intact aortic rings. S1P alone did not induce significant relaxation, the maximum relaxation observed being 11 \pm 9% (n=5) in S1P-treated rings compared to 2.2 \pm 1.4% (n=5) in untreated rings (Figure 4-2A).

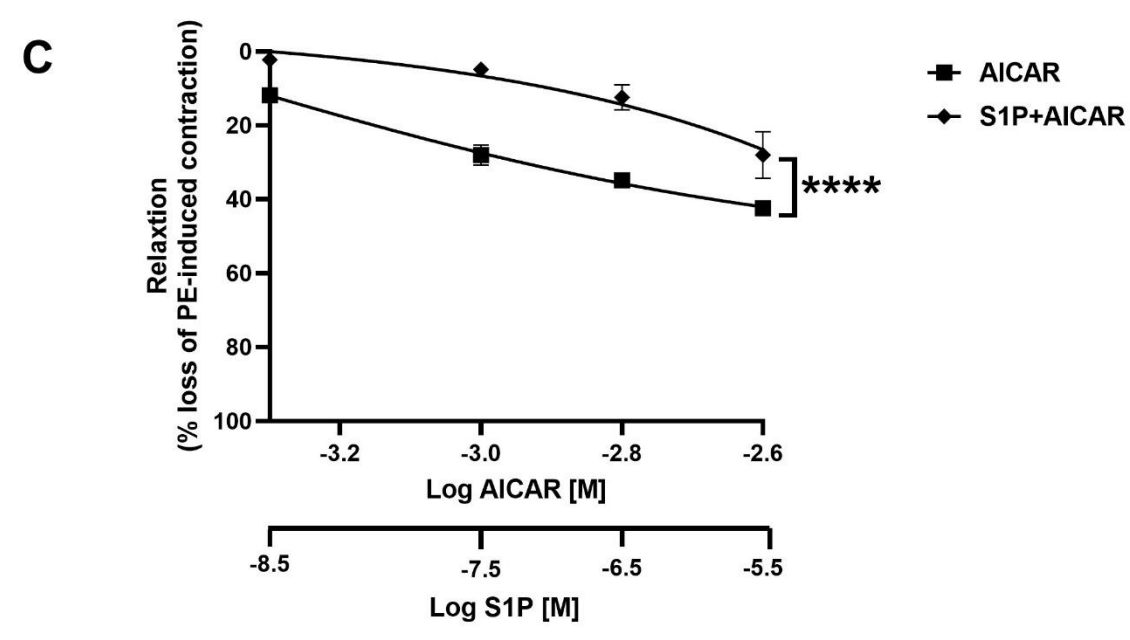
AICAR (5×10^{-4} to 2×10^{-3} M) alone in endothelium-intact aortic rings containing PVAT induced significant relaxation, with a maximum relaxation of $42.4 \pm 1.4\%$ (n=5) in treated rings compared to $2.2 \pm 1.4\%$ (n=5) in untreated rings (Figure 4-2B).

When rings were treated with a combination of S1P (3×10^{-9} to 3×10^{-6} M) and AICAR (5×10^{-4} to 2×10^{-3} M), there was no significant increase in relaxation compared to AICAR alone. The maximum relaxation observed with the combination treatment was $28 \pm 6.2\%$ (n=6), comparable to that induced by AICAR alone ($42.4 \pm 1.4\%$, n=5) (Figure 4-2C).

The combination of S1P (3×10^{-9} to 3×10^{-6} M) and AICAR (5×10^{-4} to 2×10^{-3} M) significantly augmented relaxation in endothelium-denuded PVAT-containing rings compared to endothelium-intact PVAT rings. The maximum relaxation observed with the combination treatment in endothelium-denuded rings was 72.6 \pm 6.4% (n=6), which was notably higher than that induced by the same treatment in endothelium-intact PVAT rings ($34.5\pm7.6\%$, n=6) (Figure 4-2D).







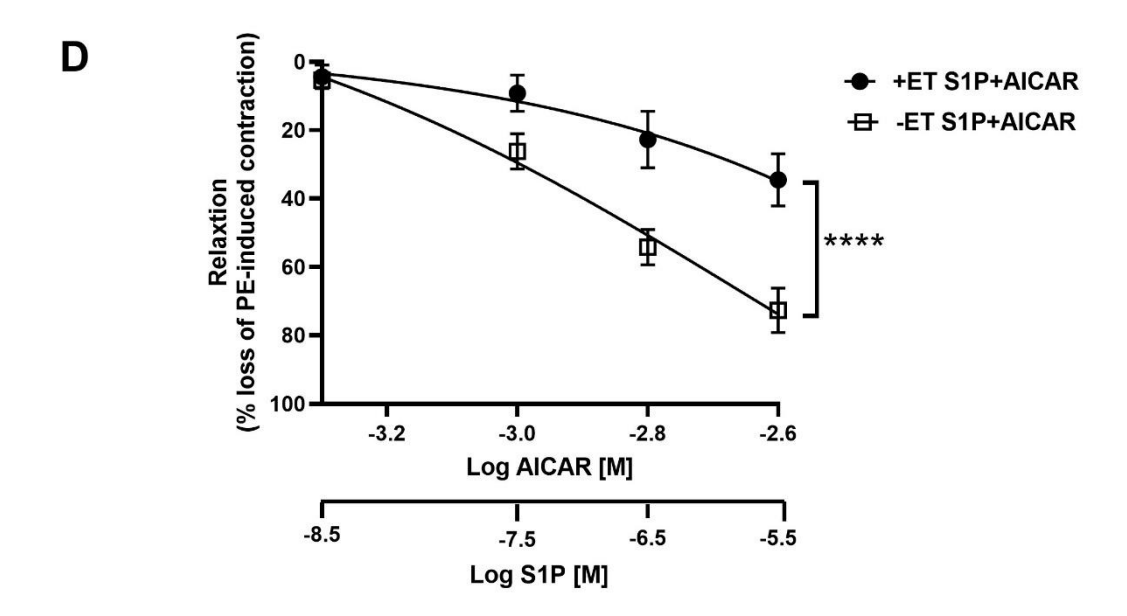


Figure 4-2: Functional assessment of endothelium-intact thoracic aortic rings with PVAT in Wild-Type mice.

(A)Relaxation responses to sphingosine-1-phosphate (S1P) were evaluated at concentrations ranging from 3×10⁻⁹ to 3×10⁻⁵ M. These results were compared to untreated PVAT-containing aortic rings (n=5). (B) The relaxation responses to the AMP-activated protein kinase (AMPK) activator AICAR were measured over a concentration range of 5×10⁻⁴ to 2×10⁻³ M. Data were compared with untreated PVAT-containing aortic rings (n=5). (C) The combined effects of S1P and AICAR on concentration–response curves were analyzed in PVAT-containing aortic rings (n=6). The results were compared to those observed with AICAR treatment alone in aortic rings with PVAT. (D) The combined effects of S1P and AICAR on concentration–response curves were analyzed in PVAT-containing aortic rings from endothelium-intact mice and compared to those from endothelium-denuded mice (n=6). Statistical analyses were conducted using two-way ANOVA followed by Tukey's post hoc test with ****P < 0.001.

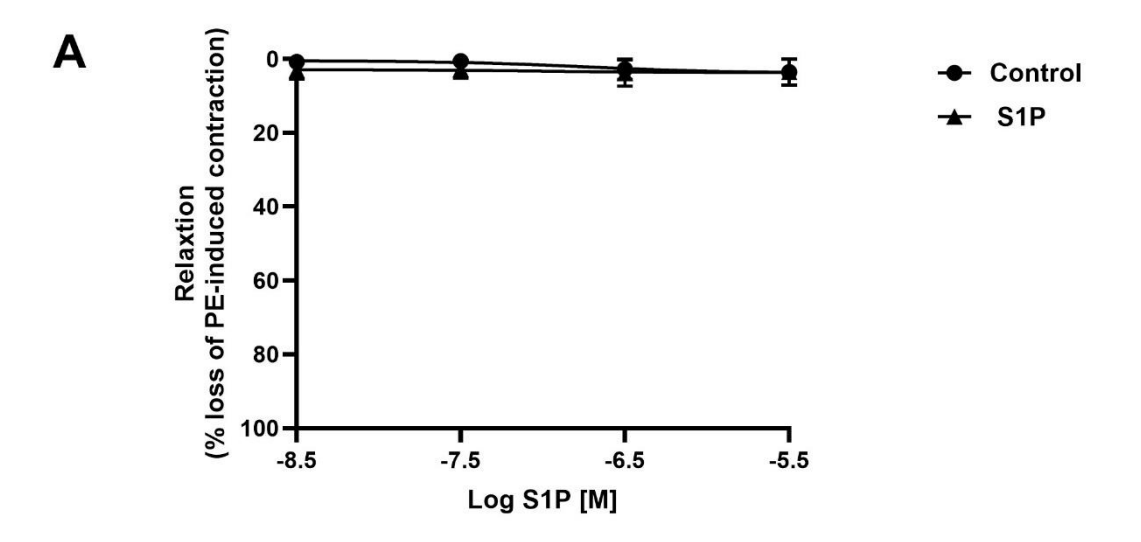
4.3.3 Vascular relaxation to the combination of S1P and AICAR is attenuated in WT denuded thoracic rings without PVAT

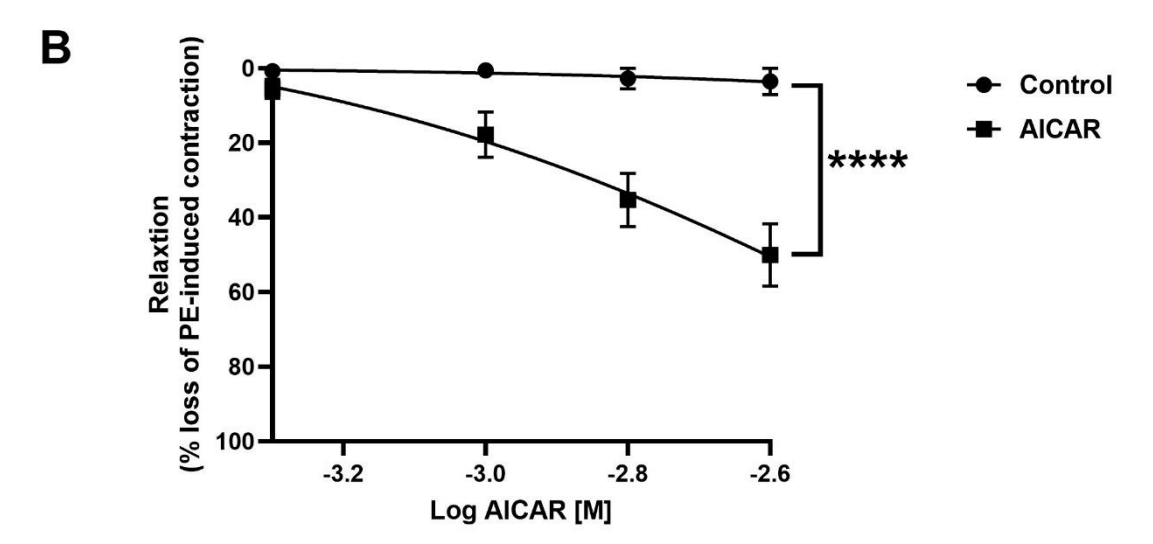
Building upon the observed augmented relaxation to a combination of AICAR and S1P in denuded thoracic aortic rings containing perivascular adipose tissue (PVAT), (Figure 4-1D), the next stage was to study endothelium-denuded thoracic aortic rings in the absence of PVAT. WT rings with PVAT removed were mounted on a wire myograph and pre-contracted with 1 μ M phenylephrine, following the protocol detailed in the methods section.

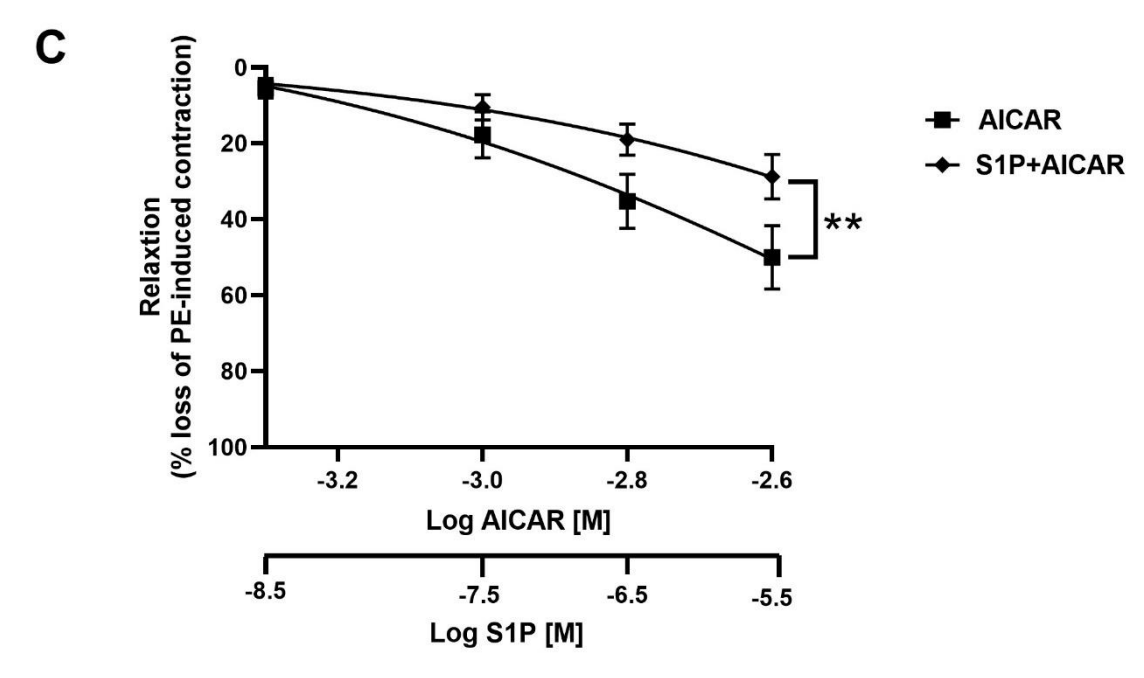
Cumulative concentration-response curves to S1P (3×10^{-9} to 3×10^{-6} M) were applied to endothelium-denuded aortic rings without PVAT. S1P alone did not result in any significant relaxation in these rings. The maximum relaxation observed was 3.5 \pm 3.5% (n=4) in S1P-treated rings compared to 3.5 \pm 3.5% (n=4) in untreated control rings (Figure 4-3A).

Separately, AICAR (5×10^{-4} to 2×10^{-3} M) significantly enhanced relaxation in these rings, with a maximum relaxation of $50 \pm 8.3\%$ (n=4) observed in treated rings compared to $3.5 \pm 3.5\%$ (n=4) in untreated rings (Figure 4-3B).

Treating rings with a combination of S1P (3×10^{-9} to 3×10^{-6} M) and AICAR (5×10^{-4} to 2×10^{-3} M) did not produce any significant additional relaxation compared to AICAR alone. The maximum relaxation observed with the combination treatment was $28.8 \pm 5.8\%$ (n=6), which was actually significantly reduced compared to AICAR alone ($50 \pm 8.3\%$, n=4) (Figure 4-3C). This may suggest that S1P inhibits the action or AICAR in this case. Interestingly, the combination of S1P and AICAR induced significantly greater relaxation in endothelium-denuded PVAT-containing rings compared to endothelium-denuded rings in the absence of PVAT. The maximum relaxation observed with the combination treatment in endothelium-denuded PVAT-containing rings was ($72.7 \pm 6.4\%$, n=6), which notably exceeded the relaxation seen in endothelium-denuded rings without PVAT ($28.8 \pm 5.8\%$, n=6) (Figure 4-3D).







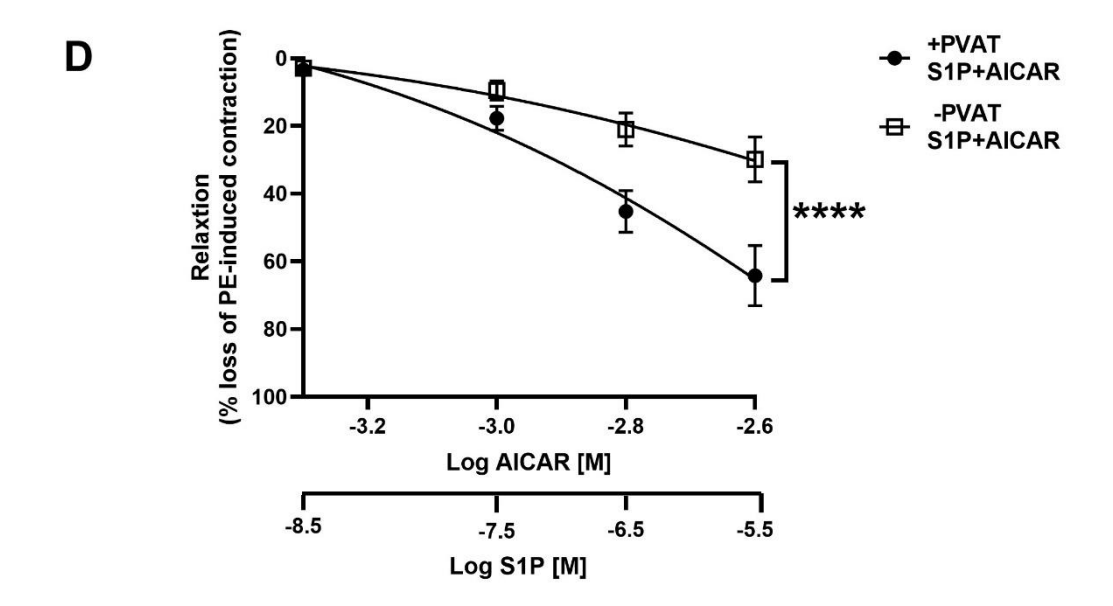


Figure 4-3: Functional assessment of endothelium-denuded thoracic aortic rings without PVAT in Wild-Type mice.

(A)Relaxation responses to sphingosine-1-phosphate (S1P) were assessed across a concentration range of 3×10⁻⁹ to 3×10⁻⁶ M. These results were compared to untreated endothelium-denuded aortic rings without PVAT (n=4). (B) Relaxation responses to AMPK activator AlCAR were measured at concentrations ranging from 5×10⁻⁴ to 2×10⁻³ M. Data were compared to untreated endothelium-denuded aortic rings without PVAT (n=4). (C) The combined effects of S1P and AlCAR on concentration-response curves were analyzed in aortic rings lacking PVAT. These results were compared to those obtained with AlCAR treatment alone in aortic rings without PVAT (n=6). (D) The combined effects of S1P and AlCAR on concentration-response curves were assessed in endothelium-denuded aortic rings containing PVAT (n=6) and compared to those in endothelium-denuded aortic rings without PVAT (n=6). Statistical analyses were performed using two-way ANOVA followed by Tukey's post hoc test with **P < 0.01 and ****P < 0.001 considered statistically significant.

4.3.4 Effect of AMPKα1 subunit knockout on vascular relaxation to the combination of S1P+AlCAR in thoracic PVAT rings

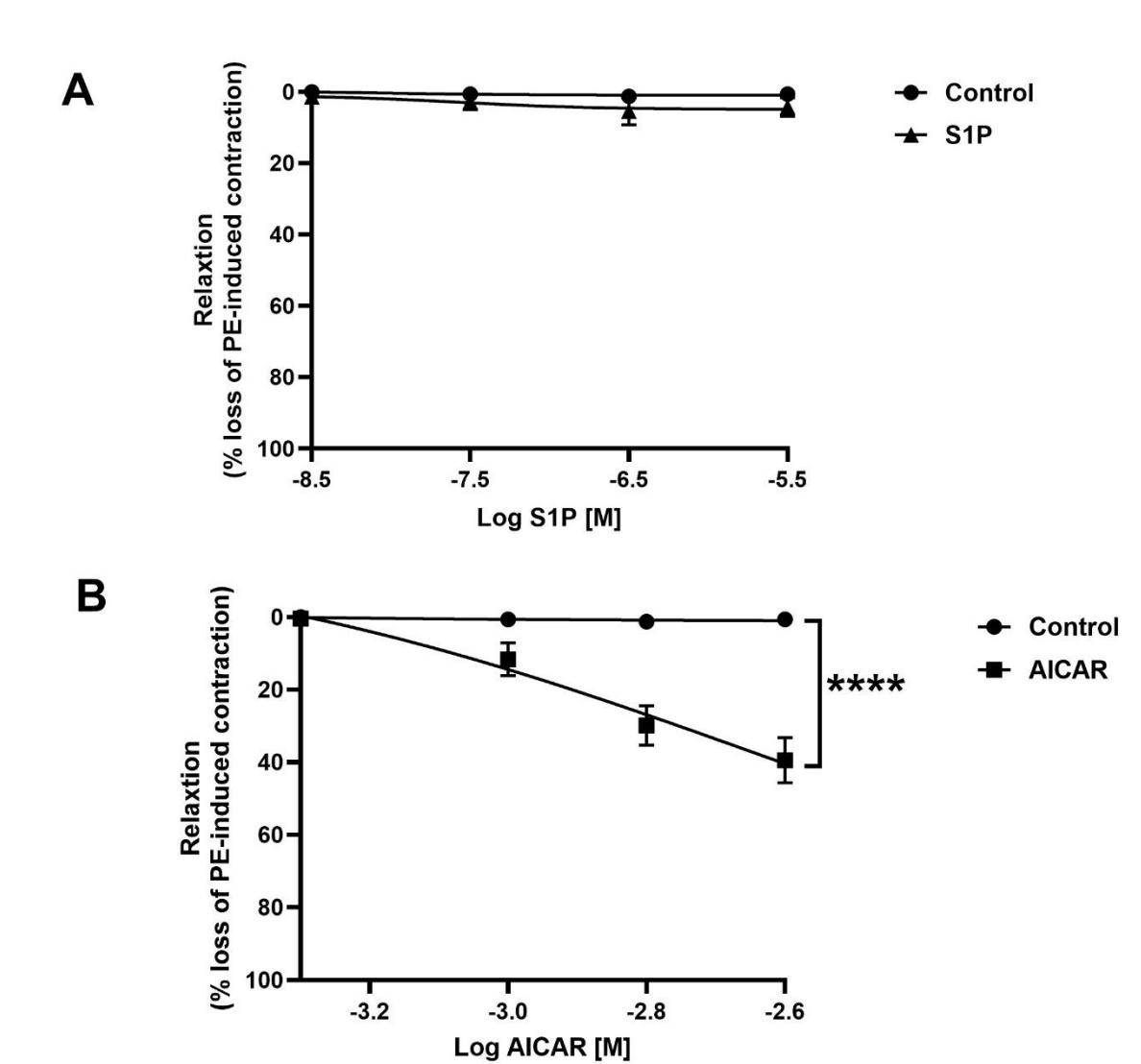
The next stage of the study was to further investigate vascular function in endothelium-denuded thoracic aortic rings derived from AMPK α 1 knockout (KO) mice, this time in the presence of PVAT. Following the methods described in detail earlier, the rings were mounted on a wire myograph and pre-contracted with 1 μ M phenylephrine.

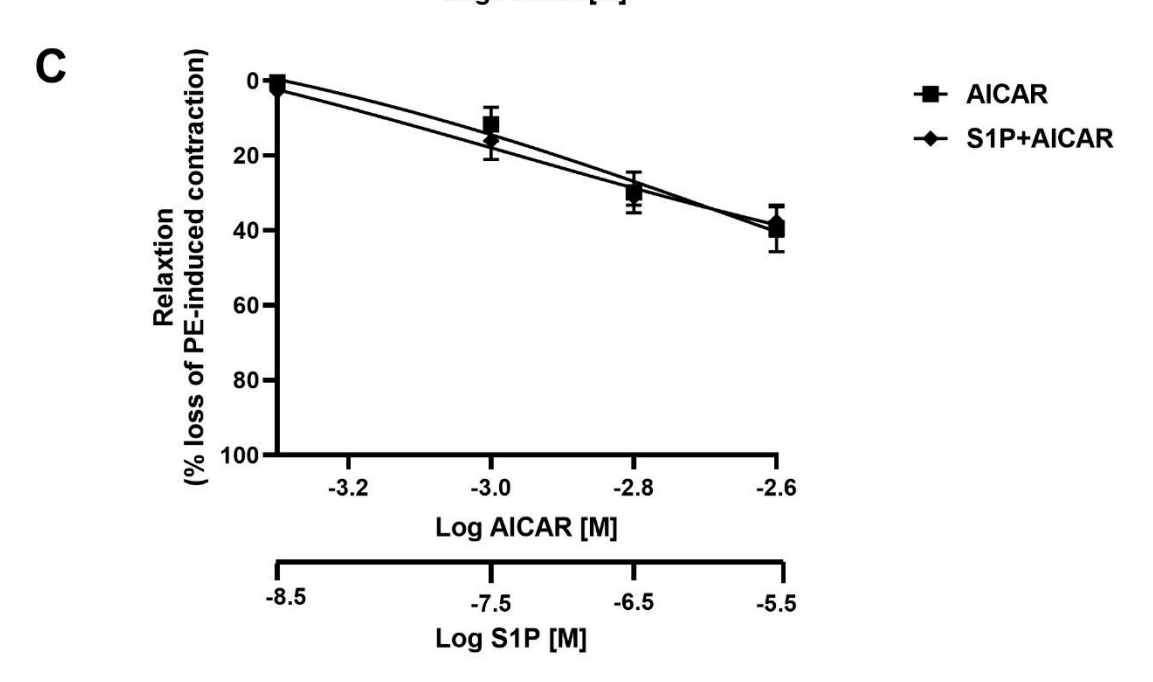
Cumulative concentration-response curves for S1P (ranging from 3×10^{-9} to 3×10^{-6} M) were generated in endothelium-denuded aortic rings with PVAT. S1P alone failed to produce significant relaxation in these rings. The maximum relaxation observed in S1P-treated rings was $4.2 \pm 2.6\%$ (n=5), compared to $0.6 \pm 0.6\%$ (n=5) in untreated control rings (Figure 4-4A).

AICAR (at concentrations from 5×10^{-4} to 2×10^{-3} M) was applied to a different set of aortic rings where relaxation was observed with a maximum of $39.4 \pm 6.1\%$ (n=5). This was significantly higher than the $0.6 \pm 0.6\%$ (n=5) which was observed in untreated, control rings (Figure 4-4B).

Applying a combination of S1P (3×10^{-9} to 3×10^{-6} M) and AICAR (5×10^{-4} to 2×10^{-3} M) did not lead to any significant additional relaxation beyond that induced by AICAR alone. The maximum relaxation observed with the combination treatment was $37.6 \pm 3.9\%$ (n=5), compared to $39.4 \pm 6.1\%$ (n=5) in AICAR alone rings (Figure 4-4C).

This lack of augmented relaxation to the combination of AICAR and S1P was on contrast to what has been observed in WT aortic rings with intact PVAT and denuded endothelium. The maximum relaxation observed in the AMPK α 1 KO PVAT-containing rings with the combination treatment was 37.6 \pm 3.9% (n=5), while the WT PVAT-containing rings exhibited relaxation levels of 67.4 \pm 10.1% (n=5) (Figure 4-3D).





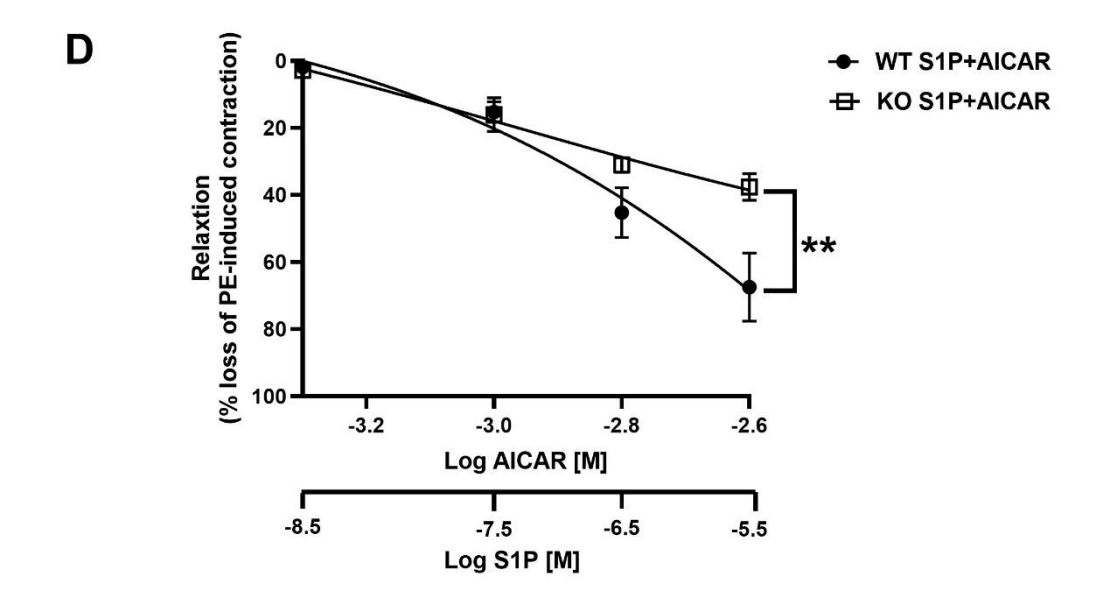


Figure 4-4: Functional evaluation of endothelium-denuded thoracic aortic rings with perivascular adipose tissue in AMPKα1 KO mice.

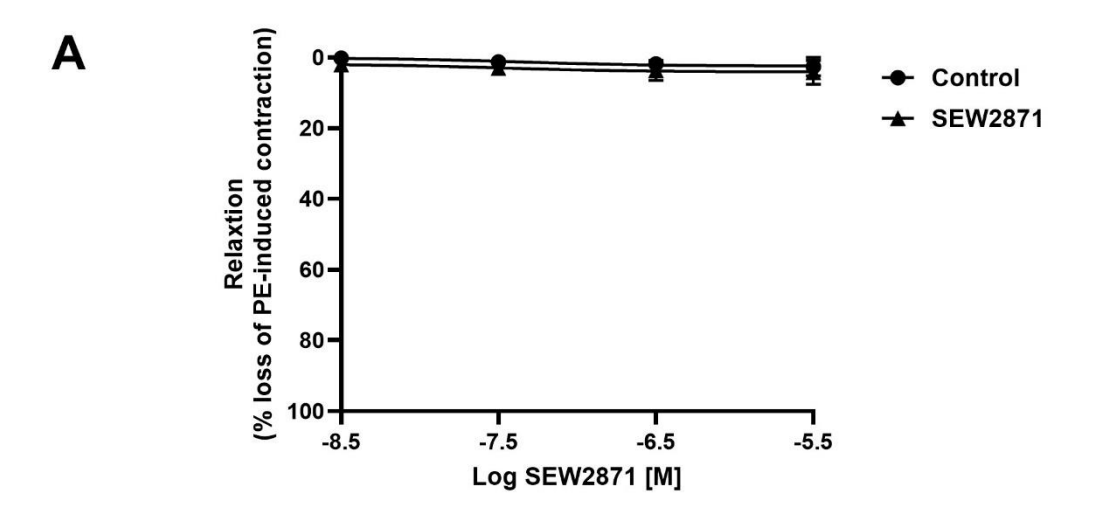
(A)Relaxation responses to sphingosine-1-phosphate (S1P) were evaluated at concentrations ranging from 3×10^{-9} to 3×10^{-6} M. These responses were compared to those of untreated (control) PVAT-containing aortic rings (n=5). (B) Relaxation responses to AMPK activator AICAR were assessed over a concentration range of 5×10^{-4} to 2×10^{-3} M. These were compared to the responses of untreated PVAT-containing aortic rings (n=5). (C) The effects of combined treatment with S1P and AICAR on the concentration–response curves were analyzed in PVAT-containing aortic rings from AMPK α 1 KO mice. Results were compared to those obtained with AICAR treatment alone in PVAT-containing aortic rings (n=5). (D) The combined effects of S1P and AICAR on the concentration–response curves in PVAT-containing aortic rings from AMPK α 1 KO mice were compared to those observed with the same treatment in PVAT-containing aortic rings from WT mice (n=5). Statistical analyses were performed using two-way ANOVA followed by Tukey's post hoc test with **P < 0.01 and ****P < 0.001.

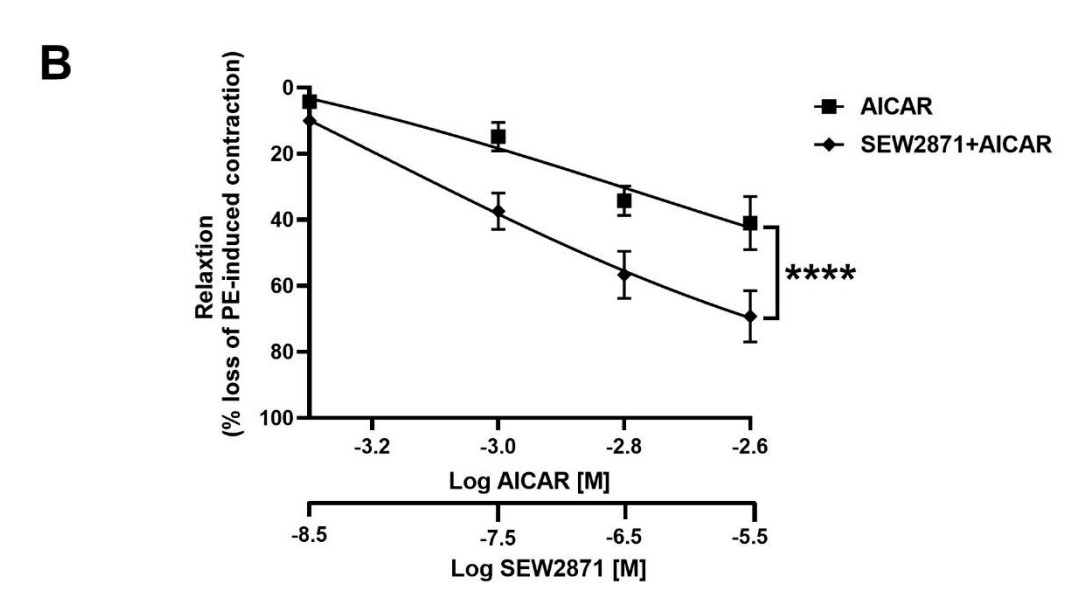
4.3.5 Effect of S1PR₁ agonists (SEW2871) and antagonists (W146) and AICAR on vascular smooth muscle wild-type thoracic PVAT rings

Vasorelaxation was observed in endothelium-denuded thoracic aortic rings with intact PVAT from wild-type (WT) mice following treatment with the combination of sphingosine-1-phosphate (S1P) and AICAR (Figure 4-1D). In contrast, no significant relaxation was observed in endothelium-intact rings, AMPKα1 knockout (KO) PVAT rings, or in denuded rings lacking PVAT under the same conditions.

To investigate whether S1P acts through specific S1P receptors to mediate this response, selective pharmacological agents were used. The S1PR1 agonist SEW2871 and antagonist W146 were applied alongside AICAR in WT PVAT rings to assess the contribution of S1PR1 to the observed vasorelaxation. This approach aimed to determine whether S1PR1 activation is required for the effect, and whether receptor blockade could uncover any receptor-specific contributions not evident from S1P alone. Thoracic aortic rings with intact PVAT were isolated from WT mice and then subjected to endothelial removal prior to mounting in the wire myograph. The rings were pre-contracted with 1 µM phenylephrine as described previously.

Cumulative concentration-response curves were generated for SEW2871, a selective S1PR1 agonist, at concentrations ranging from 3×10^{-9} to 3×10^{-6} M, in endothelium-denuded rings with PVAT. However, SEW2871 did not induce significant relaxation, effecting a maximum response of only $2.6\pm2.6\%$ (n=5), compared to $4.2\pm3.3\%$ (n=5) in untreated control rings (Figure 4-5A). However, when SEW2871 was combined with AICAR (5×10^{-4} to 2×10^{-3} M), the treatment significantly enhanced relaxation (in the rings with PVAT) compared to AICAR alone. The maximum relaxation observed with the combination was $69.2\pm7.7\%$ (n=5), compared to $41\pm8\%$ (n=5) in rings treated solely with AICAR (Figure 4-5B). In separate rings, W146, an S1PR1 antagonist, was pre-incubated at a concentration of $10~\mu$ M for 15 minutes in endothelium-denuded rings with PVAT. Pre-treatment with W146 markedly attenuated relaxation in response to the combination of S1P and AICAR. The maximum relaxation in the presence of W146 was significantly reduced to $38.6\pm5.7\%$ (n=5), compared to $70.8\pm8.1\%$ (n=5) in rings treated with the combination of S1P and AICAR (Figure 4-5C).





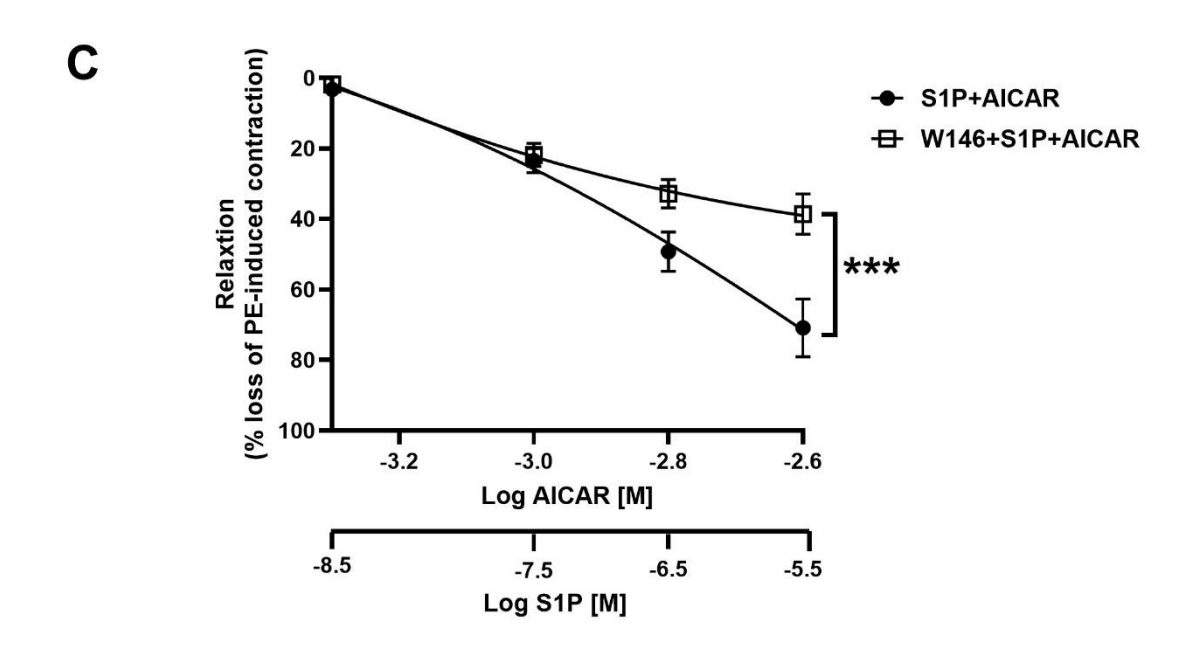


Figure 4-5: Functional assessment of SEW2871, a selective S1PR1 agonist, in endothelium-denuded thoracic aortic rings with PVAT in Wild-Type (WT) mice.

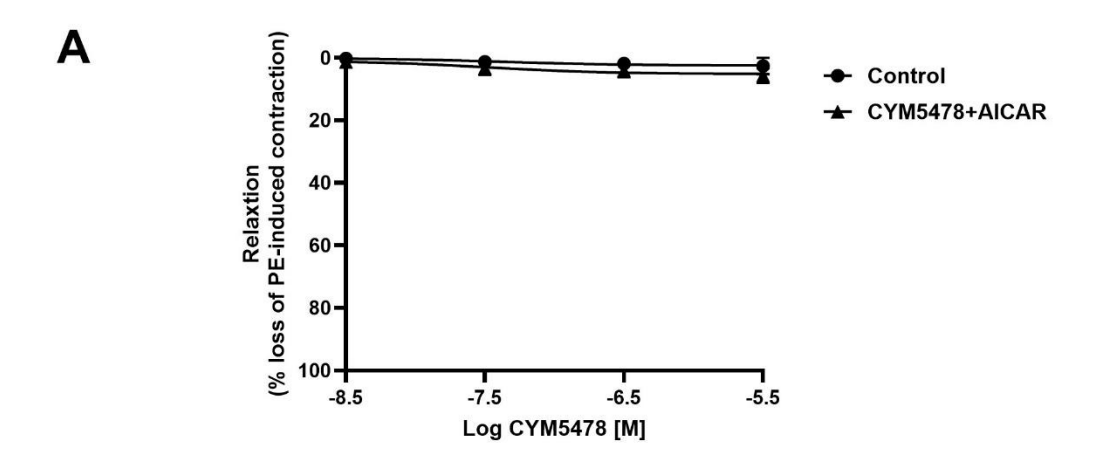
(A) A selective agonist of sphingosine-1-phosphate receptor1 (SEW2871), relaxation responses were measured across a concentration range of 3×10^{-9} to 3×10^{-6} M. These responses were compared with those from untreated PVAT-containing aortic rings (n=5). (B) The combined effects of SEW2871 and AICAR were assessed by analysing concentration–response curves. SEW2871 was applied at concentrations from 3×10^{-9} to 3×10^{-6} M, while AICAR was used at concentrations ranging from 5×10^{-4} to 2×10^{-3} M. The combined responses were compared to those elicited by AICAR treatment alone in PVAT-containing rings (n=5). (C) The role of S1PR1 in mediating the combined effects of S1P and AICAR was investigated by pre-treating PVAT-containing aortic rings with W146, a selective S1PR1 antagonist (10 μ M). The influence of W146 on concentration–response curves for the combined treatment with S1P and AICAR was analyzed. Results were compared with those obtained from S1P and AICAR treatment in the absence of W146 (n=5). All data were analysed using two-way ANOVA followed by Tukey's post hoc test with ***P < 0.001 and ****P < 0.001.

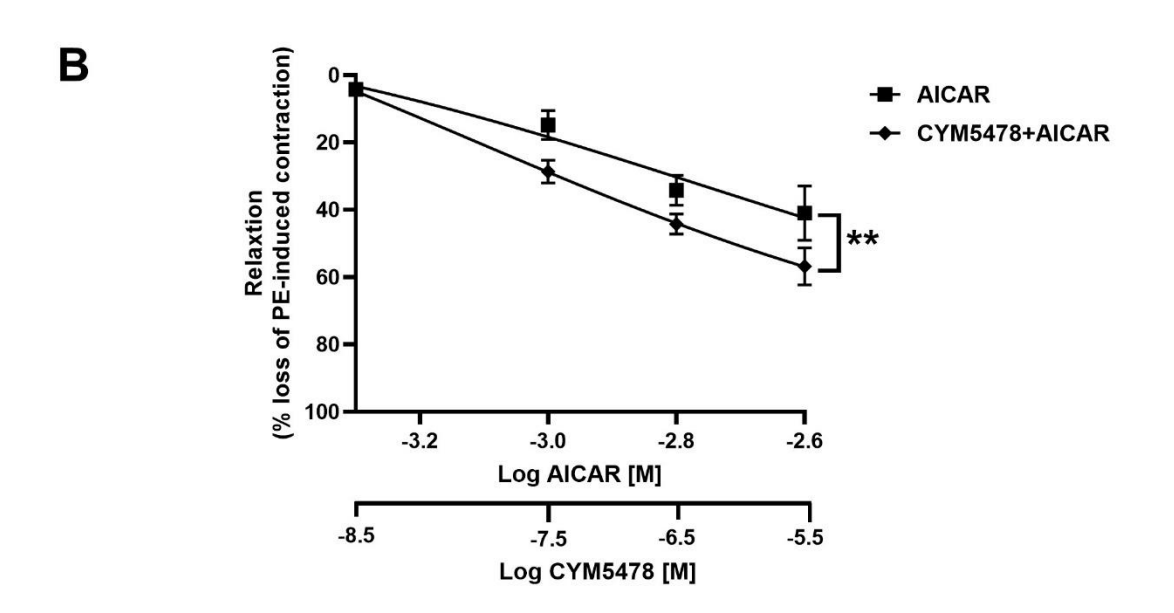
4.3.6 Effect of S1PR₂ agonists (CYM5478) and antagonists (JTE013) combined with AICAR on vascular smooth muscle in WT thoracic aorta

To further investigate the effects of S1P receptor agonists and antagonists in conjunction with AICAR, experiments were performed using endothelium-denuded thoracic aortic rings obtained from WT mice in the presence of PVAT. Rings were pre-contracted with 1 μ M phenylephrine following established protocols.

Cumulative concentration-response curves were generated for CYM5478 at concentrations ranging from 3×10^{-9} to 3×10^{-6} M. CYM5478 in isolation did not produce any significant evidence of relaxation, with a maximum relaxation of 5.6 \pm 2.2% (n=5), compared to 2.6 \pm 2.6% (n=5) in untreated control rings (Figure 4-6A). However, when applied in combination with AICAR (5×10^{-4} to 2×10^{-3} M), a significantly enhanced relaxation was observed when compared to AICAR alone. The maximum relaxation achieved with the combination treatment was 56.8 \pm 5.4% (n=5), compared to 41 \pm 8% (n=5) in rings treated only with AICAR (Figure 4-6B).

In a separate set of rings, JTE013, a selective S1PR2 antagonist, was pre-incubated at a concentration of 10 μ M for 15 minutes in endothelium-denuded aortic rings with PVAT. Pre-incubation with JTE013 significantly reduced the relaxation response to the combined treatment of S1P and AICAR. In the presence of JTE013, the maximum relaxation was reduced to 46.4 \pm 5.2% (n=5), compared to 70.8 \pm 8.1% (n=5) observed in rings treated with the combination of S1P and AICAR without the antagonist (Figure 4-6C).





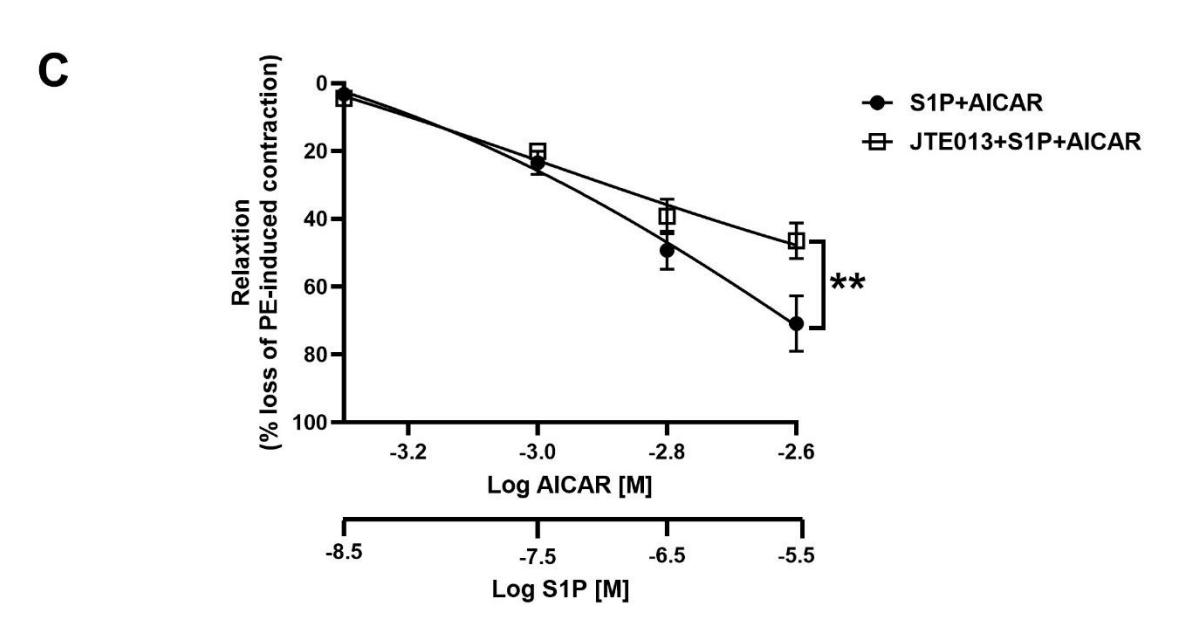


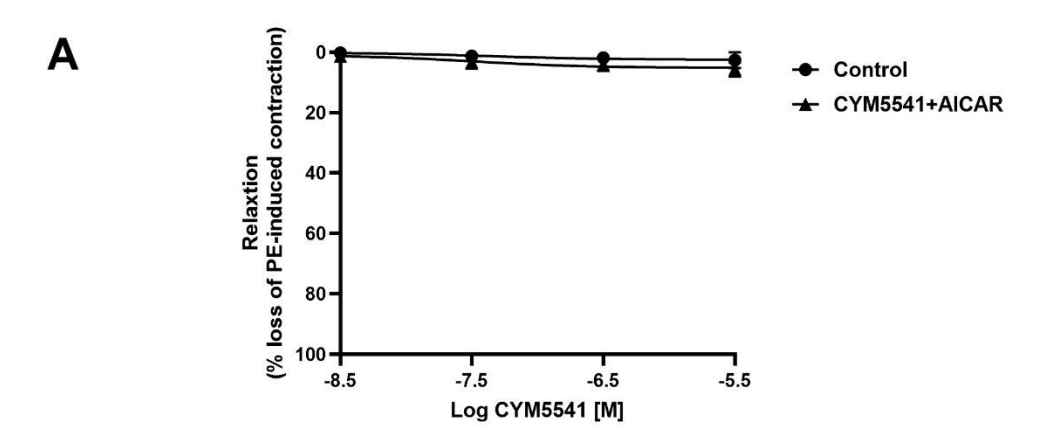
Figure 4-6: Functional evaluation of CYM5478, a selective S1PR2 agonist, in endothelium-denuded thoracic aortic rings with PVAT in Wild-Type (WT) mice.

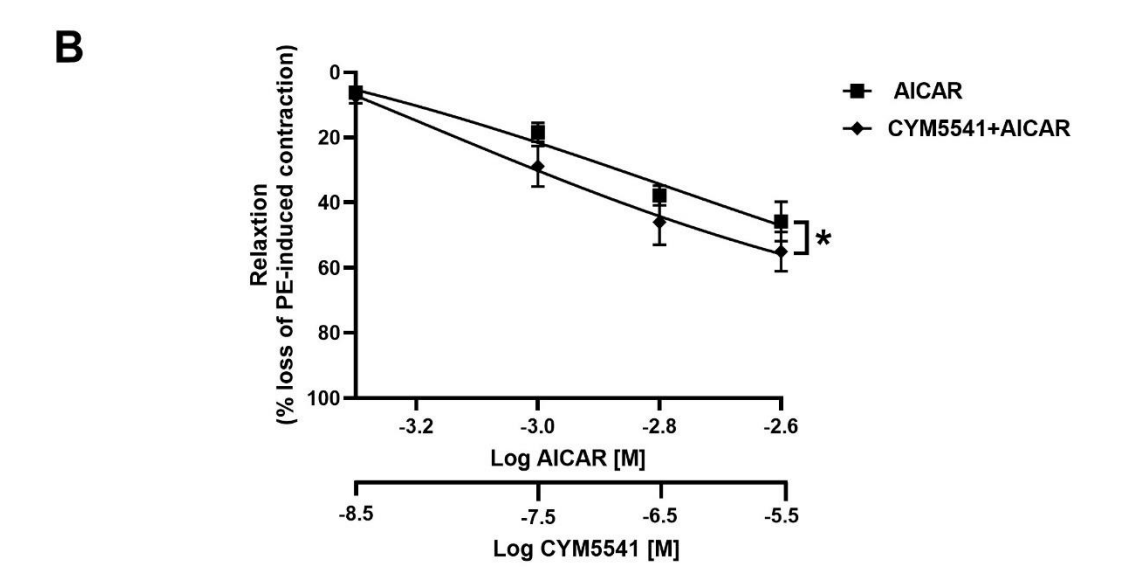
(A) CYM5478, a selective S1PR2 agonist, was tested for its ability to induce relaxation in PVAT-containing aortic rings. Responses were evaluated at concentrations ranging from 3×10^{-9} to 3×10^{-6} M and compared to the responses of untreated rings containing PVAT (n=5). (B) The interaction between CYM5478 and AICAR was explored by examining their combined effects on concentration–response curves. CYM5478 was tested at concentrations of 3×10^{-9} to 3×10^{-6} M, while AICAR was applied at concentrations ranging from 5×10^{-4} to 2×10^{-3} M. These combined effects were compared to those observed with AICAR alone in PVAT-containing aortic rings (n=5). (C) To investigate the role of S1PR2 in mediating the effects of S1P and AICAR, PVAT-containing aortic rings were pre-treated with JTE013 (10 μ M), a selective S1PR2 antagonist. The impact of this pre-treatment on the concentration–response curves to the combination of S1P and AICAR was evaluated. Results were compared to those from rings treated with S1P and AICAR without JTE013 pre-treatment (n=5). Statistical analysis was performed using two-way ANOVA, followed by Tukey's post hoc test with **P < 0.01.

4.3.7 Effect of S1PR₃ agonists (CYM5541) and antagonists (CAY10444) in combination with AICAR on vascular smooth muscle in WT thoracic aorta.

Cumulative concentration-response curves were also generated for CYM5541, a selective S1PR3 agonist, at concentrations ranging from 3×10^{-9} to 3×10^{-6} M in endothelium-denuded rings with PVAT. CYM5541 alone did not produce significant relaxation, with a maximum response of $5.6\pm2.2\%$ (n=5), compared to $2.6\pm2.6\%$ (n=5) in untreated control rings (Figure 4-7A). However, when combined with AICAR (5×10^{-4} to 2×10^{-3} M), a significant enhancement in relaxation was compared to AICAR treatment alone. The maximum relaxation achieved with the combination was also $55\pm5.9\%$ (n=5), compared to $45.8\pm6.1\%$ (n=5) in rings treated solely with AICAR (Figure 4-7B).

In separate rings, CAY10444, a selective S1PR3 antagonist, was pre-incubated at a concentration of 10 μ M for 15 minutes in endothelium-denuded rings with PVAT. Pre-treatment with CAY10444 significantly reduced the relaxation response to the combination of S1P and AICAR. The maximum relaxation in the presence of CAY10444 was markedly attenuated to 51.4 \pm 4.9% (n=5), compared to 70.8 \pm 8.1% (n=5) observed in rings treated with the combination of S1P and AICAR alone (Figure 4-7C).





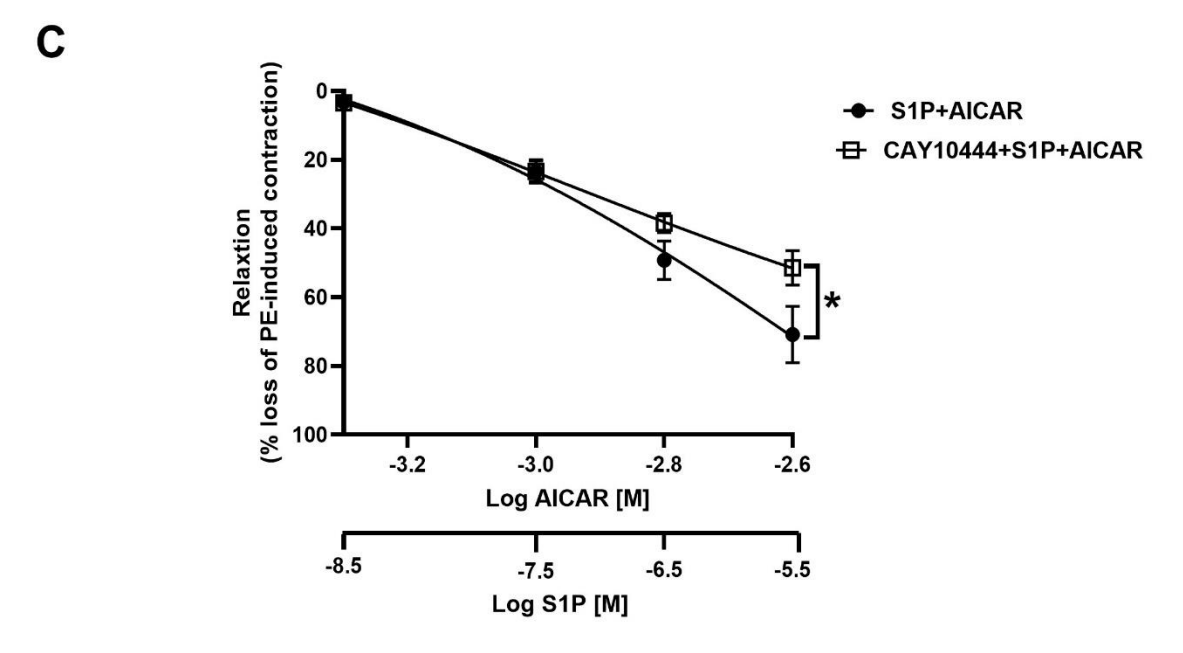


Figure 4-7: Functional assessment of CYM5541, a selective S1PR3 agonist, in endothelium-denuded thoracic aortic rings with PVAT in Wild-Type (WT) mice.

(A) A selective S1PR3 agonist, were assessed in PVAT-containing aortic rings at concentrations ranging from 3×10^{-9} to 3×10^{-6} M. The resulting responses were compared with untreated PVAT-containing rings (n=5) to determine the specific effect of CYM5541. (B) To explore the combined effects of CYM5541 and AlCAR, concentration–response curves were generated using CYM5541 at concentrations of 3×10^{-9} to 3×10^{-6} M in conjunction with AlCAR at concentrations ranging from 5×10^{-4} to 2×10^{-3} M. The relaxation responses from this combined treatment were compared with those observed from AlCAR treatment alone in PVAT-containing aortic rings (n=5). (C) Rings were pre-treated with CAY10444 (10 μ M), a selective S1PR3 antagonist. The effects of this pre-treatment on the concentration–response curves for the combination of S1P and AlCAR were analyzed and compared to responses from rings treated with S1P and AlCAR in the absence of CAY10444 (n=5). Statistical analyses were performed using two-way ANOVA followed by Tukey's post hoc test with *P < 0.05.

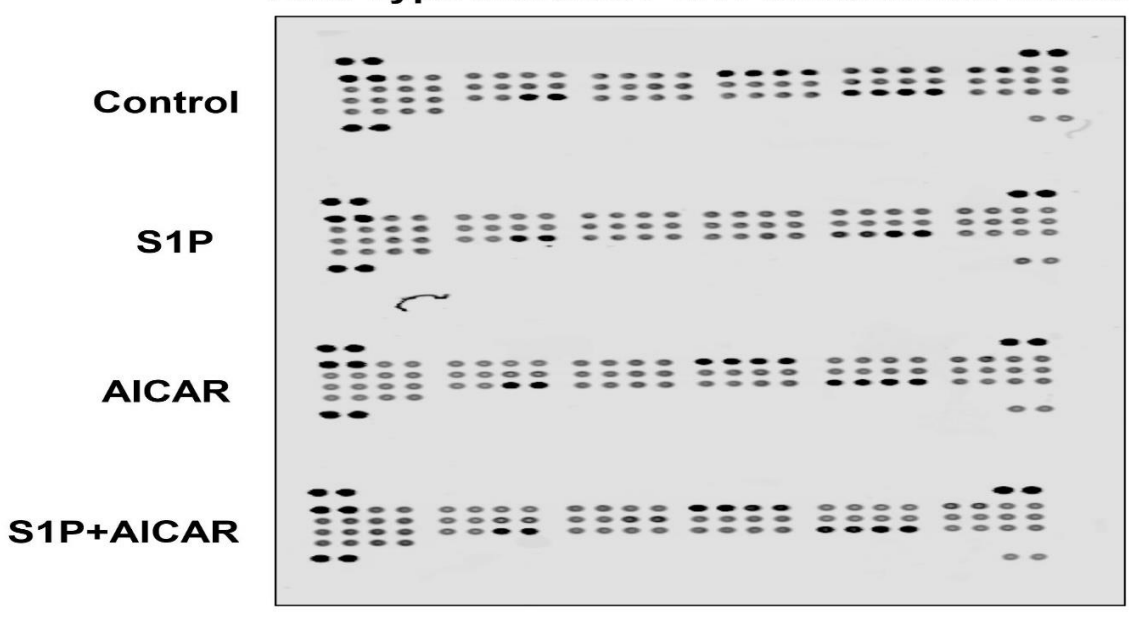
4.3.8 Mouse adipokine array (proteome profile)

We previously observed enhanced relaxation in response to AICAR in PVAT-containing rings from WT mice and the data presented here shows that this effect is also seen to a combination of sphingosine-1-phosphate (S1P) and the AMPK activator AICAR (refer to Figure 4-1D). Notably, this effect was absent in aortic rings lacking PVAT (refer to Figure 4-3C). To further investigate, the secretion of adipokines and the presence of these adipokine within the thoracic aortic PVAT from WT mice was examined. Conditioned media were analyzed using the Proteome Profiler Adipokine Array from R&D Systems, a tool described in detail in the methods section that enables the detection of 38 different adipokines.

As shown in Figure 4.8, analysis of conditioned media PVAT samples revealed that treatment with the combination of S1P and AICAR slightly increased the levels of several adipokines in WT mice. These included adiponectin (Acrp30/AdipoQ), dipeptidyl peptidase-4 (CD26/DPP4), insulin-like growth factor binding protein-3 (IGFBP-3), IGFBP-6, and lipocalin-2 (NGAL).

A





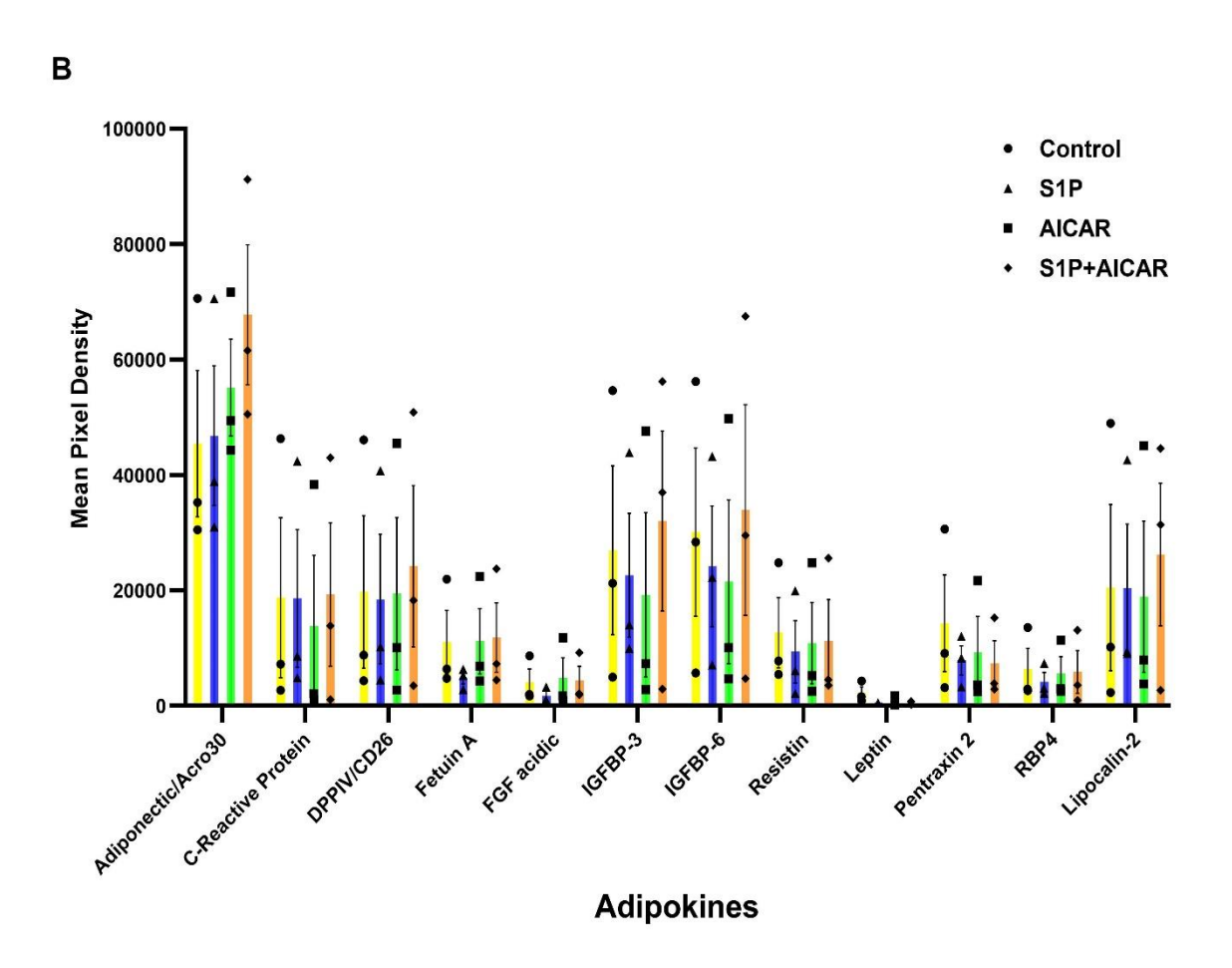


Figure 4-8: Adipokine profiling of thoracic PVAT-conditioned media following S1P and AICAR treatments in Wild-Type mice.

Thoracic PVAT isolated from WT mice was incubated in 1 mL of physiological saline solution (PSS) at 37°C under continuous oxygenation. Conditioned media were collected from thoracic aortic PVAT of WT mice after exposure to various treatments, including untreated control, sphingosine-1-phosphate (S1P, 1 mM), AICAR (2 mM), and a combination of S1P and AICAR. The incubation period for all treatments was 4 hours. Adipokine levels in the conditioned media were analyzed using the Proteome Profiler Mouse Adipokine Array kit, which contains antibodies for 38 mouse adipokines and adipokine-related proteins, presented in duplicate. Panel (A)- representative arrays showing chemiluminescent reaction spots on the membranes of the adipokine profiler. Panel (B) illustrates the comparative levels of adipokines released by WT PVAT (n=3).

4.3.9 Effect of S1P and AlCAR in combination on nitric oxide (NO) production in wild-type (WT) thoracic PVAT

To evaluate whether generation of NO by PVAT could be involved in the augmented relaxation responses observed, this was measured following combined application of S1P and AICAR to WT thoracic aortic PVAT. The PVAT was incubated under different treatments, including an untreated control, S1P (10 μ M), AICAR (2 mM), and a combination of S1P and AICAR for a duration of four hours. NO levels in the conditioned media were quantified using a Sievers 280 NO analyzer, as outlined in the methods section.

The findings, illustrated in Figure 4-9, demonstrate that the combination of S1P and AICAR significantly enhanced NO synthesis by PVAT. In contrast, neither S1P nor AICAR alone produced a significant effect on NO levels when compared to the untreated control. This indicates an interaction between S1P and AICAR which seem to enhance NO from the PVAT.

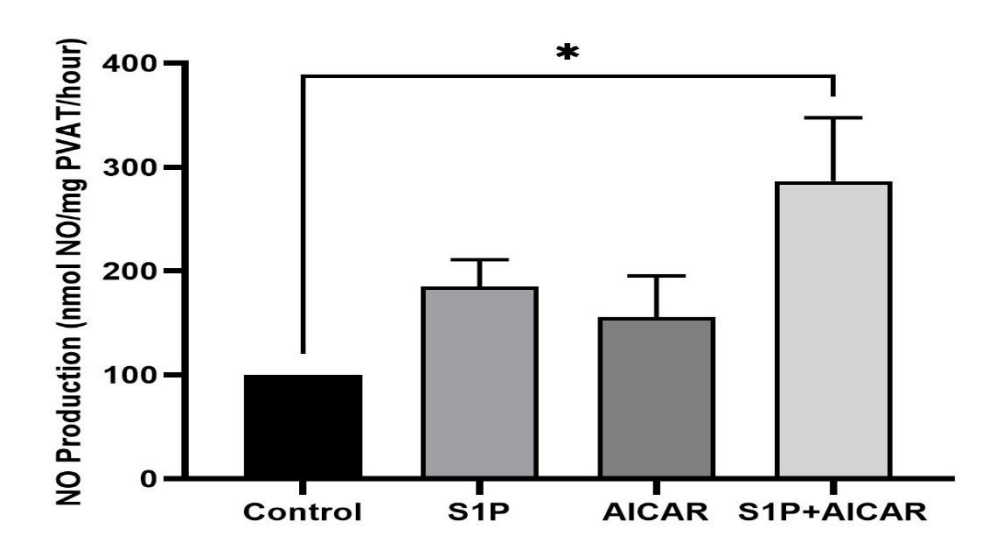


Figure 4-9: Combined effects of S1P and AICAR on nitric oxide production in thoracic aortic PVAT of Wild-Type mice.

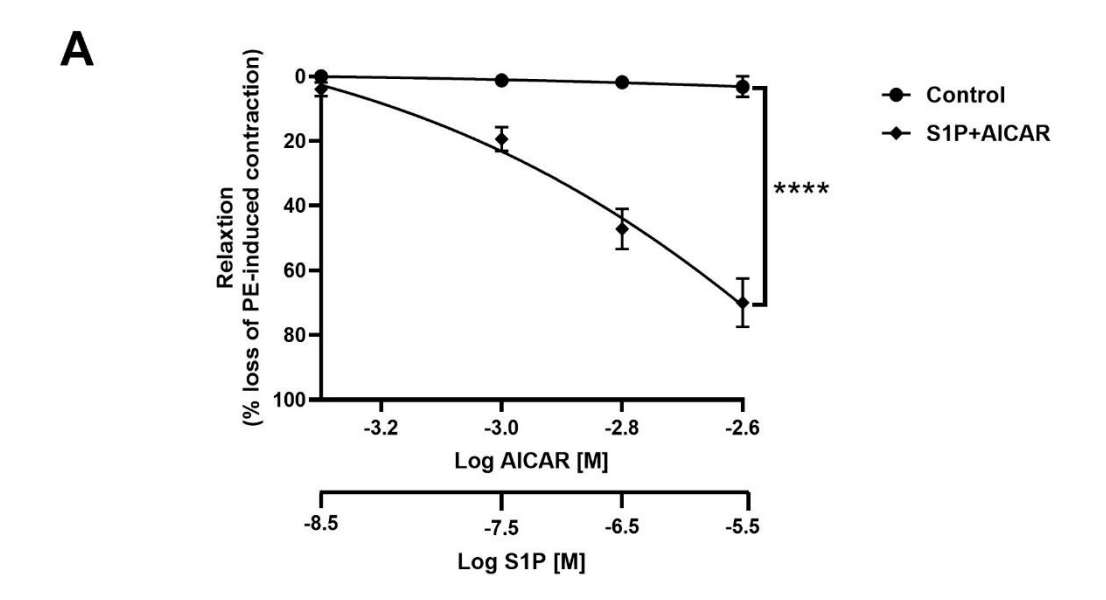
Thoracic PVAT from wild-type (WT) mice was incubated in physiological saline solution (PSS) at 37°C with continuous oxygenation. The tissue was then treated under four conditions, as shown on the figure. Results are expressed as the mean ± SEM for NO production (nmol NO/mg PVAT/hour, n=6). Statistical significance was determined by one-way ANOVA, with *P < 0.05.

4.3.10 Effect of NO inhibitor (L-NAME) on combination of S1P and AICAR in WT denuded thoracic PVAT

Building on the enhanced NO production in response to the combination of S1P and AlCAR, (Figure 4-9), further investigations were conducted to examine the effects of this combination on vascular function. A deficiency of AMPKα1 disrupts the phosphorylation of endothelial nitric oxide synthase (eNOS) and impairs nitric oxide (NO) production in PVAT, leading to a reduction in vasodilation (Hwej et al., 2024). This experiment used endothelium-denuded WT thoracic aortic in the presence of PVAT. The objective was to evaluate the impact of combination of S1P with AlCAR on PVAT-derived NO and its impact on relaxation using the NO inhibitor L-NAME.

Following the previously detailed methods, thoracic aortic rings were mounted on a wire myograph and pre-contracted with phenylephrine (1 μ M). The rings were then treated with combination of S1P (3×10⁻⁹ to 3×10⁻⁶ M) and AICAR (5×10⁻⁴ to 2×10⁻³ M). The combination of S1P and AICAR significantly enhanced relaxation, the maximum relaxation observed with the combination treatment was 71 ± 7.4% (n=5), which was considerably higher than the relaxation in untreated control rings 3.2 ± 3.2% (n=5) (Figure 4-10A).

Endothelium-denuded rings with PVAT were pre-incubated with the NO inhibitor L-NAME (200 μ M). Pre-treatment with L-NAME significantly attenuated the relaxation response to the combination of S1P and AICAR. The maximum relaxation in the presence of L-NAME was reduced to 27 ± 3.5% (n=5), compared to 71 ± 7.4% (n=5) in rings treated with the combination of S1P and AICAR (Figure 4-10B). These findings highlight the role of NO synthesis in mediating the relaxation effects induced by the combination of S1P and AICAR.



В

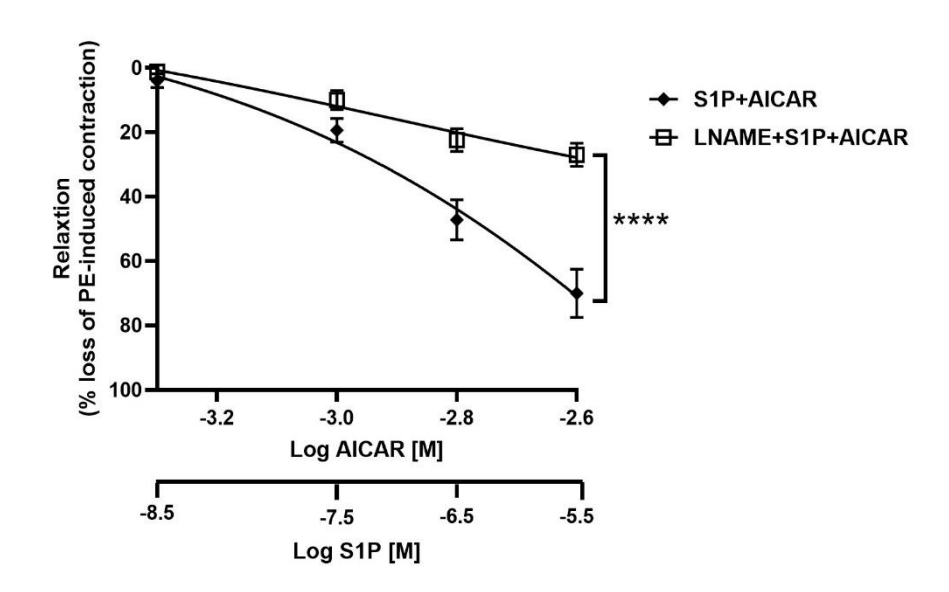


Figure 4-10: Relaxation to S1P and AlCAR and the role of Nitric Oxide (NO) in endothelium-denuded mouse thoracic aortic rings with PVAT.

(A)S1P was tested at concentrations ranging from 3×10^{-9} to 3×10^{-6} M, while AICAR was applied at concentrations between 5×10^{-4} and 2×10^{-3} M. The responses observed from the combination of S1P and AICAR were compared to those of untreated control vessels with intact PVAT (n=5). (B) Aortic rings were pre-treated with the NO inhibitor L-NAME (200 µM). The effect of L-NAME pre-treatment on the concentration–response curves to the combined application of S1P and AICAR was compared to responses in rings treated with S1P and AICAR alone, without L-NAME pre-treatment (n=5). All results are presented as mean \pm SEM. Statistical significance was assessed using two-way ANOVA followed by Tukey's post hoc test, with ****P < 0.001.

4.4 Discussion

This study explored the effects of S1P and the AMPK activator AICAR on vascular relaxation in thoracic aortic rings, with a particular focus on the roles of perivascular adipose tissue, AMPKα1, nitric oxide, and adiponectin. The findings revealed that S1P and agonist of S1P receptors alone did not induce relaxation, whereas AICAR did induce significant relaxation, particularly in aortic rings containing PVAT. Notably, the combined treatment with S1P and AICAR resulted in augmented relaxation, more pronounced in endothelium-denuded rings with PVAT (Figure 4-1) compared to those without (Figure 4-3), highlighting the critical role of PVAT in mediating these effects.

In figure 4-9, the data suggests that addition of S1P to PVAT induces as much production of NO as AICAR does; yet S1P does not cause relaxation of the aortic rings. This paradox could be explained because, while both stimulate the production of NO, they activate different pathways and also interact differently with vascular cells.

The enhanced relaxation observed with the combined treatment was significantly diminished in AMPKα1 knockout (KO) mice (Figure 4-4), underscoring the essential role of AMPKα1 in this interaction. Nitric oxide production was identified as a key mediator, as the NO synthase inhibitor L-NAME markedly attenuated the relaxation responses (Figure 4-10). Further analysis of PVAT-derived factors indicated a slight increase in adiponectin secretion in response to S1P and AICAR (Figure 4-9), linking this adipokine to the observed vascular effects, however the effects of adiponectin would need to be investigated more fully in functional experiments.

The enhanced vasorelaxation induced by the combined treatment of S1P and AICAR was markedly attenuated in vessels with intact endothelium compared to endothelium-denuded aortic rings (Figure 4-2), indicating that these agents could exert vasorelaxant effects directly on vascular smooth muscle cells (VSMCs) independent of endothelial influence. This observation aligns with findings that AICAR induces endothelium-independent vasorelaxation through activation of AMPK in VSMCs, leading to smooth muscle relaxation without reliance on intact endothelium (Goirand et al., 2007). Highlighting potential roles of AICAR in modulating vascular function independently of the endothelium.

In this study, a pharmacological approach was employed using selective agonists and antagonists to investigate the receptor-specific effects of S1P on vascular relaxation (Table 4-1).

Table 4-1 Semi-quantitative assessment of vasorelaxation in mouse thoracic aorta in response to S1P receptor agonists, AICAR, and their co-application; plus signs indicate degree of qualitative relaxation.

Mouse	PVAT	ET	S1PR agonists	AICAR	S1PR agonists + AICAR
WT	Yes	No	- S1P	++	+++
WT	Yes	Yes	- S1P	++	+
WT	No	No	- S1P	++	+
AMPKα1 KO	Yes	No	- S1P	++	++
WT	Yes	No	- SEW2871	++	+++
WT	Yes	No	- CYM5478	++	+++
WT	Yes	No	- CYM5541	++	+++

SEW2871 and W146 were used as a selective S1PR1 agonist and antagonist, respectively (Figure 4-5); CYM5478 and JTE013 targeted S1PR2 as agonist and antagonist (Figure 4-6); and CYM5541 and CAY10444 were employed as selective agonist and antagonist for S1PR3 (Figure 4-7). This strategy aimed to assess whether activation of specific S1P receptors is necessary for the observed effects and whether receptor blockade could reveal receptor-dependent mechanisms that

may not be evident with S1P treatment alone. Receptor-specific studies implicated S1PR1 as a potent mediator of vasorelaxation, while S1PR2 and S1PR3 exhibited less pronounced effects when combined with AICAR. Inhibition of these receptors reduced the relaxation responses, further supporting their involvement. Overall, these findings highlight the interplay between S1P signalling, AMPK activation, PVAT-derived factors, and NO in regulating vascular relaxation.

The findings of this study indicate that S1P alone does not induce significant relaxation in thoracic aortic rings under most experimental conditions, underscoring its limited role as an independent vasorelaxant. This aligns with the established understanding that S1P exerts its effects through the activation of sphingosine-1-phosphate receptors (S1PR1-S1PR5), with each receptor subtype contributing uniquely to vascular tone regulation (Chun et al., 2002). The weak or absent relaxation responses observed in this study suggest that the effects of S1P are mediated by a balance between vasodilatory and vasoconstrictive pathways, where certain receptor subtypes may favour vasoconstriction, thereby limiting the vasorelaxant potential of S1P. This interpretation is supported by evidence that S1P signalling can mediate both vasoconstriction and vasodilation, depending on the specific receptor subtype activated, the vascular bed involved, and interactions with other signalling mediators (WaeberBlondeau and Salomone, 2004). For example, S1PR1 is often associated with vasodilation through its role in enhancing endothelial nitric oxide synthase activity and promoting nitric oxide production. Conversely, S1PR2 and S1PR3 are more commonly linked to vasoconstrictive effects, potentially through pathways that counteract S1PR1mediated vasodilation (Katunaric et al., 2022). The findings of this study are consistent with existing literature, confirming that S1P alone is not a potent independent vasodilator. S1P binds to S1PR1 on endothelial cells. Once activated, S1PR1 triggers intracellular signalling pathways that lead to the activation of eNOS, which catalyses the production of NO from L-arginine. NO then diffuses into the surrounding VSMC, which leads to relaxation of the smooth muscle and subsequent vasodilation. On the other hand, S1PR2 primarily signals through the Ga12/13 and Gaq pathways, leading to the activation of Rho kinase, which encourages smooth muscle tissues to contract. S1PR3, in a similar way to S1PR2, also utilizes the $G\alpha q$ and $G\alpha 12/13$ pathways. But can also activate the $G\alpha i$ pathway, reducing cyclic AMP levels and enhancing calcium signalling in VSMC,

thus contributing to vasoconstriction. Given these observations, further investigation into S1P alone is unlikely to yield significant new insights. Instead, future research should prioritize selective targeting of S1PR1 or combination therapies that enhance its vasorelaxant effects, such as co-activation with AMPK using agents like AICAR.

In contrast, AICAR - a pharmacological activator of AMPK - consistently induced significant relaxation in thoracic aortic rings, particularly in those containing perivascular adipose tissue (PVAT). This finding is consistent with the established role of AMPK as a key regulator of vascular homeostasis. AMPK activation enhances the activity of endothelial nitric oxide synthase, leading to increased nitric oxide production, which serves as a critical mediator of vascular relaxation. Additionally, it also plays a crucial role in maintaining vascular homeostasis (Ewart and Kennedy, 2011). AICAR, an adenosine analogue, is transported into cells via adenosine transporters and phosphorylated by adenosine kinase to generate ZMP, an AMP mimetic (Hardie, 2016). This ability to activate AMPK has made AICAR a tool of choice in studies involving intact cells, tissues, and animal models. However, despite its broad utility, AICAR exhibits limited specificity and has been associated with several off-target effects, as reported in recent studies (Kopietz et al., 2021; Ahwazi et al., 2021a, 2021b).

The effectiveness of AICAR in inducing vascular relaxation has been supported by evidence from studies on human aortic smooth muscle cells and isolated rabbit aortas. AICAR treatment induces the phosphorylation of AMPK and its downstream target, acetyl-CoA carboxylase, leading to the inhibition of growth factor-induced cell proliferation (Igata et al., 2005). Furthermore, AICAR-induced activation of AMPK within PVAT has been shown to stimulate nitric oxide (NO) release, thereby contributing to the regulation of vascular function via NO-dependent pathways (Abdulqader & Kennedy, 2020). These findings highlight the dominant role of AMPK signalling in promoting vascular relaxation, particularly in the context of NO-mediated pathways. The stronger relaxation responses to AICAR compared to S1P alone underscore the critical contribution of AMPK activation in this experimental setting.

The differential effects of S1P and AICAR on vascular relaxation highlight their distinct roles in vascular biology. While S1P primarily functions through receptor-mediated pathways, AMPK exerts its effects by directly modulating cellular metabolism, enhancing NO production, and reducing oxidative stress. These findings emphasize the importance of metabolic signalling in promoting vascular relaxation and suggest that S1P may require interactions with other pathways, such as AMPK or PVAT-derived factors, to exert significant vasorelaxant effects. One noticeable finding of this study is the enhanced relaxation observed in endothelium-denuded aortic rings containing PVAT when treated with a combination of S1P and selective agonists for its receptors, including S1PR1, S1PR2, and S1PR3, alongside AICAR. This enhancement was greater than the relaxation induced by AICAR alone, suggesting an interaction between S1P signalling and AMPK activation in the presence of PVAT. Importantly, this augmented relaxation was absent in PVAT-free rings, highlighting the critical role of PVAT in mediating the combined effects of S1P and AICAR.

PVAT is well-established as a source of various bioactive molecules, including adipokines and gaseous mediators such as nitric oxide and hydrogen sulfide (H2S). These factors contribute to vascular relaxation by modulating the function of endothelial and smooth muscle cells. In this study, the combined treatment with S1P and AICAR likely enhanced the secretion of vasorelaxant factors from PVAT, thereby amplifying the relaxation response. Adiponectin, a key anti-inflammatory and vasoprotective adipokine secreted predominantly by PVAT, emerges as a potential mediator of this effect. Adiponectin is known to activate eNOS, leading to increase NO production, which is essential for vascular relaxation (Chen et al., 2003). Furthermore, adiponectin reduces oxidative stress in the vascular wall, further contributing to its vasoprotective effects. The observed augmentation of relaxation in thoracic aortic rings containing PVAT may reflect a positive feedback mechanism. In this model, the combined activation of PVAT by S1P and AICAR could stimulate adiponectin secretion, which, in turn, enhances NO synthesis and amplifies the relaxation response. The significant reduction in relaxation observed following treatment with NOS inhibitor L-NAME provides strong evidence that NO serves as a primary mediator of the vascular effects induced by S1P and AICAR. This finding underscores the important role of NO in facilitating vascular relaxation in response to these stimuli. The inhibition of this pathway by L-NAME further confirms the value of NO in mediating the synergistic effects of S1P and AICAR on vascular function. This study reinforces the importance of the NO pathway as a key downstream effector in the context of S1P- and AICAR-mediated vascular relaxation. Previous studies have demonstrated that S1P influences the secretion of PVAT-derived factors, such as adipokines and NO, highlighting its role in modulating vascular function through paracrine signalling (Kwon et al., 2001). Additionally, PVAT surrounds blood vessels and exerts paracrine effects through the release of bioactive molecules such as adipokines, reactive oxygen species (ROS), and gaseous mediators like NO and H₂S (Szasz and Webb, 2012). The interplay of these factors creates a vascular microenvironment conducive to relaxation, particularly under conditions of combined S1P and AICAR stimulation. The interplay is complex, but may be outlined as follows: anti-inflammatory adipokines, such as adiponectin, encourage more NO to be produced, which promotes vasodilation. Excessive ROS acts to lower NO bioavailability, which can result in dysfunction in the endothelial cells. H2S counteracts oxidative stress and supports NO-mediated relaxation. The result of this complex network is enhanced relaxation and vascular homeostasis.

These findings underscore the critical role of PVAT-derived factors, such as adiponectin, in mediating vascular relaxation through NO-dependent mechanisms. They also highlight the effects of S1P and AICAR in enhancing PVAT function and promoting vascular homeostasis. This research adds to the growing body of evidence supporting the importance of PVAT as a modulator of vascular tone and its potential as a target for therapeutic interventions in cardiovascular diseases.

Interestingly, the absence of augmented relaxation in AMPK α 1 knockout (KO) mice strongly suggests that AMPK activation is essential for the interplay between S1P and PVAT in modulating vascular tone. AMPK is required for the downstream effects of PVAT-derived factors, including NO production and the reduction of oxidative stress. Without AMPK signalling, as in AMPK α 1 KO mice, these critical processes are impaired, resulting in diminished relaxation responses. Both AMPK α 1 and α 2 isoforms are expressed in arterial smooth muscle cells, although their relative abundance varies between different arteries (Rubin et al., 2005; Evans et al., 2006). Importantly, AMPK α 1 is the predominant isoform responsible for inducing vascular relaxation. Studies have demonstrated that AMPK induces aortic

ring relaxation through the direct activation of AMPKα1 in smooth muscle cells (Goirand et al., 2007). Research involving AMPKα1 KO mice has shown significantly reduced vascular relaxation responses, emphasizing the critical role of this isoform in AMPK-mediated vascular effects (Almabrouk et al., 2017). The absence of AMPKα1 disrupts eNOS phosphorylation and NO production also by the PVAT itself, impairing vasodilation (Hwej et al., 2024). Additionally, other PVAT-derived factors, such as adiponectin, are less effective in promoting relaxation in vessels from AMPKα1 KO mice. This finding highlights the essential role of AMPKα1 in facilitating the interaction between PVAT and the vascular wall, emphasizing its importance in maintaining vascular homeostasis (Almabrouk et al., 2017). The role of AMPKα1 is further supported by the observation that the vasorelaxant effects of AICAR, a pharmacological activator of AMPK, are completely abolished in AMPK α 1-deficient mice but remain intact in α 2-deficient mice. This evidence strongly suggests the dominant role of the AMPKα1 isoform in mediating vascular relaxation responses (Goirand et al., 2007). The interplay between S1P, AMPK, adiponectin, and NO underscores the importance of PVAT in modulating vascular function. By enhancing adiponectin secretion and amplifying its NO effects, the combination of S1P and AICAR creates a positive feedback loop that promotes vascular relaxation.

Implications and Future Directions

The findings of this study have significant implications for our understanding of vascular biology and the treatment of cardiovascular diseases. The interplay between S1P, AMPK activation and perivascular adipose tissue highlights a complex regulatory network that governs vascular relaxation through the secretion of NO and adipokines like adiponectin. These results suggest that targeting PVAT and AMPK pathways could provide new therapeutic strategies for mitigating disease with a component of vascular dysfunction. Therapeutic strategies targeting PVAT and AMPK activation, including pharmacological AMPK activators such as AICAR or selective modulation of S1PR to enhance NO and adiponectin secretion, could represent innovative approaches for improving endothelial function and alleviating vascular dysfunction, particularly in the context of metabolic and cardiovascular diseases. Future experiments will aim to

elucidate the mechanisms by which S1P and AMPK activation regulate vascular relaxation, with a particular focus on the role of PVAT-derived factors.

In vivo studies could be conducted using WT and AMPKα1 KO mice treated with the combination of S1P and AICAR, with PVAT-conditioned media from these mice being analyzed to determine adiponectin concentrations using an ELISA. To further investigate the role of adiponectin in PVAT-mediated vascular relaxation, endothelium-denuded thoracic aortic rings from both WT and AMPKα1 KO mice, with and without PVAT, could be incubated with an AdipoR1 receptor blocker peptide. Following incubation, dose-response curves to S1P and AICAR would assess the extent of vascular relaxation and determine the specific contribution of adiponectin signalling through AdipoR1. Additionally, adiponectin knockout mice could be used to assess whether the absence of adiponectin alters S1P and AICAR-induced vasorelaxation. Vascular function could also be assessed in abdominal and mesenteric rings, both with and without PVAT, to compare vascular responses across different vascular beds. Furthermore, an interesting future direction would be testing sequence dependence by holding S1P at a single low (minimally active) concentration and constructing a cumulative concentrationresponse curve to AICAR, and vice versa. This approach could clarify whether the order of activation alters the magnitude of vasorelaxation, potentially revealing priming effects or synergistic interactions between these signalling pathways. To examine the impact of metabolic disorders, high-fat diet (HFD)-induced obese mice could be used to evaluate how obesity affects PVAT function, AMPK activation, and vascular relaxation. These studies would provide critical insights into the interplay between S1P signalling, AMPK activation, and PVAT-derived adipokines in regulating vascular function under physiological and pathological conditions. Given the established role of hydrogen sulfide (H2S) in vascular function, its potential contribution to S1P and AMPK-induced vasorelaxation would also be interesting to study. H2S levels in PVAT-conditioned media treated with S1P and AICAR can be quantified using gas chromatography-mass spectrometry (GC-MS) and colorimetric assays to determine whether these treatments influence H₂S production and pharmacological inhibition of H2S production can be achieved using DL-propargylglycine (PAG), a cystathionine y-lyase (CSE) inhibitor, to evaluate its effect on vascular relaxation. Furthermore, studies using CSE knockout (KO) mice would clarify the endogenous role of H2S in S1P and AMPK-

induced vascular effects, providing deeper insights into its contribution to PVAT-mediated vasoregulation.

Future work could also employ in vitro studies using 3T3-L1 adipocytes, WT and AMPKα1&α2 KO MEFs to examine the molecular mechanisms involved. Cells would be treated with S1P and AICAR, and adipokine secretion assessed using ELISA and Western blot analysis, while qPCR and immunoblotting used to analyse the expression of S1P receptors (S1PR1, S1PR2, and S1PR3) and AMPK signalling components. Furthermore, conditioned media from treated with S1P and AICAR could be applied to vascular smooth muscle cells (VSMCs) to examine their effects on vasorelaxation.

4.5 Conclusion

This study provides novel insights into the mechanisms by which S1P and AICAR regulate vascular relaxation, emphasizing the complex interplay between perivascular adipose tissue (PVAT), AMPKα1, nitric oxide (NO), and adiponectin. The findings establish PVAT as an active regulator of vascular function, rather than a passive structural component, primarily through its secretion of vasoprotective adipokines and enhancement of NO production. The significant attenuation of these effects in AMPKα1 knockout (KO) mice highlights AMPK signalling as a key mediator of PVAT-induced vasorelaxation. This study extends our understanding of PVAT as a metabolic regulator of vascular tone, suggesting that targeting PVATderived signalling and AMPK activation could serve as a potential therapeutic strategy for vascular dysfunction in cardiovascular diseases. Beyond reinforcing the vasodilatory role of adiponectin and NO, this study opens new research directions into other PVAT-derived mediators, such as hydrogen sulfide (H2S), which may also contribute to S1P and AMPK-induced vascular effects. Furthermore, the differential responses observed in AMPKα1 KO mice suggest the possibility of isoform-specific functions of AMPK, warranting further investigation into AMPKα2 and its compensatory mechanisms in vascular homeostasis. However, certain limitations should be considered. While this study establishes a functional relationship between PVAT, AMPK activation, and vascular relaxation, the precise molecular mechanisms and downstream signalling pathways require further validation through targeted gene knockdown and pharmacological inhibition.

Additionally, the reliance on in vitro wire myography, although valuable for mechanistic studies, does not fully capture the systemic vascular responses in physiological and pathological conditions. Future research should extend these findings to in vivo disease models to assess their clinical significance. Overall, this study presents PVAT as an active metabolic contributor to vascular function, shifting the perspective from a structural support role to a dynamic regulator of vascular homeostasis. These findings highlight the potential of PVAT-targeted therapies and AMPK modulation in developing novel interventions for metabolic and cardiovascular diseases.

Chapter 5 - How Sphingsine-1-Phosphate (S1P) and AMPK activators-compound 991 and A769662 affect perivascular adipose tissue functions

5.1 Introduction

In Chapter 4, it was shown that a combination of S1P and the AMPK activator AICAR, induced significantly enhanced vascular relaxation in endothelium-denuded thoracic aortic rings containing PVAT compared to each agent individually. These findings emphasize the critical role of AMPK activation in regulating vascular smooth muscle function and highlight the importance of PVAT-derived factors in facilitating relaxation responses. Notably, the presence of PVAT amplified the effects of both S1P, which had no significant vasorelaxant effects when administered alone, and AICAR, illustrating its dynamic role as an active endocrine tissue. PVAT releases key adipokines, such as adiponectin, and vasorelaxant mediators, including nitric oxide. These PVAT-derived factors are fundamental to the regulation of vascular tone and play a crucial role in maintaining vascular homeostasis under physiological conditions (Queiroz and Sena, 2024).

The findings further underscored the pivotal role of AMPK activation in modulating PVAT functionality. The augmented relaxation observed when S1P and AICAR were combined in PVAT-containing vascular rings was significantly diminished in AMPKa1 knockout (KO) mice, highlighting the essential function of AMPKa1, the principal catalytic subunit of AMPK in vascular tissues. These results provide a foundation for future research aimed at exploring the impact of various AMPK activators on vascular function in relation to PVAT.

Building on these findings, the experiments presented in this chapter investigate the effects of two other AMPK activators, namely Compound 991 and A-769662, in thoracic aortic rings containing PVAT, both individually and in combination with S1P. These two AMPK activators differ significantly from AICAR in terms of their mechanisms of activation (Sanders et al., 2007). AICAR, an adenosine analogue, is transported into cells via adenosine transporters and subsequently phosphorylated by adenosine kinase to become ZMP, an AMP mimetic (Merrill et al., 1997; Gao et al., 2018). Unlike traditional activators, AICAR activates AMPK without altering adenine nucleotide ratios, that is ADP/ATP or AMP/ATP. However, ZMP can also modulate other metabolic enzymes that are allosterically regulated by AMP, leading to potential off-target effects (RenaHardie and Pearson, 2017). In contrast, A769662 is a direct allosteric activator of AMPK that targets the AMPK

isoforms containing the β1 subunit. The drug binds to the subunit between the β-CBM and the N-lobe on the α subunit, known as the allosteric drug and metabolite (ADaM) site. This interaction also inhibits the dephosphorylation of Thr172 by protein phosphatases, thus keeping the enzyme activated. Similarly, Compound 991 (C991) is another direct allosteric activator of AMPK (Willows et al., 2017). Like A769662, C991 binds to the ADaM site but demonstrates activity in both AMPKβ1- and AMPKβ2-containing complexes, with a stronger preference for β1 (Xiao et al., 2013). These distinct mechanisms of AMPK activation offer a valuable opportunity to investigate the specific effects of various activation pathways on vascular relaxation, particularly in the presence of PVAT.

The motivation for investigating C991 and A-769662 arises from the need to determine whether the previously observed effects of S1P and AlCAR are specific and dependent on the mode of AMPK activation or represent a broader interaction between S1P signalling and AMPK pathways. The roles of both activators in regulating nitric oxide (NO) production and oxidative stress in cultured endothelial cells have not been extensively investigated, and current understanding remains limited (Strembitska et al., 2018). By comparing the effects of C991 and A-769662 with those of AlCAR, this study seeks to clarify whether variations in AMPK activation mechanisms lead to differences in vascular relaxation responses, particularly in the context of S1P signalling and PVAT.

Chapter 4 highlighted that the effects of S1P and AICAR were partly associated with a slight increase in adiponectin secretion and a significant enhancement of NO from PVAT. This observation suggests that AMPK activation may condition PVAT to release vasoprotective factors, thereby amplifying the vasorelaxant effects of S1P. However, it remains uncertain whether this priming effect is unique to AICAR or can be achieved with other AMPK activators, such as C991 and A-769662. To address this question, the current study examines the combined effects of S1P and these activators on vascular relaxation in thoracic aortic rings containing PVAT.

This chapter further explores the role of AMPKα1 in mediating vascular relaxation responses by utilizing thoracic aortic rings from AMPKα1 knockout mice. The global absence of AMPKα1 in these mice offers a valuable model to distinguish between AMPK-dependent and AMPK-independent mechanisms underlying vascular relaxation. In Chapter 4, the combination of S1P and AICAR resulted in enhanced relaxation, which was markedly reduced in AMPKα1 KO mice, underscoring the

critical role of this isoform in AMPK-mediated effects. Building on these findings, the current study examines whether the compounds C991 and A-769662 exhibit similar AMPKa1 dependency in their effects on vascular relaxation. By comparing responses in wild-type and AMPKa1 KO mice, this research aims to elucidate the extent to which AMPKa1 contributes to the interplay between S1P signalling and PVAT-mediated vascular effects.

In summary, the findings presented in Chapter 4 are extended in this chapter through an exploration of the effects of two additional AMPK activators, C991 and A-769662, on vascular relaxation in thoracic aortic rings with PVAT. By comparing these results with those observed using AICAR, the study seeks to elucidate how distinct mechanisms of AMPK activation influence S1P-mediated vascular effects and PVAT-driven vascular responses.

5.2 Aim and Objectives

The primary aim of this chapter is to investigate the role of AMPK activators C991 and A-769662 in modulating vascular relaxation in thoracic aortic rings with intact PVAT, both individually and in combination with S1P. The aim is to determine how different mechanisms of AMPK activation influence vascular function, particularly in the context of PVAT-derived factors and AMPKα1 signalling. Objectives include:

- 1. To evaluate the effects of S1P and C991 on vascular relaxation in WT endothelium-denuded thoracic aortic rings with PVAT and in AMPK α 1 KO thoracic aortic rings with PVAT.
- To evaluate the effects of S1P and A-769662 (A76) on vascular relaxation in WT endothelium-denuded thoracic aortic rings with PVAT and in AMPKα1 KO thoracic aortic rings with PVAT.

5.3 Results

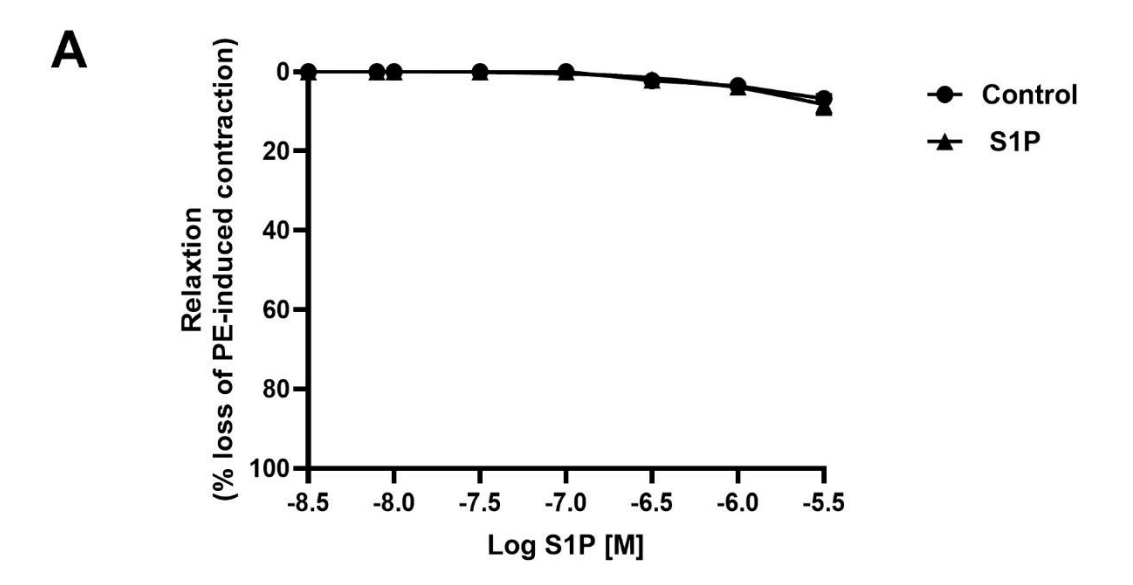
5.3.1 Effect of the combination of S1P and Compound 991 (C991) on vascular smooth muscle relaxation in wild-type (WT) thoracic rings with intact PVAT

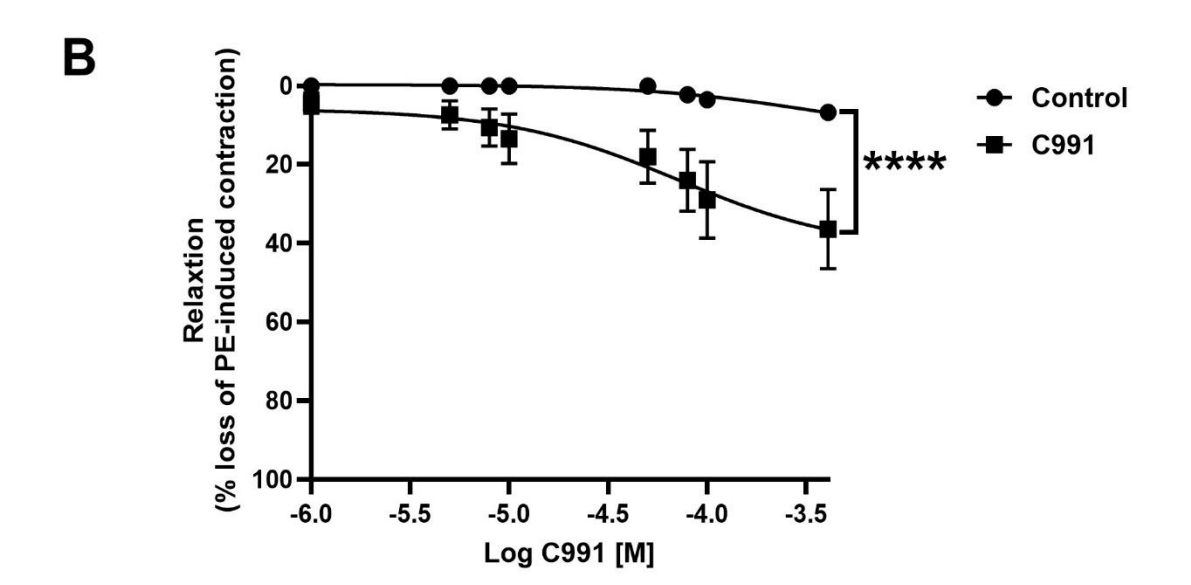
Chapter 4 reported enhanced relaxation in denuded thoracic aortic rings containing perivascular adipose tissue (PVAT) when treated with a combination of sphingosine-1-phosphate (S1P) and the AMPK activator AICAR (Figure 4-1D). To further explore the roles of sphingolipids and AMPK in vascular function, the AMPK activator C991 was utilized. Thoracic aortic rings with intact PVAT were isolated from wild-type (WT) mice, and the endothelium was removed before use. These rings were mounted on a wire myograph and pre-contracted using 1 μ M phenylephrine, following the protocol detailed in the methods section. Subsequently, the effects of S1P and C991 on vascular function were assessed in rings with intact PVAT.

Cumulative concentration-response curves for S1P alone (3×10^{-9} to 3×10^{-6} M) were generated in endothelium-denuded aortic rings with PVAT. S1P alone did not induce significant relaxation in these rings, with maximum relaxation recorded at $8.3 \pm 2.4\%$ (n=5) in S1P-treated rings compared to $6.8 \pm 1.6\%$ (n=5) in untreated controls (Figure 5-1A).

In separate rings, C991 (1×10^{-6} to 5×10^{-4} M) was administered. C991 treatment induced a significant relaxation, with a maximum relaxation of $36.4 \pm 9.9\%$ (n=5) observed in treated rings, compared to $6.8 \pm 1.6\%$ (n=5) in untreated controls (Figure 5-1B).

A combination of S1P (3×10^{-9} to 3×10^{-6} M) and C991 (1×10^{-6} to 5×10^{-4} M) was applied, but there was no augmented relaxation beyond the effect of C991 alone. The maximum relaxation observed with the combination treatment was 34.8 \pm 7.7% (n=6), comparable to that achieved with C991 alone ($36.4 \pm 9.9\%$, n=5) (Figure 5-1C).





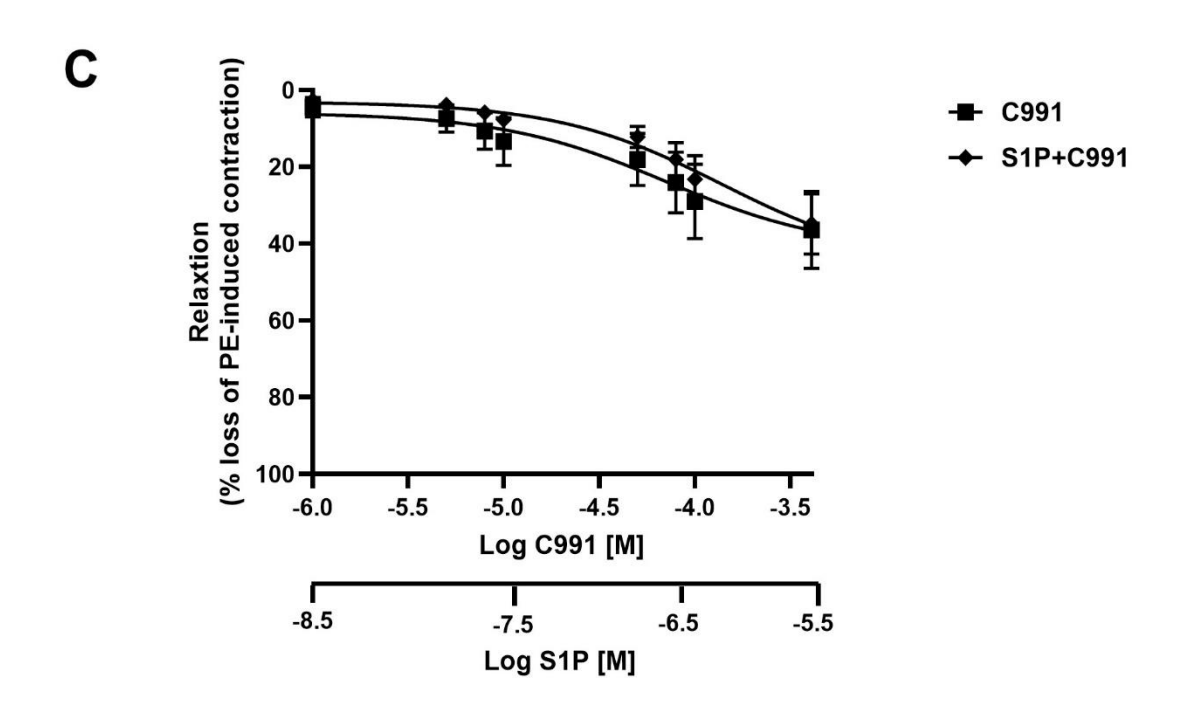


Figure 5-1: Functional assessment of relaxation in endothelium-denuded thoracic aortic rings with PVAT from wild-type (WT) mice.

(A)Sphingosine-1-phosphate (S1P) were investigated over a range of concentrations (3×10^{-9} to 3×10^{-9} M). These data were compared with the responses of time control PVAT-containing aortic rings (n=5). (B) The effects of the AMPK activator C991 were evaluated at concentrations between 1×10^{-6} and 5×10^{-4} M. Results were compared to the untreated PVAT-containing aortic rings (n=5). (C) The combined effects of S1P and C991 on the concentration-response curves were assessed in PVAT-containing aortic rings. These responses were compared to those observed with C991 treatment alone (n=6). All results are expressed as mean \pm SEM. Statistical comparisons were performed using two-way ANOVA followed by Tukey's post hoc test, ****P < 0.001 vs control.

5.3.2 Effect of the combination of S1P plus Compound 991 (C991) on vascular smooth muscle relaxation in AMPKα1 KO thoracic rings with intact PVAT

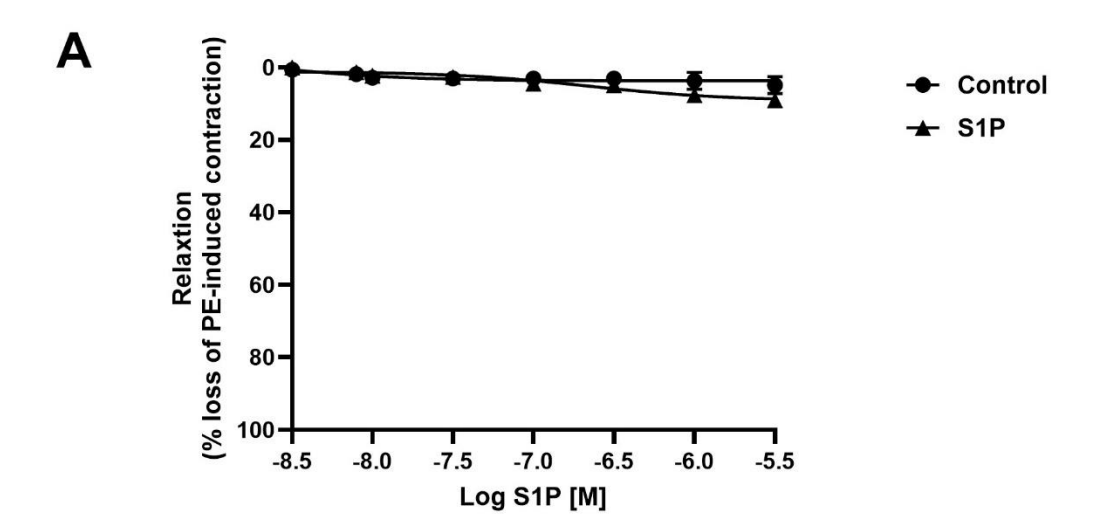
Vascular function in endothelium-denuded thoracic aortic rings derived from global AMPK α 1 KO mice in the presence of PVAT was examined. The primary objective was to assess the effects of S1P and the AMPK activator C991 on vascular relaxation in these tissues. Following the previously described methodology, the aortic rings were mounted on a wire myograph and pre-contracted with 1 μ M phenylephrine.

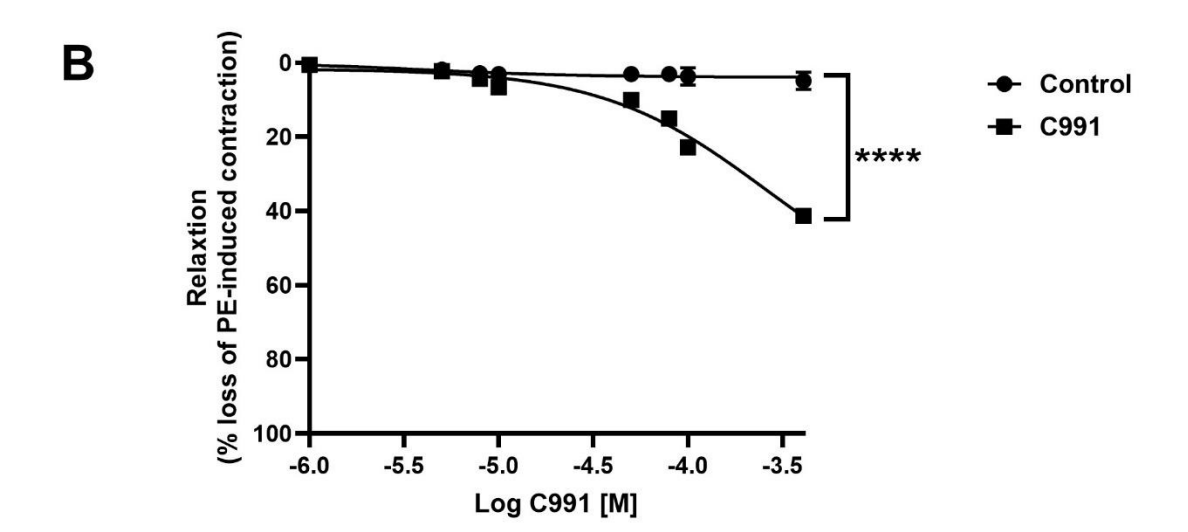
Cumulative concentration-response curves were generated for S1P (3×10^{-9} to 3×10^{-6} M) in endothelium-denuded aortic rings containing PVAT. S1P alone did not induce significant relaxation in the KO rings, with the maximum relaxation recorded at 9 ± 1% (n=5), compared to 4.8 ± 2.2% (n=5) in untreated control rings (Figure 5-2A).

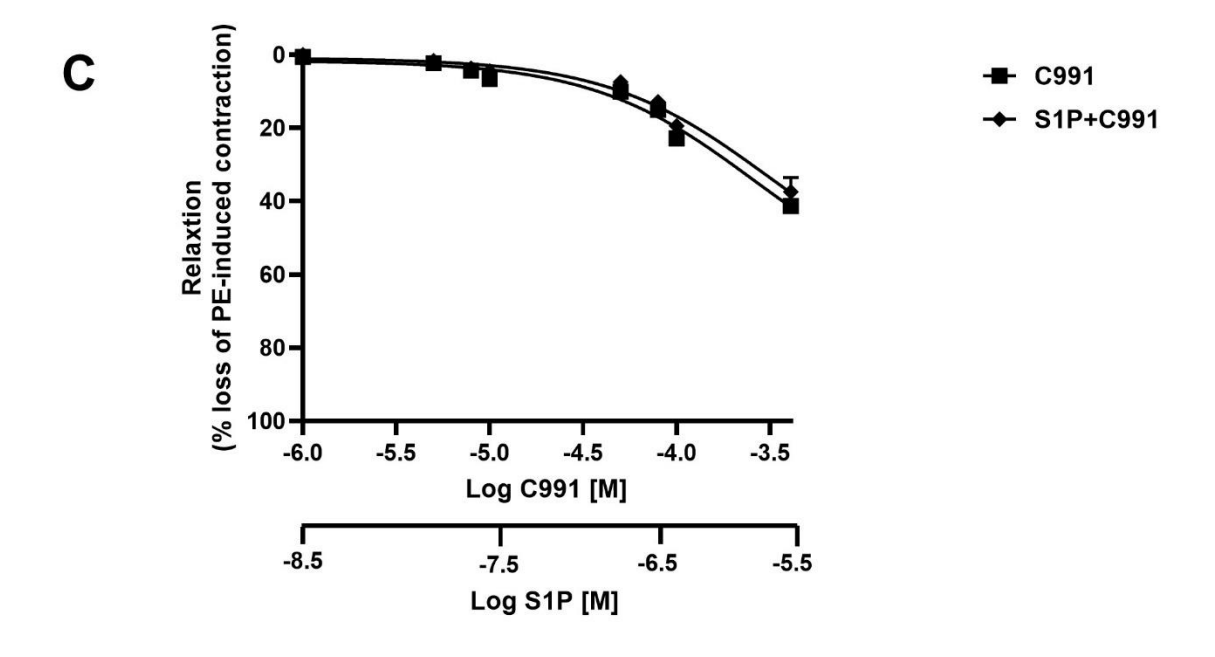
In separate rings, C991 caused a significant degree of vascular relaxation in these rings, achieving a maximum relaxation of $41.3 \pm 1.4\%$ (n=4), substantially greater than the $4.8 \pm 2.2\%$ (n=5) observed in untreated controls (Figure 5-2B).

When a combination of S1P (3×10^{-9} to 3×10^{-6} M) and C991 (1×10^{-6} to 5×10^{-4} M) was applied to AMPK α 1 KO aortic rings with PVAT, no additional relaxation was observed beyond that produced by C991 alone. The maximum relaxation achieved with the combination treatment was $37.4 \pm 3.8\%$ (n=5), similar in magnitude to the response to C991 alone ($41.3 \pm 1.4\%$, n=4) (Figure 5-2C).

When comparing the relaxation responses in WT and KO aortic rings, it was observed that there was no difference in the maximum relaxation observed following combination treatment with S1P and C991 where the value was $37.4 \pm 3.8\%$ (n=5) in KO mice compared to $34.8 \pm 7.7\%$ in WT mice (n=6; (Figure 5-2D).







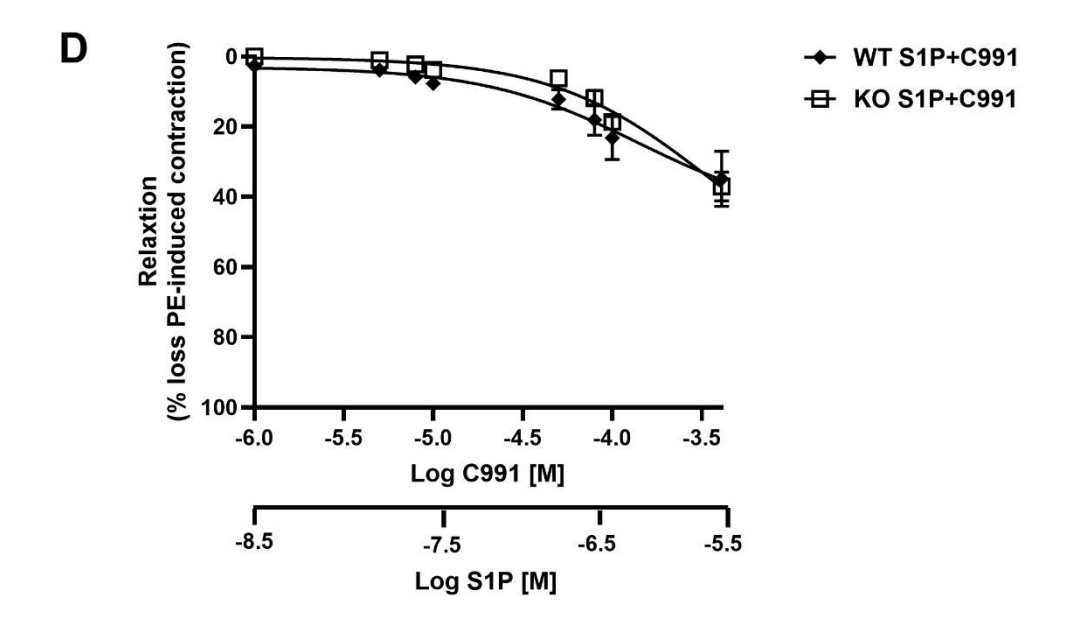


Figure 5-2: Functional evaluation of endothelium-denuded thoracic aortic rings with PVAT in AMPKα1 knockout (KO) mice.

(A) Sphingosine-1-phosphate (S1P)-induced relaxation was analyzed across a concentration range of 3×10^{-6} M. Results were compared with those obtained from untreated PVAT-containing aortic rings (n=5). (B) The impact of the AMPK activator C991 on vascular relaxation was assessed at concentrations ranging from 1×10^{-6} to 5×10^{-4} M. These results were compared to those observed in untreated PVAT-containing aortic rings (n=4). (C) The combined effects of S1P and C991 on relaxation responses were evaluated. Comparisons were made with data from PVAT-containing rings treated with C991 alone (n=5). (D) The combined effects of C991 and AICAR on relaxation responses in PVAT-containing aortic rings from AMPK α 1 KO mice (n=5) were compared with the corresponding responses in PVAT-containing aortic rings from wild-type (WT) mice (n=6). All results are presented as mean \pm SEM. Statistical analyses were performed using two-way ANOVA, followed by Tukey's post hoc test. ****P < 0.001 vs. control.

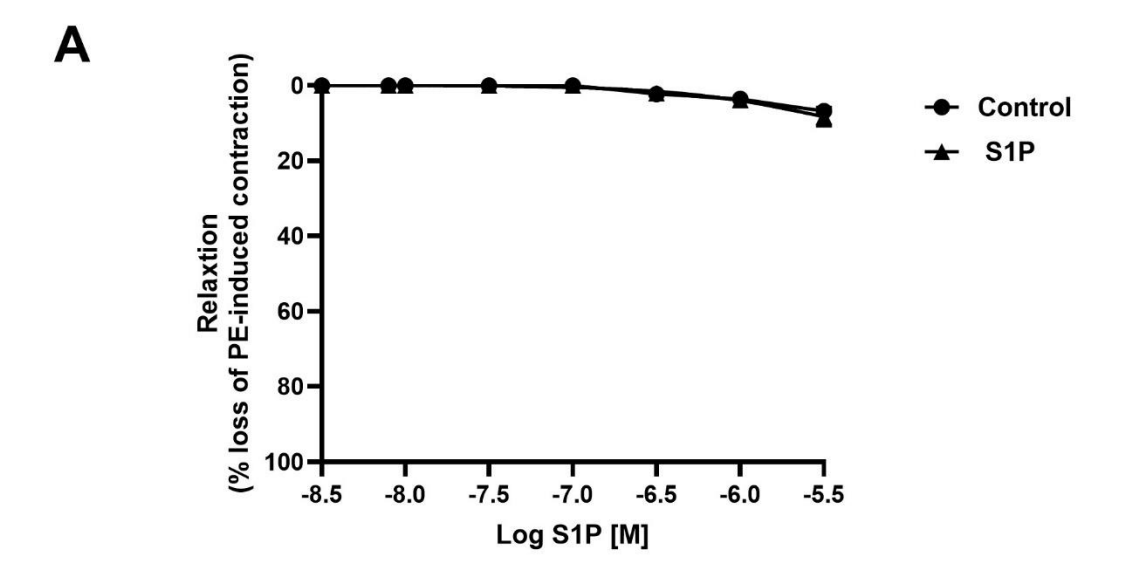
5.3.3 Effect of the combination of S1P plus A769662 on vascular smooth muscle relaxation in wild-type thoracic aortic rings with intact PVAT

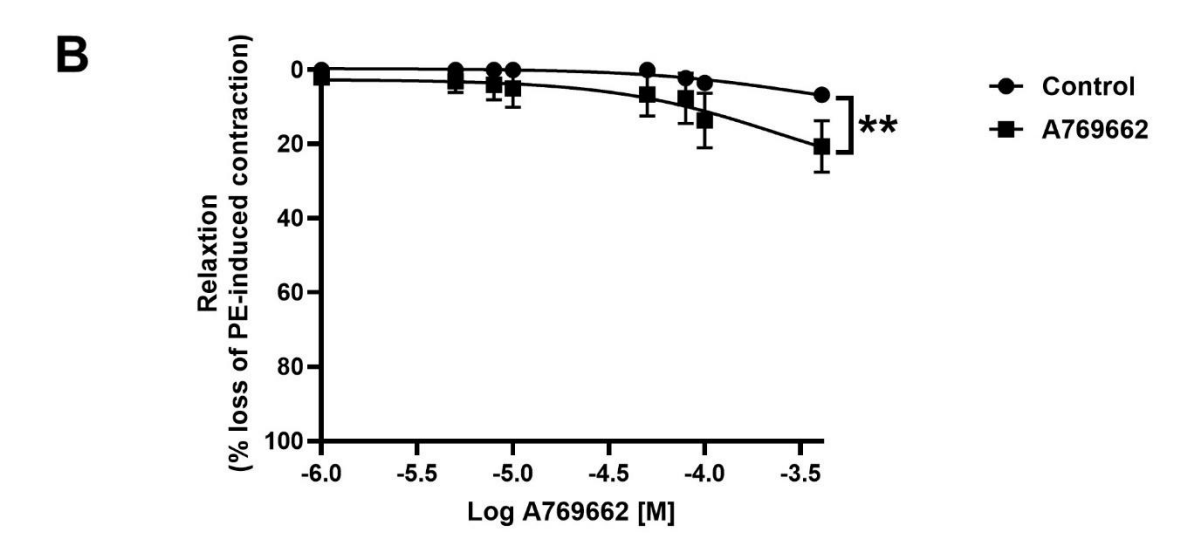
The combination of S1P and the AMPK activator C991 did not enhance relaxation in denuded thoracic aortic rings containing PVAT in either WT mice (Figure 5-1C) or AMPK α 1 KO mice (Figure 5-2C). To investigate if the lack of effect was specific to C991 or shared with other allosteric AMPK modulators, additional experiments were conducted using the AMPK activator A769662 on mouse aortic tissues. Denuded thoracic aortic rings with intact PVAT were isolated from WT mice, mounted on a wire myograph, and pre-contracted with 1 μ M phenylephrine, as described in the methods section. The effects of S1P and A769662 on vascular function were subsequently assessed in the presence of PVAT.

Cumulative concentration-response curves for S1P alone (3×10^{-9} to 3×10^{-6} M) were constructed using endothelium-denuded aortic rings with PVAT. S1P on its own did not produce significant relaxation in these rings, with a maximum relaxation of 8.3 \pm 2.4% (n=4) observed in S1P-treated rings compared to 6.8 \pm 1.6% (n=4) in untreated controls (Figure 5-3A).

In another set of rings, A769662 (1×10^{-6} to 5×10^{-4} M) was added and induced a significant degree of relaxation, achieving a maximum relaxation of 20.6 ± 6.8% (n=3), compared to 6.8 ± 1.6% (n=4) in untreated rings (Figure 5-3B).

Finally, the effect of a combined treatment with S1P (3×10^{-9} to 3×10^{-6} M) and A769662 (1×10^{-6} to 5×10^{-4} M) was evaluated. However, the combination did not provide any augmentation of relaxation beyond that observed with A769662 alone. The maximum relaxation recorded with the combination treatment was 21.8 \pm 6.6% (n=4), comparable to the relaxation achieved with A769662 alone (20.6 \pm 6.8%, n=3) (Figure 5-3C).





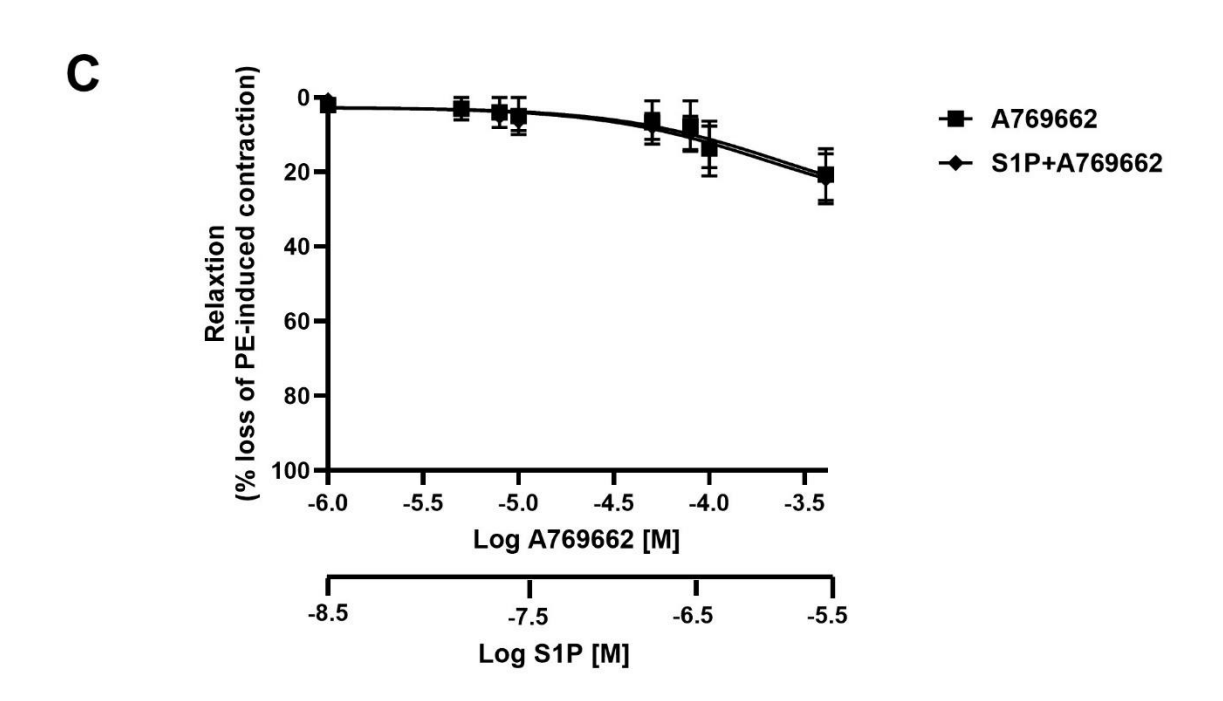


Figure 5-3: Functional evaluation of endothelium-denuded thoracic aortic rings with PVAT in wild-type (WT) mice.

A) The vasorelaxation effects of sphingosine-1-phosphate (S1P) were assessed over a concentration range of 3×10⁻⁶ to 3×10⁻⁶ M. These responses were compared to those of a time control PVAT-containing aortic rings (n=4). (B) The impact of the AMPK activator A769662 on vascular relaxation was evaluated at concentrations ranging from 1×10⁻⁶ to 5×10⁻⁴ M. Results were analysed in comparison to untreated PVAT-containing aortic rings (n=3). (C) The effects of S1P and A769662 on vascular relaxation were explored by assessing the concentration–response curves. These data were compared to the relaxation responses observed with A769662 alone (n=4). All results are presented as mean ± SEM. Statistical significance was evaluated using two-way ANOVA followed by Tukey's post hoc test. ****P< 0.01 vs control.

5.3.4 Effect of a combination of S1P plus A-769662 on relaxation in aortic rings from AMPKα1 KO mice with intact PVAT

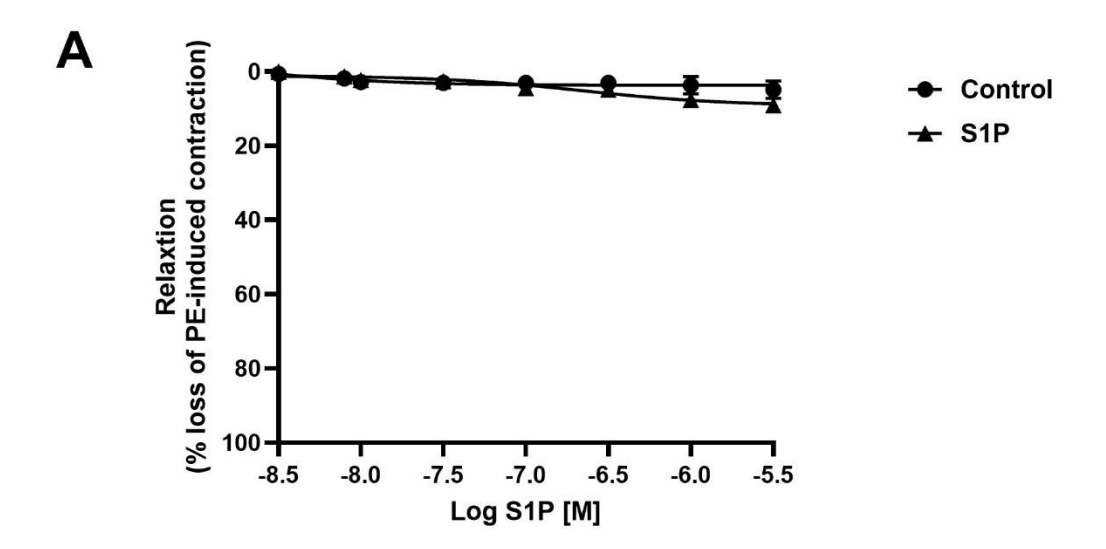
To investigate the role of AMPK in mediating relaxation in endothelium-denuded thoracic aortic rings, tissue from global AMPK α 1 KO mice with the PVAT left intact was studied. In these experiments, the effects of S1P and the AMPK activator A-769662 were studied alone and in combination. Using the previously described methodology, the aortic rings were mounted on a wire myograph and precontracted with 1 μ M phenylephrine.

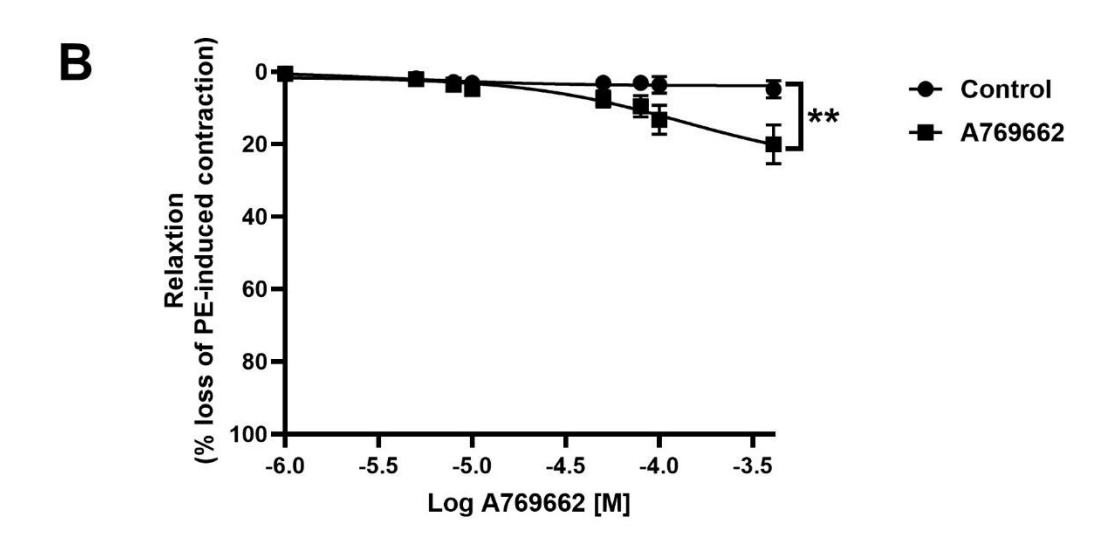
Cumulative concentration-response curves for S1P (3×10^{-9} to 3×10^{-6} M) were generated in endothelium-denuded aortic rings containing PVAT. S1P alone did not induce any significant relaxation in AMPK α 1 KO rings, with a maximum relaxation of 9 ± 1% (n=5), compared to 4.8 ± 2.2% (n=4) in untreated control rings (Figure 5-4A).

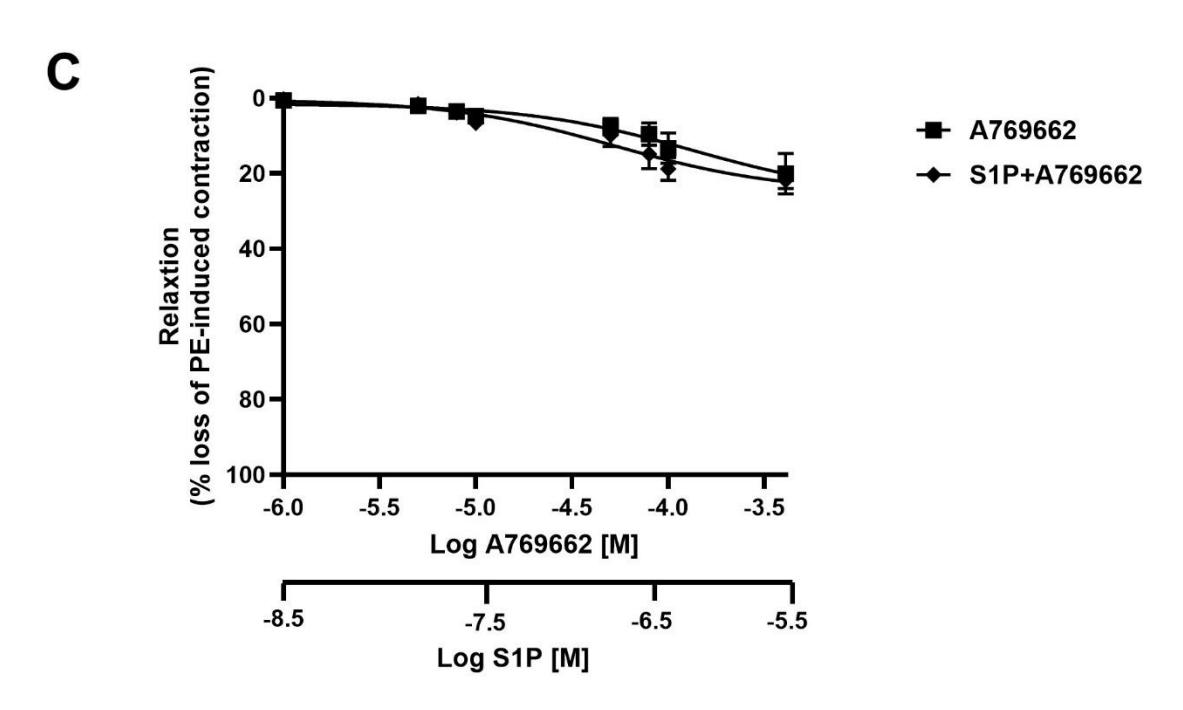
In a separate set of rings, A-769662 (1×10^{-6} to 5×10^{-4} M) was applied to endothelium-denuded aortic rings with PVAT. A-769662 treatment induced a significant degree of relaxation, achieving a maximum relaxation of $20 \pm 5.3\%$ (n=4), markedly higher than the $4.8 \pm 2.2\%$ (n=4) observed in untreated control rings (Figure 5-4B).

When the combination of S1P (3×10^{-9} to 3×10^{-6} M) and A-769662 (1×10^{-6} to 5×10^{-4} M) was applied to AMPK α 1 KO aortic rings with PVAT, no additional relaxation was observed beyond that produced by A-769662 alone. The maximum relaxation recorded for the combination treatment was 21.8 \pm 2.1% (n=4), consistent with the response to A-769662 alone ($20\pm5.3\%$, n=4) (Figure 5-4C).

When comparing the relaxation responses in WT and KO aortic rings, it was observed that there was no difference in the maximum relaxation observed following combination treatment with S1P and A-769662. The maximum relaxation observed with the combination treatment remained at $21.8 \pm 2.1\%$ (n=4), comparable to the relaxation observed in WT endothelium-denuded rings with PVAT under similar conditions ($21.8 \pm 6.6\%$, n=4) (Figure 5-4D).







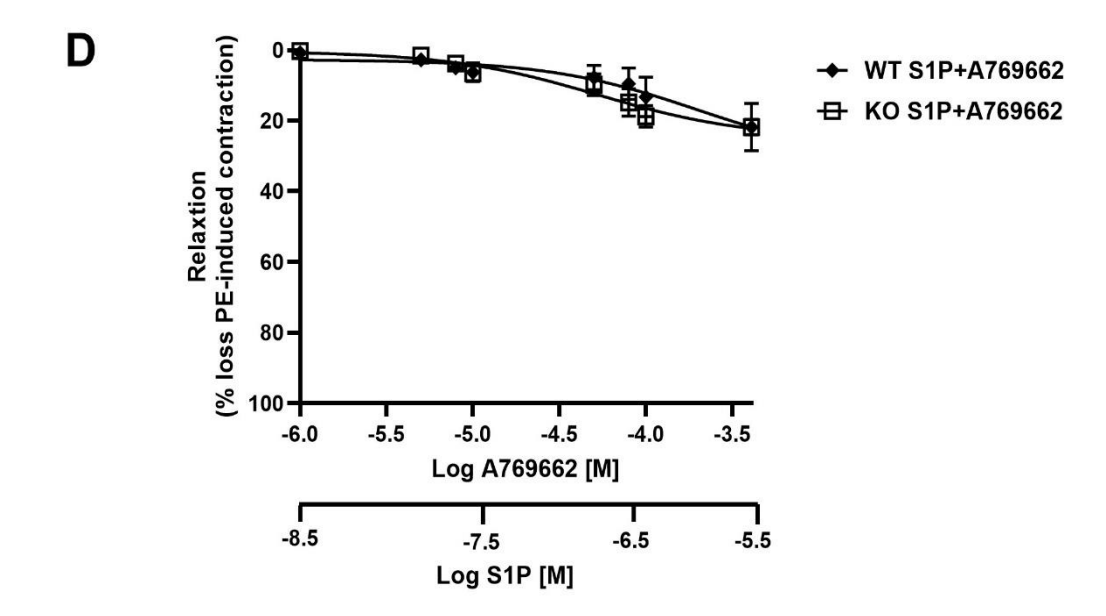


Figure 5-4: Functional evaluation of endothelium-denuded thoracic aortic rings with PVAT in AMPKα1 knockout (KO) mice.

(A) The vasorelaxation responses to sphingosine-1-phosphate (S1P) were evaluated across a concentration range of 3×10^{-9} to 3×10^{-6} M. These data were compared to the relaxation responses observed in a time control PVAT-containing aortic rings (n=5). (B) The effects of the AMPK activator A769662 on vascular relaxation were analyzed over a concentration range of 1×10^{-6} to 5×10^{-4} M. Results were compared with those obtained in untreated PVAT-containing aortic rings (n=4). (C) The effects of S1P and A769662 on relaxation responses were examined. These responses were compared to those of PVAT-containing aortic rings treated with A769662 alone (n=4). (D) The combined relaxation effects of A769662 and AICAR were compared between PVAT-containing aortic rings from AMPK α 1 KO mice (n=4) and wild-type (WT) mice (n=4). All results are expressed as mean \pm SEM. Statistical significance was assessed using two-way ANOVA followed by Tukey's post hoc test, **P < 0.01 vs. control.

5.4 Discussion

Chapter 5 explored the effects of S1P in combination with two AMPK activators, C991 and A-769662, on vascular relaxation in thoracic aortic rings from wild-type and AMPKα1 knockout mice. The findings demonstrated that both AMPK activators, C991 and A-769662, induced a significant vascular relaxation in WT and AMPKα1 KO rings. While these results suggest that AMPK activation facilitates vascular relaxation, the persistence of this effect in AMPKα1-deficient mice implies the involvement of alternative AMPK isoforms or compensatory mechanisms. Therefore, although AMPK α 1 plays a contributory role, it may not be solely responsible for the vasorelaxation observed. Notably, the combination of S1P with either C991 or A-769662 did not result in further relaxation beyond that achieved by the AMPK activator alone, indicating a lack of synergistic or additive effects. This contrasts with the enhanced relaxation observed when S1P was combined with AICAR, which may be due to differences in the mechanism of AMPK activation. This can be explained because AICAR activates AMPK indirectly, but C991 and A-769662 are direct AMPK activators. By using these agents in combination, such as S1P with AICAR, there be a synergistic effect that more effectively activates AMPK, leading to increase NO production from PVAT, thereby promoting vascular relaxation.

The lack of enhanced relaxation in the combined treatments such as S1P with A-769662 or S1P with C991 suggests that S1P and AMPK activators likely engage convergent signalling pathways, with both influencing nitric oxide. Some evidence suggests that S1P can influence VSMC and other tissues through its receptors, potentially modulating NO-related pathways. In a similar way, AMPK activators may have indirect effects on NO production in non-endothelial tissues (Igarash and Michel, 2009). The almost absent vasorelaxation observed with S1P alone further supports the possibility that S1P's role in vascular relaxation may be secondary or modulatory rather than primary.

Chapter 4 demonstrated that the combination of S1P and the AMPK activator AICAR induced a significantly augmented vascular relaxation in endothelium-denuded thoracic aortic rings containing PVAT. The relaxation response to the combined treatment was notably greater than that achieved by AICAR alone,

suggesting an interaction between S1P and AICAR in the presence of PVAT (see Chapter 4). This effect was attributed to the enhanced secretion of PVAT-derived factors such as adiponectin and increased NO production, both of which are known to contribute to vasorelaxation. To understand why the interaction was so effective, it is useful to note that S1P interacts with its receptors (S1PR1-S1PR5) on different kinds of cells, including adipocytes and endothelial cells. This may stimulate pathways that encourage adipokines like adiponectin to be released and enhance the production of NO. AICAR indirectly activates AMPK, a key regulator of cellular energy homeostasis, which in turn stimulates NO production from PVAT, thereby enhancing vascular NO availability. Furthermore, it encourages the secretion of anti-inflammatory adipokines (e.g., adiponectin) from PVAT. These individual effects may operate synergistically, with amplified effects through their targeting of pathways that are different, but complementary. S1P's signalling, mediated by its receptors, and AICAR's activation of AMPK might combine to speed the production of PVAT-derived factors and NO, with greater effect together than individually. The augmented relaxation in Chapter 4 highlights a contextdependent interaction between S1P and AMPK activators, mediated by the presence of PVAT and, crucially AMPKα1 because the effect was lost in KO mouse rings.

In contrast, the findings in Chapter 5 revealed no additive effects between S1P and the AMPK activators C991 and A-769662. This discrepancy may stem from differences in the mechanisms of AMPK activation. These two AMPK activators exhibit distinct activation mechanisms compared to AICAR (Sanders et al., 2007). AICAR, an adenosine analogue, is phosphorylated intracellularly to form ZMP, an AMP mimetic that activates AMPK without significantly altering cellular ADP/ATP or AMP/ATP ratios (Merrill et al., 1997; Hardie & Pearson, 2017). However, ZMP is not exclusively selective for AMPK. It can also interact with a range of AMP-sensitive enzymes and signalling pathways independent of AMPK activation. Notably, ZMP has been shown to affect the activity of metabolic enzymes such as glycogen phosphorylase and fructose-1,6-bisphosphatase, as well as other key regulators of cellular metabolism (Corton et al., 1995; Merrill et al., 1997). In vascular smooth muscle cells (VSMCs), these off-target interactions may alter metabolic activity and cellular responses in ways that are unrelated to AMPK signalling.

In contrast, A769662 and Compound 991 are direct allosteric AMPK activators targeting the ADaM site between the β -CBM and the N-lobe on the α subunit, enhancing AMPK activity and inhibiting Thr172 dephosphorylation (Xiao et al., 2013). A769662 is specific to the AMPKB1 isoform, while C991 shows activity in both β 1- and β 2-containing complexes, with a preference for β 1 (Cool et al., 2006; Xiao et al., 2013; Willows et al., 2017) (Figure 5-5).

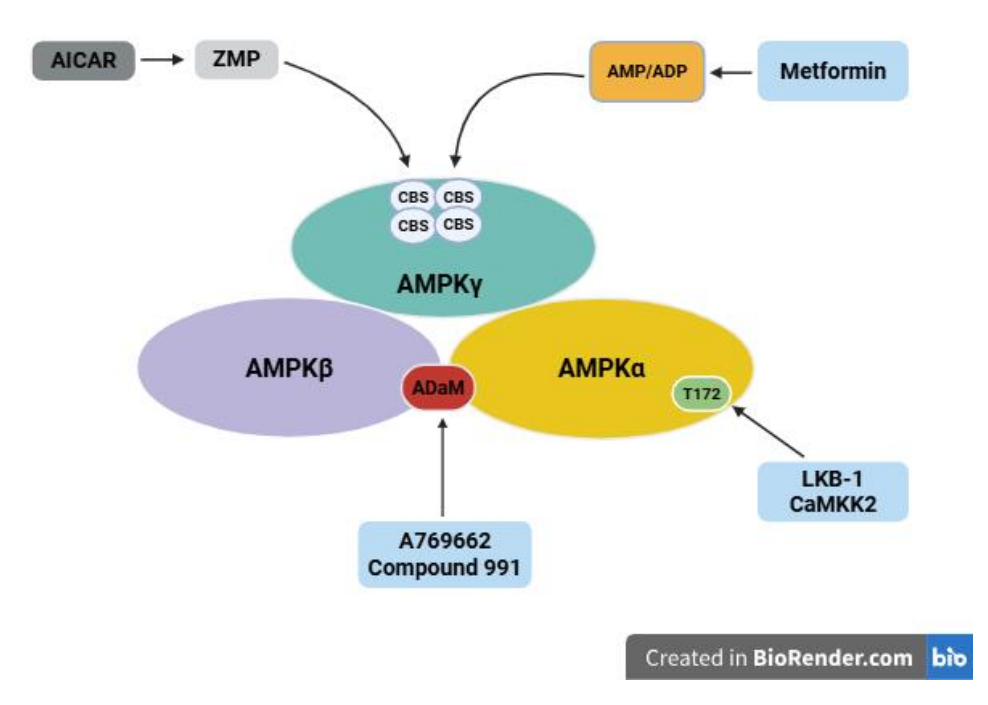


Figure 5-5: Mechanisms of AMPK regulation by pharmacological activators.

AMP-activated protein kinase (AMPK) is a heterotrimeric complex composed of a catalytic α -subunit and regulatory β - and γ -subunits. The γ -subunit contains cystathionine β -synthase (CBS) motifs that bind AMP and ADP, promoting allosteric activation and facilitating phosphorylation of the α -subunit at threonine 172 (Thr172) by the upstream kinase LKB1. This phosphorylation is essential for full AMPK activation. Conversely, ATP binding to the CBS sites inhibits AMPK activity. AICAR, an AMP analog, is metabolized intracellularly to ZMP, which mimics AMP by binding to the CBS motifs and activating AMPK. Additionally, AMPK α can be phosphorylated at Thr172 by Ca²+/calmodulin-dependent protein kinase kinase 2 (CaMKK2), independent of AMP levels, in response to elevated intracellular calcium. Synthetic activators such as A-769662 and compound 991 bind to the allosteric drug and metabolite (ADaM) site located between the β -subunit's carbohydrate-binding module and the α -subunit's kinase domain, thereby directly activating AMPK independently of cellular energy status.

AICAR, an AMP analog, activates AMPK by mimicking cellular energy stress and has been shown to enhance adiponectin expression, improve NO-mediated vascular function, and promote insulin sensitivity in peripheral tissues (Lihn et al., 2004;

Davis et al., 2006). These effects may help explain the more pronounced vasorelaxation observed with AICAR in this study compared to direct AMPK activators, highlighting the importance of activation mechanism in modulating PVAT-derived signalling and vascular responses.

In contrast to AICAR, A-769662 is a direct AMPK activator that binds to the B1subunit at the ADaM site. However, it has been reported to inhibit insulinstimulated glucose uptake in adipocytes through an AMPK-independent mechanism, leading to impaired insulin signaling (Kopietz et al., 2021). This disruption may have downstream consequences on adipokine regulation, particularly adiponectin. Adiponectin has been shown to promote adipocyte differentiation and enhance insulin-stimulated glucose uptake by upregulating GLUT4 gene expression and facilitating its translocation to the plasma membrane, thereby improving insulin sensitivity and lipid accumulation (Fu et al., 2005). In addition to its metabolic functions, PVAT-derived adiponectin and nitric oxide (NO) play important roles in vascular regulation by exerting direct vasorelaxant effects on vascular smooth muscle cells (VSMCs), independent of the endothelium. Adiponectin, in particular, has been recognised not only for its metabolic functions but also for its vascular actions. As demonstrated by Jüttner et al. (2024), both adiponectin and NO serve as key mediators in modulating vascular tone through their direct influence on VSMCs. Therefore, the impairment of insulin signaling and glucose uptake caused by A-769662 may reduce adiponectin release by PVAT, potentially diminishing its ability to promote nitric oxide (NO) production and relax vascular smooth cells via hyperpolarisation. This could account for why relaxation to A-769662 was lower than with AICAR. In the context of perivascular adipose tissue (PVAT), where adiponectin contributes to the anticontractile phenotype, a reduction in its secretion could blunt PVAT's regulatory effect on vascular tone. This suggests that while A-769662 effectively activates AMPK, its off-target interference with insulin signaling may inadvertently impair key adipocyte-derived mediators like adiponectin, which are essential for maintaining endothelial function and vascular health. Consequently, this could limit the therapeutic utility of A-769662 in conditions such as metabolic syndrome and cardiovascular disease, where both improved insulin sensitivity and vascular function are desired.

C991, another direct AMPK activator with greater potency than A-769662, also targets the ADaM site and shares the B-subunit binding interface. Adiponectin, a key adipokine involved in metabolic regulation, enhances insulin sensitivity and, together with nitric oxide (NO), directly promotes vasorelaxation in vascular smooth muscle cells (VSMCs), contributing to the regulation of vascular tone independently of endothelial involvement. However, the specific role of C991 in modulating adiponectin expression and nitric oxide (NO) production remains underexplored.

The findings from Chapters 4 and 5 collectively reinforce our understanding of the intricate interplay between S1P, AMPK activators, and PVAT in regulating vascular relaxation. While S1P and AICAR demonstrate an augmented relaxation, particularly in the presence of PVAT, the addition of S1P to C991 or A-769662 does not enhance the vasodilation induced by these AMPK activators alone. This could be down to potential differences in their mechanisms of action and their target pathways. S1P primarily acts through its specific receptors to influence cellular signalling. However, C991 and A-769662 are direct AMPK activators. It is possible that the different pathways may not always synergise effectively, depending on the context, which could tend to limit the accumulated effects. Furthermore, the effects of S1P and the AMPK activators might overlap when affecting targets downstream (for example, adiponectin and NO production). This could result in redundancy, again limiting any potential additional effects. Finally, the effects of these compounds might be influenced by factors such as the cell type, experimental conditions, or the presence of other regulatory factors. This indicates that the specific pathways of AMPK activation and the influence of PVATderived factors play a critical role in shaping the vascular response.

Implications and Future Plans

The dynamics between S1P, AMPK activators C991 and A769662, and perivascular adipose tissue (PVAT) in regulating vascular relaxation are complex. S1P alone failed to show significant vasorelaxant effects in any experiments, while AMPK activation induced a significant relaxation, particularly in PVAT-containing endothelium-denuded aortic rings. This emphasises the critical role of AMPK in mediating vascular tone, likely through increased production of PVAT-derived

vasorelaxant factors such as adiponectin and nitric oxide. However, the inability of S1P to augment the effects of some AMPK activators suggests a receptor-mediated, context-specific role for S1P signalling that is less reliant on PVAT-derived factors. Furthermore, the different pathways used may not always be conducive to synergies, and there may be competition between the two, leading to redundancy. The comparable responses between wild-type and AMPKα1 knockout tissues suggest that while AMPKα1 contributes specifically to certain vascular signalling pathways, other AMPK isoforms or compensatory mechanisms may partially offset its absence to maintain vascular relaxation.

Future experiments should aim to clarify the specific mechanisms by which C991 and A-769662 mediate vascular relaxation. Given that the combination of C991 or A-769662 with S1P did not enhance relaxation beyond the effect of the AMPK activators alone, further research is needed to determine whether these compounds fully saturate AMPK-mediated vasorelaxation pathways. In vitro studies could focus on optimizing dose-response curves using wire myography in WT and AMPKα1 KO mice. In vitro experiments utilizing vascular smooth muscle cells (VSMCs) and endothelial cells could be used to investigate whether these activators differentially regulate downstream AMPK targets, such as eNOS activation and oxidative stress reduction, using techniques including Western blot, gPCR, and live-cell metabolic assays. Additionally, MEF cells with KO of both AMPKα1 and AMPKα2 could be employed to determine isoform-specific contributions of AMPK to vascular relaxation. Furthermore, RNA sequencing and proteomic analysis of PVAT-conditioned media from mice treated with C991, A-769662, and S1P could be used to assess whether these activators influence PVATderived adipokine secretion, such as adiponectin and hydrogen sulfide (H2S), in an AMPK-dependent manner. Collectively, these experiments would provide a comprehensive understanding of AMPK activator-induced vascular relaxation and help identify additional signaling pathways regulated by C991, A-769662, and S1P beyond AMPK activation.

5.5 Conclusion

This study underscores the critical role of AMPK activation in vascular relaxation, demonstrating that C991 and A-769662 induce significant relaxation responses especially in rings with intact PVAT. In contrast, S1P alone had no direct effect on vascular tone, and its combination with these two AMPK activators did not yield synergistic relaxation. These findings refine our understanding of AMPK's role in vascular homeostasis, reinforcing its therapeutic potential in conditions associated with vascular dysfunction. Notably, the preserved relaxation responses in AMPKα1 knockout (KO) tissues indicate that other AMPK isoforms may compensate for the loss of AMPKα1 and sustain vascular function. This highlights the need for further investigation into the potential contributions of other AMPK isoforms or other compensatory signalling pathways in mediating vascular relaxation. Additionally, given the central role of PVAT in AMPK-mediated vasorelaxation, future research should aim to identify key PVAT-derived mediators, such as nitric oxide (NO) and hydrogen sulfide (H2S), which may enhance the vasoprotective effects of AMPK activation. Further studies should evaluate whether chronic AMPK activation using C991 or A-769662 can improve endothelial function, restore vascular tone, and mitigate cardiovascular risk. By uncovering unexpected relaxation responses in AMPKα1 KO tissues, this study opens new avenues for research into alternative AMPK isoforms and non-canonical vasorelaxation mechanisms, paving the way for the development of targeted therapeutic interventions for vascular disorders.

Chapter 6 - General discussion

6.1 Summary and General discussion

The interplay between metabolic regulation, adipose tissue biology, and vascular function is increasingly recognised as a critical determinant in the development of cardiovascular and metabolic diseases. This thesis systematically examined these interactions, with a particular focus on the role of AMPK and SphK1 in adipose tissues, and the contribution of PVAT to vascular function. Through a series of experimental approaches involving genetic models and pharmacological interventions, the work presented here delineates how AMPK activation or deficiency modulates SphK1 expression, inflammatory signalling, and vascular relaxation. These findings advance current understanding of the functional heterogeneity of adipose tissue and its impact on vascular health and provide further support for developing novel therapeutic strategies targeting AMPK-dependent mechanisms in future.

Chapter 3 investigated the regulatory relationship between AMP-activated protein kinase and SphK1 in adipose tissue and adipocyte-derived cell models. The findings reveal a complex interaction between metabolic and inflammatory signalling pathways, which appears to differ depending on the location of the specific adipose depot.

SphK1 protein expression was found to increase progressively during the differentiation of 3T3-L1 preadipocytes into mature adipocytes, reaching a peak in fully differentiated cells. This observation supports earlier studies that identified SphK1 as a promoter of adipogenesis by enhancing lipid accumulation and supporting adipocyte maturation (Hashimoto et al., 2009). The results suggest, therefore, that SphK1 is not simply a marker of differentiation. Instead, it can be understood to make an active contribution to the regulation of adipocyte function.

Deletion of AMPK α 1 and α 2 in mouse embryonic fibroblast cells resulted in significantly increased SphK1 protein levels without a corresponding increase in SphK1 mRNA, suggesting that AMPK may regulate SphK1 through post-transcriptional mechanisms such as modulation of protein stability or translation. This is consistent with the broader role of AMPK in regulating energy balance and post-translational signalling in cells (Hardie, 2014). Moreover, AMPK deficiency was associated with increased activation of ERK1/2 and JNK pathways, both of

which are critical mediators of inflammation (Kyriakis and Avruch, 2012). These findings suggest that AMPK normally acts to suppress SphK1 expression and limit activation of pro-inflammatory signalling cascades, emphasising its anti-inflammatory role.

Analyses of fat from mice revealed a depot-specific pattern of SphK1 regulation. In abdominal perivascular adipose tissue (PVAT), no significant differences in SphK1 expression were detected between wild-type and AMPK α 1 knockout mice. However, in thoracic PVAT, SphK1 protein expression was significantly elevated in AMPK α 1-deficient mice. This observation highlights the functional differences between thoracic and abdominal PVAT. Thoracic PVAT shares characteristics with brown adipose tissue (BAT), including a high mitochondrial content and greater metabolic activity (Fitzgibbons et al., 2011). It is likely that BAT-like thoracic PVAT is more reliant on AMPK signalling to maintain its anti-inflammatory and metabolic functions, whereas WAT-like abdominal PVAT may be less dependent on AMPK activity.

The upregulation of SphK1 in thoracic PVAT under AMPK-deficient conditions may contribute to the development of local inflammation and metabolic dysfunction, which are important contributors to vascular disease. Previous studies have shown that PVAT inflammation impairs its normal protective effects on vascular tone and promotes vascular stiffness (Greenstein et al., 2009). Thus, loss of AMPK activity and the resulting increase in SphK1 may represent an important mechanism linking adipose tissue inflammation to vascular pathology.

Overall, these findings suggest that AMPK plays a critical role in regulating SphK1 expression and inflammatory signalling in adipose tissues, particularly in metabolically active depots such as thoracic PVAT. The results provide important insights into depot-specific differences in adipose tissue biology and suggest that targeting the AMPK-SphK1-MAPK signalling axis may offer a novel therapeutic approach for metabolic and vascular diseases.

Chapter4 provides novel insights into the regulatory interplay between sphingosine-1-phosphate (S1P) signalling, AMPK activation via AICAR, and the functional role of PVAT in modulating vascular relaxation in mouse thoracic aorta. The primary findings reveal that while S1P alone exhibits limited vasorelaxant properties, its combination with AICAR significantly enhances vascular relaxation,

particularly in the presence of PVAT. These findings emphasize the complexity of vascular regulation and the critical involvement of PVAT-derived factors, notably adiponectin and nitric oxide.

The limited vasorelaxant effect of S1P when used alone supports previous observations that S1P can mediate both vasodilation and vasoconstriction depending on receptor subtype activation and vascular bed context (Waeber et al., 2004; Chun et al., 2002). Specifically, S1PR1 activation has been associated with vasodilation through NO production (Wilkerson and Argraves, 2014), whereas S1PR2 and S1PR3 are often linked with vasoconstrictive pathways (Katunaric et al., 2022). This dual role may explain why S1P alone did not robustly induce relaxation in this study.

Importantly, the augmented relaxation observed with the combination of S1P and AICAR suggests a synergistic interaction between S1P receptor signalling and AMPK metabolic pathways. Activation of AMPK, particularly through the α 1 subunit, has been shown to enhance endothelial nitric oxide synthase (eNOS) activity, promote NO production, and facilitate vascular relaxation (Goirand et al., 2007; Davis et al., 2006). AICAR, an AMP analogue, effectively activates AMPK by mimicking cellular energy deprivation and has been previously reported to promote vascular relaxation through NO-dependent mechanisms (Igata et al., 2005; Hardie, 2016).

PVAT emerged as a crucial modulator in this study, amplifying the relaxation response to the S1P and AICAR combination. PVAT is increasingly recognized as an active endocrine organ, capable of secreting adipokines such as adiponectin and anti-inflammatory mediators such as NO (Szasz and Webb, 2012; Xia and Li, 2017). The enhancement of NO production in PVAT in response to S1P and AICAR, and the attenuation of relaxation by the NOS inhibitor L-NAME, strongly suggest that NO is a principal mediator of the observed vasorelaxation.

Furthermore, adiponectin, a key PVAT-derived adipokine, may significantly contribute to the relaxation responses observed. Adiponectin has been demonstrated to activate AMPK and enhance NO bioavailability, providing vasoprotective effects (Chen et al., 2003; Almabrouk et al., 2017). The slight increase in adiponectin secretion following S1P and AICAR treatment reinforces the hypothesis that PVAT-derived factors are central to mediating vascular relaxation.

Experiments with selective S1P receptor agonists and antagonists identified S1PR1 as a major contributor to the augmented relaxation, aligning with studies showing S1PR1-mediated enhancement of eNOS activity and NO production (Wang et al., 2023; Constantinescu et al., 2022). Antagonism of S1PR1 with W146 significantly reduced relaxation responses, further confirming the importance of S1PR1 signalling in this process.

The use of AMPKα1 KO mice provided critical mechanistic insights, as the absence of AMPKα1 abolished the enhanced relaxation response to the S1P and AICAR combination. These findings are consistent with previous studies emphasizing the dominance of the AMPKα1 isoform in vascular smooth muscle cells and its key role in maintaining vascular tone (Evans et al., 2005; Almabrouk et al., 2017). AMPKα1 KO mice exhibit impaired eNOS phosphorylation and reduced NO production, leading to vascular dysfunction (Hwej et al., 2024). Moreover, the differential responses observed in rings with and without PVAT highlight the indispensable role of PVAT in modulating vascular tone. PVAT-derived adipokines and NO act locally to promote vasodilation and modulate vascular smooth muscle responsiveness to other vasoactive stimuli (Szasz and Webb, 2012).

In summary, this study extends the current understanding of vascular biology by demonstrating that the combination of S1P and AMPK activation promotes vascular relaxation primarily through PVAT-mediated NO production and adiponectin signalling. The findings emphasize the therapeutic potential of targeting PVAT-AMPK signalling pathways to improve vascular function, particularly in conditions associated with endothelial dysfunction, such as obesity, diabetes, and hypertension (Ketonen et al., 2010; Qi et al., 2018).

Further research is warranted to elucidate the detailed molecular mechanisms underlying S1P and AMPK crosstalk within PVAT and to explore the therapeutic potential of modulating these pathways in cardiovascular disease models.

Chapter5 expanded upon previous findings by evaluating the effects of AMPK activators A-769662 and Compound 991 (C991) on vascular function, with a specific focus on thoracic aortic rings containing PVAT. The outcomes were compared to those observed with AICAR, an indirect AMPK activator. Notably, while co-treatment with S1P and AICAR significantly enhanced vascular relaxation,

the combination of S1P with either A-769662 or C991 did not result in further relaxation beyond that induced by the AMPK activators alone.

A-769662 and C991 are recognized as direct allosteric AMPK activators, interacting at the allosteric drug and metabolite (ADaM) site to increase AMPK activity (Sanders et al., 2007; Xiao et al., 2013). By contrast, AICAR functions as an AMP mimetic, indirectly activating AMPK through intracellular accumulation of ZMP (Hardie, 2016). These mechanistic distinctions likely underpin the differing vascular responses observed in this study.

Both A-769662 and C991 induced significant relaxation in PVAT-containing aortic rings, affirming the vasorelaxant potential of AMPK activation. However, the absence of augmented relaxation upon co-treatment with S1P suggests that direct AMPK activation may engage a distinct mechanism or converge on a shared downstream pathway with S1P, thereby limiting any additive or synergistic effect. In contrast, the enhanced relaxation seen with S1P and AICAR co-treatment implies a broader interaction between S1P signalling and AICAR-mediated pathways, potentially engaging additional downstream mechanisms beyond canonical AMPK activation.

This distinction may relate to AICAR's lack of specificity and its ability to influence multiple AMP-sensitive pathways (Kopietz et al., 2021; Ahwazi et al., 2021a; Ahwazi et al., 2021b). AICAR is metabolised intracellularly to ZMP, an AMP mimetic capable of activating not only AMPK but also a variety of other AMP-sensitive enzymes, such as glycogen phosphorylase and fructose-1,6-bisphosphatase (Corton et al., 1995; Merrill et al., 1997). These off-target interactions may influence cellular metabolism and functional responses through AMPK-independent pathways.

The critical role of PVAT-derived factors in mediating vasorelaxation is reinforced by these findings. Adipokines, notably adiponectin, and NO contribute significantly to vascular homeostasis by promoting vasodilation and reducing oxidative stress (Chen et al., 2003; Szasz and Webb, 2012). The results suggest that while direct AMPK activators such as A-769662 and C991 efficiently stimulate PVAT to release vasorelaxant factors, the indirect activator AICAR may additionally synergize with S1P signalling to amplify these effects.

The attenuation of relaxation responses in AMPK α 1 KO mice across all experimental conditions further underscores the pivotal role of the AMPK α 1 isoform in regulating PVAT function and vascular tone, consistent with previous reports (Almabrouk et al., 2017; Hwej et al., 2024).

In conclusion, although all three AMPK activators; AICAR, A-769662, and C991 promote vascular relaxation in PVAT-containing thoracic aortic rings, only AICAR demonstrates a synergistic enhancement when combined with S1P. This highlights critical differences in the cellular mechanisms engaged by direct versus indirect AMPK activation and suggests that AICAR's broader intracellular effects may confer unique therapeutic advantages in modulating PVAT function and vascular relaxation.

6.2 Limitations

Chpter3 provides meaningful insights, but several methodological limitations must be acknowledged. First, the use of MEF cells and isolated mouse PVAT tissues may not fully capture the complexity and integrated metabolic responses of whole organisms. Bearing in mind the complex interactions that have been seen to operate in the moderation of vascular function, it cannot be ruled out that differences may prove to be significant. Secondly, our findings of increased protein expression without corresponding mRNA changes strongly suggest posttranscriptional regulation, but the specific mechanisms (e.g., protein degradation rates or translation initiation) remain unidentified. Addressing this would require detailed investigations such as cycloheximide chase assays or polysome fractionation studies and may be suited to follow-up studies. Lastly, our study did not measure the direct functional impact of altered SphK1 expression on metabolic or inflammatory processes in cells or tissues, leaving open questions regarding the physiological relevance of observed changes. Future research focused on these aspects would significantly enhance our understanding of AMPK and SphK1 interactions.

In Chapter 4, several limitations must be acknowledged in interpreting the results. Firstly, the study relied primarily on ex vivo thoracic aortic ring preparations, which, while informative for mechanistic understanding, may not fully reflect in vivo vascular responses. Insights obtained through the ex vivo experiments need to be compared to results found using in vivo studies. Such further validation

would provide additional physiological relevance and signal different responses, which would need investigation, or support the findings made ex vitro. Secondly, although selective receptor agonists and antagonists were employed to dissect S1P receptor involvement, the specific downstream signalling pathways remain to be fully elucidated. Additional molecular analyses could clarify these mechanisms. Lastly, the AMPK activator AICAR, despite its well-characterized use, has known off-target effects that may influence the observed outcomes (Hardie, 2016). Future studies employing more selective AMPK activators could help confirm the specificity of AMPK-mediated effects observed in this study.

Chapter5 mainly investigated the effects of the AMPK activators A-769662 and Compound 991 on vascular relaxation. Although important findings were made, there are several limitations that should be considered.

First, both A-769662 and Compound 991 activate AMPK through direct binding to the enzyme, but they might not fully reflect the natural activation of AMPK that happens during metabolic stress in the body. Also, while these compounds are selective, they can sometimes affect other cellular pathways, which could influence the results.

Second, while vascular relaxation was clearly induced with A-769662 and Compound 991, the exact molecular mechanisms responsible for the relaxation were not fully studied in this chapter. Important factors like nitric oxide release, adiponectin levels, or oxidative stress markers were not directly measured after treatment with these activators.

Third, the experiments were only carried out on thoracic aortic rings with PVAT from mice. Blood vessels from other parts of the body might respond differently, and the results might not be the same in other types of arteries.

6.3 Conclusion

In summary, this thesis provides new insights into the regulatory interplay between AMPK, SphK1, and perivascular adipose tissue (PVAT) in the modulation of vascular tone. A key novel finding of this work is the synergistic enhancement of vascular relaxation observed for the first time with the combined treatment of AICAR and sphingosine-1-phosphate (S1P). This effect appears to be mediated by PVAT-derived factors, particularly nitric oxide (NO) and adiponectin, underscoring the importance of indirect AMPK activation in facilitating adipose-vascular signalling. In contrast, direct AMPK activators, such as A-769662 and Compound 991, induced vasorelaxation independently but lacked the synergistic interaction observed with AICAR, indicating distinct underlying mechanisms. Furthermore, the upregulation of SphK1 expression in AMPK-deficient PVAT and associated proinflammatory signalling suggest a critical role for AMPK in restraining vascular inflammation and maintaining adipose tissue homeostasis. Collectively, the work presented highlights the central role of AMPK and S1P in maintaining vascular and adipose tissue homeostasis and suggests that therapeutic strategies aimed at enhancing AMPK signalling may offer promising avenues for the treatment of vascular and metabolic disorders. Moreover, studies in human volunteers demonstrate that AICAR is pharmacologically active in vivo, acutely stimulating skeletal muscle glucose uptake and modulating relevant signalling pathways, thereby underscoring the clinical relevance of indirect AMPK activation (Cuthbertson et al., 2007; Babraj et al., 2009).

Chapter 7 References

- Aaronson, P. I., Ward, J. P. and Connolly, M. J. (2020). *The cardiovascular system at a glance*. John Wiley & Sons.
- Abdulqader, A. and Kennedy, S. (2020). 'The influence of perivascular adipose tissue on vascular function in a rabbit model', *Pharmacology and Pharmacy*, 11, pp. 331-349.
- Agabiti-Rosei, C., Paini, A., De Ciuceis, C., Withers, S., Greenstein, A., Heagerty, A. M. and Rizzoni, D. (2018). 'Modulation of vascular reactivity by perivascular adipose tissue (PVAT)', *Current hypertension reports*, 20, pp. 1-11.
- Aghamohammadzadeh, R., Greenstein, A. S., Yadav, R., Jeziorska, M., Hama, S., Soltani, F., Pemberton, P. W., Ammori, B., Malik, R. A. and Soran, H. (2013). 'Effects of bariatric surgery on human small artery function: evidence for reduction in perivascular adipocyte inflammation, and the restoration of normal anticontractile activity despite persistent obesity', *Journal of the American College of Cardiology*, 62(2), pp. 128-135.
- Ahwazi, D., Neopane, K., Markby, G. R., Kopietz, F., Ovens, A. J., Dall, M., Hassing, A. S., Gräsle, P., Alshuweishi, Y. and Treebak, J. T. (2021a). 'Investigation of the specificity and mechanism of action of the ULK1/AMPK inhibitor SBI-0206965', *Biochemical Journal*, 478(15), pp. 2977-2997.
- Ahwazi, D., Neopane, K., Markby, G. R., Kopietz, F., Ovens, A. J., Dall, M., Hassing, A. S., Gräsle, P., Alshuweishi, Y., Treebak, J. T., Salt, I. P., Göransson, O., Zeqiraj, E., Scott, J. W. and Sakamoto, K. (2021b). 'Investigation of the specificity and mechanism of action of the ULK1/AMPK inhibitor SBI-0206965', *Biochemical Journal*, 478(15), pp. 2977-2997.
- Alemany, R., van Koppen, C. J., Danneberg, K., Ter Braak, M. and Meyer zu Heringdorf, D. (2007). 'Regulation and functional roles of sphingosine kinases', *Naunyn-Schmiedeberg's archives of pharmacology*, 374, pp. 413-428.
- Alewijnse, A. E., Peters, S. L. and Michel, M. C. (2004). 'Cardiovascular effects of sphingosine-1-phosphate and other sphingomyelin metabolites', *British journal of pharmacology*, 143(6), pp. 666-684.
- Alganga, H., Almabrouk, T. A., Katwan, O. J., Daly, C. J., Pyne, S., Pyne, N. J. and Kennedy, S. (2019). 'Short periods of hypoxia upregulate sphingosine kinase 1 and increase vasodilation of arteries to sphingosine 1-phosphate (S1P) via S1P3', *The Journal of Pharmacology and Experimental Therapeutics*, 371(1), pp. 63-74.
- Alkafaas, S. S., Elsalahaty, M. I., Ismail, D. F., Radwan, M. A., Elkafas, S. S., Loutfy, S. A., Elshazli, R. M., Baazaoui, N., Ahmed, A. E. and Hafez, W. (2024). 'The emerging roles of sphingosine 1-phosphate and SphK1 in cancer resistance: a promising therapeutic target', *Cancer Cell International*, 24(1), pp. 89.

- Almabrouk, T. A., Ugusman, A. B., Katwan, O. J., Salt, I. P. and Kennedy, S. (2017). 'Deletion of AMPKα1 attenuates the anticontractile effect of perivascular adipose tissue (PVAT) and reduces adiponectin release', *British journal of pharmacology*, 174(20), pp. 3398-3410.
- Almabrouk, T. A., White, A. D., Ugusman, A. B., Skiba, D. S., Katwan, O. J., Alganga, H., Guzik, T. J., Touyz, R. M., Salt, I. P. and Kennedy, S. (2018). 'High fat diet attenuates the anticontractile activity of aortic PVAT via a mechanism involving AMPK and reduced adiponectin secretion', *Frontiers in physiology*, 9, pp. 51.
- Almabrouk, T.A.M., Ugusman, A.B., Katwan, O.J., Guzik, T.J., Neves, K.B., Lopes, R.A., Walker, B.R., Salt, I.P. and Kennedy, S. (2014). 'Deletion of AMP-activated protein kinase α1 attenuates the anticontractile effects of perivascular adipose tissue', *British Journal of Pharmacology*, 171(15), pp.3547-3561.
- Anderson, A. K., Lambert, J. M., Montefusco, D. J., Tran, B. N., Roddy, P., Holland, W. L. and Cowart, L. A. (2020). 'Depletion of adipocyte sphingosine kinase 1 leads to cell hypertrophy, impaired lipolysis, and nonalcoholic fatty liver disease', *Journal of Lipid Research*, 61(10), pp. 1328-1340.
- Anelli, V., Gault, C. R., Cheng, A. B. and Obeid, L. M. (2008). 'Sphingosine kinase 1 is up-regulated during hypoxia in U87MG glioma cells: role of hypoxia-inducible factors 1 and 2', *Journal of Biological Chemistry*, 283(6), pp. 3365-3375.
- Argraves, K. M., Wilkerson, B. A. and Argraves, W. S. (2010). 'Sphingosine-1-phosphate signaling in vasculogenesis and angiogenesis', *World journal of biological chemistry*, 1(10), pp. 291.
- Asano, M., Kajita, K., Fuwa, M., Kajita, T., Mori, I., Akahoshi, N., Ishii, I. and Morita, H. (2023). 'Opposing roles of sphingosine 1-phosphate receptors 1 and 2 in fat deposition and glucose tolerance in obese male mice', *Endocrinology*, 164(3), pp. bgad019.
- Babraj, J.A., Mustard, K., Sutherland, C., Towler, M.C., Chen, S., Smith, K., Green, K., Leese, G., Hardie, D.G., Rennie, M.J. and Cuthbertson, D.J. (2009). Blunting of AICAR-induced human skeletal muscle glucose uptake in type 2 diabetes is dependent on age rather than diabetic status. *American Journal of Physiology-Endocrinology and Metabolism*, 296(5), pp.E1042-E1048.
- Bektas, M., Allende, M. L., Lee, B. G., Chen, W., Amar, M. J., Remaley, A. T., Saba, J. D. and Proia, R. L. (2010). 'Sphingosine 1-phosphate lyase deficiency disrupts lipid homeostasis in liver', *Journal of Biological Chemistry*, 285(14), pp. 10880-10889.
- Berbée, J. F., Boon, M. R., Khedoe, P. P. S., Bartelt, A., Schlein, C., Worthmann, A., Kooijman, S., Hoeke, G., Mol, I. M. and John, C. (2015). 'Brown fat activation reduces hypercholesterolaemia and protects from atherosclerosis development', *Nature communications*, 6(1), pp. 6356.
- Berryman, D. E. and List, E. O. (2017). 'Growth hormone's effect on adipose tissue: quality versus quantity', *International Journal of Molecular Sciences*, 18(8), pp. 1621.

- Bijland, S., Mancini, S. J. and Salt, I. P. (2013). 'Role of AMP-activated protein kinase in adipose tissue metabolism and inflammation', *Clinical science*, 124(8), pp. 491-507.
- Billich, A., Bornancin, F., Mechtcheriakova, D., Natt, F., Huesken, D. and Baumruker, T. (2005). 'Basal and induced sphingosine kinase 1 activity in A549 carcinoma cells: function in cell survival and IL-1β and TNF-α induced production of inflammatory mediators', *Cellular signalling*, 17(10), pp. 1203-1217.
- Bischoff, A., Czyborra, P., Fetscher, C., Meyer zu Heringdorf, D., Jakobs, K. H. and Michel, M. C. (2000). 'Sphingosine-1-phosphate and sphingosylphosphorylcholine constrict renal and mesenteric microvessels in vitro', *British journal of pharmacology*, 130(8), pp. 1871-1877.
- Boutari, C. and Mantzoros, C. S. (2022). A 2022 update on the epidemiology of obesity and a call to action: as its twin COVID-19 pandemic appears to be receding, the obesity and dysmetabolism pandemic continues to rage on. Elsevier.
- Boyle, J. G., Logan, P. J., Ewart, M.-A., Reihill, J. A., Ritchie, S. A., Connell, J. M., Cleland, S. J. and Salt, I. P. (2008). 'Rosiglitazone stimulates nitric oxide synthesis in human aortic endothelial cells via AMP-activated protein kinase', *Journal of Biological Chemistry*, 283(17), pp. 11210-11217.
- Brinkmann, V., Billich, A., Baumruker, T., Heining, P., Schmouder, R., Francis, G., Aradhye, S. and Burtin, P. (2010). 'Fingolimod (FTY720): discovery and development of an oral drug to treat multiple sclerosis', *Nature reviews Drug discovery*, 9(11), pp. 883-897.
- Brouet, A., Sonveaux, P., Dessy, C., Balligand, J.-L. and Feron, O. (2001). 'Hsp90 ensures the transition from the early Ca2+-dependent to the late phosphorylation-dependent activation of the endothelial nitric-oxide synthase in vascular endothelial growth factor-exposed endothelial cells', *Journal of Biological Chemistry*, 276(35), pp. 32663-32669.
- Brown, N. K., Zhou, Z., Zhang, J., Zeng, R., Wu, J., Eitzman, D. T., Chen, Y. E. and Chang, L. (2014). 'Perivascular adipose tissue in vascular function and disease: a review of current research and animal models', *Arteriosclerosis*, thrombosis, and vascular biology, 34(8), pp. 1621-1630.
- Bruno, G., Cencetti, F., Bernacchioni, C., Donati, C., Blankenbach, K. V., Thomas, D., Zu Heringdorf, D. M. and Bruni, P. (2018). 'Bradykinin mediates myogenic differentiation in murine myoblasts through the involvement of SK1/Spns2/S1P2 axis', *Cellular Signalling*, 45, pp. 110-121.
- Bu, Y., Wu, H., Deng, R. and Wang, Y. (2021). 'Therapeutic potential of SphK1 inhibitors based on abnormal expression of SphK1 in inflammatory immune related-diseases', *Frontiers in Pharmacology*, 12, pp. 733387.
- Buchwalow, I.B., Cacanyiova, S., Neumann, J., Samoilova, V.E., Boecker, W. and Kristek, F. (2008). The role of arterial smooth muscle in vasorelaxation. *Biochemical and Biophysical Research Communications*, 377(2), pp.504-507.

- Byun, H.-S., Pyne, S., MacRitchie, N., Pyne, N. J. and Bittman, R. (2013). 'Novel sphingosine-containing analogues selectively inhibit sphingosine kinase (SK) isozymes, induce SK1 proteasomal degradation and reduce DNA synthesis in human pulmonary arterial smooth muscle cells', *Medchemcomm*, 4(10), pp. 1394-1399.
- Cacanyiova, S., Majzunova, M., Golas, S. and Berenyiova, A. (2019). 'The role of perivascular adipose tissue and endogenous hydrogen sulfide in vasoactive responses of isolated mesenteric arteries in normotensive and spontaneously hypertensive rats', *Journal of Physiology & Pharmacology*, 70(2).
- Calabrese, M. F., Rajamohan, F., Harris, M. S., Caspers, N. L., Magyar, R., Withka, J. M., Wang, H., Borzilleri, K. A., Sahasrabudhe, P. V. and Hoth, L. R. (2014). 'Structural basis for AMPK activation: natural and synthetic ligands regulate kinase activity from opposite poles by different molecular mechanisms', *Structure*, 22(8), pp. 1161-1172.
- Cannavo, A., Liccardo, D., Komici, K., Corbi, G., De Lucia, C., Femminella, G. D., Elia, A., Bencivenga, L., Ferrara, N. and Koch, W. J. (2017). 'Sphingosine kinases and sphingosine 1-phosphate receptors: signaling and actions in the cardiovascular system', *Frontiers in pharmacology*, 8, pp. 556.
- Carling, D. (2017). 'AMPK signalling in health and disease', *Current opinion in cell biology*, 45, pp. 31-37.
- Cartier, A. and Hla, T. (2019). 'Sphingosine 1-phosphate: Lipid signaling in pathology and therapy', *Science*, 366(6463), pp. eaar5551.
- Chakrabarty, S., Bui, Q., Badeanlou, L., Hester, K., Chun, J., Ruf, W., Ciaraldi, T. P. and Samad, F. (2022). 'S1P/S1PR3 signalling axis protects against obesity-induced metabolic dysfunction', *Adipocyte*, 11(1), pp. 69-83.
- Chang, L., Garcia-Barrio, M. T. and Chen, Y. E. (2020). 'Perivascular adipose tissue regulates vascular function by targeting vascular smooth muscle cells', *Arteriosclerosis*, *thrombosis*, *and vascular biology*, 40(5), pp. 1094-1109.
- Chaudhry, R., Miao, J. H., & Rehman, A. (2022). Physiology, Cardiovascular. In *StatPearls*. StatPearls Publishing.
- Chen, H., Ahmed, S., Zhao, H., Elghobashi-Meinhardt, N., Dai, Y., Kim, J. H., McDonald, J. G., Li, X. and Lee, C.-H. (2023). 'Structural and functional insights into Spns2-mediated transport of sphingosine-1-phosphate', *Cell*, 186(12), pp. 2644-2655. e16.
- Chen, H., Montagnani, M., Funahashi, T., Shimomura, I. and Quon, M. J. (2003). 'Adiponectin stimulates production of nitric oxide in vascular endothelial cells', *Journal of Biological Chemistry*, 278(45), pp. 45021-45026.
- Chen, H., Vanhoutte, P. M. and Leung, S. W. (2019). 'Acute activation of endothelial AMPK surprisingly inhibits endothelium-dependent hyperpolarization-like relaxations in rat mesenteric arteries', *British journal of pharmacology*, 176(16), pp. 2905-2921.

- Chen, R., McVey, D. G., Shen, D., Huang, X. and Ye, S. (2023). 'Phenotypic switching of vascular smooth muscle cells in atherosclerosis', *Journal of the American Heart Association*, 12(20), pp. e031121.
- Chen, Y., Xu, X., Zhang, Y., Liu, K., Huang, F., Liu, B. and Kou, J. (2016). 'Diosgenin regulates adipokine expression in perivascular adipose tissue and ameliorates endothelial dysfunction via regulation of AMPK', *The Journal of Steroid Biochemistry and Molecular Biology*, 155, pp. 155-165.
- Chen, Z., Peng, I.-C., Sun, W., Su, M.-I., Hsu, P.-H., Fu, Y., Zhu, Y., DeFea, K., Pan, S. and Tsai, M.-D. (2009). 'AMP-activated protein kinase functionally phosphorylates endothelial nitric oxide synthase Ser633', *Circulation research*, 104(4), pp. 496-505.
- Cheng, K. K., Lam, K. S., Wang, Y., Huang, Y., Carling, D., Wu, D., Wong, C. and Xu, A. (2007). 'Adiponectin-induced endothelial nitric oxide synthase activation and nitric oxide production are mediated by APPL1 in endothelial cells', *Diabetes*, 56(5), pp. 1387-1394.
- Chun, J., Goetzl, E. J., Hla, T., Igarashi, Y., Lynch, K. R., Moolenaar, W., Pyne, S. and Tigyi, G. (2002). 'International union of pharmacology. XXXIV. Lysophospholipid receptor nomenclature', *Pharmacological reviews*, 54(2), pp. 265-269.
- Cinti, S. (2011). 'Between brown and white: novel aspects of adipocyte differentiation', *Annals of medicine*, 43(2), pp. 104-115.
- Coelho, M., Oliveira, T. and Fernandes, R. (2013). 'State of the art paper Biochemistry of adipose tissue: an endocrine organ', *Archives of medical science*, 9(2), pp. 191-200.
- Colombo, S. L. and Moncada, S. (2009). 'AMPKα1 regulates the antioxidant status of vascular endothelial cells', *Biochemical Journal*, 421(2), pp. 163-169.
- Constantinescu, V., Haase, R., Akgün, K. and Ziemssen, T. (2022). 'S1P receptor modulators and the cardiovascular autonomic nervous system in multiple sclerosis: a narrative review', *Therapeutic advances in neurological disorders*, 15, pp. 17562864221133163.
- Contos, J. J., Ishii, I. and Chun, J. (2000). 'Lysophosphatidic acid receptors', *Molecular pharmacology*, 58(6), pp. 1188-1196.
- Cool, B., Zinker, B., Chiou, W., Kifle, L., Cao, N., Perham, M., Dickinson, R., Adler, A., Gagne, G. and Iyengar, R. (2006). 'Identification and characterization of a small molecule AMPK activator that treats key components of type 2 diabetes and the metabolic syndrome', *Cell metabolism*, 3(6), pp. 403-416.
- Corton, J.M., Gillespie, J.G., Hawley, S.A. and Hardie, D.G. (1995). 5-Aminoimidazole-4-carboxamide ribonucleoside: a specific method for activating AMP-activated protein kinase in intact cells?. *European journal of biochemistry*, 229(2), pp.558-565.

- Coussin, F., Scott, R. H., Wise, A. and Nixon, G. F. (2002). 'Comparison of sphingosine 1-phosphate-induced intracellular signaling pathways in vascular smooth muscles: differential role in vasoconstriction', *Circulation research*, 91(2), pp. 151-157.
- Coyle, P. K., Freedman, M. S., Cohen, B. A., Cree, B. A. and Markowitz, C. E. (2024). 'Sphingosine 1-phosphate receptor modulators in multiple sclerosis treatment: A practical review', *Annals of clinical and translational neurology*, 11(4), pp. 842-855.
- Cuthbertson, D.J., Babraj, J.A., Mustard, K.J., Towler, M.C., Green, K.A., Wackerhage, H., Leese, G.P., Baar, K., Thomason-Hughes, M., Sutherland, C. and Hardie, D.G. (2007). 5-Aminoimidazole-4-carboxamide 1-B-D-ribofuranoside acutely stimulates skeletal muscle 2-deoxyglucose uptake in healthy men. *Diabetes*, 56(8), pp.2078-2084.
- Daly, C. J. (2019). 'Examining vascular structure and function using confocal microscopy and 3D imaging techniques', *Biomedical Visualisation: Volume 1*, pp. 97-106.
- Dantas, A. P. V., Igarashi, J. and Michel, T. (2003). 'Sphingosine 1-phosphate and control of vascular tone', *American Journal of Physiology-Heart and Circulatory Physiology*, 284(6), pp. H2045-H2052.
- Davies, S. P., Helps, N. R., Cohen, P. T. and Hardie, D. G. (1995). '5'-AMP inhibits dephosphorylation, as well as promoting phosphorylation, of the AMP-activated protein kinase. Studies using bacterially expressed human protein phosphatase-2Cα and native bovine protein phosphatase-2AC', *FEBS letters*, 377(3), pp. 421-425.
- Davis, B. J., Xie, Z., Viollet, B. and Zou, M.-H. (2006). 'Activation of the AMP-activated kinase by antidiabetes drug metformin stimulates nitric oxide synthesis in vivo by promoting the association of heat shock protein 90 and endothelial nitric oxide synthase', *Diabetes*, 55(2), pp. 496-505.
- Davis, B. J., Xie, Z., Viollet, B. and Zou, M.-H. (2006). 'Activation of the AMP-activated kinase by antidiabetes drug metformin stimulates nitric oxide synthesis in vivo by promoting the association of heat shock protein 90 and endothelial nitric oxide synthase', *Diabetes*, 55(2), pp. 496-505.
- Deanfield, J. E., Halcox, J. P. and Rabelink, T. J. (2007). 'Endothelial function and dysfunction: testing and clinical relevance', *Circulation*, 115(10), pp. 1285-1295.
- Dschietzig, T., Brecht, A., Bartsch, C., Baumann, G., Stangl, K. and Alexiou, K. (2012). Relaxin improves TNF-α-induced endothelial dysfunction: the role of glucocorticoid receptor and phosphatidylinositol 3-kinase signalling. *Cardiovascular research*, 95(1), pp.97-107.
- Dolinsky, V. W., Chakrabarti, S., Pereira, T. J., Oka, T., Levasseur, J., Beker, D., Zordoky, B. N., Morton, J. S., Nagendran, J. and Lopaschuk, G. D. (2013). 'Resveratrol prevents hypertension and cardiac hypertrophy in hypertensive rats and mice', *Biochimica et Biophysica Acta (BBA)-Molecular Basis of Disease*, 1832(10), pp. 1723-1733.

- Dong, Y., Zhang, M., Wang, S., Liang, B., Zhao, Z., Liu, C., Wu, M., Choi, H. C., Lyons, T. J. and Zou, M.-H. (2010). 'Activation of AMP-activated protein kinase inhibits oxidized LDL-triggered endoplasmic reticulum stress in vivo', *Diabetes*, 59(6), pp. 1386-1396.
- Dubrovska, G., Verlohren, S., Luft, F. C. and Gollasch, M. (2004). 'Mechanisms of ADRF release from rat aortic adventitial adipose tissue', *American Journal of Physiology-Heart and Circulatory Physiology*, 286(3), pp. H1107-H1113.
- El-Shewy, H. M., Parnham, S., Fedarovich, D., Bullesbach, E. and Luttrell, L. M. (2018). 'Sphingosine 1 Phosphate Regulates Store-Operated Calcium Entry through binding to STIM1', *The FASEB Journal*, 32, pp. 815.10-815.10.
- Evans, A. M., Hardie, D. G., Galione, A., Peers, C., Kumar, P. and Wyatt, C. N. (2006). 'AMP-Activated Protein Kinase Couples Mitochondrial Inhibition by Hypoxia to Cell-Specific Ca2+ Signalling Mechanisms in Oxygensensing Cells'. Signalling Pathways in Acute Oxygen Sensing: Novartis Foundation Symposium 272: Wiley Online Library, 234-258.
- Evans, A. M., Mustard, K. J., Wyatt, C. N., Peers, C., Dipp, M., Kumar, P., Kinnear, N. P. and Hardie, D. G. (2005). 'Does AMP-activated protein kinase couple inhibition of mitochondrial oxidative phosphorylation by hypoxia to calcium signaling in O2-sensing cells?', *Journal of Biological Chemistry*, 280(50), pp. 41504-41511.
- Ewart, M.-A. and Kennedy, S. (2011). 'AMPK and vasculoprotection', *Pharmacology & therapeutics*, 131(2), pp. 242-253.
- Ewart, M.-A., Kohlhaas, C. F. and Salt, I. P. (2008). 'Inhibition of tumor necrosis factor α-stimulated monocyte adhesion to human aortic endothelial cells by AMP-activated protein kinase', *Arteriosclerosis*, *Thrombosis*, *and Vascular Biology*, 28(12), pp. 2255-2257.
- Ewart, M.A., Ugusman, A., Vishwanath, A., Almabrouk, T.A., Alganga, H., Katwan, O.J., Hubanova, P., Currie, S. and Kennedy, S. (2017). Changes in IP3 receptor expression and function in aortic smooth muscle of atherosclerotic mice. *Journal of Vascular Research*, 54(2), pp.68-78.
- Fang, Z., Pyne, S. and Pyne, N. J. (2019). 'Ceramide and sphingosine 1-phosphate in adipose dysfunction', *Progress in lipid research*, 74, pp. 145-159.
- Fésüs, G., Dubrovska, G., Gorzelniak, K., Kluge, R., Huang, Y., Luft, F. C. and Gollasch, M. (2007). 'Adiponectin is a novel humoral vasodilator', *Cardiovascular research*, 75(4), pp. 719-727.
- Fitzgibbons, T. P., Kogan, S., Aouadi, M., Hendricks, G. M., Straubhaar, J. and Czech, M. P. (2011). 'Similarity of mouse perivascular and brown adipose tissues and their resistance to diet-induced inflammation', *American Journal of Physiology-Heart and Circulatory Physiology*, 301(4), pp. H1425-H1437.
- Ford, R. J. and Rush, J. W. (2011). 'Endothelium-dependent vasorelaxation to the AMPK activator AICAR is enhanced in aorta from hypertensive rats and is NO and EDCF

- dependent', American Journal of Physiology-Heart and Circulatory Physiology, 300(1), pp. H64-H75.
- Förstermann, U. and Sessa, W. C. (2012). 'Nitric oxide synthases: regulation and function', *European heart journal*, 33(7), pp. 829-837.
- Förstermann, U., Mülsch, A., Böhme, E. and Busse, R. (1986). Stimulation of soluble guanylate cyclase by an acetylcholine-induced endothelium-derived factor from rabbit and canine arteries. *Circulation research*, 58(4), pp.531-538.
- French, K. J., Schrecengost, R. S., Lee, B. D., Zhuang, Y., Smith, S. N., Eberly, J. L., Yun, J. K. and Smith, C. D. (2003). 'Discovery and evaluation of inhibitors of human sphingosine kinase', *Cancer research*, 63(18), pp. 5962-5969.
- Fu, Y., Luo, N., Klein, R. L. and Garvey, W. T. (2005). 'Adiponectin promotes adipocyte differentiation, insulin sensitivity, and lipid accumulation', *Journal of lipid research*, 46(7), pp. 1369-1379.
- Fujita, T., Okada, T., Hayashi, S., Jahangeer, S., Miwa, N. and Nakamura, S.-i. (2004). 'δ-Catenin/NPRAP (neural plakophilin-related armadillo repeat protein) interacts with and activates sphingosine kinase 1', *Biochemical Journal*, 382(2), pp. 717-723.
- Furchgott, R.F. and Zawadzki, J.V. (1980). The obligatory role of endothelial cells in the relaxation of arterial smooth muscle by acetylcholine. *nature*, 288(5789), pp.373-376.
- Fukuda, Y., Aoyama, Y., Wada, A. and Igarashi, Y. (2004). 'Identification of PECAM-1 association with sphingosine kinase 1 and its regulation by agonist-induced phosphorylation', *Biochimica et Biophysica Acta (BBA)-Molecular and Cell Biology of Lipids*, 1636(1), pp. 12-21.
- Fukuhara, S., Simmons, S., Kawamura, S., Inoue, A., Orba, Y., Tokudome, T., Sunden, Y., Arai, Y., Moriwaki, K. and Ishida, J. (2012). 'The sphingosine-1-phosphate transporter Spns2 expressed on endothelial cells regulates lymphocyte trafficking in mice', *The Journal of clinical investigation*, 122(4), pp. 1416-1426.
- Gabriel, T. L., Mirzaian, M., Hooibrink, B., Ottenhoff, R., van Roomen, C., Aerts, J. M. and van Eijk, M. (2017). 'Induction of Sphk1 activity in obese adipose tissue macrophages promotes survival', *PLoS One*, 12(7), pp. e0182075.
- Gálvez-Prieto, B., Somoza, B., Gil-Ortega, M., García-Prieto, C. F., De las Heras, A. I., González, M. C., Arribas, S., Aranguez, I., Bolbrinker, J. and Kreutz, R. (2012). 'Anticontractile effect of perivascular adipose tissue and leptin are reduced in hypertension', *Frontiers in pharmacology*, 3, pp. 103.
- Gandy, K. A. O. and Obeid, L. M. (2013). 'Targeting the sphingosine kinase/sphingosine 1-phosphate pathway in disease: review of sphingosine kinase inhibitors', *Biochimica et Biophysica Acta (BBA)-Molecular and Cell Biology of Lipids*, 1831(1), pp. 157-166.

- Gao, J., Xiong, R., Xiong, D., Zhao, W., Zhang, S., Yin, T., Zhang, X., Jiang, G. and Yin, Z. (2018). 'The adenosine monophosphate (AMP) analog, 5-aminoimidazole-4-carboxamide ribonucleotide (AICAR) inhibits hepatosteatosis and liver tumorigenesis in a high-fat diet murine model treated with diethylnitrosamine (DEN)', Medical Science Monitor: International Medical Journal of Experimental and Clinical Research, 24, pp. 8533.
- Gao, Y. and Lee, R. (2001). 'Hydrogen peroxide induces a greater contraction in mesenteric arteries of spontaneously hypertensive rats through thromboxane A2 production', *British journal of pharmacology*, 134(8), pp. 1639-1646.
- Gao, Y. J. and Lee, R. M. (2005). 'Hydrogen peroxide is an endothelium-dependent contracting factor in rat renal artery', *British journal of pharmacology*, 146(8), pp. 1061-1068.
- Gao, Y. J., Lu, C., Su, L. Y., Sharma, A. and Lee, R. (2007). 'Modulation of vascular function by perivascular adipose tissue: the role of endothelium and hydrogen peroxide', *British journal of pharmacology*, 151(3), pp. 323-331.
- Gao, Y.-J., Takemori, K., Su, L.-Y., An, W.-S., Lu, C., Sharma, A. M. and Lee, R. M. (2006). 'Perivascular adipose tissue promotes vasoconstriction: the role of superoxide anion', *Cardiovascular research*, 71(2), pp. 363-373.
- Gauthier, M.-S., O'Brien, E. L., Bigornia, S., Mott, M., Cacicedo, J. M., Xu, X. J., Gokce, N., Apovian, C. and Ruderman, N. (2011). 'Decreased AMP-activated protein kinase activity is associated with increased inflammation in visceral adipose tissue and with whole-body insulin resistance in morbidly obese humans', *Biochemical and biophysical research communications*, 404(1), pp. 382-387.
- Giri, S., Rattan, R., Haq, E., Khan, M., Yasmin, R., Won, J.-s., Key, L., Singh, A. K. and Singh, I. (2006). 'AICAR inhibits adipocyte differentiation in 3T3L1 and restores metabolic alterations in diet-induced obesity mice model', *Nutrition & metabolism*, 3, pp. 1-20.
- Goetzl, E. J., Wang, W., McGiffert, C., Huang, M. C. and Gräler, M. H. (2004). 'Sphingosine 1-phosphate and its G protein-coupled receptors constitute a multifunctional immunoregulatory system', *Journal of cellular biochemistry*, 92(6), pp. 1104-1114.
- Goirand, F., Solar, M., Athea, Y., Viollet, B., Mateo, P., Fortin, D., Leclerc, J., Hoerter, J., Ventura-Clapier, R. and Garnier, A. (2007). 'Activation of AMP kinase α1 subunit induces aortic vasorelaxation in mice', *The Journal of physiology*, 581(3), pp. 1163-1171.
- Gómez-Galeno, J. E., Dang, Q., Nguyen, T. H., Boyer, S. H., Grote, M. P., Sun, Z., Chen, M., Craigo, W. A., van Poelje, P. D. and MacKenna, D. A. (2010). 'A potent and selective AMPK activator that inhibits de novo lipogenesis', *ACS medicinal chemistry letters*, 1(9), pp. 478-482.
- Gonda, K., OKAMOTO, H., TAKUWA, N., YATOMI, Y., OKAZAKI, H., SAKURAI, T., KIMURA, S., SILLARD, R., HARII, K. and TAKUWA, Y. (1999). 'The novel

- sphingosine 1-phosphate receptor AGR16 is coupled via pertussis toxin-sensitive and-insensitive G-proteins to multiple signalling pathways', *Biochemical Journal*, 337(1), pp. 67-75.
- Greenstein, A. S., Khavandi, K., Withers, S. B., Sonoyama, K., Clancy, O., Jeziorska, M., Laing, I., Yates, A. P., Pemberton, P. W. and Malik, R. A. (2009). 'Local inflammation and hypoxia abolish the protective anticontractile properties of perivascular fat in obese patients', *Circulation*, 119(12), pp. 1661-1670.
- Guitton, J., Bandet, C. L., Mariko, M. L., Tan-Chen, S., Bourron, O., Benomar, Y., Hajduch, E. and Le Stunff, H. (2020). 'Sphingosine-1-phosphate metabolism in the regulation of obesity/type 2 diabetes', *Cells*, 9(7), pp. 1682.
- Hait, N. C., Bellamy, A., Milstien, S., Kordula, T. and Spiegel, S. (2007). 'Sphingosine kinase type 2 activation by ERK-mediated phosphorylation', *Journal of Biological Chemistry*, 282(16), pp. 12058-12065.
- Hardie, D. G. (2011). 'Adenosine monophosphate-activated protein kinase: a central regulator of metabolism with roles in diabetes, cancer, and viral infection'. *Cold Spring Harbor Symposia on Quantitative Biology*: Cold Spring Harbor Laboratory Press, 155-164.
- Hardie, D. G. (2011). 'AMP-activated protein kinase—an energy sensor that regulates all aspects of cell function', *Genes & development*, 25(18), pp. 1895-1908.
- Hardie, D. G. (2014). 'AMP-activated protein kinase: maintaining energy homeostasis at the cellular and whole-body levels', *Annual review of nutrition*, 34(1), pp. 31-55.
- Hardie, D. G. (2016). 'Regulation of AMP-activated protein kinase by natural and synthetic activators', *Acta Pharmaceutica Sinica B*, 6(1), pp. 1-19.
- Hardie, D. G. (2018). 'Keeping the home fires burning: AMP-activated protein kinase', *Journal of the Royal Society Interface*, 15(138), pp. 20170774.
- Hashimoto, T., Igarashi, J. and Kosaka, H. (2009). 'Sphingosine kinase is induced in mouse 3T3-L1 cells and promotes adipogenesis', *Journal of lipid research*, 50(4), pp. 602-610.
- Hattori, Y., Suzuki, K., Hattori, S. and Kasai, K. (2006). 'Metformin inhibits cytokine-induced nuclear factor κB activation via AMP-activated protein kinase activation in vascular endothelial cells', *Hypertension*, 47(6), pp. 1183-1188.
- Hawley, S. A., Davison, M., Woods, A., Davies, S. P., Beri, R. K., Carling, D. and Hardie, D. G. (1996). 'Characterization of the AMP-activated protein kinase kinase from rat liver and identification of threonine 172 as the major site at which it phosphorylates AMP-activated protein kinase', *Journal of Biological Chemistry*, 271(44), pp. 27879-27887.
- Hawley, S. A., Pan, D. A., Mustard, K. J., Ross, L., Bain, J., Edelman, A. M., Frenguelli, B. G. and Hardie, D. G. (2005). 'Calmodulin-dependent protein kinase kinase-ß is an alternative upstream kinase for AMP-activated protein kinase', *Cell metabolism*, 2(1), pp. 9-19.

- Hayabuchi, Y., Nakaya, Y., Matsuoka, S. and Kuroda, Y. (1998). 'Hydrogen peroxide-induced vascular relaxation in porcine coronary arteries is mediated by Ca 2+activated K+ channels', *Heart and Vessels*, 13, pp. 9-17.
- Hazar-Rethinam, M., de Long, L. M., Gannon, O. M., Topkas, E., Boros, S., Vargas, A. C., Dzienis, M., Mukhopadhyay, P., Simpson, F. and Endo-Munoz, L. (2015). 'A novel E2F/sphingosine kinase 1 axis regulates anthracycline response in squamous cell carcinoma', *Clinical Cancer Research*, 21(2), pp. 417-427.
- He, C., Li, H., Viollet, B., Zou, M.-H. and Xie, Z. (2015). 'AMPK suppresses vascular inflammation in vivo by inhibiting signal transducer and activator of transcription-1', *Diabetes*, 64(12), pp. 4285-4297.
- Hemmings, D. G. (2006). 'Signal transduction underlying the vascular effects of sphingosine 1-phosphate and sphingosylphosphorylcholine', *Naunyn-Schmiedeberg's archives of pharmacology*, 373(1), pp. 18-29.
- Hemmings, D. G., Hudson, N. K., Halliday, D., O'Hara, M., Baker, P. N., Davidge, S. T. and Taggart, M. J. (2006). 'Sphingosine-1-phosphate acts via rho-associated kinase and nitric oxide to regulate human placental vascular tone', *Biology of reproduction*, 74(1), pp. 88-94.
- Herr, D. R., Reolo, M. J., Peh, Y. X., Wang, W., Lee, C.-W., Rivera, R., Paterson, I. C. and Chun, J. (2016). 'Sphingosine 1-phosphate receptor 2 (S1P2) attenuates reactive oxygen species formation and inhibits cell death: implications for otoprotective therapy', *Scientific reports*, 6(1), pp. 24541.
- Herzig, S. and Shaw, R. J. (2018). 'AMPK: guardian of metabolism and mitochondrial homeostasis', *Nature reviews Molecular cell biology*, 19(2), pp. 121-135.
- Hisano, Y., Kobayashi, N., Kawahara, A., Yamaguchi, A. and Nishi, T. (2011). 'The sphingosine 1-phosphate transporter, SPNS2, functions as a transporter of the phosphorylated form of the immunomodulating agent FTY720', *Journal of Biological Chemistry*, 286(3), pp. 1758-1766.
- Hla, T. and Maciag, T. (1990). 'An abundant transcript induced in differentiating human endothelial cells encodes a polypeptide with structural similarities to G-protein-coupled receptors', *Journal of Biological Chemistry*, 265(16), pp. 9308-9313.
- Horman, S., Morel, N., Vertommen, D., Hussain, N., Neumann, D., Beauloye, C., El Najjar, N., Forcet, C., Viollet, B. and Walsh, M. P. (2008). 'AMP-activated Protein Kinase Phosphorylates and Desensitizes Smooth Muscle Myosin Light Chain Kinase*♦', Journal of Biological Chemistry, 283(27), pp. 18505-18512.
- Hwej, A., Al-Ferjani, A., Alshuweishi, Y., Naji, A., Kennedy, S. and Salt, I. P. (2024). Lack of AMP-activated protein kinase-α1 reduces nitric oxide synthesis in thoracic aorta perivascular adipose tissue', *Vascular Pharmacology*, 157, pp. 107437.
- Ibrahim, M. M. (2010). 'Subcutaneous and visceral adipose tissue: structural and functional differences', *Obesity reviews*, 11(1), pp. 11-18.

- Igarashi, J. and Michel, T. (2009). 'Sphingosine-1-phosphate and modulation of vascular tone', *Cardiovascular research*, 82(2), pp. 212-220.
- Igata, M., Motoshima, H., Tsuruzoe, K., Kojima, K., Matsumura, T., Kondo, T., Taguchi, T., Nakamaru, K., Yano, M. and Kukidome, D. (2005). 'Adenosine monophosphate-activated protein kinase suppresses vascular smooth muscle cell proliferation through the inhibition of cell cycle progression', *Circulation research*, 97(8), pp. 837-844.
- Im, H., Park, J.-H., Im, S., Han, J., Kim, K. and Lee, Y.-H. (2021). 'Regulatory roles of G-protein coupled receptors in adipose tissue metabolism and their therapeutic potential', *Archives of pharmacal research*, 44, pp. 133-145.
- Ishii, I., Friedman, B., Ye, X., Kawamura, S., McGiffert, C., Contos, J. J., Kingsbury, M. A., Zhang, G., Brown, J. H. and Chun, J. (2001). 'Selective loss of sphingosine 1-phosphate signaling with no obvious phenotypic abnormality in mice lacking its G protein-coupled receptor, LPB3/EDG-3', *Journal of Biological Chemistry*, 276(36), pp. 33697-33704.
- Ito, S., Iwaki, S., Koike, K., Yuda, Y., Nagasaki, A., Ohkawa, R., Yatomi, Y., Furumoto, T., Tsutsui, H. and Sobel, B. E. (2013). 'Increased plasma sphingosine-1-phosphate in obese individuals and its capacity to increase the expression of plasminogen activator inhibitor-1 in adipocytes', *Coronary artery disease*, 24(8), pp. 642-650.
- Jansen, T., Kvandová, M., Daiber, A., Stamm, P., Frenis, K., Schulz, E., Münzel, T. and Kröller-Schön, S. (2020). 'The AMP-activated protein kinase plays a role in antioxidant defense and regulation of vascular inflammation', *Antioxidants*, 9(6), pp. 525.
- Jarman, K. E., Moretti, P. A., Zebol, J. R. and Pitson, S. M. (2010). 'Translocation of sphingosine kinase 1 to the plasma membrane is mediated by calcium-and integrin-binding protein 1', *Journal of Biological Chemistry*, 285(1), pp. 483-492.
- Jeong, J.-K., Moon, M.-H. and Park, S.-Y. (2015). 'Modulation of the expression of sphingosine 1-phosphate 2 receptors regulates the differentiation of preadipocytes', *Molecular medicine reports*, 12(5), pp. 7496-7502.
- Jo, E., Bhhatarai, B., Repetto, E., Guerrero, M., Riley, S., Brown, S. J., Kohno, Y., Roberts, E., Schürer, S. C. and Rosen, H. (2012). 'Novel selective allosteric and bitopic ligands for the S1P3 receptor', *ACS chemical biology*, 7(12), pp. 1975-1983.
- Jozefczuk, E., Guzik, T. and Siedlinski, M. (2020). 'Significance of sphingosine-1-phosphate in cardiovascular physiology and pathology', *Pharmacological research*, 156, pp. 104793.
- Jun, D.-J., Lee, J.-H., Choi, B.-H., Koh, T.-K., Ha, D.-C., Jeong, M.-W. and Kim, K.-T. (2006). 'Sphingosine-1-phosphate modulates both lipolysis and leptin production in differentiated rat white adipocytes', *Endocrinology*, 147(12), pp. 5835-5844.

- Juszczak, F., Caron, N., Mathew, A. V. and Declèves, A.-E. (2020). 'Critical role for AMPK in metabolic disease-induced chronic kidney disease', *International journal of molecular sciences*, 21(21), pp. 7994.
- Jüttner, A.A., Ataabadi, E.A., Golshiri, K., de Vries, R., Garrelds, I.M., Danser, A.H.J., Visser, J.A. and Roks, A.J.M. (2024). Adiponectin secretion by perivascular adipose tissue supports impaired vasodilation in a mouse model of accelerated vascular smooth muscle cell and adipose tissue aging. *Vascular Pharmacology*, 154, p.107281.
- Kang, S.-C., Kim, B.-R., Lee, S.-Y. and Park, T.-S. (2013). 'Sphingolipid metabolism and obesity-induced inflammation', *Frontiers in endocrinology*, 4, pp. 67.
- Karuppuchamy, T., Behrens, E., González-Cabrera, P., Sarkisyan, G., Gima, L., Boyer, J. D., Bamias, G., Jedlicka, P., Veny, M. and Clark, D. (2017). 'Sphingosine-1-phosphate receptor-1 (S1P1) is expressed by lymphocytes, dendritic cells, and endothelium and modulated during inflammatory bowel disease', *Mucosal Immunology*, 10(1), pp. 162-171.
- Katerelos, M., Mudge, S. J., Stapleton, D., Auwardt, R. B., Fraser, S. A., Chen, C. G., Kemp, B. E. and Power, D. A. (2010). '5-aminoimidazole-4-carboxamide ribonucleoside and AMP-activated protein kinase inhibit signalling through NF-κB', *Immunology and cell biology*, 88(7), pp. 754-760.
- Katunaric, B., SenthilKumar, G., Schulz, M. E., De Oliveira, N. and Freed, J. K. (2022). 'S1P (sphingosine-1-phosphate)-induced vasodilation in human resistance arterioles during health and disease', *Hypertension*, 79(10), pp. 2250-2261.
- Kawahara, A., Nishi, T., Hisano, Y., Fukui, H., Yamaguchi, A. and Mochizuki, N. (2009). 'The sphingolipid transporter spns2 functions in migration of zebrafish myocardial precursors', *Science*, 323(5913), pp. 524-527.
- Ketonen, J., Shi, J., Martonen, E. and Mervaala, E. (2010). 'Periadventitial adipose tissue promotes endothelial dysfunction via oxidative stress in diet-induced obese C57Bl/6 mice', *Circulation Journal*, 74(7), pp. 1479-1487.
- Khaddaj Mallat, R., Mathew John, C., Kendrick, D. J. and Braun, A. P. (2017). 'The vascular endothelium: A regulator of arterial tone and interface for the immune system', *Critical reviews in clinical laboratory sciences*, 54(7-8), pp. 458-470.
- Khedoe, P. P., Hoeke, G., Kooijman, S., Dijk, W., Buijs, J. T., Kersten, S., Havekes, L. M., Hiemstra, P. S., Berbée, J. F. and Boon, M. R. (2015). 'Brown adipose tissue takes up plasma triglycerides mostly after lipolysis', *Journal of lipid research*, 56(1), pp. 51-59.
- Kim, H. W., Shi, H., Winkler, M. A., Lee, R. and Weintraub, N. L. (2020). 'Perivascular adipose tissue and vascular perturbation/atherosclerosis', *Arteriosclerosis*, *thrombosis*, *and vascular biology*, 40(11), pp. 2569-2576.
- Kim, J.-E., Song, S. E., Kim, Y.-W., Kim, J.-Y., Park, S.-C., Park, Y.-K., Baek, S.-H., Lee, I. K. and Park, S.-Y. (2010). 'Adiponectin inhibits palmitate-induced apoptosis through suppression of reactive oxygen species in endothelial cells:

- involvement of cAMP/protein kinase A and AMP-activated protein kinase', *Journal of endocrinology*, 207(1), pp. 35.
- Kim, V. N., Han, J. and Siomi, M. C. (2009). 'Biogenesis of small RNAs in animals', *Nature reviews Molecular cell biology*, 10(2), pp. 126-139.
- Kitada, Y., Kajita, K., Taguchi, K., Mori, I., Yamauchi, M., Ikeda, T., Kawashima, M., Asano, M., Kajita, T. and Ishizuka, T. (2016). 'Blockade of sphingosine 1-phosphate receptor 2 signaling attenuates high-fat diet-induced adipocyte hypertrophy and systemic glucose intolerance in mice', *Endocrinology*, 157(5), pp. 1839-1851.
- Kluk, M. J. and Hla, T. (2002). 'Signaling of sphingosine-1-phosphate via the S1P/EDG-family of G-protein-coupled receptors', *Biochimica et Biophysica Acta (BBA)-Molecular and Cell Biology of Lipids*, 1582(1-3), pp. 72-80.
- Koenen, M., Hill, M. A., Cohen, P. and Sowers, J. R. (2021). 'Obesity, adipose tissue and vascular dysfunction', *Circulation research*, 128(7), pp. 951-968.
- Kopietz, F., Alshuweishi, Y., Bijland, S., Alghamdi, F., Degerman, E., Sakamoto, K., Salt, I. P. and Göransson, O. (2021). 'A-769662 inhibits adipocyte glucose uptake in an AMPK-independent manner', *Biochemical Journal*, 478(3), pp. 633-646.
- Krawutschke, C., Koesling, D. and Russwurm, M. (2015). 'Cyclic GMP in vascular relaxation: export is of similar importance as degradation', *Arteriosclerosis*, thrombosis, and vascular biology, 35(9), pp. 2011-2019.
- Krüger-Genge, A., Blocki, A., Franke, R.-P. and Jung, F. (2019). 'Vascular endothelial cell biology: an update', *International journal of molecular sciences*, 20(18), pp. 4411.
- Kwaifa, I. K., Bahari, H., Yong, Y. K. and Noor, S. M. (2020). 'Endothelial dysfunction in obesity-induced inflammation: molecular mechanisms and clinical implications', *Biomolecules*, 10(2), pp. 291.
- Kyriakis, J. M. and Avruch, J. (2012). 'Mammalian MAPK signal transduction pathways activated by stress and inflammation: a 10-year update', *Physiological reviews*, 92(2), pp. 689-737.
- Lacaná, E., Maceyka, M., Milstien, S. and Spiegel, S. (2002). 'Cloning and characterization of a protein kinase A anchoring protein (AKAP)-related protein that interacts with and regulates sphingosine kinase 1 activity', *Journal of Biological Chemistry*, 277(36), pp. 32947-32953.
- Lambert, J. M. (2021). 'Sphingosine Kinase 1 in Adipose Tissue: Roles in Metabolism, Adipogenesis, and Glucocorticoid Signaling'.
- Lee, C.-F., Dang, A., Hernandez, E., Pong, R.-C., Chen, B., Sonavane, R., Raj, G., Kapur, P., Lin, H.-Y. and Wu, S.-R. (2019). 'Activation of sphingosine kinase by lipopolysaccharide promotes prostate cancer cell invasion and metastasis via SphK1/S1PR4/matriptase', *Oncogene*, 38(28), pp. 5580-5598.

- Lee, H.-Y., Després, J.-P. and Koh, K. K. (2013). 'Perivascular adipose tissue in the pathogenesis of cardiovascular disease', *Atherosclerosis*, 230(2), pp. 177-184.
- Lee, J. M., Kim, S. R., Yoo, S. J., Hong, O., Son, H. and Chang, S. A. (2009). 'The relationship between adipokines, metabolic parameters and insulin resistance in patients with metabolic syndrome and type 2 diabetes', *Journal of International Medical Research*, 37(6), pp. 1803-1812.
- Lee, R. M., Lu, C., Su, L.-Y. and Gao, Y.-J. (2009). 'Endothelium-dependent relaxation factor released by perivascular adipose tissue', *Journal of hypertension*, 27(4), pp. 782-790.
- Lee, S.-Y., Lee, H.-Y., Song, J.-H., Kim, G.-T., Jeon, S., Song, Y.-J., Lee, J. S., Hur, J.-H., Oh, H. H. and Park, S.-Y. (2017). 'Adipocyte-specific deficiency of de novo sphingolipid biosynthesis leads to lipodystrophy and insulin resistance', *Diabetes*, 66(10), pp. 2596-2609.
- Li, H.-F., Liu, H.-T., Chen, P.-Y., Lin, H. and Tseng, T.-L. (2022). 'Role of PVAT in obesity-related cardiovascular disease through the buffering activity of ATF3', *Iscience*, 25(12).
- Li, W., Xu, H. and Testai, F. D. (2016). 'Mechanism of action and clinical potential of fingolimod for the treatment of stroke', *Frontiers in neurology*, 7, pp. 139.
- Lian, X. and Gollasch, M. (2016). 'A clinical perspective: contribution of dysfunctional perivascular adipose tissue (PVAT) to cardiovascular risk', *Current hypertension reports*, 18, pp. 1-9.
- Lidell, M. E., Betz, M. J., Leinhard, O. D., Heglind, M., Elander, L., Slawik, M., Mussack, T., Nilsson, D., Romu, T. and Nuutila, P. (2013). 'Evidence for two types of brown adipose tissue in humans', *Nature medicine*, 19(5), pp. 631-634.
- Lihn, A. S., Jessen, N., Pedersen, S. B., Lund, S. and Richelsen, B. (2004). 'AICAR stimulates adiponectin and inhibits cytokines in adipose tissue', *Biochemical and biophysical research communications*, 316(3), pp. 853-858.
- Lim, K. G., Sun, C., Bittman, R., Pyne, N. J. and Pyne, S. (2011). '(R)-FTY720 methyl ether is a specific sphingosine kinase 2 inhibitor: Effect on sphingosine kinase 2 expression in HEK 293 cells and actin rearrangement and survival of MCF-7 breast cancer cells', *Cellular signalling*, 23(10), pp. 1590-1595.
- Löhn, M., Dubrovska, G., Lauterbach, B., Luft, F. C., Gollasch, M. and Sharma, A. M. (2002). 'Periadventitial fat releases a vascular relaxing factor', *The FASEB Journal*, 16(9), pp. 1057-1063.
- Lu, Z., Zhang, W., Gao, S., Jiang, Q., Xiao, Z., Ye, L. and Zhang, X. (2015). 'MiR-506 suppresses liver cancer angiogenesis through targeting sphingosine kinase 1 (SPHK1) mRNA', *Biochemical and biophysical research communications*, 468(1-2), pp. 8-13.
- Lynch, F. M., Withers, S. B., Yao, Z., Werner, M. E., Edwards, G., Weston, A. H. and Heagerty, A. M. (2013). 'Perivascular adipose tissue-derived adiponectin

- activates BKCa channels to induce anticontractile responses', *American Journal of Physiology-Heart and Circulatory Physiology*, 304(6), pp. H786-H795.
- Ma, Y., Li, L., Shao, Y., Bai, X., Bai, T. and Huang, X. (2017). 'Methotrexate improves perivascular adipose tissue/endothelial dysfunction via activation of AMPK/eNOS pathway', *Molecular Medicine Reports*, 15(4), pp. 2353-2359.
- Maceyka, M., Alvarez, S. E., Milstien, S. and Spiegel, S. (2008). 'Filamin A links sphingosine kinase 1 and sphingosine-1-phosphate receptor 1 at lamellipodia to orchestrate cell migration', *Molecular and cellular biology*, 28(18), pp. 5687-5697.
- Mair, K., Robinson, E., Kane, K., Pyne, S., Brett, R., Pyne, N. and Kennedy, S. (2010). 'Interaction between anandamide and sphingosine-1-phosphate in mediating vasorelaxation in rat coronary artery', *British journal of pharmacology*, 161(1), pp. 176-192.
- Mancini, S. J. and Salt, I. P. (2018). 'Investigating the role of AMPK in inflammation', *AMPK: Methods and protocols*, pp. 307-319.
- Mancini, S. J., Boyd, D., Katwan, O. J., Strembitska, A., Almabrouk, T. A., Kennedy, S., Palmer, T. M. and Salt, I. P. (2018). 'Canagliflozin inhibits interleukin-18-stimulated cytokine and chemokine secretion in vascular endothelial cells by AMP-activated protein kinase-dependent and-independent mechanisms', *Scientific reports*, 8(1), pp. 5276.
- Mancini, S. J., White, A. D., Bijland, S., Rutherford, C., Graham, D., Richter, E. A., Viollet, B., Touyz, R. M., Palmer, T. M. and Salt, I. P. (2017). 'Activation of AMP-activated protein kinase rapidly suppresses multiple pro-inflammatory pathways in adipocytes including IL-1 receptor-associated kinase-4 phosphorylation', *Molecular and cellular endocrinology*, 440, pp. 44-56.
- Mastrandrea, L. D. (2013). 'Role of sphingosine kinases and sphingosine 1-phosphate in mediating adipogenesis'.
- Mastrandrea, L. D., Sessanna, S. M. and Laychock, S. G. (2005). 'Sphingosine kinase activity and sphingosine-1 phosphate production in rat pancreatic islets and INS-1 cells: response to cytokines', *Diabetes*, 54(5), pp. 1429-1436.
- Matienzo, D. and Bordoni, B. (2020). 'Anatomy, blood flow'.
- Matrone, G., Meng, S., Gu, Q., Lv, J., Fang, L., Chen, K. and Cooke, J. P. (2017). 'Lmo2 (LIM-Domain-Only 2) modulates Sphk1 (Sphingosine Kinase) and promotes endothelial cell migration', *Arteriosclerosis*, *thrombosis*, *and vascular biology*, 37(10), pp. 1860-1868.
- Mendelson, K., Evans, T. and Hla, T. (2014). 'Sphingosine 1-phosphate signalling', *Development*, 141(1), pp. 5-9.
- Mendizábal, Y., Llorens, S. and Nava, E. (2013). 'Vasoactive effects of prostaglandins from the perivascular fat of mesenteric resistance arteries in WKY and SHROB rats', *Life sciences*, 93(25-26), pp. 1023-1032.

- Merrill, G. F., Kurth, E. J., Hardie, D. and Winder, W. (1997). 'AICA riboside increases AMP-activated protein kinase, fatty acid oxidation, and glucose uptake in rat muscle', *American Journal of Physiology-Endocrinology and Metabolism*, 273(6), pp. E1107-E1112.
- Meyer, M. R., Fredette, N. C., Barton, M. and Prossnitz, E. R. (2013). 'Regulation of vascular smooth muscle tone by adipose-derived contracting factor', *PloS one*, 8(11), pp. e79245.
- Mitra, P., Oskeritzian, C. A., Payne, S. G., Beaven, M. A., Milstien, S. and Spiegel, S. (2006). 'Role of ABCC1 in export of sphingosine-1-phosphate from mast cells', *Proceedings of the national academy of sciences*, 103(44), pp. 16394-16399.
- Moon, M. H., Jeong, J. K. and Park, S. Y. (2015). 'Activation of S1P2 receptor, a possible mechanism of inhibition of adipogenic differentiation by sphingosine 1-phosphate', *Molecular medicine reports*, 11(2), pp. 1031-1036.
- Moon, M.-H., Jeong, J.-K., Lee, Y.-J., Seol, J.-W. and Park, S.-Y. (2014). 'Sphingosine-1-phosphate inhibits the adipogenic differentiation of 3T3-L1 preadipocytes', *International journal of molecular medicine*, 34(4), pp. 1153-1158.
- Morishige, J.-i., Yoshioka, K., Nakata, H., Ishimaru, K., Nagata, N., Tanaka, T., Takuwa, Y. and Ando, H. (2023). 'Sphingosine kinase 1 is involved in triglyceride breakdown by maintaining lysosomal integrity in brown adipocytes', *Journal of Lipid Research*, 64(11), pp. 100450.
- Morrow, V. A., Foufelle, F., Connell, J. M., Petrie, J. R., Gould, G. W. and Salt, I. P. (2003). 'Direct activation of AMP-activated protein kinase stimulates nitric-oxide synthesis in human aortic endothelial cells', *Journal of Biological Chemistry*, 278(34), pp. 31629-31639.
- Murakami, M., Ichihara, M., Sobue, S., Kikuchi, R., Ito, H., Kimura, A., Iwasaki, T., Takagi, A., Kojima, T. and Takahashi, M. (2007). 'RET signaling-induced SPHK1 gene expression plays a role in both GDNF-induced differentiation and MEN2-type oncogenesis', *Journal of neurochemistry*, 102(5), pp. 1585-1594.
- Nagata, D., Mogi, M. and Walsh, K. (2003). 'AMP-activated protein kinase (AMPK) signaling in endothelial cells is essential for angiogenesis in response to hypoxic stress', *Journal of Biological Chemistry*, 278(33), pp. 31000-31006.
- Neubauer, H. A. and Pitson, S. M. (2013). 'Roles, regulation and inhibitors of sphingosine kinase 2', *The FEBS journal*, 280(21), pp. 5317-5336.
- Nijnik, A., Clare, S., Hale, C., Chen, J., Raisen, C., Mottram, L., Lucas, M., Estabel, J., Ryder, E. and Adissu, H. (2012). 'The role of sphingosine-1-phosphate transporter Spns2 in immune system function', *The Journal of Immunology*, 189(1), pp. 102-111.
- Nojiri, T., Kurano, M., Tokuhara, Y., Ohkubo, S., Hara, M., Ikeda, H., Tsukamoto, K. and Yatomi, Y. (2014). 'Modulation of sphingosine-1-phosphate and

- apolipoprotein M levels in the plasma, liver and kidneys in streptozotocin-induced diabetic mice', *Journal of Diabetes Investigation*, 5(6), pp. 639-648.
- Okamoto, H., Takuwa, N., Gonda, K., Okazaki, H., Chang, K., Yatomi, Y., Shigematsu, H. and Takuwa, Y. (1998). 'EDG1 is a functional sphingosine-1-phosphate receptor that is linked via a Gi/o to multiple signaling pathways, including phospholipase C activation, Ca2+ mobilization, Ras-mitogen-activated protein kinase activation, and adenylate cyclase inhibition', *Journal of Biological Chemistry*, 273(42), pp. 27104-27110.
- Okazaki, H., Ishizaka, N., Sakurai, T., Kurokawa, K., Goto, K., Kumada, M. and Takuwa, Y. (1993). 'Molecular cloning of a novel putative G protein-coupled receptor expressed in the cardiovascular system', *Biochemical and biophysical research communications*, 190(3), pp. 1104-1109.
- Olefsky, J. M. and Glass, C. K. (2010). 'Macrophages, inflammation, and insulin resistance', *Annual review of physiology*, 72(1), pp. 219-246.
- Olivera, A. and Spiegel, S. (1993). 'Sphingosine-1-phosphate as second messenger in cell proliferation induced by PDGF and FCS mitogens', *Nature*, 365(6446), pp. 557-560.
- Osborn, O. and Olefsky, J. M. (2012). 'The cellular and signaling networks linking the immune system and metabolism in disease', *Nature medicine*, 18(3), pp. 363-374.
- O'Sullivan, C. and Dev, K. K. (2013). 'The structure and function of the S1P1 receptor', *Trends in pharmacological sciences*, 34(7), pp. 401-412.
- Ouchi, N., Kobayashi, H., Kihara, S., Kumada, M., Sato, K., Inoue, T., Funahashi, T. and Walsh, K. (2004). 'Adiponectin stimulates angiogenesis by promoting crosstalk between AMP-activated protein kinase and Akt signaling in endothelial cells', *Journal of Biological Chemistry*, 279(2), pp. 1304-1309.
- Padilla, J., Jenkins, N. T., Vieira-Potter, V. J. and Laughlin, M. H. (2013). 'Divergent phenotype of rat thoracic and abdominal perivascular adipose tissues', *American Journal of Physiology-Regulatory, Integrative and Comparative Physiology*, 304(7), pp. R543-R552.
- Palmer, T. M. and Salt, I. P. (2021). 'Nutrient regulation of inflammatory signalling in obesity and vascular disease', *Clinical Science*, 135(13), pp. 1563-1590.
- Parrill, A. L., Sardar, V. M. and Yuan, H. (2004). 'Sphingosine 1-phosphate and lysophosphatidic acid receptors: agonist and antagonist binding and progress toward development of receptor-specific ligands'. Seminars in cell & developmental biology: Elsevier, 467-476.
- Paugh, B. S., Bryan, L., Paugh, S. W., Wilczynska, K. M., Alvarez, S. M., Singh, S. K., Kapitonov, D., Rokita, H., Wright, S. and Griswold-Prenner, I. (2009). 'Interleukin-1 regulates the expression of sphingosine kinase 1 in glioblastoma cells', *Journal of Biological Chemistry*, 284(6), pp. 3408-3417.

- Peters, S. L. and Alewijnse, A. E. (2007). 'Sphingosine-1-phosphate signaling in the cardiovascular system', *Current opinion in pharmacology*, 7(2), pp. 186-192.
- Pitman, M. R. and Pitson, S. M. (2010). 'Inhibitors of the sphingosine kinase pathway as potential therapeutics', *Current cancer drug targets*, 10(4), pp. 354-367.
- Pitman, M.R., Lewis, A.C., Davies, L.T., Moretti, P.A., Anderson, D., Creek, D.J., Powell, J.A. and Pitson, S.M. (2022). The sphingosine 1-phosphate receptor 2/4 antagonist JTE-013 elicits off-target effects on sphingolipid metabolism. *Scientific reports*, 12(1), p.454.
- Pitson, S. M., Moretti, P. A., Zebol, J. R., Lynn, H. E., Xia, P., Vadas, M. A. and Wattenberg, B. W. (2003). 'Activation of sphingosine kinase 1 by ERK1/2-mediated phosphorylation', *The EMBO journal*.
- Powell-Wiley, T. M., Poirier, P., Burke, L. E., Després, J.-P., Gordon-Larsen, P., Lavie, C. J., Lear, S. A., Ndumele, C. E., Neeland, I. J. and Sanders, P. (2021). 'Obesity and cardiovascular disease: a scientific statement from the American Heart Association', *Circulation*, 143(21), pp. e984-e1010.
- Pulkoski-Gross, M. J., Donaldson, J. C. and Obeid, L. M. (2015). 'Sphingosine-1-phosphate metabolism: A structural perspective', *Critical reviews in biochemistry and molecular biology*, 50(4), pp. 298-313.
- Pyne, N. J. and Pyne, S. (2010). 'Sphingosine 1-phosphate and cancer', *Nature Reviews Cancer*, 10(7), pp. 489-503.
- Pyne, S. and Pyne, N. J. (2000). 'Sphingosine 1-phosphate signalling in mammalian cells', *Biochemical Journal*, 349(2), pp. 385-402.
- Qi, X.-Y., Qu, S.-L., Xiong, W.-H., Rom, O., Chang, L. and Jiang, Z.-S. (2018). 'Perivascular adipose tissue (PVAT) in atherosclerosis: a double-edged sword', *Cardiovascular diabetology*, 17, pp. 1-20.
- Ramirez, J., O'Malley, E. and Ho, W. (2017). 'Pro-contractile effects of perivascular fat in health and disease', *British Journal of Pharmacology*, 174(20), pp. 3482-3495.
- Rao, X., Huang, X., Zhou, Z. and Lin, X. (2013). 'An improvement of the 2[^] (-delta delta CT) method for quantitative real-time polymerase chain reaction data analysis', *Biostatistics, bioinformatics and biomathematics*, 3(3), pp. 71.
- Reihill, J. A., Ewart, M.-A., Hardie, D. G. and Salt, I. P. (2007). 'AMP-activated protein kinase mediates VEGF-stimulated endothelial NO production', *Biochemical and biophysical research communications*, 354(4), pp. 1084-1088.
- Rena, G., Hardie, D. G. and Pearson, E. R. (2017). 'The mechanisms of action of metformin', *Diabetologia*, 60(9), pp. 1577-1585.
- Richard, A. J., White, U., Elks, C. M. and Stephens, J. M. (2020). 'Adipose tissue: physiology to metabolic dysfunction', *Endotext [internet]*.

- Robinson, S. (2021). 'Priorities for health promotion and public health', London: Routledge. Rodgers, B. and Knafl, K.(2000) Concept Development in Nursing. 2nd edn. Montreal: WB Saunders. Roger, K. and Hatala, A.(2018) 'Religion, spirituality & chronic illness: A scoping review and implications for health care practitioners.' Journal of Religion & Spirituality in Social Work: Social Thought, 37(1), pp. 24-44.
- Rodríguez, C., Contreras, C., Sáenz-Medina, J., Muñoz, M., Corbacho, C., Carballido, J., García-Sacristán, A., Hernandez, M., López, M. and Rivera, L. (2020). 'Activation of the AMP-related kinase (AMPK) induces renal vasodilatation and downregulates Nox-derived reactive oxygen species (ROS) generation', *Redox Biology*, 34, pp. 101575.
- Rodríguez, C., Muñoz, M., Contreras, C. and Prieto, D. (2021). 'AMPK, metabolism, and vascular function', *The FEBS Journal*, 288(12), pp. 3746-3771.
- Roger, K. S. and Hatala, A. (2018). 'Religion, spirituality & chronic illness: A scoping review and implications for health care practitioners', *Journal of Religion & Spirituality in Social Work: Social Thought*, 37(1), pp. 24-44.
- Ross, F. A., Jensen, T. E. and Hardie, D. G. (2016). 'Differential regulation by AMP and ADP of AMPK complexes containing different γ subunit isoforms', *Biochemical Journal*, 473(2), pp. 189-199.
- Ross, J. S., Hu, W., Rosen, B., Snider, A. J., Obeid, L. M. and Cowart, L. A. (2013). 'Sphingosine kinase 1 is regulated by peroxisome proliferator-activated receptor α in response to free fatty acids and is essential for skeletal muscle interleukin-6 production and signaling in diet-induced obesity', *Journal of Biological Chemistry*, 288(31), pp. 22193-22206.
- Rossoni, L. V., Wareing, M., Wenceslau, C. F., Al-Abri, M., Cobb, C. and Austin, C. (2011). 'Acute simvastatin increases endothelial nitric oxide synthase phosphorylation via AMP-activated protein kinase and reduces contractility of isolated rat mesenteric resistance arteries', *Clinical Science*, 121(10), pp. 449-458.
- Roviezzo, F., Bucci, M., Delisle, C., Brancaleone, V., Lorenzo, A. D., Mayo, I. P., Fiorucci, S., Fontana, A., Gratton, J. P. and Cirino, G. (2006). 'Expression of Concern: Essential requirement for sphingosine kinase activity in eNOS-dependent NO release and vasorelaxation', *The FASEB journal*, 20(2), pp. 340-342.
- Rubin, L. J., Magliola, L., Feng, X., Jones, A. W. and Hale, C. C. (2005). 'Metabolic activation of AMP kinase in vascular smooth muscle', *Journal of applied physiology*, 98(1), pp. 296-306.
- Salomone, S. and Waeber, C. (2011). 'Selectivity and specificity of sphingosine-1-phosphate receptor ligands: caveats and critical thinking in characterizing receptor-mediated effects', *Frontiers in pharmacology*, 2, pp. 9.
- Salomone, S., Potts, E.M., Tyndall, S., Ip, P.C., Chun, J., Brinkmann, V. and Waeber, C. (2008). Analysis of sphingosine 1-phosphate receptors involved in constriction

- of isolated cerebral arteries with receptor null mice and pharmacological tools. *British journal of pharmacology*, 153(1), pp.140-147.
- Salt, I. P. and Hardie, D. G. (2017). 'AMP-activated protein kinase: an ubiquitous signaling pathway with key roles in the cardiovascular system', *Circulation research*, 120(11), pp. 1825-1841.
- Salt, I. P. and Palmer, T. M. (2012). 'Exploiting the anti-inflammatory effects of AMP-activated protein kinase activation', *Expert opinion on investigational drugs*, 21(8), pp. 1155-1167.
- Samad, F., Hester, K. D., Yang, G., Hannun, Y. A. and Bielawski, J. (2006). 'Altered adipose and plasma sphingolipid metabolism in obesity: a potential mechanism for cardiovascular and metabolic risk', *Diabetes*, 55(9), pp. 2579-2587.
- Sanchez, T. and Hla, T. (2004). 'Structural and functional characteristics of S1P receptors', *Journal of cellular biochemistry*, 92(5), pp. 913-922.
- Sanders, M. J., Ali, Z. S., Hegarty, B. D., Heath, R., Snowden, M. A. and Carling, D. (2007). 'Defining the mechanism of activation of AMP-activated protein kinase by the small molecule A-769662, a member of the thienopyridone family', *Journal of biological chemistry*, 282(45), pp. 32539-32548.
- Sandoo, A., van Zanten, J. J. V., Metsios, G. S., Carroll, D. and Kitas, G. D. (2010). 'The endothelium and its role in regulating vascular tone', *The open cardiovascular medicine journal*, 4, pp. 302.
- Sanna, M.G., Liao, J., Jo, E., Alfonso, C., Ahn, M.Y., Peterson, M.S., Webb, B., Lefebvre, S., Chun, J., Gray, N. and Rosen, H. (2004). Sphingosine 1-phosphate (S1P) receptor subtypes S1P1 and S1P3, respectively, regulate lymphocyte recirculation and heart rate. *Journal of Biological Chemistry*, 279(14), pp.13839-13848.
- Sanna, M. G., Wang, S.-K., Gonzalez-Cabrera, P. J., Don, A., Marsolais, D., Matheu, M. P., Wei, S. H., Parker, I., Jo, E. and Cheng, W.-C. (2006). 'Enhancement of capillary leakage and restoration of lymphocyte egress by a chiral S1P1 antagonist in vivo', *Nature chemical biology*, 2(8), pp. 434-441.
- Sato, K., Malchinkhuu, E., Horiuchi, Y., Mogi, C., Tomura, H., Tosaka, M., Yoshimoto, Y., Kuwabara, A. and Okajima, F. (2007). 'Critical role of ABCA1 transporter in sphingosine 1-phosphate release from astrocytes', *Journal of neurochemistry*, 103(6), pp. 2610-2619.
- Schneider, H., Schubert, K. M., Blodow, S., Kreutz, C.-P., Erdogmus, S., Wiedenmann, M., Qiu, J., Fey, T., Ruth, P. and Lubomirov, L. T. (2015). 'AMPK dilates resistance arteries via activation of SERCA and BKCa channels in smooth muscle', *Hypertension*, 66(1), pp. 108-116.
- Schnute, M. E., McReynolds, M. D., Kasten, T., Yates, M., Jerome, G., Rains, J. W., Hall, T., Chrencik, J., Kraus, M. and Cronin, C. N. (2012). 'Modulation of cellular S1P levels with a novel, potent and specific inhibitor of sphingosine kinase-1', *Biochemical Journal*, 444(1), pp. 79-88.

- Schulz, E., Anter, E., Zou, M.-H. and Keaney Jr, J. F. (2005). 'Estradiol-mediated endothelial nitric oxide synthase association with heat shock protein 90 requires adenosine monophosphate-dependent protein kinase', *Circulation*, 111(25), pp. 3473-3480.
- Sena, C. M., Pereira, A., Fernandes, R., Letra, L. and Seiça, R. M. (2017). 'Adiponectin improves endothelial function in mesenteric arteries of rats fed a high-fat diet: role of perivascular adipose tissue', *British journal of pharmacology*, 174(20), pp. 3514-3526.
- Shaw, R. J., Kosmatka, M., Bardeesy, N., Hurley, R. L., Witters, L. A., DePinho, R. A. and Cantley, L. C. (2004). 'The tumor suppressor LKB1 kinase directly activates AMP-activated kinase and regulates apoptosis in response to energy stress', *Proceedings of the National Academy of Sciences*, 101(10), pp. 3329-3335.
- Shimokawa, H. and Godo, S. (2020). 'Nitric oxide and endothelium-dependent hyperpolarization mediated by hydrogen peroxide in health and disease', *Basic & Clinical Pharmacology & Toxicology*, 127(2), pp. 92-101.
- Sobue, S., Hagiwara, K., Banno, Y., Tamiya-Koizumi, K., Suzuki, M., Takagi, A., Kojima, T., Asano, H., Nozawa, Y. and Murate, T. (2005). 'Transcription factor specificity protein 1 (Sp1) is the main regulator of nerve growth factor-induced sphingosine kinase 1 gene expression of the rat pheochromocytoma cell line, PC12', *Journal of neurochemistry*, 95(4), pp. 940-949.
- Soltis, E. E. and Cassis, L. A. (1991). 'Influence of perivascular adipose tissue on rat aortic smooth muscle responsiveness', *Clinical and Experimental Hypertension*. *Part A: Theory and Practice*, 13(2), pp. 277-296.
- Spiegel, S. and Milstien, S. (2003). 'Sphingosine-1-phosphate: an enigmatic signalling lipid', *Nature reviews Molecular cell biology*, 4(5), pp. 397-407.
- Stahmann, N., Woods, A., Carling, D. and Heller, R. (2006). 'Thrombin activates AMP-activated protein kinase in endothelial cells via a pathway involving Ca2+/calmodulin-dependent protein kinase kinase B', *Molecular and cellular biology*, 26(16), pp. 5933-5945.
- Stahmann, N., Woods, A., Spengler, K., Heslegrave, A., Bauer, R., Krause, S., Viollet, B., Carling, D. and Heller, R. (2010). 'Activation of AMP-activated protein kinase by vascular endothelial growth factor mediates endothelial angiogenesis independently of nitric-oxide synthase', *Journal of Biological Chemistry*, 285(14), pp. 10638-10652.
- Stanek, A., Brożyna-Tkaczyk, K. and Myśliński, W. (2021). 'The role of obesity-induced perivascular adipose tissue (PVAT) dysfunction in vascular homeostasis', *Nutrients*, 13(11), pp. 3843.
- Strembitska, A., Mancini, S. J., Gamwell, J. M., Palmer, T. M., Baillie, G. S. and Salt, I. P. (2018). 'A769662 inhibits insulin-stimulated Akt activation in human macrovascular endothelial cells independent of AMP-activated protein kinase', *International Journal of molecular sciences*, 19(12), pp. 3886.

- Sun, J., Yan, G., Ren, A., You, B. and Liao, J. K. (2006). 'FHL2/SLIM3 decreases cardiomyocyte survival by inhibitory interaction with sphingosine kinase-1', *Circulation research*, 99(5), pp. 468-476.
- Sun, W., Lee, T.-S., Zhu, M., Gu, C., Wang, Y., Zhu, Y. and Shyy, J. Y. (2006). 'Statins activate AMP-activated protein kinase in vitro and in vivo', *Circulation*, 114(24), pp. 2655-2662.
- Sun, Y., Li, J., Xiao, N., Wang, M., Kou, J., Qi, L., Huang, F., Liu, B. and Liu, K. (2014). 'Pharmacological activation of AMPK ameliorates perivascular adipose/endothelial dysfunction in a manner interdependent on AMPK and SIRT1', *Pharmacological Research*, 89, pp. 19-28.
- Szasz, T. and Webb, R. C. (2012). 'Perivascular adipose tissue: more than just structural support', *Clinical science*, 122(1), pp. 1-12.
- Ter Braak, M., Danneberg, K., Lichte, K., Liphardt, K., Ktistakis, N. T., Pitson, S. M., Hla, T., Jakobs, K. H. and zu Heringdorf, D. M. (2009). 'Gαq-mediated plasma membrane translocation of sphingosine kinase-1 and cross-activation of S1P receptors', *Biochimica et Biophysica Acta (BBA)-Molecular and Cell Biology of Lipids*, 1791(5), pp. 357-370.
- Theodoulou, F. L. and Kerr, I. D. (2015). 'ABC transporter research: going strong 40 years on', *Biochemical Society Transactions*, 43(5), pp. 1033-1040.
- Thuy, A. V., Reimann, C.-M., Hemdan, N. Y. and Gräler, M. H. (2014). 'Sphingosine 1-phosphate in blood: function, metabolism, and fate', *Cellular Physiology and Biochemistry*, 34(1), pp. 158-171.
- Tolle, M., Levkau, B., Keul, P., Brinkmann, V., Giebing, G. n., Schönfelder, G., Schäfers, M., Lipinski, K. v. W., Jankowski, J. and Jankowski, V. (2005). 'Immunomodulator FTY720 induces eNOS-dependent arterial vasodilatation via the lysophospholipid receptor S1P3', *Circulation research*, 96(8), pp. 913-920.
- Tous, M., Ferrer-Lorente, R. and Badimon, L. (2014). 'Selective inhibition of sphingosine kinase-1 protects adipose tissue against LPS-induced inflammatory response in Zucker diabetic fatty rats', *American Journal of Physiology-Endocrinology and Metabolism*, 307(5), pp. E437-E446.
- Touyz, R. M., Alves-Lopes, R., Rios, F. J., Camargo, L. L., Anagnostopoulou, A., Arner, A. and Montezano, A. C. (2018). 'Vascular smooth muscle contraction in hypertension', *Cardiovascular research*, 114(4), pp. 529-539.
- Towler, M. C. and Hardie, D. G. (2007). 'AMP-activated protein kinase in metabolic control and insulin signaling', *Circulation research*, 100(3), pp. 328-341.
- Tsao, C. W., Aday, A. W., Almarzooq, Z. I., Alonso, A., Beaton, A. Z., Bittencourt, M. S., Boehme, A. K., Buxton, A. E., Carson, A. P. and Commodore-Mensah, Y. (2022). 'Heart disease and stroke statistics—2022 update: a report from the American Heart Association', *Circulation*, 145(8), pp. e153-e639.

- Van Dam, A. D., Boon, M. R., Berbée, J. F., Rensen, P. C. and van Harmelen, V. (2017). 'Targeting white, brown and perivascular adipose tissue in atherosclerosis development', *European journal of pharmacology*, 816, pp. 82-92.
- Venkataraman, K., Thangada, S., Michaud, J., Oo, M. L., Ai, Y., Lee, Y.-M., Wu, M., Parikh, N. S., Khan, F. and Proia, R. L. (2006). 'Extracellular export of sphingosine kinase-1a contributes to the vascular S1P gradient', *Biochemical Journal*, 397(3), pp. 461-471.
- Verlohren, S., Dubrovska, G., Tsang, S.-Y., Essin, K., Luft, F. C., Huang, Y. and Gollasch, M. (2004). 'Visceral periadventitial adipose tissue regulates arterial tone of mesenteric arteries', *Hypertension*, 44(3), pp. 271-276.
- Victorio, J. A., Fontes, M. T., Rossoni, L. V. and Davel, A. P. (2016). 'Different anticontractile function and nitric oxide production of thoracic and abdominal perivascular adipose tissues', *Frontiers in physiology*, 7, pp. 295.
- Waeber, C., Blondeau, N. and Salomone, S. (2004). 'Vascular sphingosine-1-phosphate S1P1 and S1P3 receptors', *Drug news & perspectives*, 17(6), pp. 365-382.
- Walford, G. and Loscalzo, J. (2003). 'Nitric oxide in vascular biology', *Journal of Thrombosis and Haemostasis*, 1(10), pp. 2112-2118.
- Wang, J., Alexanian, A., Ying, R., Kizhakekuttu, T. J., Dharmashankar, K., Vasquez-Vivar, J., Gutterman, D. D. and Widlansky, M. E. (2012). 'Acute exposure to low glucose rapidly induces endothelial dysfunction and mitochondrial oxidative stress: role for AMP kinase', *Arteriosclerosis*, thrombosis, and vascular biology, 32(3), pp. 712-720.
- Wang, J., Badeanlou, L., Bielawski, J., Ciaraldi, T. P. and Samad, F. (2014). 'Sphingosine kinase 1 regulates adipose proinflammatory responses and insulin resistance', *American Journal of Physiology-Endocrinology and Metabolism*, 306(7), pp. E756-E768.
- Wang, N., Li, J.-Y., Zeng, B. and Chen, G.-L. (2023). 'Sphingosine-1-phosphate signaling in cardiovascular diseases', *Biomolecules*, 13(5), pp. 818.
- Wang, Q., Sun, J., Liu, M., Zhou, Y., Zhang, L. and Li, Y. (2021). 'The new role of AMP-activated protein kinase in regulating fat metabolism and energy expenditure in adipose tissue', *Biomolecules*, 11(12), pp. 1757.
- Wang, S., Zhang, M., Liang, B., Xu, J., Xie, Z., Liu, C., Viollet, B., Yan, D. and Zou, M.-H. (2010). 'AMPKα2 deletion causes aberrant expression and activation of NAD (P) H oxidase and consequent endothelial dysfunction in vivo: role of 26S proteasomes', *Circulation research*, 106(6), pp. 1117-1128.
- Watson, D. G., Tonelli, F., Alossaimi, M., Williamson, L., Chan, E., Gorshkova, I., Berdyshev, E., Bittman, R., Pyne, N. J. and Pyne, S. (2013). 'The roles of sphingosine kinases 1 and 2 in regulating the Warburg effect in prostate cancer cells', *Cellular signalling*, 25(4), pp. 1011-1017.

- Wattenberg, B. W., Pitson, S. M. and Raben, D. M. (2006). 'The sphingosine and diacylglycerol kinase superfamily of signaling kinases: localization as a key to signaling function', *Journal of lipid research*, 47(6), pp. 1128-1139.
- Watterson, K. R., Ratz, P. H. and Spiegel, S. (2005). 'The role of sphingosine-1-phosphate in smooth muscle contraction', *Cellular signalling*, 17(3), pp. 289-298.
- Wilkerson, B. A. and Argraves, K. M. (2014). 'The role of sphingosine-1-phosphate in endothelial barrier function', *Biochimica et Biophysica Acta (BBA)-Molecular and Cell Biology of Lipids*, 1841(10), pp. 1403-1412.
- Willows, R., Navaratnam, N., Lima, A., Read, J. and Carling, D. (2017). 'Effect of different γ-subunit isoforms on the regulation of AMPK', *Biochemical Journal*, 474(10), pp. 1741-1754.
- Willows, R., Sanders, M. J., Xiao, B., Patel, B. R., Martin, S. R., Read, J., Wilson, J. R., Hubbard, J., Gamblin, S. J. and Carling, D. (2017). 'Phosphorylation of AMPK by upstream kinases is required for activity in mammalian cells', *Biochemical Journal*, 474(17), pp. 3059-3073.
- Wilson, D. (2011). Vascular smooth muscle structure and function. *Mechanisms of vascular disease*, pp.13-24.
- Woods, A., Dickerson, K., Heath, R., Hong, S.-P., Momcilovic, M., Johnstone, S. R., Carlson, M. and Carling, D. (2005). 'Ca2+/calmodulin-dependent protein kinase kinase-B acts upstream of AMP-activated protein kinase in mammalian cells', *Cell metabolism*, 2(1), pp. 21-33.
- Wu, C.C. and Bohr, D.F. (1990). Role of endothelium in the response to endothelin in hypertension. *Hypertension*, 16(6), pp.677-681.
- Xia, N. and Li, H. (2017). 'The role of perivascular adipose tissue in obesity-induced vascular dysfunction', *British journal of pharmacology*, 174(20), pp. 3425-3442.
- Xia, N., Horke, S., Habermeier, A., Closs, E. I., Reifenberg, G., Gericke, A., Mikhed, Y., Münzel, T., Daiber, A. and Förstermann, U. (2016). 'Uncoupling of endothelial nitric oxide synthase in perivascular adipose tissue of diet-induced obese mice', *Arteriosclerosis*, thrombosis, and vascular biology, 36(1), pp. 78-85.
- Xia, P., Wang, L., Moretti, P. A., Albanese, N., Chai, F., Pitson, S. M., D'Andrea, R. J., Gamble, J. R. and Vadas, M. A. (2002). 'Sphingosine kinase interacts with TRAF2 and dissects tumor necrosis factor-α signaling', *Journal of Biological Chemistry*, 277(10), pp. 7996-8003.
- Xiao, B., Sanders, M. J., Carmena, D., Bright, N. J., Haire, L. F., Underwood, E., Patel, B. R., Heath, R. B., Walker, P. A. and Hallen, S. (2013). 'Structural basis of AMPK regulation by small molecule activators', *Nature communications*, 4(1), pp. 3017.
- Xue, G., Chen, J.-p., Li, Y., Zhang, Z.-q., Zhu, J.-l. and Dong, W. (2020). 'MicroRNA-6862 inhibition elevates sphingosine kinase 1 and protects neuronal cells from MPP+-induced apoptosis', *Aging (Albany NY)*, 13(1), pp. 1369.

- Yang, Q., Liang, X., Sun, X., Zhang, L., Fu, X., Rogers, C. J., Berim, A., Zhang, S., Wang, S. and Wang, B. (2016). 'AMPK/α-ketoglutarate axis dynamically mediates DNA demethylation in the Prdm16 promoter and brown adipogenesis', *Cell metabolism*, 24(4), pp. 542-554.
- Yang, Z., Kahn, B. B., Shi, H. and Xue, B.-z. (2010). 'Macrophage α1 AMP-activated protein kinase (α1AMPK) antagonizes fatty acid-induced inflammation through SIRT1', *Journal of Biological Chemistry*, 285(25), pp. 19051-19059.
- Yao, C., Ruan, J.-W., Zhu, Y.-R., Liu, F., Wu, H.-m., Zhang, Y. and Jiang, Q. (2020). The therapeutic value of the SphK1-targeting microRNA-3677 in human osteosarcoma cells', *Aging (Albany NY)*, 12(6), pp. 5399.
- Yi, X., Tang, X., Li, T., Chen, L., He, H., Wu, X., Xiang, C., Cao, M., Wang, Z. and Wang, Y. (2023). 'Therapeutic potential of the sphingosine kinase 1 inhibitor, PF-543', *Biomedicine & Pharmacotherapy*, 163, pp. 114401.
- Yoh, T., Noriko, T. and Naotoshi, S. (2002). 'The Edg Family G Protein-Coupled Receptors for Lysophospholipids: Their Signaling Properties and Biological Activities', *The Journal of Biochemistry*, 131(6), pp. 767-771.
- Zhang, H., Wang, Q., Zhao, Q. and Di, W. (2013). 'MiR-124 inhibits the migration and invasion of ovarian cancer cells by targeting SphK1', *Journal of ovarian research*, 6, pp.1-9.
- Zhang, M., Dong, Y., Xu, J., Xie, Z., Wu, Y., Song, P., Guzman, M., Wu, J. and Zou, M.-H. (2008). 'Thromboxane receptor activates the AMP-activated protein kinase in vascular smooth muscle cells via hydrogen peroxide', *Circulation research*, 102(3), pp. 328-337.
- Zhang, W., Mottillo, E. P., Zhao, J., Gartung, A., VanHecke, G. C., Lee, J.-F., Maddipati, K. R., Xu, H., Ahn, Y.-H. and Proia, R. L. (2014). 'Adipocyte lipolysis-stimulated interleukin-6 production requires sphingosine kinase 1 activity', *Journal of Biological Chemistry*, 289(46), pp. 32178-32185.
- Zhang, Y., Lee, T.-S., Kolb, E. M., Sun, K., Lu, X., Sladek, F. M., Kassab, G. S., Garland Jr, T. and Shyy, J. Y.-J. (2006). 'AMP-activated protein kinase is involved in endothelial NO synthase activation in response to shear stress', *Arteriosclerosis*, *thrombosis*, *and vascular biology*, 26(6), pp. 1281-1287.
- Zhang, Y., Qiu, J., Wang, X., Zhang, Y. and Xia, M. (2011). 'AMP-activated protein kinase suppresses endothelial cell inflammation through phosphorylation of transcriptional coactivator p300', *Arteriosclerosis*, thrombosis, and vascular biology, 31(12), pp. 2897-2908.
- Zou, L., Wang, W., Liu, S., Zhao, X., Lyv, Y., Du, C., Su, X., Geng, B. and Xu, G. (2016). 'Spontaneous hypertension occurs with adipose tissue dysfunction in perilipin-1 null mice', *Biochimica et Biophysica Acta (BBA)-Molecular Basis of Disease*, 1862(2), pp. 182-191.

Appendices

Table 7-1 Contractile responses (mean \pm SEM) to KPSS and phenylephrine under varying ET (\pm) and PVAT (\pm) conditions.

WT	AMPKα1 KO	PVAT	ET	KPSS (mN)	PE (mN)	Number of experiments
+	•	+	1	8.5 ± 0.4	8.2 ± 0.5	6
+	1	+	+	6.4 ± 0.4	5.4 ± 0.4	6
+	-	-	-	5.3 ± 0.3	5.1 ± 0.5	6
-	+	+	-	7.4 ± 0.5	7.3 ± 0.9	5